# Regulatory B and T cells in *Helicobacter pylori* infection

Dona Reddiar

Thesis submitted to the University of Nottingham

for the degree of Doctor of Philosophy.

September 2017

## Dedication

This thesis is dedicated to David Raju Soosai Reddiar,

my grandfather and first teacher.

I wish you were here to see this.

## Abstract

In the human gastric mucosa, an inflammatory response stimulated by *H. pylori* infection can lead to gastric cancer and peptic ulcer disease. Expression of the i1 active variant of Vacuolating Cytotoxin A (VacA) by the colonising bacterial strain has been identified as an independent risk factor for disease. VacA skews the adaptive immune response towards a regulatory phenotype to promote persistent *H. pylori* colonisation. In *H. pylori*-infected individuals, regulatory T cells (Tregs), which suppress inflammation through mechanisms including interleukin-10 (IL-10) production, are thought to play a role in protection against extra-gastric diseases such as multiple sclerosis and oesophageal cancer. IL-10 is an immunomodulatory cytokine which is expressed by several immune cell types including regulatory B cells (Bregs), whose role in *H. pylori* infection is unclear.

Blood was donated by uninfected and infected patients, and those who underwent successful eradication of their *H. pylori* infection. A flow cytometry antibody panel was developed to quantify the relative frequencies of peripheral blood Bregs and Tregs, and investigate differences according to *H. pylori* status. Mice were also infected with *H. pylori* to determine VacA i1 versus i2 differences in the induced regulatory B and T cell frequencies. Stool samples were collected from patients to develop a VacA i-region PCR-based diagnostic test.

Results showed that compared to during *H. pylori* infection, the proportion of IL-10-producing Tregs in the peripheral blood of patients declined after successful eradication therapy. A pilot study in mice revealed B lymphocytes to be another important source of IL-10, and the population expanded after *H. pylori* infection. In a study of *H. pylori*-positive, *H. pylori*-negative and *H. pylori*-eradicated patients, there were no significant differences in peripheral blood Breg or IL-$10^{+}$ Breg frequencies.

Data from an expanded mouse study using blood and spleen showed that VacA variants in a colonising *H. pylori* strain did not induce differences in Breg or Treg frequencies 9 weeks after wildtype or mutant *H. pylori* SS1 infection. The *H. pylori 16S* gene was successfully detected in stool DNA samples and could be used to determine infection status, but the development of a *vacA* i-region PCR-based typing stool test was unsuccessful.

Previous work in the research group has identified how Treg frequencies are associated with *H. pylori* infection and disease. While Bregs are capable of producing IL-10 after stimulation, their role in *H. pylori* infection in mice and humans appears to be limited. The consistency of peripheral blood Treg frequencies in patients from their infected state until two years post-eradication is a start to understanding whether *H. pylori*-induced extra-gastric protection may also be maintained after eradication. While stool remains a promising resource for non-invasively diagnosing *H. pylori* infection worldwide, there are strong concerns about contamination and reproducibility which are unlikely to be overcome for use in a clinical setting.

## Presented research

### Oral presentations

Reddiar, D., Kaneko, K., White, J., Atherton, J., and Robinson, K.
**IL-10-secreting lymphocytes in the immune response to *H. pylori* infection.**

- School of Medicine Sue Watson Oral Presentation Event, November 2015. (Joint third prize)
- LINK'16 student-led research conference, Nottingham, June 2016.

Reddiar, D., Kaneko, K., White, J., Atherton, J., and Robinson, K.
**IL-10-producing B and T lymphocytes during *H. pylori* infection.**

- 12th International Workshop on Pathogenesis and Host Response in *Helicobacter* Infections, Helsingør, Denmark, June-July 2016.

### Poster presentations

Reddiar, D., Kaneko, K., White, J., Atherton, J., and Robinson, K.
**Optimisation of a polychromatic flow cytometry panel to identify human regulatory B and T cells.**

- M5 Flow Cytometry Meeting, Nottingham, December 2015.
- Immunology Showcase, Nottingham, February 2016.

Reddiar, D., Kaneko, K., White, J., Atherton, J., and Robinson, K.
**IL-10-producing lymphocytes in the immune response to *Helicobacter pylori* infection.**

- Immunology Showcase, Nottingham, February 2016.
- Microbiology Society Annual Meeting, Liverpool, March 2016.

Reddiar, D., Kaneko, K., White, J., Atherton, J., and Robinson, K.
**It's hard to stomach *H. pylori* infection: identifying those at risk of disease.**

- Nottingham Research Showcase, June 2016.

Reddiar, D., Kaneko, K., White, J., Atherton, J., and Robinson, K.
**IL-10-producing B and T lymphocytes during *H. pylori* infection.**

- 12th International Workshop on Pathogenesis and Host Response in *Helicobacter* Infections, Helsingør, Denmark, June-July 2016.

Reddiar, D.
**Identifying new risk factors for stomach cancer.**

- STEM for Britain exhibition, House of Commons, London, March 2017.

## Acknowledgements

I've always liked reading other people's acknowledgements. It provides a unique glimpse into the depth of their gratitude for the support they've been given, both personally and professionally.

For me, this PhD has been a definite adventure. In a training session at the beginning of my first year, I was told to write down the reason why I was doing a PhD and keep it in my wallet. This was because I'd need to remember the reason in difficult moments. This is what I wrote:

I'm doing a PhD because I want to learn more about my subject (*H. pylori*).

I am proud to say that even now, after the exhaustion and anxiety of writing this thesis (and correcting it), I still feel that way. As you will read in my Introduction, *H. pylori* is an incredible bacterium, with a past and a future that is irrevocably entwined with human disease.

However, it would be the height of dishonour to suggest that my interest in this subject has been enough to get me through this degree on its own. I would like to profusely thank the following people for their role in getting me to this position.

Firstly, secondly, and lastly, to my supervisor Dr. Karen Robinson. Thank you for accepting me as your PhD student, for pushing me, and for always reminding me of the bigger perspectives of my work. I have learned so much from you, and I will always be grateful for it.

Dr. Kazuyo Kaneko, thank you for answering every question I ever had on flow cytometry. You are an excellent mentor and an amazing scientist, and I deeply appreciated your feedback on my work and my writing.

It would be difficult to describe what I owe to Dr. Jon White. As well as a colleague on two of the projects listed in my thesis, he has become a great friend. I know him to be a fantastic doctor, who worked so hard to obtain the samples I needed for my work on patients. Thank you, Jon.

Thank you to all the members of the *H. pylori* research group; to Prof. John Atherton for his enthusiasm and encouragement on even the smallest achievement, and for the samples he obtained for me, and to Dr. Darren Letley, Mrs. Jo Rhead and Dr. Rob Delahay for making a great working environment. Kwadwo Boampong (future doctor), thank you for your positive attitude and your friendship.

Thank you to everyone in CBS office B51 for all the happy memories we made.

Thank you to NDDBRC for funding this PhD, and to all the patients and volunteers who consented to donate to my projects. Without you all, none of this would have been possible.

This next person crosses the line between supporting me personally and professionally. I first met Dr. Annastazia Learoyd in the animal facility in QMC, and complimented her on her Harry Potter-themed jumper. She then turned out to be my housemate the following year, and has been a good friend ever since. Thank you, Anna, for never letting me feel like I was ever alone in my thesis writing period.

Thank you to my friends, Dr. Aishah Nasir, Ms. Tanya Leonard, Mr. Horatio Caine and Mr. Gordon Smith, who checked in on me, listened to my ramblings, and always provided me with the encouragement to continue with my work.

Rossby Awadzi (future doctor) has been my rock throughout this whole PhD. He was there when I applied for this position, he was there every time I needed him, and he will be there when I finish. Thank you, Ross.

To my partner in life, William Norwood-Grundy. You've held my hand and walked with me through some truly difficult moments. You've been a critic when I've needed it, but a fierce supporter whenever I've questioned myself. Your love and kindness are the armour I wear to face my worst doubts. Thank you for choosing to be with me on this journey.

Thank you to my grandmothers, Theresa and Soosaiammal, for their daily prayers and thoughts. There was never a moment when your good thoughts did not reach me and lift my spirits. Sadly, my grandfather Isaac passed away before this PhD was completed. I remember him as a pious man, who freely gave us his smiles, blessings and love. An added thank you to all my maternal family in India. You all prayed for me and rejoiced in all my successes. Thank you.

My siblings have put up with an awful lot from me this past year. I would like to thank my brother, Paul, for his quiet kindnesses and encouragement during my thesis writing. Thank you to my sister, Fiona, for being herself. (She once told me to fail this degree so that I could return home to be with her.) Bugs, you always make me laugh. Thank you for all the healing hugs you've given me all these years.

For all the feeling you can put into the words 'thank you', it will never be enough to convey the gratitude I feel for my parents, Fatima and Stephen. This thesis is testament to all the sacrifices you have made for me. You sent me food parcels when I was homesick, you prayed unremittingly for me when I needed it most, you picked me up every time I fell, and you have done all this for me for 26 years.

I consider it the highest honour in the world to be your daughter.

Thank you.

## Contents

**Dedication** ... **ii**

**Abstract** ... **iii**

**Presented research** ... **v**

Oral presentations ... v

Poster presentations ... v

**Acknowledgements** ... **vi**

**Contents** ... **ix**

**Abbreviations** ... **xi**

**List of tables** ... **xv**

**List of figures** ... **xvii**

**Chapter 1: Introduction to *Helicobacter pylori* infection** ... **1**

1.1 General background ... 1

1.2 Association between *H. pylori* and disease ... 3

1.3 Current treatment ... 8

1.4 Factors that influence disease outcomes ... 9

1.5 The innate immune response to *H. pylori* infection ... 20

1.6 The adaptive immune response to *H. pylori* infection ... 23

1.7 Research objectives ... 47

**Chapter 2: Studying the effect of *H. pylori* eradication on Treg responses** ... **49**

2.1 Introduction ... 49

2.2 Hypotheses ... 50

2.3 Aims ... 51

2.4 Materials and methods ... 52

2.5 Results ... 61

2.6 Discussion ... 71

**Chapter 3: Pilot study characterising IL-10-producing B cells in mice** ... **82**

3.1 Introduction ... 82

3.2 Hypotheses ... 83

3.3 Aims ... 83

3.4 Materials and methods ... 84

3.5 Results ... 88

3.6 Discussion ... 102

**Chapter 4: Quantifying human Bregs and Tregs in *H. pylori* infection ..... 111**
4.1 Introduction ..... 111
4.2 Hypotheses ..... 111
4.3 Aims ..... 112
4.4 Materials and methods ..... 113
4.5 Results ..... 118
4.6 Discussion ..... 138
**Chapter 5: Characterising the effect of VacA on Bregs and Tregs in mice ..... 148**
5.1 Introduction ..... 148
5.2 Hypotheses ..... 148
5.3 Aims ..... 149
5.4 Materials and methods ..... 150
5.5 Results ..... 155
5.6 Discussion ..... 182
**Chapter 6: Developing a *H. pylori vacA* type stool-based PCR test ..... 190**
6.1 Introduction ..... 190
6.2 Rationale ..... 198
6.3 Aims ..... 199
6.4 Materials and methods ..... 200
6.5 Results ..... 206
6.6 Discussion ..... 221
**Chapter 7: General discussion ..... 237**
7.1 General findings and conclusions ..... 237
7.2 Critique of experimental design ..... 242
7.3 Future work and unanswered questions ..... 244
7.4 Final summary ..... 246
**Bibliography ..... 247**
**Appendix ..... 272**
**Quotation ..... 299**

## Abbreviations

Abl – Abelson murine leukemia viral oncogene homolog 1 and 2

ANOVA – Analysis of Variance

APC – Antigen Presenting Cell

ATCC ID – American Type Culture Collection identification number

B cells – B lymphocytes

BabA – Blood group Antigen-Binding antigen A

BFA – Brefeldin A

BHI – Brain-Heart Infusion

Bp – Base pairs

Breg – Regulatory B cell

BSA – Bovine Serum Albumin

CagA – Cytotoxin-associated Antigen A

CagPAI – Cytotoxin-associated Antigen Pathogenicity Island

CFSE - Carboxyfluorescein Succinimidyl Ester

CFU – Colony Forming Units

CLO – *Campylobacter*-Like Organism

CLR – C-type Lectin Receptor

$CO_2$ – Carbon Dioxide

C+S – *H. pylori* culture and sensitivity

CtkA – Cell Translocating Kinase A

CTLA-4 – Cytotoxic T lymphocyte Antigen 4

DC – Dendritic Cell

DC-SIGN - DC-Specific Intercellular adhesion molecule-3-Grabbing Non-integrin

DNA – Deoxyribonucleic Acid

DupA – Duodenal Ulcer Promoting gene A

EAE – Experimental Autoimmune Encephalomyelitis

EDTA - Ethylenediaminetetraacetic acid

ELISA – Enzyme-Linked Immuno-Sorbent Assay

FACS – Fluorescence and Cell Sorting

FCS – Fetal Calf Serum

FISH - Fluorescence *in Situ* Hybridization

FMO – Fluorescence-Minus-One

Foxp3 – Forkhead Box P3

GA – Gastric Adenocarcinoma

GAPDH - Glyceraldehyde 3-Phosphate Dehydrogenase

GFP - Green Fluorescent Protein

GGT – Gamma-Glutamyl Transpeptidase

GI – Gastro-Intestinal

GORD – Gastro-Oesophageal Reflux Disease

HBD – Human Beta Defensin

HLA-DR – Human Leukocyte Antigen – antigen D Related

HO-1 - Heme Oxygenase-1

*Hp*SA – *Helicobacter pylori* Stool Antigen test

HRP – Horse Radish Peroxidase

IDA – Iron-Deficiency Anaemia

IFN-γ – Interferon gamma

Ig – Immunoglobulin

IKK – IκB kinase

IL – Interleukin

ITK – Interleukin-2-inducible T cell

iTreg – Induced Regulatory T cell

JAK – Janus kinase

Kb – Kilobase

KDa – Kilo Dalton

LAG3 – Lymphocyte Activation Gene 3 protein

$Le^b$ – Lewis blood group B

LPS – Lipopolysaccharide

µg – Micrograms

µl – Microlitres

MARCH-1 – Membrane-Associated RING-CH-1

MHC – Major Histocompatibility Complex

MIC – Minimum Inhibitory Concentration

MGE – Mobile Genetic Element

MALT lymphoma – Mucosa-Associated Lymphoid Tissue lymphoma

ml – Millilitres

MS – Multiple Sclerosis

MyD88 - Myeloid Differentiation primary response 88

MZ – Marginal Zone

NADPH - Nicotinamide Adenine Dinucleotide Phosphate

NDDC – Nottingham Digestive Diseases Centre

NFAT- Nuclear Factor of Activated T cells

NF-κB – Nuclear Factor Kappa light chain enhancer of activated B cells

NHPH – Non-*H. pylori Helicobacter*

NKT cells – Natural Killer T cells

NLR – NOD-Like Receptor

NO – Nitric Oxide

NOD1 - Nucleotide-binding Oligomerization Domain-containing protein 1 receptor

NS – Not Significant

NSAID – Non-Steroidal Anti-Inflammatory Drug

nTreg – Natural Regulatory T cell

OipA – Outer Inflammatory Protein A

O.D. – Optical density

PAMP – Pathogen Associated Molecular Pattern

PBA – PBS-containing 20% sodium azide

PBS - Phosphate Buffered Saline

PBMC – Peripheral Blood Mononuclear Cell

PCR – Polymerase Chain Reaction

PMA - Phorbol Myristate Acetate

PPI – Proton Pump Inhibitor

PRR – Pattern Recognition Receptor

PUD – Peptic Ulcer Disease

PZ – Plasticity Zone

qPCR – Qualitative Polymerase Chain Reaction

RIG-1 - Retinoic acid-Inducible Gene 1

RLR – RIG-1-Like Receptor

RNS – Reactive Nitrogen Species

RPM – Revolutions per Minute

RPMI – Roswell Park Memorial Institute

RT-PCR – Real Time-Polymerase Chain Reaction

RUT – Rapid Urease Test

SabA - Sialic Acid-Binding Adhesin

SEM – Scanning Electron Micrograph

S/M/I – Signal, Mid, Intermediate region of VacA

STAT – Signal Transducer and Activator of Transcription protein

TIM-1 - T cell Ig domain and Mucin domain protein 1

T2-MZP – Transitional 2 Marginal-Zone Precursor

T4SS – Type IV Secretion System

Th – Helper T $CD4^+$ lymphocyte

TLR – Toll-Like Receptor

TNF-α – Tumour Necrosis Factor alpha

TPM - Tyrosine Phosphorylation Motif

Treg – Regulatory T cell

Tresp – Responder T cell

UBT – Urease Breath Test

V - Volts

VacA – Vacuolating Cytotoxin A

WHO – World Health Organisation

## List of tables


| No. | Table description | Page |
|---|---|---|
| 1.1 | UK guidelines for *H. pylori* eradication therapy regimes. | 8 |
| 1.2 | A comparison of natural and induced regulatory T cells. | 26 |
| 1.3 | Treg markers in mice and humans. | 29 |
| 1.4 | Markers for Breg subsets in mice, and their functions. | 38 |
| 1.5 | Markers for Breg subsets in humans, and their functions. | 38 |
| 1.6 | Different Breg subsets and their features. | 39 |
| 2.1 | Clinical characteristics of patients recruited to the Treg eradication study. | 53 |
| 2.2 | Total blood samples collected in the Treg eradication study so far, at *H. pylori* diagnosis (Month 0) and a series of time points over 24 months after *H. pylori* eradication therapy. | 55 |
| 2.3 | *H. pylori* isolates incorporated into the whole cell lysate antigen, which was used to stimulate PBMCs *in* vitro. | 56 |
| 2.4 | The properties of fluorochromes used in the flow cytometry panel for the Treg eradication study. | 58 |
| 2.5 | Fluorochrome-conjugated antibodies detecting markers expressed by human regulatory T lymphocytes. | 59 |
| 3.1 | The properties of fluorochromes used in the flow cytometry panel for the pilot study. | 85 |
| 3.2 | Panel of antibodies used to identify mouse splenic populations of regulatory B cells. | 86 |
| 3.3 | Panel of antibodies used to identify mouse splenic populations of regulatory T cells. | 86 |
| 4.1 | Clinical characteristics of patients recruited to the Breg/Treg study. | 113 |
| 4.2 | The properties of fluorochromes used in the flow cytometry panel for this study. | 114 |
| 4.3 | Fluorochrome-conjugated antibodies used to detect markers expressed by human Bregs and Tregs. | 116 |
| 4.4 | The relative brightness index of various fluorophores where 1 represents the dimmest dyes, and 5 represents the brightest dyes. | 121 |
| 4.5 | Optimised panel of fluorochrome-conjugated antibodies used to detect markers expressed by human Bregs and Tregs. | 123 |
| 5.1 | Virulence factor properties in *H. pylori* SS1 wild-type and mutant strains. | 150 |
| 5.2 | Fluorochrome-conjugated antibodies used to detect markers expressed by mouse regulatory B and T lymphocytes in spleen. | 151 |
| 5.3 | Fluorochrome-conjugated antibodies used to detect markers expressed by mouse B and T lymphocytes in blood. | 153 |
| 6.1 | Types of antibiotics used in eradication therapy for *H. pylori* infection, and the bacterial polymorphisms associated with resistance. | 194 |

| | | |
|---|---|---|
| 6.2 | The results of *H. pylori* tests and the *H. pylori* status of patients undergoing an endoscopy at QMC, who consented to contribute to the *H. pylori* stool study. | 201 |
| 6.3 | Strains of *H. pylori* used as genomic DNA positive controls for stool-based PCR. | 202 |
| 6.4 | Primers used to amplify *H. pylori* specific genes in stool-based PCR, and their corresponding thermo-cycling conditions. | 204 |
| 6.5 | A comparison of tested stool DNA extraction kits and the average quality and quantity of purified DNA. | 207 |
| 6.6 | The *H. pylori* status of patients in the stool study, and the concentrations of DNA extracted from 0.2-0.5g of their donated stool samples. | 208 |
| 6.7 | Matching patients' *H. pylori* status with the resulting *H. pylori 16S* rRNA gene stool PCR result to determine the accuracy of the typing method. | 214 |

## List of figures


| No. | Figure description | Page |
|---|---|---|
| 1.1 | A coloured scanning electron micrograph (SEM) image of the *Helicobacter pylori* bacterium. | 2 |
| 1.2 | The mechanisms by which *H. pylori* can cause gastric and duodenal ulcers in the human host. | 4 |
| 1.3 | Intracellular signalling pathways induced by the injection of *H. pylori* CagA into gastric epithelial cells. | 13 |
| 1.4 | The vacuolation of rabbit kidney (RK13) cells by membrane vesicles containing active *H. pylori* VacA. | 16 |
| 1.5 | Combinations of the three regions of variation: signal (s), mid (m) and intermediate (i) regions in *vacA*, and the associated risks of future disease. | 18 |
| 1.6 | Signalling pathways induced by interleukin 10 (IL-10) upon binding to its receptor in various immune cells *in vivo*. | 32 |
| 1.7 | The regulatory B cell and its mechanisms in suppressing pro-inflammatory immune responses through the release of IL-10, TGF-β and IL-35. | 41 |
| 1.8 | Contact-mediated immunosuppressive mechanisms of Breg cells. | 42 |
| 1.9 | Representative flow cytometry plots and gating strategy schemes of $CD19^{+}CD1d^{hi}CD5^{+}$ Bregs from mouse splenic lymphocytes. | 43 |
| 1.10 | Representative flow cytometry plots and gating strategy schemes of $CD19^{+}CD24^{+/hi}CD38^{+/hi}$ Bregs from human peripheral blood samples. | 44 |
| 1.11 | Characteristics of Bregs and Tregs, their interactions, and their described roles in the context of *H. pylori* infection for mice and humans. | 46 |
| 2.1 | Protocol for patient recruitment to the Treg eradication study, and subsequent time points for blood donations. | 54 |
| 2.2 | Representative flow cytometry plots, the gating scheme, and subsequent analysis of $CD4^{+}CD25^{hi}$ T lymphocytes. | 62 |
| 2.3 | Representative flow cytometry plots, the gating scheme, and subsequent analysis of $CD4^{+}Foxp3^{+}$ T lymphocytes. | 63 |
| 2.4 | Representative flow cytometry plots and the gating analysis scheme for the analysis of $CD4^{+}CD25^{hi}Foxp3^{+}$ Treg lymphocytes. | 64 |
| 2.5 | Proportions of $CD4^{+}CD25^{hi}Foxp3^{+}$ Treg lymphocytes in PBMCs from patients treated for *H. pylori* infection. | 65 |
| 2.6 | Representative flow cytometry plots, gating strategy, and subsequent analysis of $CD4^{+}IL\text{-}10^{+}$ T lymphocytes. | 66 |
| 2.7 | Proportions of $CD4^{+}$ lymphocytes that are $IL\text{-}10^{+}$ in PBMCs from patients treated for *H. pylori* infection. | 67 |
| 2.8 | Proportions of $CD4^{+}CD25^{hi}IL\text{-}10^{+}$ lymphocytes in the peripheral blood of patients treated for *H. pylori* infection. | 68 |
| 2.9 | Proportions of $CD4^{+}IL\text{-}10^{+}$ lymphocytes in the peripheral blood of patients who failed eradication treatment for *H. pylori* infection. | 69 |

| | | |
|---|---|---|
| 2.10 | Proportion of $CD4^+CD25^{hi}Foxp3^+$ lymphocytes in the peripheral blood of patients who failed treatment for *H. pylori* infection. | 70 |
| 3.1 | Representative flow cytometry plots, the gating scheme, and analysis of splenic $CD19^+$ lymphocytes. | 89 |
| 3.2 | Representative flow cytometry plots, the gating scheme, and analysis of splenic $CD4^+$ lymphocytes. | 90 |
| 3.3 | Representative flow cytometry plots, the gating scheme, and analysis of the proportions of IL-$10^+$ lymphocytes in groups of mice orally dosed with *H. pylori* strain SS1 (SS1) or given plain Brucella broth (Broth). | 92 |
| 3.4 | Representative flow cytometry plots, the gating scheme, and analysis of the proportions of IL-$10^+$ lymphocytes in groups of mice orally dosed with *H. pylori* strain SS1 (SS1) or given plain Brucella broth (Broth). | 93 |
| 3.5 | Proportion of splenic IL-$10^+$ lymphocytes in groups of mice orally dosed with *H. pylori* strain SS1 (SS1), or given plain Brucella broth (Broth). | 95 |
| 3.6 | Representative flow cytometry plots and the gating analysis scheme for splenic $CD1d^{hi}CD5^+$ Bregs from mice orally dosed with *H. pylori* strain SS1 (SS1), or given plain Brucella broth (Broth). | 96 |
| 3.7 | Proportion of splenic $CD1d^{hi}CD5^+$ Bregs within the $CD19^+$ B cell population from mice orally dosed with *H. pylori* strain SS1 (SS1), or given plain Brucella broth (Broth). | 97 |
| 3.8 | Proportion of splenic IL-10-producing $CD19^+CD1d^{hi}CD5^+$ Bregs in mice orally dosed with *H. pylori* strain SS1 (SS1), or given plain Brucella broth (Broth). | 98 |
| 3.9 | Representative flow cytometry plots, gating strategy and analysis of the proportion of splenic $CD4^+Foxp3^+$ Tregs from Foxp3-GFP-transgenic mice orally dosed with *H. pylori* strain SS1 (SS1), or given plain Brucella broth (Broth). | 100 |
| 3.10 | Proportion of splenic IL-$10^+$ $CD4^+Foxp3^+$ regulatory T cells in mice orally dosed with *H. pylori* strain SS1 (SS1), or given plain Brucella broth (Broth). | 101 |
| 4.1 | Anti-Rat and Anti-Hamster Ig CompBeads labelled with fluorophore-conjugated antibodies on the Astrios flow cytometer. | 119 |
| 4.2 | Representative flow cytometry plots and the gating analysis scheme for the identification of B and T lymphocytes. | 125 |
| 4.3 | Proportion of lymphocyte frequencies amongst PMBCs collected from patients who were *H. pylori*-negative (Hp-), *H. pylori*-positive (Hp+) or had successfully eradicated their *H. pylori* infection (HpE). | 126 |
| 4.4 | Representative flow cytometry plots and gating strategy analysis of the proportion of IL-$10^+$ lymphocytes that were $CD19^+$ B cells in PBMCs from patients. | 128 |
| 4.5 | Representative flow cytometry plots and gating strategy analysis of the proportion of IL-$10^+$ lymphocytes that were $CD4^+$ T cells in PBMCs from patients. | 129 |

| | | |
|---|---|---|
| 4.6 | Proportions of peripheral blood IL-10$^+$ lymphocytes that were (A) CD19$^+$ B cells or (B) CD4$^+$ T cells. | 130 |
| 4.7 | Proportion of (A) CD19$^+$ lymphocytes that were IL-10$^+$ or (B) CD4$^+$ lymphocytes that were IL-10$^+$ in PBMCs from patients undergoing an upper GI endoscopy. | 131 |
| 4.8 | Representative flow cytometry plots and the gating analysis scheme for CD19$^+$CD24$^+$CD38$^{hi}$ Bregs from the peripheral blood of patients undergoing an endoscopy. | 133 |
| 4.9 | Proportion of peripheral blood CD24$^+$CD38$^{hi}$ Bregs within the CD19$^+$ B cell population. | 134 |
| 4.10 | Representative flow cytometry plots and the gating analysis scheme for CD4$^+$CD25$^{hi}$CD127$^{lo}$ Tregs from peripheral blood samples in patients. | 135 |
| 4.11 | Proportion of CD25$^{hi}$ events from the total CD4$^+$ T cell population in blood samples donated by patients undergoing an upper GI endoscopy. | 136 |
| 4.12 | Proportion of CD4$^+$CD25$^{hi}$ Tregs from the total CD45$^+$ lymphocyte population in blood samples donated by patients. | 136 |
| 4.13 | Proportion of IL-10-producing Bregs and Tregs in blood samples donated by patients undergoing an upper GI endoscopy. | 137 |
| 5.1 | Representative flow cytometry plots, the gating scheme, and subsequent analysis of splenic CD19$^+$ lymphocytes. | 156 |
| 5.2 | Representative flow cytometry plots, the gating scheme, and subsequent analysis of splenic CD4$^+$ lymphocytes. | 157 |
| 5.3 | Representative flow cytometry plots, the gating scheme, and subsequent analysis of the proportions of IL-10$^+$ lymphocytes in uninfected and *H. pylori*-infected groups of mice. | 159 |
| 5.4 | Representative flow cytometry plots, the gating scheme, and subsequent analysis of the proportions of IL-10$^+$ lymphocytes in uninfected and *H. pylori*-infected groups of mice. | 160 |
| 5.5 | Representative flow cytometry plots and the gating analysis scheme for splenic CD1d$^{hi}$CD5$^+$ Bregs from mice orally dosed with *H. pylori*. | 162 |
| 5.6 | Proportion of splenic CD1d$^{hi}$CD5$^+$ Bregs within the CD19$^+$ B cell population in mice. | 163 |
| 5.7 | Proportion of splenic IL-10-producing CD1d$^{hi}$CD5$^+$ Bregs within the CD19$^+$ B cell population in mice. | 164 |
| 5.8 | Representative flow cytometry plots and the gating analysis scheme for splenic CD25$^{hi}$Foxp3$^+$ Tregs from mice orally dosed with *H. pylori*. | 165 |
| 5.9 | Proportion of splenic CD25$^{hi}$Foxp3$^+$ Tregs within the CD4$^+$ T cell population in mice. | 166 |
| 5.10 | Proportion of splenic IL-10-producing CD25$^{hi}$Foxp3$^+$ Tregs within the CD4$^+$ T cell population in mice. | 167 |
| 5.11 | Representative flow cytometry plots, the gating scheme, and subsequent analysis of CD19$^+$ lymphocytes in mouse blood. | 169 |
| 5.12 | Representative flow cytometry plots and the gating analysis scheme for CD3$^+$, CD4$^+$ and CD8$^+$ lymphocytes in mouse blood. | 170 |
| 5.13 | Proportion of T cells amongst peripheral blood lymphocytes in mice. | 171 |

| | | |
|---|---|---|
| 5.14 | Representative flow cytometry plots, the gating scheme, and subsequent proportions of IL-10$^{+}$ lymphocytes in uninfected and *H. pylori*-infected groups of mice. | 173 |
| 5.15 | Representative flow cytometry plots and the gating analysis scheme for proportions of IL-10$^{+}$ T lymphocytes in uninfected and *H. pylori*-infected groups of mice. | 174 |
| 5.16 | Proportion of IL-10$^{+}$ lymphocytes that are CD4$^{+}$ T cells in mouse blood. | 175 |
| 5.17 | Representative flow cytometry plots and the gating analysis scheme for proportions of peripheral blood IL-10$^{+}$ T lymphocytes in uninfected and *H. pylori*-infected groups of mice. | 176 |
| 5.18 | Proportion of IL-10-producing CD8$^{+}$ T cells in peripheral blood lymphocytes from mice. | 177 |
| 5.19 | Representative flow cytometry plots and the gating analysis scheme for peripheral blood CD1d$^{hi}$CD5$^{+}$ Bregs in mice. | 178 |
| 5.20 | Representative flow cytometry plots, the gating scheme, and the analysis of the proportion of Foxp3$^{+}$ peripheral blood Tregs in mice. | 179 |
| 5.21 | Proportion of CD4$^{+}$Foxp3$^{+}$ Tregs producing IL-10 within the peripheral blood lymphocyte population in mice. | 180 |
| 5.22 | The *ex vivo* suppression capacity of splenic Tregs after *H. pylori* infection in mice. | 181 |
| 6.1 | Agarose gel of *H. pylori 16S* rRNA gene PCR products from a dilution series of DNA extracted from stool sample 779. | 210 |
| 6.2 | Agarose gel separation of *H. pylori 16S* rRNA gene PCR products from DNA extracted from stool sample #764. | 211 |
| 6.3 | Agarose gel separation of *H. pylori 16S* rRNA gene PCR products from DNA extracted from stool samples. | 212 |
| 6.4 | Agarose gel separation of *H. pylori 16S* rRNA gene PCR products from DNA extracted from stool samples. | 213 |
| 6.5 | Agarose gel separation of *H. pylori 16S* rRNA gene PCR products from DNA extracted from *H. pylori*-negative stool samples. | 214 |
| 6.6 | *H. pylori 16S* rRNA gene sequence analysis, comparing stool DNA to those from the corresponding *H. pylori* isolate genomic DNA. | 216 |
| 6.7 | Agarose gel separation of *H. pylori vacA* s-region gene PCR products from DNA extracted from stool sample #764. | 220 |

## Chapter 1: Introduction to *Helicobacter pylori* infection

### 1.1 General background

*Helicobacter pylori* (*H. pylori*) is a Gram-negative bacterium which has adapted to reside in microaerophilic conditions[1]. This is ideal for its colonisation within the human gastric mucosa, where it has co-adapted alongside humans for at least a hundred thousand years[2 3].

Due to the strong gastric acid produced by parietal cells, the human stomach was previously thought to be a sterile organ. The discovery of *H. pylori*, and the subsequent research performed identified how the bacterium is uniquely equipped to survive and thrive in this harsh environment.

15% of total protein expression by the bacterium is the enzyme urease[4 5]. This catalyses the hydrolysis of urea from interstitial fluid into ammonia, which surrounds the bacterial cell and acts as a buffer to neutralise the gastric acid[6]. Furthermore, the cluster of polar flagella present on *H. pylori* can propel the bacterium through the mucus gel which covers gastric epithelial cells and protects the host tissue from acid erosion[5].

In 1991, the World Health Organisation (WHO) listed *H. pylori* as a Class 1 carcinogen, meaning that there is sufficient evidence correlating *H. pylori* infection to the incidence of cancer in humans[7]. Originally classified as *Campylobacter pylori* due to its presence in the body of the human stomach (the pylorus), *16S* rRNA sequencing ultimately proved it to belong to a novel genus[8]. Its current name, *Helicobacter pylori*, reflects its rod-like and helical nature shown (**Figure 1.1**).



**Figure 1.1:** A coloured scanning electron micrograph (SEM) image of the *Helicobacter pylori* bacterium. Image use authorised by Juergen Berger/Science Photo Library[9]

*H. pylori* is one of the most prevalent human pathogens as it is present in almost half of the world's population[10]. The majority of infections begin in childhood and persist throughout life. It is exclusively a human pathogen. Transmission requires a close person-to-person contact; it most likely occurs through the faecal-oral route, but possibly oral-oral, vomito-oral or via the inhalation and ingestion of aerosolised bacteria[11].

Individuals are more likely to be colonised with the same strain as their close family members. It has been suggested that, within families in developed countries, crowded living conditions and poor socioeconomic status may also associate close person-to-person transmission with an increased incidence of *H. pylori* infection[5].

## 1.2 Association between *H. pylori* and disease

While the majority of infected individuals remain asymptomatic (85%), the pathogenic effect of *H. pylori* were first demonstrated in 1983, when an Australian gastroenterologist, Barry Marshall, deliberately ingested a culture of the bacterium and developed gastritis (inflammation of the stomach lining) three days later[12]. Previously, pathologist Robin Warren noticed that gastric biopsies from patients with gastritis contained curved bacteria. Together, their discovery was of critical importance for the treatment of ulcers. In 2005, Marshall and Warren were awarded a Noble Prize, in recognition of their work in this field.

Dyspepsia, which is pain within the stomach, is a common symptom of gastritis. It is estimated that 5% of individuals suffering from dyspepsia have symptoms linked to *H. pylori* infection[13]. Patients who present with chronic dyspepsia are referred for an upper Gastro-Intestinal (GI) endoscopy, should first-line treatments in primary care not resolve their symptoms. Upper GI endoscopy procedures are an exploratory examination, used to identify any abnormalities within the oesophagus, stomach and gastro-duodenal junction. Other symptoms which necessitate an endoscopy include persistent vomiting, weight loss, gastrointestinal bleeding, gastric reflux (heartburn), and iron-deficiency anaemia (IDA) (a tell-tale sign of pathology, particularly for men and post-menopausal women). *H. pylori*-induced ulcers and stomach cancer can cause bleeding from the mucosal lining, which can lead to anaemia[14].

### 1.2.1 Ulceration

Marshall and Warren were the first to propose a causative link between *H. pylori* infection and the development of chronic inflammation to cause peptic ulcer disease (PUD)[12]. An ulcer is where an open sore can form from a break in the mucosal lining. This usually takes place in the lesser curvature of the stomach as a gastric ulcer, or in the small intestine as a duodenal ulcer (**Figure 1.2**). This ulceration can lead to severe complications such as internal bleeding, perforation of the ulcer, and obstruction of the normal passage of food through the GI tract[15] [16]. *H. pylori* infection is the

predominant cause of ulceration, responsible for 80-90% of gastric or duodenal ulcer cases. PUD is the most common cause of life-threatening GI bleeding[17]. Prior to *H. pylori* infection, ulcers were associated with stressful lifestyles, and patients were prescribed antacids for relief.

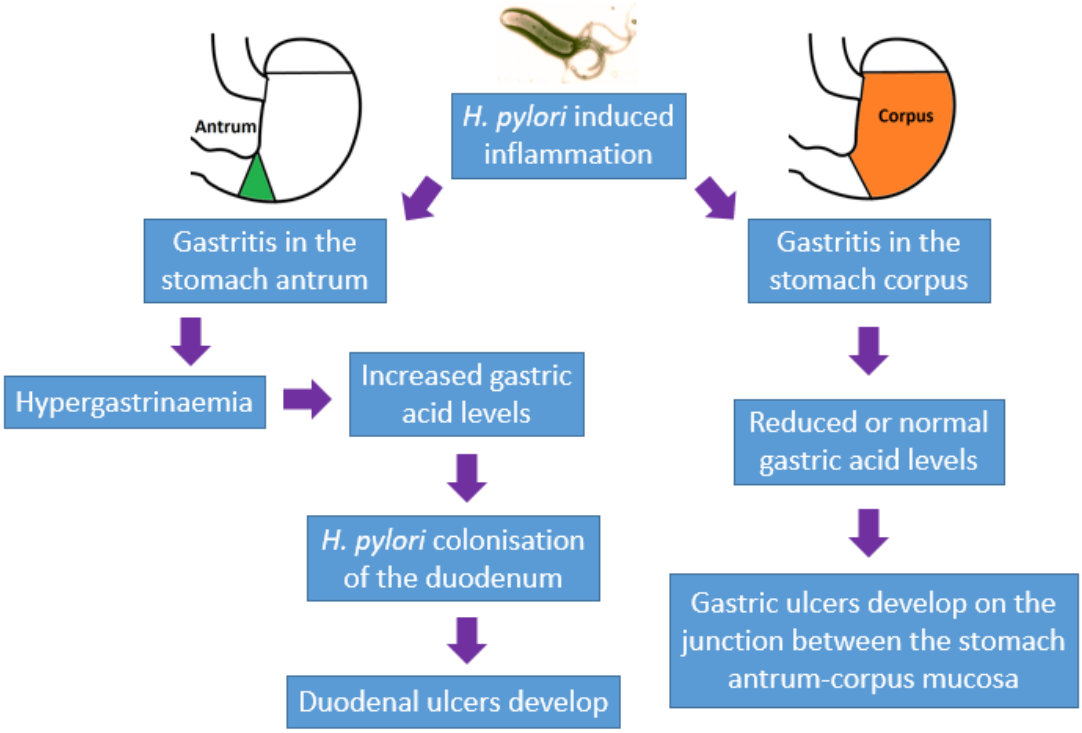



**Figure 1.2:** The mechanisms by which *H. pylori* can cause gastric and duodenal ulcers in the human host. Adapted from information provided in Atherton and Blaser[5].

### 1.2.2 Gastric MALT lymphoma

*H. pylori* infection is also associated with extranodal marginal zone lymphoma of mucosa-associated lymphoid tissue (MALT), which usually presents in the stomach. Gastric MALT lymphomas accounts for 7.6% of all Non-Hodgkin's Lymphoma cases[18], and are more likely to affect men[19]. This low-grade (slow growing) B lymphocyte cancer develops from the adaptive immune response reacting to the persistent presence of *H. pylori*. The subsequent clonal expansion of B cells after continued *H. pylori* stimulation can lead into a malignant transformation of B cells, which forms

the basis for the lymphoma[20]. After *H. pylori* eradication therapy, varying degrees of lymphoma regression have been reported[19].

### 1.2.3 Gastric adenocarcinoma

*H. pylori* infection is the most common microbial cause of human malignancy. 1-2% of infected individuals develop gastric adenocarcinoma (GA)[21-23]. *H. pylori* infection is accountable for at least 90% of GA cases[24]. *H. pylori* infection is associated with a six-fold increased risk for GA, compared to *H. pylori*-negative individuals[25]. GA is most prevalent in countries such as Korea, China, Japan, Columbia and Chile, which also have a high prevalence of *H. pylori* infection[13]. It is the fifth most prevalent type of cancer and the third most frequent cause of cancer-associated deaths worldwide[26] [27]. This may be partially attributed to a late diagnosis; 80% of diagnoses are made after stage four metastasis has already occurred. Because of this poor prognosis, there is only a 20% survival rate for patients 5 years after their primary diagnosis, despite the high standards of healthcare present in the UK[28] [29].

Although the mechanisms of cancer development are not completely understood, it is known to result from an escalating interaction of *H. pylori* with the host immune response[30]. *H. pylori* infection fulfils most of the Bradford Hill criteria for the causation of GA[13]. The current accepted model for the development of GA is that *H. pylori* infection triggers mutations in the infected stomach, which leads to a lifetime of chronic active gastritis, which can progress further into cancer[13] [31]. The gradual pathway from asymptomatic gastritis, through to atrophy, metaplasia and cancer can be clinically silent[22], which may help to explain why GA diagnoses are made at late stages so frequently.

### 1.2.4 Role of infection in extra-gastric diseases

There is a global decline of *H. pylori* infection in Western countries[3 13]. This decline is inter-generational[32]. Furthermore, the migration of parents from high risk areas mean that while their risk is maintained, their children mirror the risk of the resident population[32]. It has been suggested that this decline, combined with evolved hygiene practices, socio-economic developments, and exposure to antibiotics from a young age may have contributed to a change in human microbial populations, and a global decline in *H. pylori* colonisation[5].

Conversely, there has been a rise in oesophageal cancer, and cases of immunopathological conditions such as gastro-oesophageal reflux disease (GORD), multiple sclerosis (MS), asthma, allergies, eczema, oesophageal cancer, and Inflammatory Bowel Disease (IBD)/Crohn's Disease[33-41]. There is controversial evidence to suggest that this rise in autoimmune conditions has been linked to the decline of *H. pylori* infection in the human stomach, where it has successfully colonised for thousands of years[34-36 42].

MS is an autoimmune condition characterised by the demyelination of the neuronal sheath in the central nervous system. It is a chronic autoimmune condition seen predominantly in women, in whose genome particular combinations of polymorphisms reinforce the likelihood of disease outcomes[43 44]. In a mouse model for MS, *H. pylori* infected mice showed reduced symptoms of disease severity[33]. In humans, female *H. pylori*-sero positive MS patients also had a reduced disability score compared to sero-negative women[38]. This association was corroborated further in multiple studies, demonstrating a reduced prevalence of *H. pylori* infection in MS patients, compared to healthy individuals[33 38 45]. This protective effect of *H. pylori* infection may be linked to Vitamin D levels. This vitamin, of whose deficiency is linked to the development of autoimmunity, has been noted to be lower in patients with MS[46]. Recently, *H. pylori*-infected individuals have been shown to have an upregulated expression of the Vitamin D receptor[47].

Asthma is a long-term inflammation of the bronchial tubes of the upper respiratory tract. Approximately 5% of asthmatics suffer from severe asthma which cannot be sufficiently controlled with current medicines. Additionally, 3 people die every day from asthma attacks[48]. Research in neonatal mouse models demonstrated that infecting mice with *H. pylori* protected them from asthma-specific inflammatory processes such as airway hyperrresponsiveness and goblet cell metaplasia when challenged with allergens[39]. This protection was revoked upon the successful eradication of *H. pylori* infection with antibiotics. The presence of *H. pylori* infection in children aged 3-13 was also inversely associated with asthma diagnosis in a cross-sectional study of 7000 individuals[42]. The different manifestations of asthma were enquired about in questionnaires given to guardians of the patients. Wheezing, which is an important clinical symptom of asthma, was inversely associated with a positive *H. pylori* infection status.

Allergy and asthma are often seen as clinically related as the presence of an allergen can also trigger an asthma attack. Allergies to the 'big 8' (milk, fish, eggs, crustacean shellfish, tree nuts, peanuts, wheat and soybean) can have fatal consequences if not treated rapidly. A recent paper describes a modest protection by *H. pylori* against anaphylaxis in a peanut allergy in a mouse model. *H. pylori* infection resulted in a lower anaphylaxis score and a reduced immunoglobulin (Ig) G1 antibody response when challenged[40]. *H. pylori* infection has also been associated with protection against allergies in humans. In *H. pylori*-positive children, there was an inverse correlation between infection and the presence of allergic rhinitis[42]. *H. pylori*-positive Ethiopian children aged 3-5 were also less likely to have eczema[41]. Studying peripheral blood in *H. pylori*-positive adult patients also showed a decreased IgE antibody response, which is a key component of allergy inflammation, compared to *H. pylori*-negative patients[37].

Gastro-intestinal diseases such as IBD, GORD, Coeliac and oesophageal cancer have also been described in the literature as being inversely correlated to *H. pylori* infection[24 34-36 49]. *H. pylori* eradication is still a current recommended clinical outcome, regardless of the presence of such conditions[24]. Although some of the

studies describing a connection between *H. pylori* and atopic conditions can be underpowered, and does not identify a cause and effect, the rise in atopic diseases provides interesting questions on the nature of *H. pylori* infection in humans[34]. It is a curious phenomenon that extra-gastric protection potentially induced by *H. pylori* infection is associated with the most virulent colonising strains[37 40 49 50].

## 1.3 Current treatment

After *H. pylori* infection is diagnosed, a front-line regime of a triple drug eradication therapy is prescribed (**Table 1.1**). This includes two antibiotics and a proton pump inhibitor (PPI). If this fails to clear the infection, subsequent second and third line treatments are prescribed[24 51]. The PPI inhibits the production of gastric acid, causing the pH of the stomach to rise, creating an environment less conducive to *H. pylori* colonisation and replication. In this state, the bacterium is more susceptible to antibiotics[24] as the minimum inhibitory concentration (MIC) of the combined antibiotics against *H. pylori* is reduced in this PPI-altered background[52].

**Table 1.1**: UK guidelines for *H. pylori* eradication therapy regimes.

| Treatment regime | Drug | Concentration | Dosage | Length |
|---|---|---|---|---|
| Front line | Amoxicillin<br>Clarithromycin<br>Omeprazole | 1g<br>500mg<br>20mg | Twice daily | 7 days |
| Second line | Tetracycline<br>Metronidazole<br>Omeprazole<br>Bismuthate | 500mg<br>400mg<br>40mg<br>120mg | Four times a day<br>Three times a day<br>Twice daily<br>Four times a day | 14 days |
| Third line | Amoxicillin<br>Levofloxacin<br>Omeprazole | 1g<br>500mg<br>40mg | Twice daily | 10 days |

There is a growing global prevalence of *H. pylori* resistance to the antibiotic clarithromycin[53]. A resistance rate over 15% in a region has been suggested as a benchmark for high resistance. In Japan and Italy, a resistance rate of 30% has been

reported, and as such, clarithromycin is no longer recommended in those countries[24]. Metronidazole resistance is another problem impairing the success of eradication therapy, but this can currently be overcome by increasing the dose and duration of its use[24]. However, second and third line treatments can also have adverse effects – metronidazole is listed by WHO as a possible carcinogen to humans[7].

The widespread use of antibiotics including amoxicillin and metronidazole drives the selection of resistant strains. *H. pylori* has a large genome, with plasticity zones (PZ) that are less conserved compared to the rest of the genome. These have been associated with horizontal gene transfer and so are a hot spot for emerging antibiotic resistance genes[54]. The use of triple-therapy treatment propagates resistance already rampant in *H. pylori* strains, thus reducing the future efficacy of eradication therapy.

The increasing resistance of *H. pylori* to eradication therapy is not the only concern. This regime may be difficult for patients to comply with, particularly those on poly-pharmacy for other co-morbidities. This treatment also may not immediately relieve the patient of their complex symptoms[55]. Additionally, the reporting of adverse effects from treatment (with the most frequently described being diarrhoea and vomiting) may deter patients from complete compliance with their prescription[24]. However, these incidents have not been severe enough to warrant stopping the treatment. Following second-line and subsequent therapies, adverse events such as hepatotoxicity are more serious[13]. Other reasons for eradication failure include a resistance to clarithromycin and other antibiotics, a high bacterial load, a low gastric pH, and environmental factors such as smoking and drinking alcohol[55].

## 1.4 Factors that influence disease outcomes

### 1.4.1 Environmental factors

While *H. pylori* infection is the predominant risk factor for PUD and GA, the influence of environmental factors on the infected mucosa must be identified. Prior work has shown that when individuals migrate from an area of high GA risk, they maintain their

risk after migration, but their children's risk of GA starts to match the local population[56], highlighting the importance of understanding environmental effects. Older people and men are more likely to be infected with *H. pylori*, and its associated diseases[5 57]. A link between lifestyle choices and GA is contentious in *H. pylori* literature. Alcohol consumption has even been suggested by some to be weakly protective against infection[58 59]. A diet high in salt intake, such as in those who use salt as a means of food preservation, is suggested to be a factor in the development of cancer in infected individuals[56 60 61]. Cigarette use has been shown to increase the likelihood of ulceration; ulcers that may also be problematic to heal are more likely to recur in smokers[62]. Moreover, smoking increases the likelihood of eradication therapy failure[63], thus elevating *H. pylori* exposure to antibiotics. Smoking can reduce the efficacy of antibiotics to the gastric mucosa via reduced blood flow and mucus secretion and increased acid secretion[63].

### 1.4.2 Virulence factors

#### 1.4.2.1 CagPAI and CagA

The *cag* Pathogenicity Island (*cag*PAI) is a 40 kilobase (kb) mobile genetic element (MGE)[1], which is comprised of almost 30 genes. 17 of these genes encode a Type IV Secretion System (T4SS)[64]. The T4SS may be present in an active form, disrupted and inactive in a truncated form, or absent entirely, but is most frequently present and functional[5]. *cag*PAI is flanked by Deoxyribonucleic acid (DNA) repeats, and when the island is absent in a colonising strain, only one copy of these repeats is present[65]. *cag*PAI was acquired by *H. pylori* at some point in its evolution, and inserted into the glutamate racemase gene[56]. The T4SS can be observed microscopically as a rigid needle[66] that translocates proteins from the bacterial cytoplasm into the host epithelial cells[5].

A functional CagPAI T4SS induces the downregulation of human beta-defensin 1 (HBD) (an antimicrobial peptide) in infected mucosa by influencing Nuclear Factor Kappa light chain enhancer of activated B cells (NF-κB) signalling[67]. The CagY protein,

which is stable in the acidic gastric environment, coats the pilus structure of the T4SS. *H. pylori* T4SS is an immune evasion mechanism, because it is antigenically variable, making it difficult to develop antigen-specific responses against it[5]. At the tip of the T4SS is the CagL protein which interacts with gastric epithelial cells, and promotes the expression of $\alpha_5\beta_1$ integrin receptor on the host epithelial cell surface[64], which activates the chemokine interleukin (IL) 8[68].

Cytotoxin-associated Antigen A (CagA) is the effector protein which is injected into host cells by CagPAI, and triggers intracellular signalling mechanisms. CagL and $\alpha_5\beta_1$ signalling is required for CagA translocation[68]. There are no homologs of CagA in other *Helicobacter* species, or in other bacteria, suggesting a specific niche for this toxin in the infected human stomach[65].

Injected CagA is treated as a signalling molecule by the host cell. CagA is activated by phosphorylation of its tyrosine phosphorylation motifs (TPMs) by Src family kinases or Abelson murine leukemia viral oncogene homolog 1 and 2 (Abl) kinases[5]. This phosphorylated protein then interacts with Src Homology Phosphatase 2 (SHP-2) and CSK kinase and induces a signalling cascade promoting a morphological change in the gastric epithelial cell cytoskeleton[30]. CagA can induce the 'hummingbird phenotype' in gastric cells after attachment, causing a characteristic elongation of cells[69]. After CagA phosphorylation, SHP-2 and Grb2 signalling can activate the RAF/MEK/ERK pathway to also increase cell proliferation. CagA can also activate NF-κβ as a transducing mechanism via ERK, and thereby promote the transcription of pro-inflammatory cytokines such as IL-8[5].

Unphosphorylated CagA can also interact with E-cadherin. When E-cadherin binds with CagA over its β-catenin ligand, there is an accumulation of β-catenin in the host cell. The β-catenin functions as part of the Wnt signalling pathway. An overexpression of this protein leads to its translocation into the nucleus where it may transcribe potentially oncogenic genes such as *cdx1*, which encodes the differentiation of intestinal cells and upregulates Mucin 2 expression. Both are markers of intestinal metaplasia, which is pre-clinical oncology associated with *H. pylori* infection[1 68].

Furthermore, CagA has been implicated in MALT lymphoma, where it can inhibit the apoptosis of B cells by downregulating p53[70]. It is in part due to these effects that CagA is labelled as a bacterial oncoprotein[68]. The signalling cascades induced by the injection of CagA into host cells are summarised below (**Figure 1.3**).

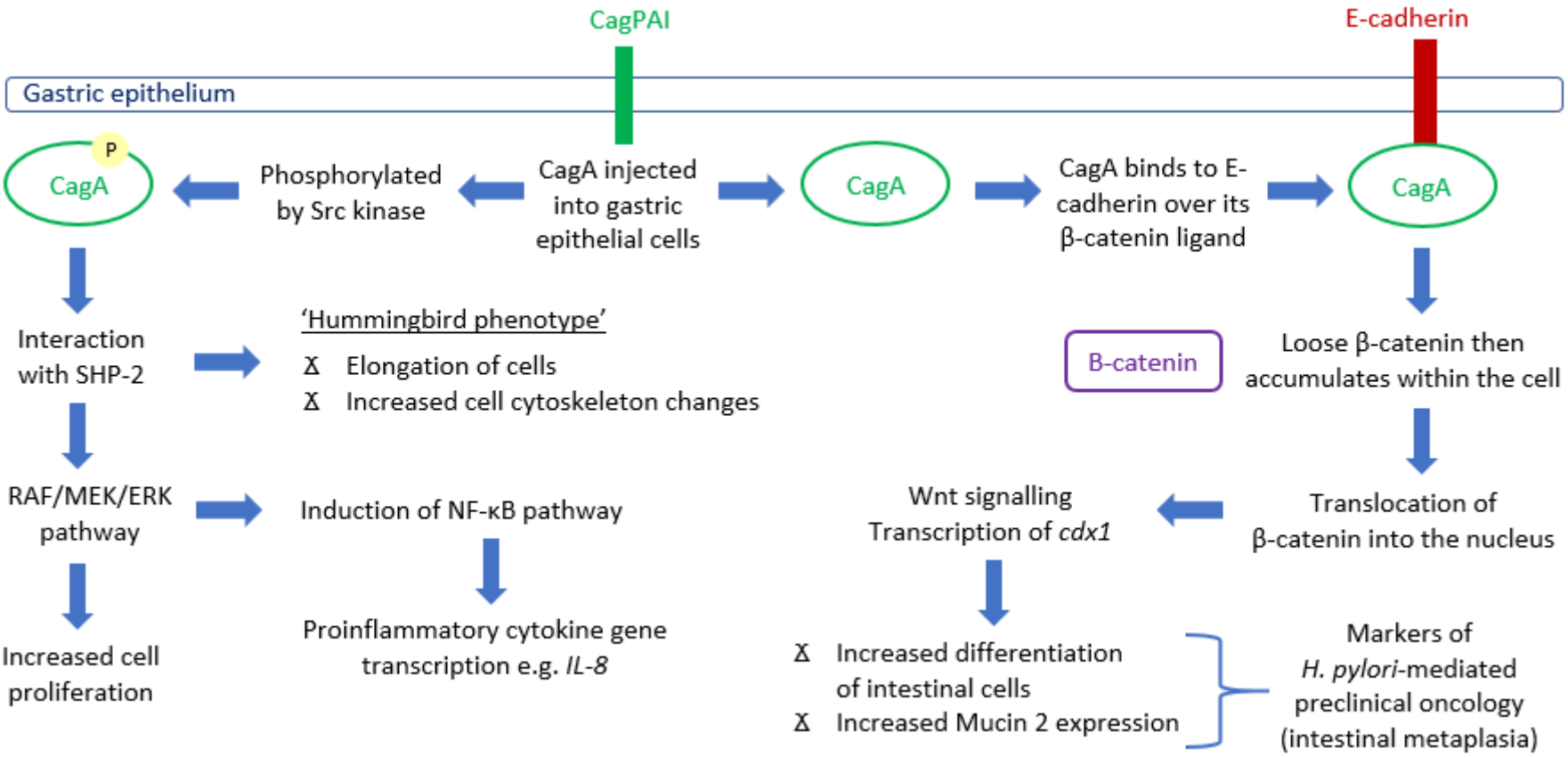

CagPAI
E-cadherin
Gastric epithelium
P
CagA
Phosphorylated by Src kinase
CagA injected into gastric epithelial cells
CagA
CagA binds to E-cadherin over its β-catenin ligand
CagA
Interaction with SHP-2
'Hummingbird phenotype'
Elongation of cells
Increased cell cytoskeleton changes
B-catenin
Loose β-catenin then accumulates within the cell
RAF/MEK/ERK pathway
Induction of NF-κB pathway
Wnt signalling
Transcription of cdx1
Translocation of β-catenin into the nucleus
Increased cell proliferation
Proinflammatory cytokine gene transcription e.g. IL-8
Increased differentiation of intestinal cells
Increased Mucin 2 expression
Markers of H. pylori-mediated preclinical oncology (intestinal metaplasia)

**Figure 1.3:** (Overleaf) Intracellular signalling pathways induced by the injection of *H. pylori* CagA into gastric epithelial cells. CagA; Cytotoxin-associated gene A, SHP-2; Src Homology Phosphatase 2, NF-κB; Nuclear Factor Kappa light chain enhancer of activated B cells, IL-8; Interleukin 8.

*H. pylori*-positive patients with GA have a 2-fold likelihood of being infected with a CagA-positive strain, compared with a CagA-negative strain[71]. There is also a higher colonisation density associated with CagA-negative genotypes[5]. Because the presence of CagA is associated with an increased risk in disease outcomes, *H. pylori* strains can be categorised by the presence or absence of this virulence factor. 60% of Western strains, and almost all East Asian strains express this gene[72].

However, there are polymorphic differences in the *cagA* gene from different strains around the world. CagA has varying numbers and types of TPMs, which in turn, affect the correlation to future risk of disease. These TPMs, made of repeating glutamic acid (E), proline (P), isoleucine (I), tyrosine (Y) and alanine (A) form distinct EPIYA motifs A, B, C and D. These are grouped under Western strains (A, B and C), or East Asian strains (A, B and D) [5]. EPIYA-D motifs have the strongest affinity for SHP-2, so that East Asian strains expressing CagA produce more inflammation and atrophy[1 73]. East Asian strains have a D-type TPM also have the strongest association with GA, compared to less-active TPMs found in Western strains[5].

#### 1.4.2.2 Vacuolating cytotoxin A (VacA)

Vacuolating cytotoxin A (VacA) is a multi-functional protein produced by *H. pylori*. VacA can be present on the surface of *H. pylori*, secreted as a monomer, but can also be present in *H. pylori* membrane vesicles directed to gastric epithelial cells. The quantity of VacA in these membrane vesicles depends on the *H. pylori* strain[74]. During secretion as a monomer, the precursor 140 kilo Dalton (kDa) protein undergoes N terminus and C terminus cleavage to form an 88 kDa protein[1 72]. VacA is composed of two subunits, P33 and P55. P33 in the N-terminus is necessary for vacuolation, and P55 is present in the C-terminus for VacA to bind to target gastric epithelial cells[75].

VacA forms hexameric anion-selective channels in biological membranes[72 76]. When activated by low pH conditions, as seen in a normal gastric environment, VacA promotes the diffusion of urea from the host cell interstitial fluid into *H. pylori* through the anion-selective channels[1 77]. This urea is converted by *H. pylori* urease into ammonium ions, to act as a buffer against gastric acid in the stomach. It is a mark of the importance of VacA to the colonisation of *H. pylori* in the stomach that nearly all strains of *H. pylori* have the *vacA* gene in their genome, and protein expression is almost ubiquitous[56 78]. Additionally, VacA has no equivalent protein in other bacterial or eukaryotic species[56 79], suggesting a unique niche for *H. pylori* in the acidic stomach.

Notably, VacA has been shown to cause mitochondrial damage which induces apoptosis in host cells. VacA reduces the electrical potential for the mitochondrial transmembrane, releasing cytochrome c, which is an early event in the cascade to cell apoptosis[72 76].

VacA was named according to the characteristic vacuolation that it induces in host epithelial cells (**Figure 1.4**). Vacuolation alone is not sufficient to induce cell death, as vacuolated cells are viable enough to exclude Trypan Blue. However, there are secondary consequences to VacA activity[80]. A full list of reported VacA functions has been reviewed previously, but the authors suggest that it is difficult to distinguish between direct effects of VacA, and secondary consequences to VacA activity on the cell[72]. This further highlights that the host signalling pathways induced by *H. pylori* VacA are still not fully understood[1].

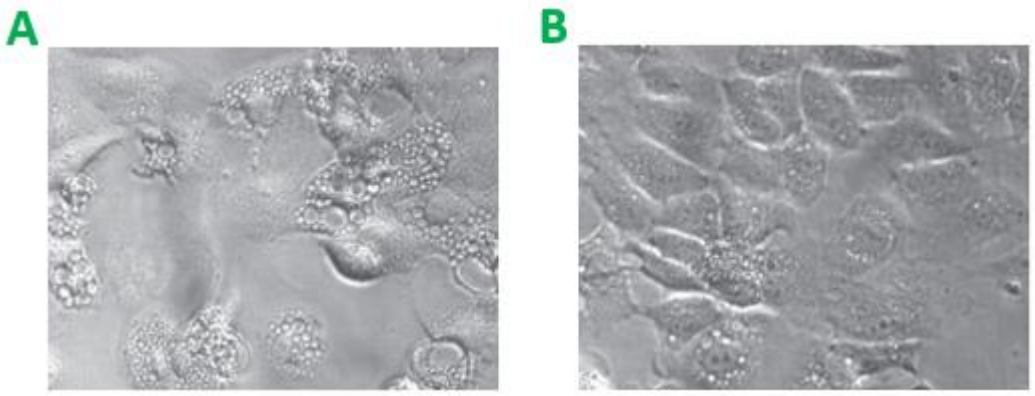



**Figure 1.4:** The vacuolation of rabbit kidney (RK13) cells by membrane vesicles containing active *H. pylori* VacA. RK13 cells were incubated for 4 hours with (A) membrane vesicles containing active VacA from *H. pylori* strain 60190 or (B) membrane vesicles containing VacA with impaired vacuolation activity from *H. pylori* strain SS1. Taken from Winter *et al.*[74].

VacA is a polymorphic protein; three regions of variation are found within its amino-terminus[1]. Each of these three regions have at least two known variants (**Figure 1.5**). The signal (s) region encodes the signal peptide, and possesses an s1 and s2 variant[81]. *H. pylori* strains expressing the s1 variant of VacA are more virulent, because this hydrophobic cleavage site can integrate more easily into the membrane of the host cell, compared to s2. *H. pylori* strains which express the s2 variant have an extension of twelve amino acids, which reduces vacuolation activity[81], decreasing the damage done to gastric epithelial cells.

The mid (m) region has an influence on *H. pylori* tropism[81]. *H. pylori* strains expressing an m1 variant allows VacA to affect toxicity on a larger range of cells, compared to m2 (**Figure 1.5**). All combinations of the signal and mid regions can occur naturally in the bacterial genome, but strains expressing VacA$^{s1/m2}$ are less commonly expressed[82]. Western strains of *H. pylori* that express the VacA$^{s1/m1}$ variant are associated with an increased likelihood of disease outcomes, because the combination of a more accessible cleavage site (s1) with a wider host cell range (m1) means an increased level of VacA cytotoxicity[5]. VacA$^{s2/m2}$ *H. pylori* strains are non-

vacuolating, and have a decreased association with risks of PUD and GA compared to VacA$^{s1/m1}$ expressing strains[82]; they are also associated with a higher colonisation density[83].

However, variations in these two regions have limited use as markers to identify an increased risk of disease. This is because East Asian strains, most commonly found in populations with a high *H. pylori* infection rate such as Korea and Japan, have almost exclusively s1/m1 variants of VacA, but with no causal link to an increased risk of disease[5]. Moreover, s and m regions of VacA are further subdivided into s1a, s1b, s1c, m1a, m1b, m1c, the expression of which varies in individuals geographically[56].

The intermediate (i) region in *vacA*, located in-between the signal and mid regions (**Figure 1.5**), has been a relatively recent discovery[84]. All VacA$^{s1/m1}$ *H. pylori* strains possess an i1 allele, while all VacA$^{s2/m2}$ carrying strains have an i2 allele. The i1 variant is associated with a stronger vacuolation activity in gastric cells, but its function is currently unknown. The presence of an i1-variant of *vacA* in a colonising *H. pylori* strain is an independent risk factor for an increased likelihood of gastric disease[84 85], when compared to an i2-variant. Introducing the i1-allele for VacA in a *H. pylori* VacA$^{s2/m2}$ strain increased vacuolation activity in an exchange mutagenesis experiment, thus confirming it as an independent risk factor[84 86]. The i1 variant was linked to the increased development of intestinal metaplasia, a sign of irreversible atrophy[87] in mice. *H. pylori*-infected patients with an i2 VacA variant did not have any intestinal metaplasia[87]. Another i-region variant, i3, was discovered in 2010, but the biological relevance of this is yet unknown[88].

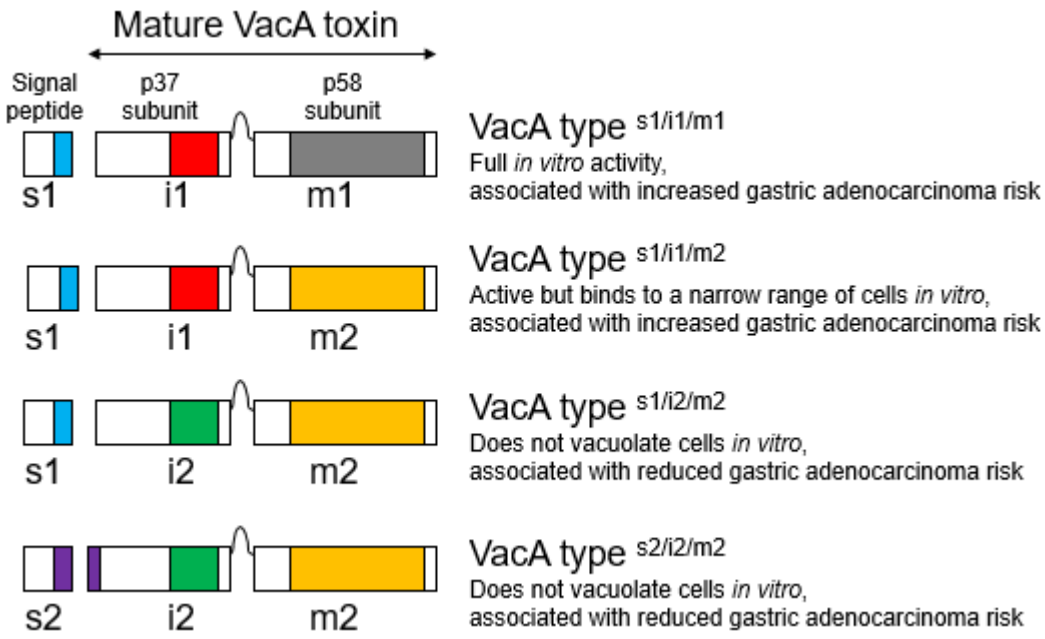



**Figure 1.5:** Combinations of the three regions of variation: signal (s), mid (m) and intermediate (i) regions in *vacA*, and the associated risks of future disease.

VacA and CagA are two of the most pathogenic virulence factors in the *H. pylori* genome. There is evidence to suggest that there may be mutual interactions, or secondary signalling effects. Both VacA and CagA interact with gastric cells to cause the accumulation of β-catenin in the WNT oncogenic pathway[1]. *In vitro* experiments with VacA and CagA show that mice infected with CagA$^{-/-}$ *H. pylori* strains had increased cellular vacuolation, while VacA$^{-/-}$ *H. pylori*-infected mice showed an increased elongation of cells (the hummingbird phenotype)[5 72 89]. This antagonistic relationship may exist to increase the lifespan of gastric cells, and help to maintain an asymptomatic infection in the stomach[89].

Conversely, these two toxins could contribute to each other's activity. Both are intracellular toxins which disrupt signalling pathways. The function of CagA in modifying the cellular cytoskeleton, and thus increasing its permeability, may help VacA to enter the cell[90]. Furthermore, a selection pressure in colonising strains could be present, as the most virulent strains for human disease express a CagA$^{+}$ VacA$^{i1}$

phenotype[90]. Whether these are direct interactions, or secondary to the signalling pathways induced by these two toxins, is yet to be clarified.

#### 1.4.2.3 Other *H. pylori* virulence factors

Other virulence factors include adhesins which are highly conserved among *H. pylori* strains. Sialic Acid-Binding Adhesin (SabA) and Blood group Antigen-Binding antigen A (BabA) attach to blood group antigens on gastric epithelial cells and mucin, of which Lewis Blood Group b ($Le^b$) is the most studied. BabA is a well-characterised adhesin in strains associated with GA[91 92]. Structurally, BabA expresses a β-sheet motif 'crown' which binds to $Le^b$ on one side. Computational modelling suggests that this interaction is mediated by hydrogen bonds and involves 8 BabA genes. This BabA 'crown' which binds to $Le^b$ in human cells is highly conserved, but with a hypervariable loop region. Modifying this loop decreased BabA affinity for $Le^b$ interactions[93].

The adherence of *H. pylori* to epithelial cells through BabA promotes the pathogenicity of VacA and CagPAI. Another adhesion protein, Outer Inflammatory Protein A (OipA), further promotes this adhesion. It is associated with an elevated IL-8 production and subsequent neutrophil chemotaxis, and an increased pro-inflammatory cytokine expression[91]. Its function is closely tied with CagPAI activity and signalling cascades, and both together can modify epithelial cell tight functions. The receptor for OipA on epithelial cells has not yet been identified[94]. OipA's functional status is determined by the number of repeats at the 5' end of genes which can be switched 'on' (functional), or 'off' (non-functional)[56]. Infection with a *H. pylori* strain expressing OipA leads to an increased risk of *H. pylori*-mediated disease as most OipA-expressing strains are also likely to be CagPAI-positive strains[16], which is a virulence factor for *H. pylori*-mediated disease in itself.

Duodenal Ulcer Promoting gene A (DupA) is a polymorphic virulence factor which promotes gastric inflammation by inducing the production of pro-inflammatory cytokines[95]. Its presence in a colonising strain of *H. pylori* is associated with an

increased risk of GA[96]. However, many strains of *H. pylori* have mutations in *dupA* which are then untranslatable[56]. The length of *dupA* is strain-dependent, with as large as a 600-base pair (bp) difference between *H. pylori* strains[56]. The gene *dupA* is also associated with a gene cluster that encodes another T4SS (*tfs3a*). One study has shown that cell translocating kinase A (CtkA) is a variable but constituent part of *tfs3a*, and that its expression induces the release of pro-inflammatory cytokines by the host immune response[97].

## 1.5 The innate immune response to *H. pylori* infection

### 1.5.1 Pattern Recognition Receptors

Micro-organisms, including bacteria like *H. pylori*, are made up of molecules with motifs such as carbohydrates, glycoproteins and lipoteichoic acid. These conserved components are integral to the structure and cell wall of the microbes, and are named Pathogen-Associated Molecular Patterns (PAMPs)[98]. Gastric epithelial cells and circulating immune surveillance cells, such as macrophages and dendritic cells, can recognise these via receptors that are expressed on their cell surface, in an endosomal compartment, or in their cytosol. These receptors are Pattern Recognition Receptors (PRRs). There are four main classes of PRRs; Toll-Like Receptors (TLRs), C-type Lectin Receptor (CLRs), NOD-Like Receptors (NLRs) and Retinoic Acid-Inducible gene I-Like Receptors (RLRs)[68]. These receptors recognise different PAMPs and trigger intracellular signalling pathways which promote the transcription of pro-inflammatory chemokines and cytokines, *e.g.* IL-8 and tumour necrosis factor alpha (TNF-α). The expression and secretion of these cytokines escalate the level of inflammation, and recruits more immune cells to the site of infection through chemotaxis[68]. Host polymorphisms in genes such as *IL-8* also result in an increase in *H. pylori*-induced inflammation[99].

Toll-Like Receptors (TLRs) are the best characterised PRR. They are transmembrane proteins with a leucine-rich extracellular domain. In humans, there are 10 TLRs[100 101] which recognise different PAMPs. Once activated, these trigger downstream

signalling pathways through either Myeloid Differentiation primary response 88 (MYD88) or TRIF/TRAM signalling molecules. This cascade leads to the translocation of transcription factors to the nucleus to induce the expression of pro-inflammatory genes.

*H. pylori* expresses many PAMPs which can be recognised by PRRs expressed by gastric epithelial cells and immune cells. As a Gram-negative bacterium, its cell envelope contains lipopolysaccharide (LPS). In other organisms, this is usually recognised by TLR4. However, *H. pylori* LPS contains a 4' phosphate attached to an ester, with a tetra-acetylated lipid A molecule[102]. These modifications prevent the ligation of TLR4 to *H. pylori* LPS, and its main ligand is thought to be TLR2. Moreover, *H. pylori* LPS has a 1000-fold reduced bio-activity in comparison to LPS from other Gram-negative bacteria, such as *E. coli*[103]. However, the expression of TLR4 is increased in *H. pylori*-infected individuals, suggesting that it plays a role in immune-mediated interactions[104]. TLR2 recognises a range of microbial molecules, such as lipoproteins, glycoproteins, peptidoglycan, lipoteichoic acid and porins[100], but it has also been shown to recognise *H. pylori* LPS *in vitro* cell lines[105]. The role of TLR2 is controversial, because its ligation induces the transcription of anti-inflammatory genes *in vivo*. This is evidenced by the presence of higher levels of immune-associated cell damage in *TLR2*-knockout mice[106]. Although TLR5 recognises bacterial flagellin[107], *H. pylori* is a flagellate micro-organism which contains mutations in the N-terminal of the *flaA* D1 domain[103]. *Salmonella* flagellin modified with *H. pylori flaA* residues prevented TLR5 recognition completely[103]. Together, these mutations show that *H. pylori* flagellin is a weak ligand of TLR5, compared to other pathogens[98]. The presence of TLR9, which binds to hypomethylated CpG motifs found in bacterial DNA[108 109], does not change the immune response to *H. pylori* in knock-out mice compared to wild-type controls[106], suggesting that TLR9 is not crucial for pro-inflammatory responses to the bacterium.

Other PRRs involved in the detection of *H. pylori* include the CLR Dendritic Cell-Specific Intercellular adhesion molecule-3-Grabbing Non-integrin (DC-SIGN). This receptor recognises mannose residues on microbes, but *H. pylori* expresses phase

variant fucosylated ligands[110]. These actively uncouple the receptor from its downstream intracellular signalling processes, and prevents the transcription of pro-inflammatory cytokines[111]. An NLR, Nucleotide-binding Oligomerization Domain-containing protein 1 receptor (NOD-1) recognises intracellular peptidoglycan that has been transferred into epithelial cells by a functional type IV secretion system[8 30]. RLRs on dendritic cells identifies *H. pylori* tri-phosphorylated RNA, and mediates Type 1 interferon induction signalling[109]. Despite the recognition of multiple *H. pylori* PAMPs by different PRRs, and their subsequent cytokine inductions, the innate immune response is not sufficient to clear the infection.

### 1.5.2 Macrophages

Reactive Nitrogen Species (RNS), such as nitric oxide, are produced by the macrophage nitric oxide synthase enzyme[68]. The function of RNS is to destroy phagocytised bacteria. *H. pylori* evades this through its conserved proteins, catalase and superoxide dismutase, which detoxifies RNS, and arginase, which limits nitric oxide production[68].

M1 macrophages are induced by interferon-gamma (IFN-γ), and promote helper T cell 1 (Th1) pro-inflammatory activity through IL-12 production[98]. M2 macrophages are involved in resolving inflammation[112]. M2 macrophages are also induced by anti-inflammatory cytokines IL-4, IL-10 and transforming growth factor beta (TGF-β)[113]. These cytokines promote the production of the extracellular matrix and may indirectly promote the persistent colonisation of *H. pylori* in the mucosa through regulatory mechanisms[114].

Macrophages in the stomach are polarized towards M1 after a *H. pylori* infection[113]. *H. pylori hmox-1* is expressed upon the phosphorylation of CagA in host cells, and is a mechanism of evading macrophage activity. Phosphorylation increases *hmox-1* gene expression, which encodes the protein heme oxygenase-1 (HO-1). HO-1 is an inducible enzyme which promotes anti-inflammatory functions. There was an increase in HO-1 expression in human gastric mononuclear cells and mouse

macrophages infected with a CagA$^+$ *H. pylori* strain[114] and this may help promote an M2 response in the infected mucosa, as a mixed M1/M2 population was observed in another study observing infected human tissue[113]. The deletion of *hmox-1* promoted an M1 macrophage response, an increased pro-inflammatory response, and a reduced *H. pylori* colonisation density[114].

As part of its mechanisms to evade the innate immune response, *H. pylori* can also inhibit phagocytosis in macrophages. Although the bacterium can be internalised within phagosomes, these phagosomes do not fuse with lysosomes to lyse the bacterium adequately[68]. This survival mechanism has been linked to a functional *cag*PAI and VacA presence[115], while other evidence suggests that this evasion mechanism is linked to the ability of *H. pylori* to glycosylate cholesterol[116].

## 1.6 The adaptive immune response to *H. pylori* infection

### 1.6.1 T lymphocytes

In mice and humans, *H. pylori* infection induces a CD4$^+$ and CD8$^+$ T cell immune response in the gastric mucosa[117]. Within the CD4$^+$ T lymphocyte response, there are subsets of helper T cell populations – Th1, Th2, Th17 and Th22. The expansion of Th1 cells are one of the predominant immune responses to *H. pylori* infection[118]. It produces increased amounts of pro-inflammatory cytokines IFN-γ, IL-2 and TNF-α[98] upon infection, which have been observed in gastric biopsy tissue[118]. IFN-γ responses are increased in *H. pylori* infection, and its presence is a major risk factor for the development of gastritis. IL-2 promotes the differentiation of effector T cells in response to *H. pylori* infection. TNF-α stimulates macrophages to secrete further pro-inflammatory factors. While a strong Th1 response results in a lower *H. pylori* colonisation density, it increases the severity of gastritis observed in the infected mucosa and may contribute to carcinogenesis[68]. The presence of Th1 and IFN-γ contributes to atrophic gastritis and intestinal metaplasia[68]. *H. pylori*-infected individuals with PUD also have increased Th1 production in their peripheral blood[119].

However, a strong Th1 response is also a marker for a good GA prognosis, as it may demonstrate a stronger anti-tumour immune response.

In response to *H. pylori* infection, Th2 cells have been detected in the infected mucosa[119]. Th2 cells promote humoral responses through IL-4, but this was not needed for protective immunity[120]. A Th1/Th2 balance may be required in the trade-off between bacterial survival and host damage. In mice, a dominant Th1 response led to gastritis, but there was an increased Th2 response in cases with GA[98 121 122].

Th17 has also been isolated from *H. pylori*-infected mucosa[122]. These cells produce IL-17A and IL-17F, which activate immune cells, fibroblasts and epithelial cells to secrete cytokines. These cytokines recruit neutrophils via chemotaxis. IL-17 expression in the infected mucosa was correlated with increased neutrophil frequencies, and the highest concentrations of IL-17 were near gastric ulcers[123]. Increased expression of IL-17 and IFN-γ was observed in the gastric tissue of *H. pylori* infected-mice[124]. It was noted that while mice developed a Th1/Th17 immune response to infection, Th17 cell population expanded prior to Th1 cells. Also, IL-17$^{-/-}$ mice showed a decreased Th1 response when challenged with *H. pylori* infection. Moreover, *H. pylori*-infected children showed reduced gastric inflammation, a smaller population of Th17 cells and a decreased expression of *IL-17* when compared to infected adults[125]. This finding may help explain why children are less likely to develop *H. pylori*-mediated immunopathology compared to adults.

Although the Th1/Th17 immune response is potent enough to induce host immunity from *H. pylori* infection, the bacterium has mechanisms of immune evasion to promote its own long-term colonisation in the human stomach[68 122 124]. *H. pylori* VacA attaches to CD18 integrin on the effector T cell receptor, which associates with CD11a to form the transmembrane receptor lymphocyte function-associated antigen 1 (LFA-1). During the recycling of LFA-1, *H. pylori* induces VacA uptake into the host cell[68]. VacA inhibits the effector T cell proliferative process, by interfering with the T cell receptor IL-2 signalling pathway. VacA also inhibits the activation of T cell genes by

preventing the nuclear translocation of the transcription factor Nuclear Factor of Activated T cells (NFAT)[75 126].

The presence of autoreactive antibodies, infectious agents and non-self antigens in the body elicits a powerful immune response from the host. Tempering these aberrant responses to prevent excessive immunopathology is one of the means of immunomodulation in the host[127]. Cells which can promote immune tolerance in mucosal tissue, alongside their other functions, include myeloid-suppressor cells (MDSC), innate lymphoid cells (ILCs) and natural killer T cells (NKT)[128 129]. MDSCs, which are comprised of granulocytic-like and monocytic-like cells, expand in response to infection, inflammation and carcinomas. They suppress effector T cell responses, and modulate the cytokine expression of macrophages[128]. However, the most discussed immunomodulatory mechanisms of the adaptive immune response are regulatory T cells. These cells, alongside potential IL-10-producing B cells, will be the focus of the work in this thesis.

### 1.6.2 Regulatory T cells (Tregs)

Regulatory T cells (Tregs) are a subset of the $CD4^+$ T helper lymphocyte population in mice and humans which are specialised for immunoregulation. Tregs are the master cells which mediate peripheral immune tolerance. They can induce anergy and apoptosis in self-reactive B and T lymphocytes which have escaped deleterious mechanisms in the thymus. In the periphery, the effect of self-reactive B cells can be curbed by deleterious immune responses, anergy induced by anti-inflammatory cytokines and immune modulation by Tregs[130]. These autoreactive responses must be contained to prevent autoimmune conditions such as type 1 diabetes and MS.

Tregs also limit tissue damage caused by long-term chronic inflammation, in conditions such as asthma and IBD by inhibiting pro-inflammatory cell activity and cytokine release. Unfortunately, in its attempt to prevent tissue damage in the host, Tregs can also prevent the successful clearance of particular pathogens such as *H. pylori* and viral infections[16 131]. As Tregs can limit pro-inflammatory responses from

sterilising the pathogen responsible, they indirectly promote the persistence and/or colonisation of the pathogen in the host. Furthermore, if the infection or chronic inflammation is maintained in the host, and develops into a tumour, the presence of Tregs can also inhibit anti-tumour immune responses[131].

Natural Tregs (nTregs) are a Treg subpopulation belonging to a distinct lineage, which are made in the thymus. They represent one of the largest Treg subset populations, and are differentiated in response to the presence of self-reactive lymphocytes in the thymus[132]. Induced Tregs (iTregs) are naïve $CD4^+$ T cells which can be induced into Treg function by a variety of cytokines. Differences between these types of Tregs are shown below (**Table 1.2**).

**Table 1.2:** A comparison of natural and induced regulatory T cells**.** Adapted from Bluestone & Abbas[133]

| Feature | Natural Tregs | Induced Tregs |
|---|---|---|
| Site of induction | Thymus | Immune periphery |
| CD28-CD80/CD86 dependent | Yes | No |
| IL-2 dependent | Yes | Yes |
| Specificity | Autoreactive lymphocytes in the thymus | Tissue-specific antigens and foreign antigens |
| Cytokine independent | Yes | No |

### 1.6.2.1 Treg markers

Regulatory T cells were first described in the 1970s, and termed 'suppressor' T cells[134]. Characterising these cells, and the factors that they secreted proved to be difficult, and the field fell into disrepute. This was due to the lack of Treg cellular markers. Different Treg subsets have since been discovered, as well as the array of markers needed to identify them (**Table 1.3**). Multiple markers are required to accurately identify Treg populations. This is because they share a common lineage

with other $CD4^+$ T cells[135], and also because there are similarities between Treg subsets, in that they secrete similar cytokines.

CD25 expression is a crucial marker for the identification of Tregs. The first regulatory T cell, (not the suppressor cell identified in the 1970s) was a $CD4^+CD25^+$ T cell[136]. CD25 is the high affinity alpha chain on the T cell IL-2 receptor[136]. IL-2 is a T cell growth factor needed for the differentiation of T cells. Lymphoproliferative disease and colitis can develop in IL-2 or CD25-deficient mice[137]. Tregs have since been labelled as $CD25^{hi}$ T cells, as there are effector T cells which are $CD25^+$ in expression[138]. This high expression of CD25 is linked to a theory suggesting that Tregs 'scavenge' IL-2 from other T cells, as Tregs do not produce their own autocrine growth factors. This process simultaneously prevents effector T cell expansion, and promotes the differentiation of other Tregs[139].

One of the most prevalent markers for Treg identification, Forkhead box protein 3 (Foxp3), was discovered after decades of research. In the 1940s, an American lab was investigating the effects of radiation exposure on mice and a new phenotype was observed in one of the mice. The animal presented with rough, scaly skin, red eyes, and an enlarged spleen and lymph nodes, before dying prematurely at three weeks. This murine phenotype was referred to as scurfy[140]. Further studies on this phenomenon were not undertaken until 1991, when Godfrey *et al.* demonstrated that there was a significant infiltration of lymphoid and myeloid cells within multiple organs of the mice[141 142]. The gene responsible (originally coined *scurfin*) was located, and eventually renamed *foxp3*[143].

Later research indicated that a two-base adenine insertion into the forkhead/winged helix domain of Foxp3 (needed for DNA interactions) was the source of the scurfy phenotype, since a non-functional protein was expressed[143 144]. This tied in with polyadenylation *foxp3* mutations identified in patients with IPEX syndrome[145], which is a rare autoimmune condition in which Tregs are not functionally sufficient to stem autoimmune reactions occurring within the individual.

Foxp3 is a transcription factor which is expressed highly in nTregs. Its Treg-specific demethylated region (TSDR) is a clear marker by which to identify nTregs[146]. It can induce or repress expression of approximately 700 genes, including cell-surface molecules and cytokines[127]. Its interactions with other transcription factors that activate $CD4^+$ cells and facilitate their differentiation into Tregs suggests that Foxp3 actively promotes the anergic and suppressive phenotype of Tregs[127]. Moreover, the induced expression of Foxp3 to $CD4^+$ cells converts them to a Treg-like phenotype[147]. Furthermore, the adoptive transfer of nTregs into Foxp3-knockout mice protected them against colitis[148]. Foxp3 is a significant factor in the development of nTregs[144] [147], however some iTreg subsets also express Foxp3[132] [149]. Other genes, including Granzyme B, that are specific to Tregs and can be used as markers, are expressed independently of *foxp3*[127]. The identification of the marker Foxp3 is not sufficient to identify cells as Tregs in humans[131]. In the Treg literature, different markers used in combination (or individually) to identify Tregs are described below (**Table 1.3**).

**Table 1.3:** Treg markers in mice and humans.

| Marker | Name and function |
|---|---|
| $CD4^+$ | T cell co-receptor |
| $CD25^{hi}$ | IL-2 receptor α-chain[150]<br>'Scavenger' marker which decreases IL-2 availability for maintaining effector T cells |
| $CD39^+/CD73^+$ | Enzymes that catalyses ATP to AMP to adenosine[151]<br>Promotes TGF-β secretion with CD73[152] |
| $CD49b^+$/LAG3 | α2 integrin subunit of very late activation antigen 2 (VLA-2)[153]<br>Co-expressed markers which identify Tr1 Tregs |
| $CD127^{lo}$ | IL-7 receptor<br>Downregulated in Tregs[131]<br>Marker expression is inversely associated with Foxp3 expression |
| $CD226^-$ | Low expression in Tregs inhibits effector T cell differentiation[154] |
| $CTLA\text{-}4^+$ | (Cytotoxic T lymphocyte antigen 4)<br>Negative immunomodulatory protein[155]<br>Crucial for suppression of autoreactive T cells[156] |
| $FCRL3^+$ | (FcR-like 3 protein)<br>FcR homolog in FCRL family<br>Possible function in maintaining immune homeostasis[157] |
| $FR4^{hi}$ | (Folate receptor 4)<br>Folic acid receptor which is a marker for natural Tregs[158] |
| $FoxA1^+$ | (HNF3α; Hepatocyte nuclear factor 3α)<br>Transcription factor[159] |
| $Foxp3^+$ | Transcription factor[140] |
| $GITR^{hi}$ | (Glucocorticoid-induced TNF receptor family-related protein)[160]<br>Marker expression is high on Tregs, low in T cells[161] |
| Granzyme B | Secreted protease for effector cell apoptosis[162] |
| Helios | Transcription factor in Ikaros family[162]<br>Promotes Foxp3 activity |
| IDO | Indoleamine 2,3-Dioxygenase<br>Immunomodulatory protein promotes Treg activity and inhibits Th17 differentiation via tryptophan metabolism[163 164] |
| $IL\text{-}10^+$ | Anti-inflammatory cytokine[131] |
| $Nrp\text{-}1^+$ | (Neuropilin-1)<br>Transmembrane glycoprotein<br>Promotes longer immature DC-Treg interactions[165] |
| $TGF\text{-}\beta^+$ | (Transforming growth factor beta 1)<br>Anti-inflammatory cytokine[131] |

#### 1.6.2.2 Treg suppression mechanisms

The anti-inflammatory cytokine IL-10 is a key mechanism of Treg suppression. IL-10 is also expressed by DCs, macrophages, mast cells, NKT cells, eosinophils, neutrophils, $CD4^+$ and $CD8^+$ T cells, and B cells[166]. It binds to its receptor on immune cells to trigger the Janus kinase (JAK)/ Signal Transducer and Activator of Transcription protein (STAT) intracellular signalling pathway. This occurs through the phosphorylation of two tyrosine residues on an IL-10 receptor cytosolic domain[166]. STAT3 is the critical transcriptional factor to promote the anti-inflammatory functions of IL-10[167], since it downregulates the transcription of pro-inflammatory genes such as *IFN-γ*, *IL-17* and MHC Class II[168]. IL-10 enhances the expression of suppressive molecules including Foxp3 and CTLA-4 and so induces and maintains the activity of Tregs[169]. In a tumour, $Foxp3^+$ Tregs can also induce the apoptosis of pro-inflammatory cells through granzyme B production in a perforin-dependent manner[138 170].

IL-10 has modulatory effects on DCs, suppressing their ability to induce the differentiation of Th1, Th2 and Th17 lymphocytes from naïve T cells[171 172]. It is also a major autocrine factor for B cells, by preventing apoptosis. When stimulated by LPS, human monocytes are induced to produce pro-inflammatory cytokines through NF-κB signalling. IL-10 rapidly inhibits this signalling cascade, thus dampening the pro-inflammatory immune response[173].

TGF-β is another suppressive cytokine which is expressed by some Treg subsets. It inhibits Th1, Th2 and $CD8^+$ cell proliferation by blocking T cell receptor (TCR) interleukin-2-inducible T cell (ITK) kinase activation and the $Ca^{2+}$ ions needed for the expression of pro-proliferative transcription factors such as GATA-3[174]. The importance of TGF-β in nTreg function and development has been disputed[131 175]. However, in iTregs, prolonged exposure to TGF-β can prevent Foxp3 expression loss. Moreover, vitamin A metabolite all-trans-retinoic acid can boost TGF-β pathways in up-regulating Foxp3 expression[138]. When tethered on the Treg membrane surface, TGF-β also induces cell-contact mediated suppression[131].

### 1.6.2.3 IL-10 immunosuppression

IL-10 is a crucial immunomodulatory cytokine produced by many immune cells. This includes $CD4^+$ T cells, $CD8^+$ T cells, mast cells, neutrophils, DCs, NKT cells and B cells[168] [176]. IL-10 functions by intracellular signalling cascades in different immune cells. Some of these functions are described below (**Figure 1.6**).

The most characterised pathway is the JAK/STAT3 pathway in which JAK is phosphorylated and induces the translocation of STAT3 into the cell nucleus[177]. This starts a signalling cascade in which the transcription of pro-inflammatory cytokines is inhibited. These cytokines include IL-1α, IL-1β, IL-6, IL-8 and TNF-α. The inhibition of these cytokines is a primary role in IL-10-induced immunosuppression[178]. IL-10 can also inhibit the phosphorylation of the IκB kinase (IKK)[177] [179]. This prevents the translocation of NF-κB into the nucleus, which would promote the transcription of pro-inflammatory cytokines.

The binding of IL-10 to its receptor in immune cells can also induce Membrane-Associated RING-CH-1 (MARCH-1) ubiquitin ligase expression[180]. MARCH-1 then interacts with and induces ubiquitination of Human Leukocyte Antigen – antigen D Related (HLA-DR). This decreases Major Histocompatibility Complex (MHC) Class II presentation by the immune cell, and inhibits the antigen presentation pathway[181]. IL-10 is a growth factor for B cells, and promotes the differentiation of B cells into antibody-secreting plasmacytes[182]. Further roles of IL-10-producing B cells have yet to be clarified.

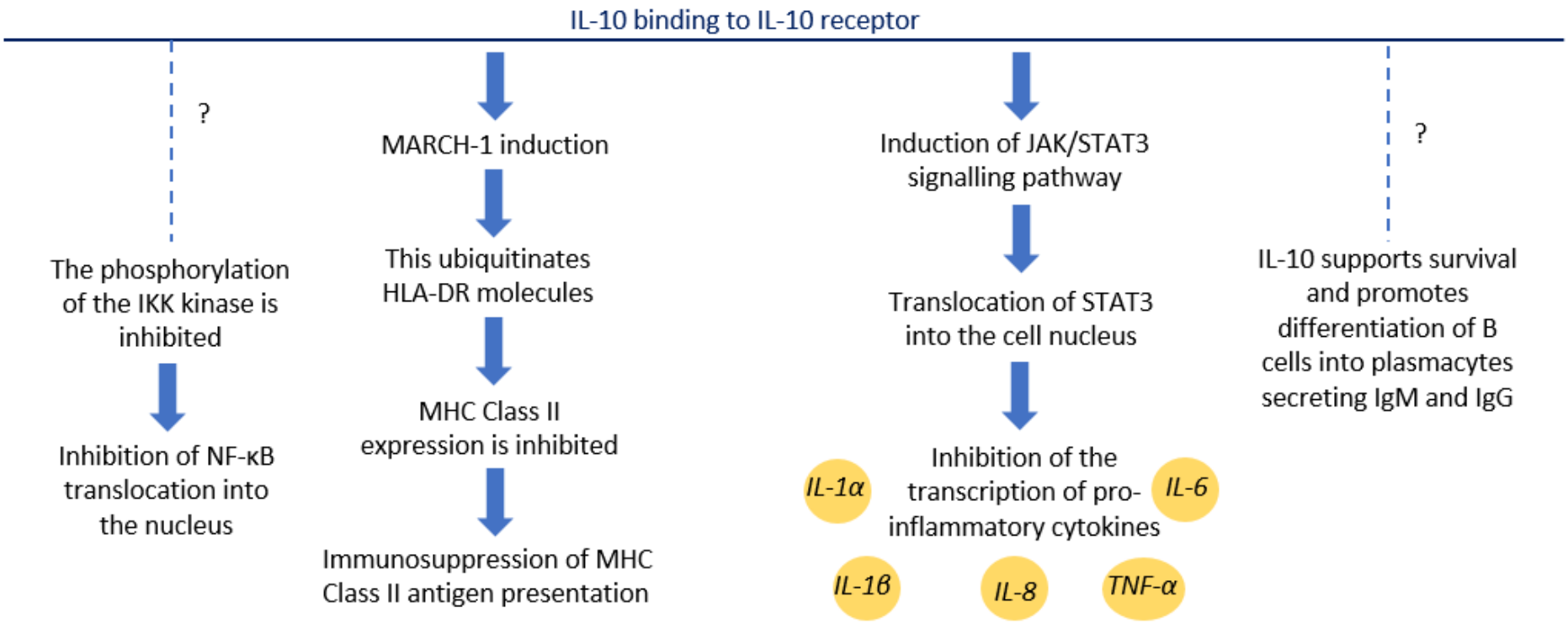



**Figure 1.6:** Signalling pathways induced by interleukin 10 (IL-10) upon binding to its receptor in various immune cells *in vivo*. Based on an IL-10 signalling pathway developed by Verma *et al*.[177] with further detail[166 167 173 176 179-182]. IKK kinase; IκB kinase, NF-κB; Nuclear Factor Kappa light chain enhancer of activated B cells, MARCH-1; Membrane-Associated RING-CH-1, HLA-DR; Human Leukocyte Antigen – antigen D Related, MHC; Major Histocompatibility Complex, JAK; Janus Kinase, STAT3; Signal Transducer and Activator of Transcription protein 3, Ig; Immunoglobulin.

### 1.6.2.4 Role of Tregs in *H. pylori* infection

An increase of $CD4^+CD25^{hi}$ Treg frequencies has been observed in the peripheral blood and gastric mucosa of *H. pylori*-infected individuals compared to uninfected controls[119 183-185]. $CD4^+$ lymphocytes from the peripheral blood of *H. pylori*-infected individuals only responded to stimulation by *H. pylori in vitro* after Tregs were depleted[183].

There was a significant increase in Foxp3 expression by Tregs in *H. pylori*-infected individuals, compared to uninfected controls[119 183 184 186 187]. There was a 19-25-fold increase in Foxp3 expression in *H. pylori*-infected antrum and cardia[186] compared to uninfected controls. Most Foxp3 was produced by $CD4^+CD25^{hi}$ Tregs, compared to $CD4^+CD25^{lo}$ cells, demonstrating an enriched Foxp3 expression in Tregs[183 184]. Foxp3 expression also increased with the level of gastric inflammation, and with TGF-β mRNA levels[186]. Furthermore, $CD4^+Foxp3^+$ Tregs were noted to be close to $CD4^+Foxp3^-$ effector T cells, implying that there may be suppressive interactions between Tregs and other T cells in infected gastric tissue[184].

$IL\text{-}10^+$ Tregs are crucial to the persistence of *H. pylori* infection in the human stomach. Increased $IL\text{-}10^+$ Treg responses have been identified in the peripheral blood and gastric mucosa of *H. pylori*-infected individuals[188 189] compared to uninfected individuals. In Chilean children, higher frequencies of $IL\text{-}10^+$ cells were observed in *H. pylori*-gastric mucosa[190]. This was accompanied by increased IL-10 and Foxp3 mRNA, and a reduced Th17 response when compared to *H. pylori*-infected adults. This strong regulatory response may help facilitate the establishment of *H. pylori* infection in children.

*H. pylori* infection can also skew the human immune response towards a regulatory phenotype as part of its immune evasion mechanisms. Through VacA and gamma-glutamyl transpeptidase (GGT), *H. pylori* can inhibit the maturation of DCs. This in turn promotes the differentiation of Tregs from naïve T cells, and suppresses Th17 proliferation[191 192]. As well as increasing Treg frequencies, *H. pylori* can also induce a

change in homing receptors on Tregs. An increased expression of CCR6, CXCR1 and CXCR2 chemokines on *H. pylori*-induced Tregs may contribute to the migration of Tregs towards the infected gastric mucosa[149].

Tregs are crucial in the development of *H. pylori*-mediated PUD. Previous work in the research group identified that *H. pylori* infected individuals who have insufficient Treg levels in blood and gastric mucosa were reported as more likely to develop PUD[119]. *H. pylori*-infected patients with PUD had a 2.4-fold reduced $CD4^{+}CD25^{hi}IL\text{-}10^{+}$ Treg frequency compared to uninfected controls. Moreover, there was a corresponding significant increase in Th1/Th2 response, which agrees with studies in the literature that a strong pro-inflammatory response to *H. pylori* infection results in increased levels of inflammation.

There was also a reported increase in the proportion of Tregs in gastric biopsies taken from *H. pylori*-infected GA patients before chemotherapy and also from MALT lymphoma patients, compared to uninfected controls[183-185 187 193]. The frequencies of Tregs in healthy tissue from GA patients was comparable with asymptomatic *H. pylori* infection. However, in GA-affected gastric tissue, Treg frequencies increased 3-fold[183]. An increase in $CD4^{+}Foxp3^{+}$ Tregs in GA-affected gastric tissue was also identified in another study[184]. Gastric Tregs suppressed *H. pylori*-induced pro-inflammatory $CD4^{+}$ T cell proliferation and IFN-γ production[184]. When these Tregs were depleted, there was an increase in $CD4^{+}CD25^{lo}$ effector T cell proliferation[184]. The increase in Treg frequencies correlated with advanced stages of GA, and linked with a decline in overall survival in a study of GA patients (reviewed in [185]).

There has been a rise in immunopathological diseases such as MS, allergy and asthma in developed countries. The decline of *H. pylori* colonisation in humans has been inversely associated with a rise in the presence of atopic conditions[33-35 37 40 42 49 194 195]. This extra-gastric protection has been connected to an increased *H. pylori*-induced Treg activity and IL-10 function[39 159 188].

### 1.6.3 B lymphocytes

*H. pylori* infection elicits a strong IgG and IgA antibody response in *H. pylori*-positive individuals. The serum IgG response is the basis for the *H. pylori* serology diagnostic test. However, it has been shown that it is the T lymphocyte cellular response, and not the humoral response, which is critical for immunity against *H. pylori* infection[5 196]. Another study demonstrated that the lack of secreted IgA did not affect the prevalence of *H. pylori* infection in patients and donors[197].

The expansion of B cell population in response to *H. pylori* infection contributes to the development of gastric MALT lymphomas; this bacterium has been identified in most MALT lymphoma cases[18-20 198-202]. However, as *H. pylori* infection is treated, the lymphoma can regress, suggesting a reliance on the *H. pylori* stimulus[201]. In the lymphoma, the presence of pro-inflammatory cytokines and ROS in response to *H. pylori* infection can lead to the development of mutations in B cells. In the tumour microenvironment, benign B cells are present and an increased frequency of $CD4^+$ T cells are recruited. Follicular lymphoma cells promote the differentiation of $CD4^+$ T cells into Tregs, which contribute to the anti-inflammatory mechanisms maintaining the lymphoma[16 201], and why the expansion of aberrant B cells is not impeded[203].

The search to create a prophylactic vaccine for *H. pylori* infection has occurred since the classification of the bacterium as the microbial cause of PUD and GA. Immunisation has been studied to test and treat *H. pylori* infection, and as an alternative to treatment regimens involving multiple antibiotics. Efforts to develop a satisfactory *H. pylori* vaccine have proved ineffective, even in mice[121]. Recently, a study in China tested an oral *H. pylori* vaccine with a corresponding placebo in a Phase 3 trial with 4000 children aged 6-15 who were *H. pylori*-negative[204]. Three doses of the vaccine were given to the children, which contained a urease B subunit. Although the study showed some success as a safe vaccine, its protective effects did not last beyond a year, when 64 children tested positive for *H. pylori* infection. Furthermore, the children had to fast for 2 hours prior to vaccination, and were given an 80ml

sodium bicarbonate/sodium citrate solution to drink, rendering it currently unfeasible for general clinical use[205].

### 1.6.4 Regulatory B cells (Bregs)

In 1974, research demonstrated that B cells had suppressive activity on delayed hypersensitivity reactions[206]. This work was only taken further almost twenty years later, when the concept of B cell subtypes and their role in immunomodulation was hypothesised by Wolf and colleagues. They showed that B cell knockout mice succumbed to more severe effects of an experimental autoimmune encephalomyelitis (EAE) infection[207], a well-established model for multiple sclerosis (MS).

Only in 2002 was the term 'regulatory B cell' coined by Mizoguchi and colleagues to describe cells that suppressed immunopathology in an IBD mouse model[208 209]. Regulatory B cells (Bregs) were so named because of their high-level IL-10 secretion, and the potent anti-inflammatory and immunomodulatory activity of this cytokine. IL-10 accounts for the majority of the regulatory activity of Bregs[210]. Bregs have been reported in the human and mouse spleen, but also in human blood, lymph nodes, Peyer's patches, intestinal tissue and the central nervous system (CNS)[210 211].

Bregs are not currently described as lineage-specific B cells, but arise from B cells at different stages of B cell development and maturation pathway. As different types of B cells have been described as Bregs, in mice and in humans, there is currently no agreement on a specific Breg phenotype in the literature[171]. This is why IL-10 is crucial to identifying Bregs. It is currently unknown whether all B cells can develop suppressive function in response to stimulation, or whether immunomodulatory function is limited to a particular subset of the $CD19^+$ B cell population[171]. There is evidence to support the theory that Bregs differentiate in response to the presence of pro-inflammatory mediators[211]. One study demonstrated that, following the induction of arthritis in a mouse model, pro-inflammatory IL-1β and IL-6 cytokines

are produced by mouse splenocytes and induce the differentiation of Bregs in the spleen and mesenteric lymph nodes[212].

Tregs can also produce anti-inflammatory cytokines for Breg development and maturation. IL-35 is a cytokine produced by Tregs and B cells which can induce Breg differentiation [213], and suppresses autoimmune disease[213 214]. The secretion of IL-35 follows from the co-stimulation of TLR-4 and CD40L in B cells[215]. Mice with functional IL-35 knockouts show signs of heightened EAE immunopathology, compared to healthy controls[215]. There is conflicting evidence that IL-35-induced-Bregs may also secrete IL-10[213 216]. IL-21 and its corresponding receptor are also reported to be crucial for Breg cell expansion and regulatory activity during effector T cell autoimmunity[217].

#### 1.6.4.1 Breg markers in mice and humans

As with Tregs before the identification of Foxp3, Bregs have no single universal marker, (surface or transcription factor), which is present in all subsets. There are differing Breg phenotypes in mice and humans, sometimes with a limited suppressive activity time-span[172]. The main marker for Bregs appears to be IL-10 production. Splenic B cells which produce IL-10 make up 1-3% of the splenic B lymphocyte population in naïve mice[210 218]. The current surface markers used are up and down-regulated in different experimental models[211] (**Tables 1.4 and 1.5**). Therefore, it is recommended that a combination of markers is used to define Breg populations reliably. This creates a standard for the evidence needed to confirm the presence of a particular Breg subset, and also to make research within this field more reproducible[219]. The most characterised Breg subset in mice is the $CD19^{+}CD1d^{hi}CD5^{+}$ Breg[171 218 220-222]. In humans, the most characterised Breg phenotype is the $CD19^{+}CD24^{+/hi}CD38^{+/hi}$ Breg population[193 223-225]. Ultimately, evidence of the functional suppressive ability of the IL-10 produced from B cells is required to show that these cells are Bregs[171].

**Table 1.4:** Markers for Breg subsets in mice, and their functions. Adapted from Breg studies in the literature[210 219 220 226 227].

| Marker | Function |
|---|---|
| $B220^{+}$ | Isoform of CD45, expressed on all haematopoietic cells[211] |
| $CD1d^{hi}$ | Presents lipid antigens to Natural Killer T cells, and maintains them[228] |
| $CD5^{+}$ | Protects B cells from apoptosis after B cell receptor stimulation[229] |
| $CD19^{+}$ | Co-stimulator surface marker for mature B cells[230] |
| $CD23^{+}$ | Low affinity IgE receptor[231], downregulated upon activation[219] |
| $CD24^{+/hi}$ | T cell co-stimulator for $CD4^{+}$ cell clonal expansion[232] |
| $CD25^{hi}$ | IL-2 receptor α-chain[169 233] |
| $CD44^{hi}$ | Glycoprotein receptor for hyaluronic acid[234] |
| $IgM^{hi}$ | B cell receptor (BCR) |
| TIM-1 | T cell Ig domain and Mucin domain protein 1<br>Necessary for the binding of apoptotic cells to B cells and their consequent IL-10 production[227] |

**Table 1.5:** Markers for Breg subsets in humans, and their functions. Adapted from Breg studies in the literature[219 225 235 223 236].

| Marker | Function |
|---|---|
| $CD1d^{hi}$ | Presents lipid antigens to Natural Killer T cells, and maintains them[228] |
| $CD5^{+}$ | Protects B cells from apoptosis after BCR stimulation[229] |
| $CD19^{+}$ | Co-stimulator surface marker for mature B cells[230] |
| $CD21^{hi}$ | Maintains BCR after B cell stimulation from T cell complement-tagged antigens[237] |
| $CD24^{+/hi}$ | T cell co-stimulator for $CD4^{+}$ cell clonal expansion[232] |
| $CD25^{hi}$ | IL-2 receptor α-chain[169 233]<br>'Scavenger' of IL-2; reducing the availability of IL-2 to maintain T cells |
| $CD27^{+}$ | TNF receptor family member<br>B cell co-stimulatory molecule[238] |
| $CD38^{+/hi}$ | B cell activation marker[219] |
| $CD71^{+}$ | Transferrin receptor |
| $CD138^{+}$ | Plasma cell marker[219] |
| $IgM^{hi}$ | B cell receptor (BCR) |
| $Pax5^{+}$ | Transcription factor essential for B lymphocyte development[239] |

Several groups have hypothesised the existence of different Breg subsets in mice and humans. Studies use these Breg subsets to name and classify particular populations within mice or humans. The table below summarises the different Breg subsets and their key identifying features (**Table 1.6**). B10 Bregs, for example, describe IL-10-producing $CD1d^{hi}CD5^{+}$ Bregs in the $CD19^{+}$ B cell population[221].

**Table 1.6:** Different Breg subsets and their features.

| Type of Breg | Found in | Location | Features |
|---|---|---|---|
| Splenic T2-MZP cell | Mouse | Spleen | Induce Tregs, suppress $CD4^{+}$ and $CD8^{+}$ T cells |
| MZ B cell | Mouse | Spleen | Induce Tregs, suppress $CD4^{+}$ and $CD8^{+}$ T cells |
| B10 cell | Mouse | Spleen | Suppress $CD4^{+}$ T cells, monocytes and DCs |
| | Human | Blood | |
| Plasma cell | Mouse | Spleen | Suppress $CD4^{+}$ T cells |
| TIM-$1^{+}$ B cell | Mouse | Spleen | Suppress $CD4^{+}$ T cells |
| Plasmablasts | Mouse | Draining lymph node | Suppress $CD4^{+}$ T cells and DCs |
| | Human | Blood | |
| Immature cell | Human | Blood<br>Site of inflammation | Induce Tregs, suppress Th1 and Th17 cells, suppress virus-specific $CD8^{+}$ cell responses |
| Br1 cells | Human | Blood | Produce IgG4 |

MZ B cell, marginal zone B cell; T2-MZP cell, transitional-2 marginal zone cell; TIM-1, T cell Ig domain and mucin domain protein 1 (TIM-1). Adapted from Rosser & Mauri[211]

### 1.6.4.2 Breg suppression mechanisms

Bregs can functionally suppress active immune responses through a number of mechanisms, but mainly through the release of anti-inflammatory cytokines such as IL-10, TGF-β, and IL-35. IL-10 is a pleiotropic anti-inflammatory cytokine which is expressed by many different types of immune cells. Although IL-10 is an important growth factor for B cells, by promoting the differentiation of B cells into plasmablasts, it is not required for Breg development[210]. The transcription factors promoting IL-10 production in B cells are unknown[210], but the influx of $Ca^{2+}$ ions induced by endoplasmic reticulum calcium sensors STIM1 and STIM2 are critical for Breg IL-10

production[240]. Without these, there is a $CD4^+$ expansion observed in mice, with an increased pro-inflammatory IFN-γ and IL-17 cytokine response. This causes them to develop an exacerbated EAE response[240]. The presence of IL-10 is crucial in modulating excessive autoimmune responses in conditions such as collagen-induced arthritis and EAE in mice[241 242]. The presence of fewer IL-10-producing-Bregs in the peripheral blood of MS patients, compared to healthy volunteers has also been observed[219].

Bregs can induce Treg differentiation from naïve T cells in mice and humans through anti-inflammatory cytokine production[169 193 224 241 243-245] (**Figure 1.7**). They can enhance Treg Foxp3, CTLA-4 and TGF-β expression[169 244]. By suppressing pro-inflammatory cytokine release from DCs, Bregs can suppress the differentiation of Th1 and Th7 cells[171 246]. TGF-β-producing Bregs can induce apoptosis of $CD4^+$ T cells, and anergy in $CD8^+$ T cells after stimulation with LPS[211]. Mice expressing Bregs lacking in IL-35 expression showed an increased pro-inflammatory Th1 response and an increased number of macrophages in mice spleen[247].

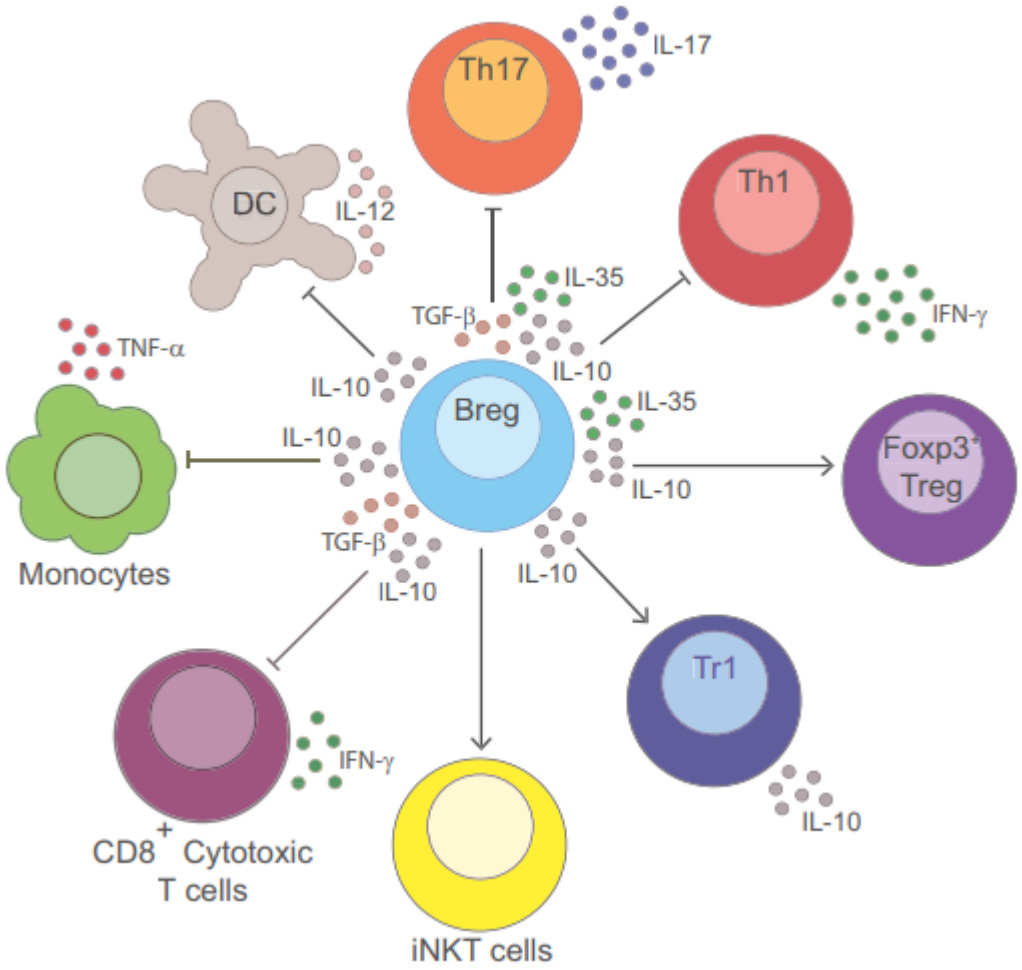



**Figure 1.7:** The regulatory B cell and its mechanisms in suppressing pro-inflammatory immune responses through the release of IL-10, TGF-β and IL-35. Adapted from Rosser *et al*[211]. DC; dendritic cell, IFN-γ; interferon gamma, iNKT cells; induced Natural Killer T cells, TGF-β; Transforming Growth Factor β, Tr1; Type 1 Regulatory T cell.

Bregs also suppress pro-inflammatory immune cell activity through contact-mediated mechanisms. Besides inducing Treg function from $CD4^+$ cells, and inhibiting other pro-inflammatory cells through IL-10, they can induce T cell anergy through CD40/CD40L interactions, or T cell apoptosis through the Fas/FasL signalling pathway[171] (**Figure 1.8**). Moreover, Bregs have been described as being able to differentiate into antibody-secreting plasmacytes *in vivo*, and thus aid in the humoral immune response[248].

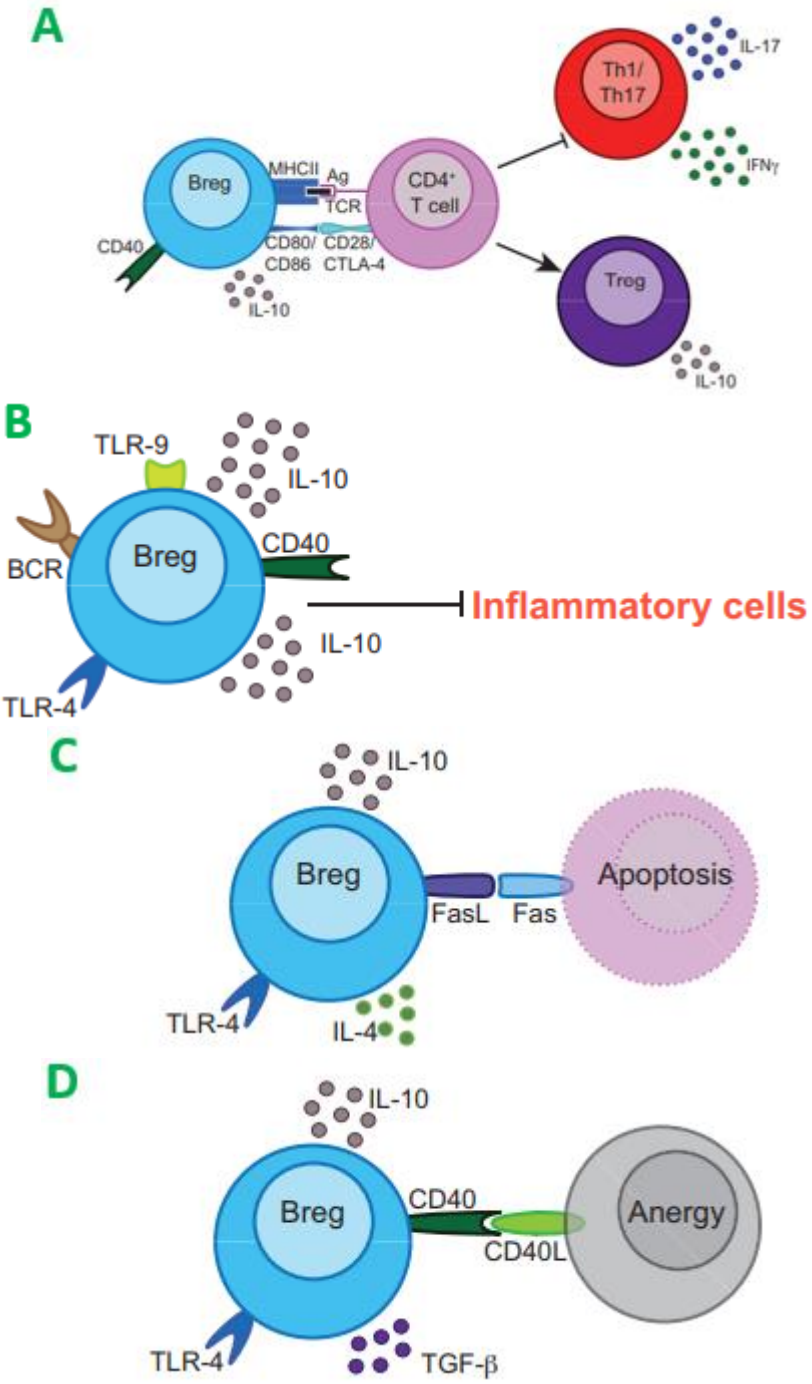



**Figure 1.8:** Contact-mediated immunosuppressive mechanisms of Breg cells. Adapted from Rosser *et al*[171]. (A) Breg interactions with $CD4^+$ effector cells, driving Treg induction. (B) Bregs can interact directly with Tregs to promote the inhibition of pro-inflammatory cells (C) Bregs can induce apoptosis in immune cells by Fas/FasL signalling. (D) Bregs can also induce anergy in activated immune cells through CD40/CD40L interactions.

### 1.6.4.3 The identification of Bregs in mouse and human studies

Bregs are a small subset of the B cell population in mice and humans. Therefore, this subtype must be clearly defined in gating strategies for flow cytometry to describe a plausible population. The gating of Bregs in published papers can be quite varied. Some studies also do not describe their Breg identification strategies[249 250]. Example gating strategies of identifying mouse $CD19^{+}CD1d^{hi}CD5^{+}$ Bregs and human $CD19^{+}CD24^{+/hi}CD38^{+/hi}$ Bregs from the literature are shown below (**Figures 1.9** and **1.10**).

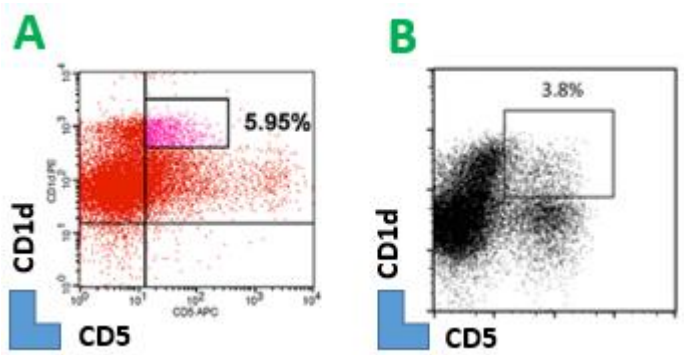



**Figure 1.9:** Representative flow cytometry plots and gating strategy schemes of $CD19^{+}CD1d^{hi}CD5^{+}$ Bregs from mouse splenic lymphocytes. Lymphocytes were harvested, stained against B cell markers CD19, CD1d and CD5 with fluorochrome-conjugated antibodies and analysed using flow cytometry. (A) Taken from Li *et al*.[251]. (B) Taken from Yokoyama *et al*.[252].

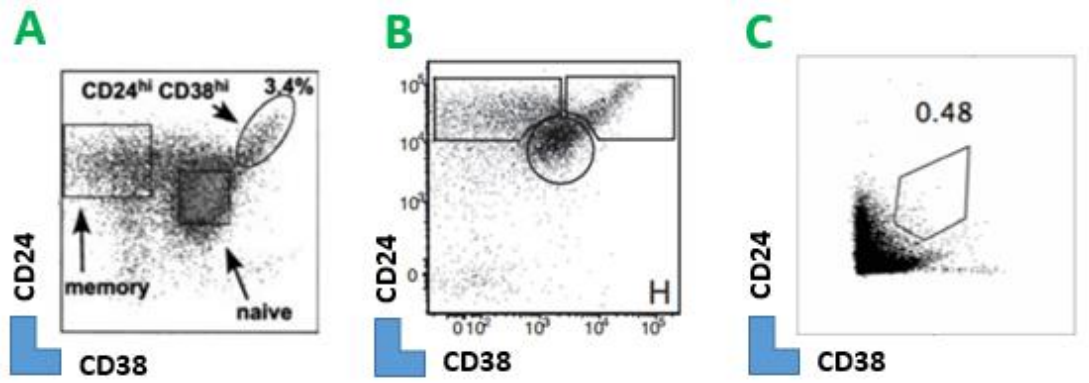



**Figure 1.10:** Representative flow cytometry plots and gating strategy schemes of $CD19^{+}CD24^{+/hi}CD38^{+/hi}$ Bregs from human peripheral blood samples. Peripheral blood mononuclear cells (PBMCs) were harvested, stained against B cell markers CD19, CD24 and CD38 with fluorochrome-conjugated antibodies and analysed using flow cytometry. (A) Taken from Cuss *et al.*[253]. (B) Taken from Flores-Borja, F. *et al.*[224]. (C) Taken from Wei *et al*. [243].

### 1.6.4.4 Role of Bregs in *H. pylori* infection

The function of Bregs is to inhibit excessive autoimmune responses, including those observed in chronic inflammatory conditions. *H. pylori* establishes a chronic inflammatory infection in the human host, which is not cleared by the innate and adaptive immune responses. There are a limited number of published studies on the role of Bregs may play in *H. pylori* infection[225 243].

IL-10 is a cytokine which suppresses gastritis in infected mice[254]. The levels of IL-10-producing B cells were indiscernible in the gastric mucosa of uninfected mice, but showed a marked increase in the stomach, spleen, mesenteric lymph nodes, small intestine and colon after *H. pylori* infection[243]. This B cell population also expanded within 2 weeks in response to *H. pylori* infection, before the expansion of $Foxp3^{+}$ Tregs at 10 weeks.

Mice lacking B cells have a reduced *H. pylori* colonisation density within the gastric mucosa when infected, but develop a more severe gastritis compared to uninfected controls[110]. This implies that the pro-inflammatory response can be suppressed by B lymphocytes. Therefore, a reduced B cell response can contribute to a disease state, as seen in chronic conditions such as systemic lupus erythematosus (SLE), asthma and rheumatoid arthritis (RA)[248]. B cells exposed to *Helicobacter felis in vitro* produced IL-10 in abundance[106]. This recognition of the *H. felis* antigen, and the following IL-10 production, was dependent on TLR2 activation and MyD88 intracellular signalling[106].

There is only one paper on human Bregs in *H. pylori* infection in *H. pylori* research literature[225]. The authors described an IL-10-producing $CD24^+CD38^+$ Breg population in peripheral blood which was almost non-existent in *H. pylori*-negative patients, but accounted for approximately 3% of peripheral blood B cells in a cohort of asymptomatic *H. pylori*-positive patients. This proportion was lower in *H. pylori*-positive patients who smoked, and in obese *H. pylori*-positive patients. The results also demonstrate a decline in Breg frequencies in these two patient cohorts with GA. This decline disagrees with the data from a study on Bregs in GA patients[193]. The association between *H. pylori* infection and GA has been previously identified. While the authors do not discuss the *H. pylori* infection status of the GA patients, the study showed that human peripheral blood Bregs suppressed $CD4^+$ T cell activity, and upregulated Tregs through TGF-β induction. The interaction between Bregs and Tregs, and their described roles in *H. pylori* infection have been shown below (**Figure 1.11**).

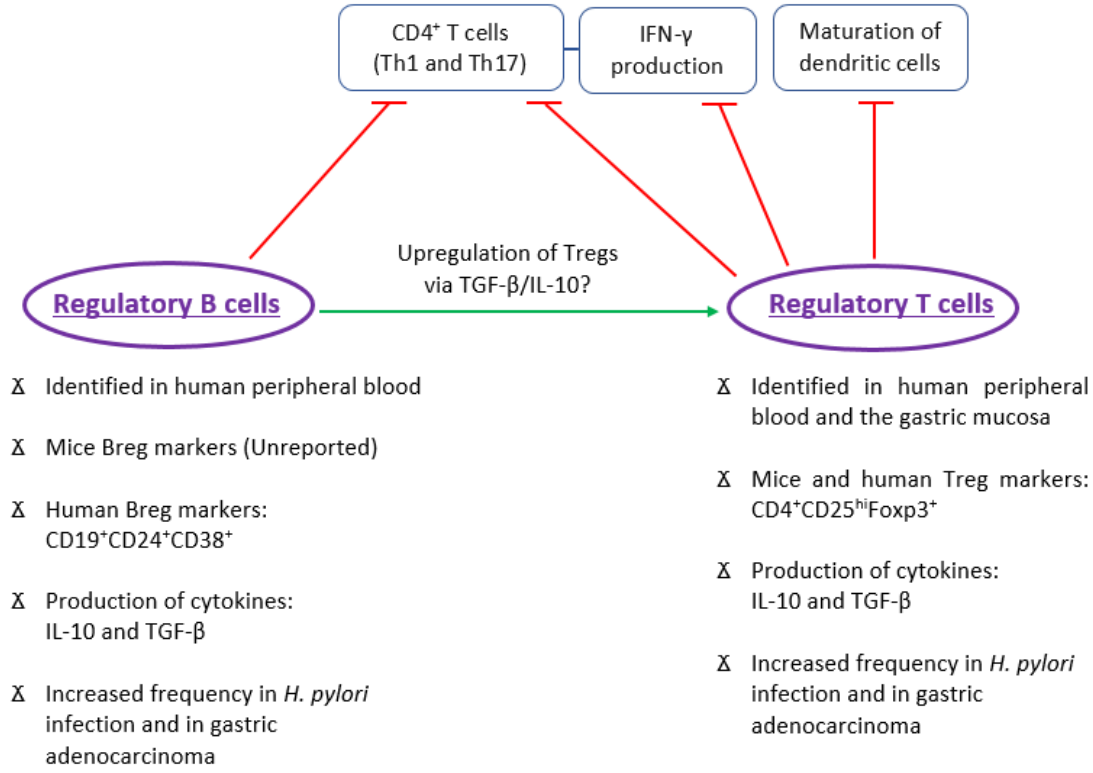



**Figure 1.11:** Characteristics of Bregs and Tregs, their interactions, and their described roles in the context of *H. pylori* infection for mice and humans.

## 1.7 Research objectives

*H. pylori* infection is associated with an increased risk of PUD and GA. Treg frequencies are shown to be increased after infection in both *in vivo* mouse models and in patient peripheral blood and gastric biopsy samples. Tregs are also a known marker for *H. pylori*-mediated disease; a reduced peripheral blood Treg frequency is associated with an increased risk for PUD.

Understanding factors which affect Treg frequency and function in the context of *H. pylori* infection would help further elucidate how host immune responses can lead to *H. pylori*-mediated disease, and potentially identify other markers for evaluating future disease risk.

The research discussed in this thesis will aim to examine recently reported subsets of IL-10-producing B cells, which have been reported to suppress pro-inflammatory $CD4^+$ T cell activity, and potentially upregulate Tregs in *H. pylori* infection.

Further experiments will also aim to further understand the role of *H. pylori* VacA, which has been reported to promote Treg differentiation through the tolerisation of DCs, and VacA i-region polymorphisms, which have been identified as an independent risk factor for *H. pylori*-mediated disease.

With these issues in mind, the objectives of the research in this thesis were as follows:

- To use patient samples to identify peripheral blood Treg frequencies during *H. pylori* infection, and subsequently observe how *H. pylori* eradication therapy affects the Treg response.

- To test an *in vivo* mouse model to identify a possible subset of IL-10-producing B cells, and whether this population is relevant in *H. pylori* infection.

- To use patient samples to develop and identify whether peripheral blood Bregs are upregulated, as Tregs are, during *H. pylori* infection.

- To observe the effect of *H. pylori* infection on the immunosuppressive capability of Tregs in an *in vivo* mouse model.

- To develop and test an *in vivo* mouse model to determine the effect of VacA polymorphisms on Breg and Treg frequencies.

- To use patient samples to develop a *vacA*-based diagnostic test to identify individuals who are at an increased risk of future *H. pylori*-mediated disease.

## Chapter 2: Studying the effect of *H. pylori* eradication on Treg responses

### 2.1 Introduction

The colonisation of *H. pylori* in the human gastric mucosa usually begins during childhood. This infection then persists over a lifetime, unless cleared by antibiotic therapy (described further in **Section 1.3**).

Following eradication therapy, ulcers heal, and their recurrence is prevented. Cases of *H. pylori*-mediated MALT lymphoma (without genetic causes) can also be cured after eradication therapy[255]. For children and younger patients, successful treatment can also reduce the risk of GA[256]. This may be due to a lack of atrophy in the gastric tissue, which usually develops after decades of persistent *H. pylori* infection[256]. As the reacquisition of *H. pylori* in adulthood is rare, the presence of atrophy may help explain why patients with autoimmune gastritis and patients who have been successfully treated for *H. pylori* infection can still go on to develop gastric cancer[5].

An analysis of the host immune response to *H. pylori* infection and subsequent eradication therapy has not yet been studied. *H. pylori* VacA and GGT components can induce Treg proliferation via the tolerisation of DCs[192 257]. This is evident by the increased frequencies of Tregs and IL-10$^{+}$ Tregs in infected mucosa[119]. A reduced Treg response in the mucosa of *H. pylori*-infected patients increases their likelihood of PUD, and pre-clinical pathology such as atrophy[119]. This is likely to be clinically important, because observational evidence suggests that *H. pylori* infection may be a protective link against GORD, oesophageal cancer, MS, IBD and asthma[33-41]. Indeed, this negative correlation between the presence of *H. pylori* infection and gastric reflux is strengthened when an individual is infected with a CagA-expressing *H. pylori* strain[50].

Work on neonatally-infected mouse models suggests that this extra-gastric protection from asthma is dependent on Treg activity[39], and stronger protection is observed from CagA-expressing strains[194]. This data was further corroborated in

humans[37]. *H. pylori*-mediated protection against IBD has also been correlated to CagA presence[49]. It is not known whether this extra-gastric protection remains after successful *H. pylori* eradication. Filling this gap in knowledge is crucial to understanding whether *H. pylori* could increase the risk of or exacerbate existing autoimmune conditions such as MS and Crohn's disease.

## 2.2 Hypotheses

In this interventional study, the consequences of eradication therapy on peripheral blood Treg frequencies and IL-10 production were studied. It was hypothesised that:

- When *H. pylori* infection is successfully treated, the damage done to the gastric epithelium ceases, there is a reduced exposure of immune cells to *H. pylori* antigens, and a decreased differentiation of Tregs from $CD4^+$ T cells.

- As IL-10 production has been previously linked with Treg suppressive activity, IL-10 production by T lymphocytes also declines after *H. pylori* infection has been cleared and gastritis is resolved after several months.

- If *H. pylori* eradication fails, the infection remains. The frequencies of Tregs and level of IL-10 production in peripheral blood T lymphocytes should be similar to that found in blood samples collected directly after the initial diagnosis.

## 2.3 Aims

- To observe the occurrence of *H. pylori* eradication failure after first line treatment in comparison to reported levels in Europe.

- To devise a strategy to consistently identify $CD4^{+}CD25^{hi}Foxp3^{+}$ regulatory T cells in human peripheral blood.

- To compare the frequencies of $CD4^{+}$ T cells and Treg subsets in the peripheral blood of individual patients before and after successful *H. pylori* eradication.

- To follow IL-10 production by peripheral blood $CD4^{+}$ T lymphocytes and Tregs prior to, and after successful *H. pylori* eradication treatment.

- To compare peripheral blood immune responses between patients who have cleared their *H. pylori* infection, and those who failed eradication therapy.

## 2.4 Materials and methods

### 2.4.1 Study management

This study was a single centre cohort study based at the Queen's Medical Centre in Nottingham, designed by Dr. Karen Robinson and Prof. John Atherton. Power calculations based on preliminary data by the research group estimated that a sample size of 42 patients would be adequate to detect a difference in peripheral blood Treg frequencies following eradication therapy. Factoring in a 15% drop out ratio by volunteers, 50 patients were recruited. Dr. Jon White completed and submitted the documentation to obtain ethical approval from Nottingham Research Ethics Committee 2 (REC Ref: 08/H0408/195). Dr. White also processed 140 blood samples, and completed 50% of the final analysis. In this analysis, I carried out the processing of 30 blood samples, devised the flow cytometry analysis gating strategy and completed 50% of the final analysis.

### 2.4.2 Patient recruitment

50 *H. pylori*-positive individuals were recruited from patients undergoing a routine upper GI endoscopy at Queen's Medical Centre in Nottingham, UK (**Table 2.1**). This study was performed with informed written patient consent (see **Appendices A** and **B** for information given to patients and the consent form). Gastric tissue biopsies were collected from patients to initially determine *H. pylori* infection status using gold-standard diagnostic tools; by histopathology, *H. pylori* culture, or a urease test. *H. pylori*-positive patients were then recruited by research nurses in the Nottingham Digestive Diseases Centre (NDDC). Individuals who were under 18 or over 70 years of age, or were taking any non-steroidal anti-inflammatory drugs (NSAIDs), antibiotics, or PPIs in the previous 14 days were excluded from participation in the study. Patients recruited to this study were then anonymised and sequentially assigned a study number from T001 to T050. CagA status of the colonising *H. pylori* strain was determined by CagA Enzyme-Linked Immuno-Sorbent Assay (ELISA) (Genesis) using serum donated by the patients. The ELISA kit was used according to the

manufacturer's instructions. This was completed by Yirga Falcone, Melanie Lingaya and Dr. Jon White (NDDC, Nottingham).

**Table 2.1:** Clinical characteristics of patients recruited to the Treg eradication study.

| | |
|---|---|
| Total patients | 50 |
| Age | Median (54), Range (21-70) |
| Male: female ratio | 0.92 |
| Ethnicity | White (43), Black (3), Asian (3), Biracial (1) |
| CagA status | 19 negative, 39 positive |
| Peptic ulcer disease | 12/50 |
| Smoking status | Non-smoker (26), current smoker (14), ex-smoker (10) |
| Asthma/allergies | 3/50 |
| Indication for endoscopy | Dyspepsia (24), IDA (7), Reflux (7), PUD (4), Other (8) |

### 2.4.3 Study timeline

After patients were diagnosed with *H. pylori* infection, they were recruited to the study. Full, written, informed consent was obtained from patients who agreed to contribute a blood sample (Month 0), and to also return for donations of further blood samples. The patients were then prescribed eradication therapy (**Table 1.1**). Before the second sample was collected (Month 2), and within 4-10 weeks of eradication treatment being prescribed, a Urease Breath Test (UBT) was performed for a *H. pylori* status to determine whether eradication therapy had been successful. If negative for *H. pylori* infection, blood was then taken at specific time points (2, 6, 12, and 24 months after eradication) and labelled accordingly e.g. T001M0, T001M2, T001M6, T001M12, and T001M24 (**Figure 2.1**). If the patient remained infected, a second-line treatment regimen was prescribed until a negative UBT result was obtained. Individuals with eradication failure were analysed as a separate control group.

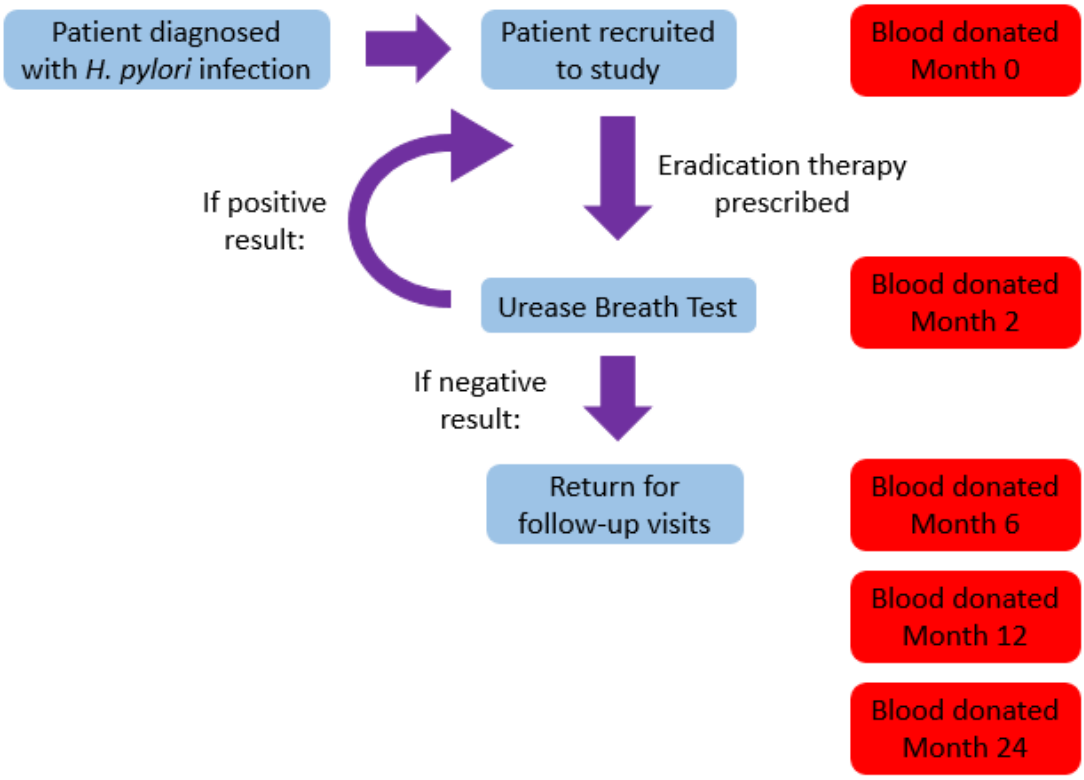



**Figure 2.1**: Protocol for patient recruitment to the Treg eradication study, and subsequent time points for blood donations.

### 2.4.4 Donation of blood samples

Informed written consent to continue participating in this study was obtained after every blood sample donation. 11 patients withdrew their consent after Month 0, and 9 simply dropped out after various time points in the study. 15 patients donated blood samples at all 5 time points, with 13 more samples due to be collected at Month 24. Samples collected to date were analysed in this study (**Table 2.2**).

**Table 2.2**: Total blood samples collected in the Treg eradication study so far, at *H. pylori* diagnosis (Month 0) and a series of time points over 24 months after *H. pylori* eradication therapy.

| Time point | Month 0 | Month 2 | Month 6 | Month 12 | Month 24 |
|---|---|---|---|---|---|
| Samples | 50/50 | 32/50 | 29/50 | 30/50 | 17/50 |

The power calculation describing a suitable number of patients to show a meaningful difference was 42. With an estimated 15% drop out rate, this was factored to a total of 50. 50/50 patients were successfully recruited to this study, with a current dropout rate of 36% before Month 12, but, reassuringly, all of the patients who returned for Month 12 visits also returned at Month 24.

### 2.4.5 Eradication failure

In 6 patients, the first line eradication therapy failed. Therefore the blood samples they donated were analysed separately. After a positive UBT at Month 2, the blood sample was labelled M2V2, to differentiate it from a successfully eradicated patient sample. In four of these patients, there were multiple rounds of treatment failure. Subsequent positive samples from these patients were labelled M2V3, M2V4 and onwards, until a negative UBT result confirmed eradication. 1 patient (T048) remained infected with *H. pylori*, even after 1 year of ongoing treatment.

### 2.4.6 Isolation and stimulation of lymphocytes from human PBMCs

#### 2.4.6.1 PBMC isolation

50ml of venous blood was collected in Ethylenediaminetetraacetic acid (EDTA) vacutainers to prevent coagulation**.** The blood was then transferred into 15ml Falcon tubes and centrifuged at 2000 revolutions per minute (RPM) for 10 minutes. Serum was then isolated and collected in cryotubes and stored at -80°C for further analysis. Centrifugation of the blood sample layered over Biocoll separating solution (Biochrom) then allowed isolation of PBMCs in an enriched interphase[37]. This was completed at 2000 RPM for 20 minutes. Cells were then washed and spun at 1500 RPM for 5 minutes repeatedly with Roswell Park Memorial Institute (RPMI) culture medium (Sigma), (augmented with 10% heat-inactivated fetal calf serum (FCS) (Sigma) and 0.1 mg/ml penicillin and streptomycin (Sigma)). The cells were then counted with 0.4% Trypan Blue solution (Thermo Scientific), before being resuspended at 1 x $10^6$/ml in culture medium.

#### 2.4.6.2 Preparation of *H. pylori* whole cell antigen lysate

6 *H. pylori* clinical isolates of varying virulence types (**Table 2.3**) were thawed from frozen stocks, and streaked onto 5% horse blood agar plates (Oxoid) and incubated at 37°C in a microaerophilic incubator. and resuspended in sterile phosphate-buffered saline (PBS).

**Table 2.3:** *H. pylori* isolates incorporated into the whole cell lysate antigen, which was used to stimulate PBMCs *in* vitro.

| ***H. pylori* isolate** | **Isolate virulence genotype** | **Gastro-duodenal disease status of patient:** |
|---|---|---|
| Q86B | *vacA* s1/m1, CagA$^+$ | Duodenal ulcer |
| Q109A | *vacA* s2/m2, CagA$^-$ | None (gastritis only) |
| Q110A | *vacA* s2/m2, CagA$^-$ | Oesophagitis |
| Q122B | *vacA* s1/m1, CagA$^+$ | Hiatus hernia |
| Q126B | *vacA* s1/m2, CagA$^+$ | Gastric cancer |
| Q131B | *vacA* s1/m2, CagA$^+$ | Duodenal ulcer |

After 48 hours, *H. pylori* colonies were extracted and passaged onto new plates for a further 48 hours. For each strain, confluent growth was then collected aseptically. The bacterial suspensions were diluted to an O.D. of 1.0 at a wavelength of 600nm, before combining equal volumes into a single tube for sonication. This cell suspension was then centrifuged for 10 mins at 4000 RPM, before the pellet was resuspended in 1ml sterile PBS.

Sonication was performed on ice using Soniprep 150 (MSE) with appropriate safety protocol, in a Class I cabinet to prevent the spread of aerosolised bacteria. The cells were sonicated in six 10 second bursts at 10 microns, with each burst being followed by 30 seconds of cooling.

To obtain a working concentration of 250µg/ml, the protein concentration of the sonicate was determined. This was done using the Pierce BCA Protein Assay kit (Thermo Scientific), according to the manufacturer's instructions. The sonicate was then stored in single-use *H. pylori* lysate aliquots at -20°C, before being diluted to 250µg/ml. This was completed by Dr. Darren Letley and Dr. Jon White, as previously described by the research group[119].

#### 2.4.6.3 *In vitro* stimulation

After resuspension of the PBMCs in 1 x $10^6$/ml in culture medium, the PBMCs were either stimulated with 100µl *H. pylori* lysate, or left unstimulated[119]. Following this stimulation, all tubes were incubated at 37°C for an hour before Brefeldin A (BFA) (10µg/ml) was added to all tubes. The leukocytes were then incubated at 37°C for a further fifteen hours. The leukocytes were then refrigerated at 4°C until they were used in cell staining protocols[119].

### 2.4.7 Flow cytometry analysis

#### 2.4.7.1 Fluorochromes

Fluorochromes are chemicals that absorb light energy at a specific wavelength upon excitation and re-emit light at a longer wavelength. Fluorochrome-conjugated antibodies raised against various cellular markers are excited at different light wavelengths within the flow cytometer to produce fluorescent signals. These are filtered into different detection channels, so that the events arising from the stained cells can be sorted into distinct populations by their expression of the markers. The properties of the fluorochrome dyes used in this study for the FC 500 MCL flow cytometer (Beckman Coulter) are described below (**Table 2.4**).

**Table 2.4:** The properties of fluorochromes used in the flow cytometry panel for the Treg eradication study.

| Fluorophore | Abbreviation | Excitation laser (nm) | Emission bandwidth (nm) |
|---|---|---|---|
| Alexa Fluor 488 | AF488 | Argon Ion-488 | 519-525 |
| Phycoerythrin-Texas Red Energy-coupled-dye | ECD | | 610-635 |
| Phycoerythrin | PE | | 568-590 |
| Phycoerythrin-Cyanin 7 | PE/Cy7 | | 750-810 |

The antibodies against helper T cell and Treg markers were used according to the manufacturer's instructions and are described overleaf (**Table 2.5**). Isotype controls are described as 'iso', e.g. 'iso-Foxp3' indicates the isotype control antibody for anti-Foxp3 staining.

**Table 2.5:** Fluorochrome-conjugated antibodies detecting markers expressed by human regulatory T lymphocytes.

| Marker/Isotype | Fluorochrome | Species subtype | Company | Catalogue no. | Clone | Concentration | Volume |
|---|---|---|---|---|---|---|---|
| CD4 | ECD | mouse IgG1 | Beckman Coulter | 6604727 | SFCI12T4D11 | 0.5 mg/ml | 2.5µl |
| CD25 | PE/Cy7 | mouse IgG1, κ | BioLegend | 302612 | BC96 | 0.1 mg/ml | 10µl |
| Foxp3 | AF488 | mouse IgG1, κ | BioLegend | 320212 | 259D | 0.1 mg/ml | 5µl |
| Iso-Foxp3 | AF488 | mouse IgG1, κ | BioLegend | 400134 | MOPC-21 | 0.1 mg/ml | 5µl |
| IL-10 | PE | rat IgG2a | ABD Serotec | MCA2250 | JES3-12G8 | 0.5 mg/ml | 2.5µl |
| Iso-IL-10 | PE | rat IgG1, κ | BioLegend | 400408 | RTK2071 | 0.2 mg/ml | 1µl |

#### 2.4.7.2 Extracellular and intracellular staining

The PBMCs were centrifuged briefly at 1100 RPM for 5 minutes, before the fluorochrome-conjugated antibodies for extracellular markers (anti-CD4 and anti-CD25) were added. These were gently mixed by pipette and incubated on ice for 30 minutes, with occasional mixing. All incubations described took place in the dark. The cells were then washed 3 times with 1ml PBS with 2.5ml 20% sodium azide (PBA) /2% FCS before being fixed in 0.5% formaldehyde in PBS for 20 minutes.

After fixation, the cells were washed with Cell Staining Buffer (BioLegend), and then with Foxp3 buffer (BioLegend) diluted in PBS. The cells were resuspended in Foxp3 buffer for permeabilisation, and incubated on a shaker for 15 minutes at room temperature. These permeabilised cells were then washed, before the anti-IL-10 antibody and isotype control were added to the appropriate tubes and incubated for 1.5 hours at 4°C. Afterwards, 100µl Foxp3 buffer was added to each tube, followed by the anti-Foxp3 antibody or corresponding isotype control, for a further incubation period of 30 minutes at room temperature. The cells were then washed 3 times with Cell Staining Buffer, before being resuspended in 0.5ml PBS containing 0.5% formaldehyde for flow cytometry analysis.

#### 2.4.7.3 Flow cytometry analysis

Multi-colour flow cytometry data acquisition was completed using a FC 500 MCL cell sorter (Beckman Coulter). Using a predetermined lymphocyte gate, data on 250,000 events was collected and analysed using Kaluza software (Beckman Coulter), with respect to appropriate isotype controls. Samples were gated on forward and side scatter under the 488nm laser to exclude dead cells and debris.

## 2.5 Results

Following analysis on Kaluza software, a gating strategy was developed to ensure the consistent identification of positive and negative populations of each helper T cell and Treg marker individually, and in combination with each other. The gating strategy was applied to all blood samples. Samples were excluded from final analysis when data on fewer than 50,000 events per tube could be collected.

Subpopulations of $CD4^+$ helper T cells were first analysed to observe any change in frequency following successful *H. pylori* eradication. $CD4^+CD25^{hi}$ events were gated according to previous work by the research group[119] (**Figure 2.2B**). At two years post-treatment, it was observed that $CD4^+CD25^{hi}$ and $CD4Foxp3^+$ lymphocyte frequencies did not change significantly (**Figures 2.2C** and **2.3C**).

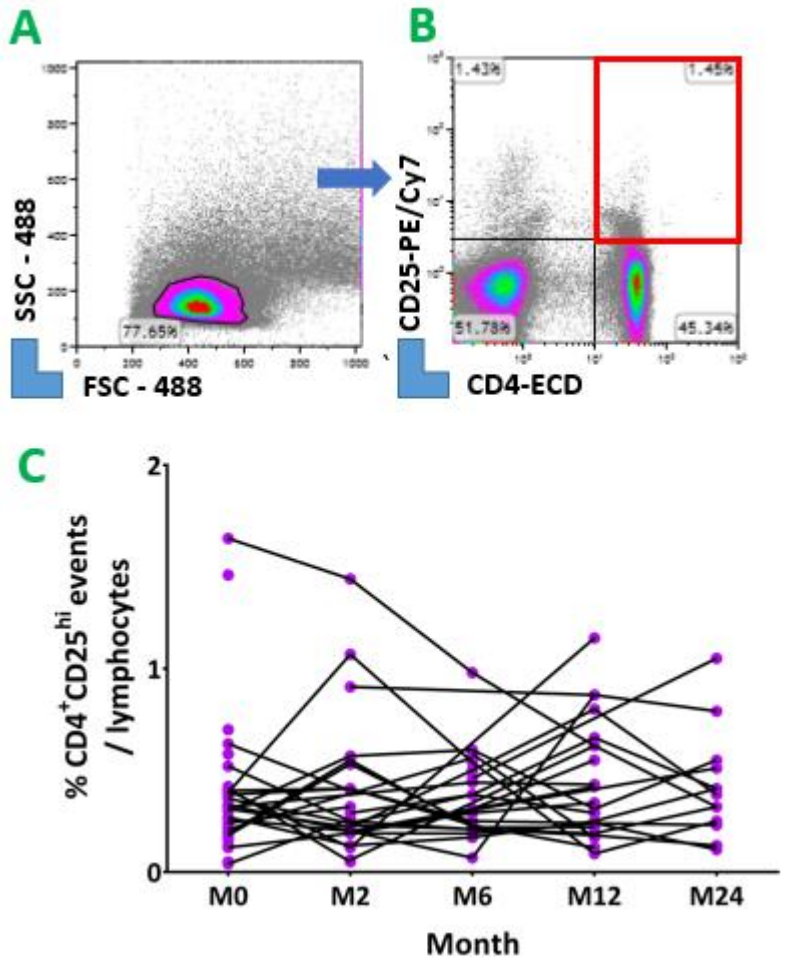



**Figure 2.2:** Representative flow cytometry plots, the gating scheme, and subsequent analysis of $CD4^{+}CD25^{hi}$ T lymphocytes. Human PBMCs were stained with mouse fluorochrome-conjugated antibodies to identify $CD4^{+}$ T cells. (A) Lymphocyte population gated by forward (FSC) and side (SSC) scatter under the 488nm laser. (B) Representative CD4-CD25 flow cytometry plot from the lymphocyte gated population. (C) Proportions of $CD4^{+}CD25^{hi}$ events from patients treated for *H. pylori* infection. After diagnosis and treatment at Month 0, patients donated further blood samples at Months 2, 6, 12 and 24.

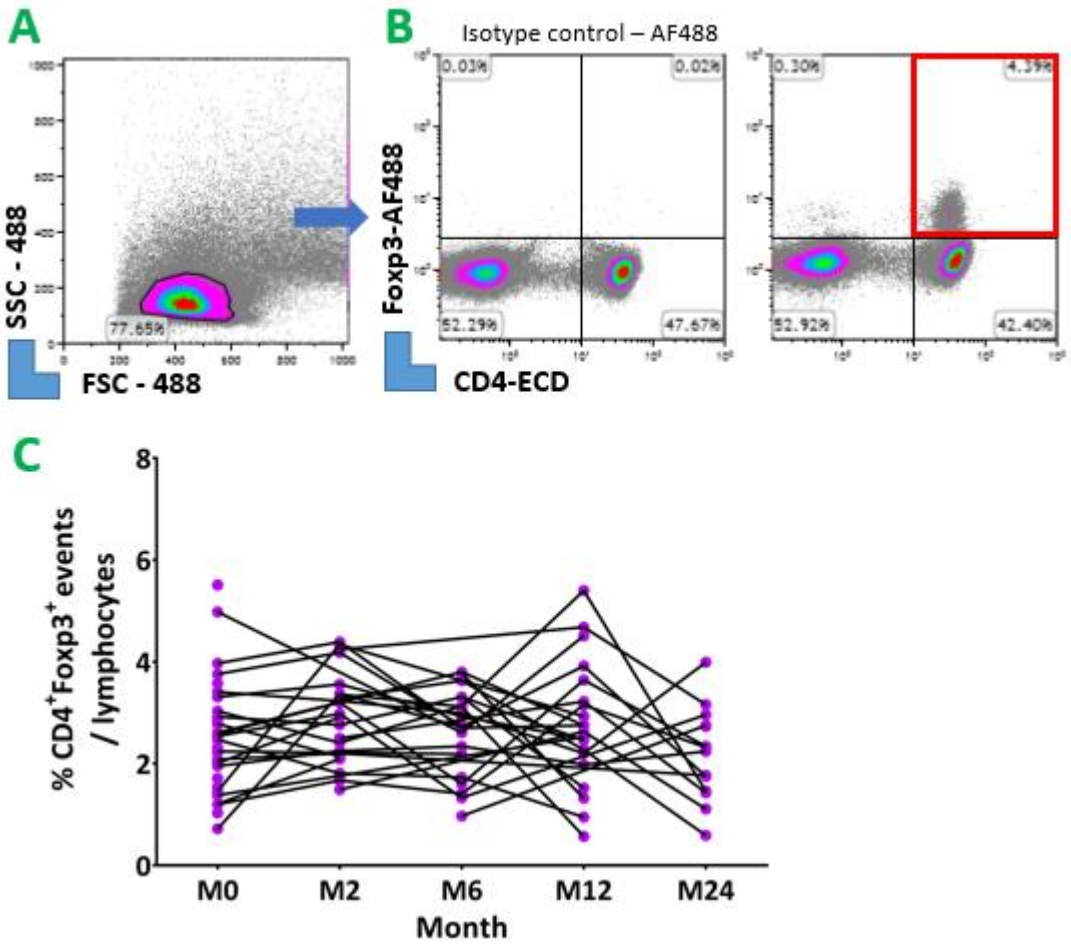



**Figure 2.3:** Representative flow cytometry plots, the gating scheme, and subsequent analysis of $CD4^+Foxp3^+$ T lymphocytes. Human PBMCs were stained with mouse fluorochrome-conjugated antibodies to identify $CD4^+$ T cells. (A) Lymphocyte population gated by forward (FSC) and side (SSC) scatter under the 488nm laser. (B) Representative CD4-Foxp3 flow cytometry plot and corresponding isotype control from the lymphocyte gated population. (C) Proportions of $CD4^+Foxp3^+$ events from patients treated for *H. pylori* infection. After diagnosis and treatment at Month 0, patients donated further blood samples at Months 2, 6, 12 and 24. The linked lines represent samples donated by the same patient over time.

Foxp3 and CD25 are markers for Tregs within the $CD4^+$ T helper population. A triple positive Treg population was then identified within the $CD4^+$ T lymphocytes in flow cytometry plots (**Figure 2.4**). Further analysis of the $CD4^+CD25^{hi}Foxp3^+$ peripheral blood Treg population demonstrated no change in frequency one year after successful *H. pylori* eradication therapy (**Figure 2.5**).

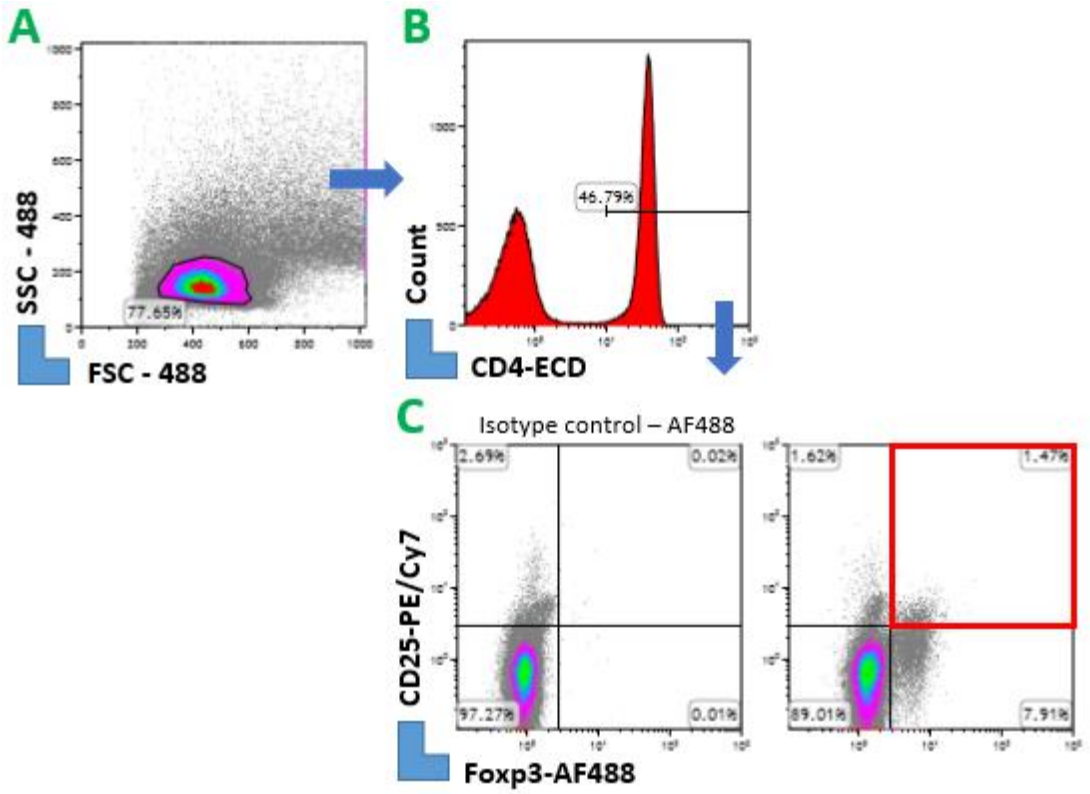



**Figure 2.4:** Representative flow cytometry plots and the gating analysis scheme for the analysis of $CD4^+CD25^{hi}Foxp3^+$ Treg lymphocytes. Human PBMCs were stained with anti-human fluorochrome-conjugated antibodies to identify regulatory T cells within the lymphocyte population. (A) Lymphocyte population gated by forward (FSC) and side (SSC) scatter under the 488nm laser. (B) Histogram showing $CD4^+$ events amongst gated lymphocytes. (C) Representative plot of $CD25^{hi}Foxp3^+$ lymphocytes gated from $CD4^+$ positive events identified in (B), and its corresponding isotype.

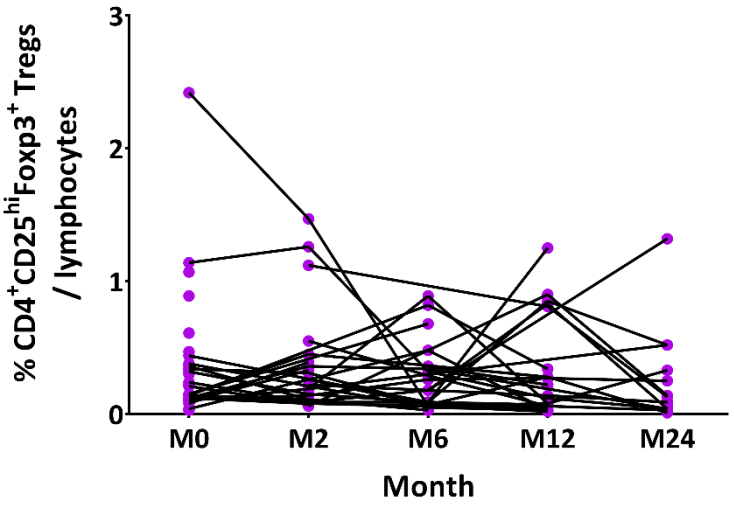



**Figure 2.5:** Proportions of $CD4^+CD25^{hi}Foxp3^+$ Treg lymphocytes in PBMCs from patients treated for *H. pylori* infection. After diagnosis and treatment at Month 0, patients donated blood samples at Months 2, 6, 12 and 24. The linked lines represent samples donated by the same patient over time. Statistical analysis between Month 0 (infected state) and Months 2-24 (eradicated state) was carried out using a Wilcoxon signed rank test.

After stimulation with *H. pylori* lysate antigen (**Table 2.3**) for 16 hours, the frequencies of $CD4^+IL\text{-}10^+$ lymphocytes were analysed (**Figure 2.6**). $CD4^+IL\text{-}10^+$ events were gated according to previous work by the research group[95 119] (**Figure 2.6B**). At Month 6 after eradication therapy, there were decreased frequencies of IL-10-producing $CD4^+$ T cells compared to pre-treatment (medians: 0.17 and 0.19 respectively; $p = 0.0397$). This trend continued at 1 year (median: 0.12, $p = 0.0038$) and at 2 years (median: 0.07, $p = 0.0313$).

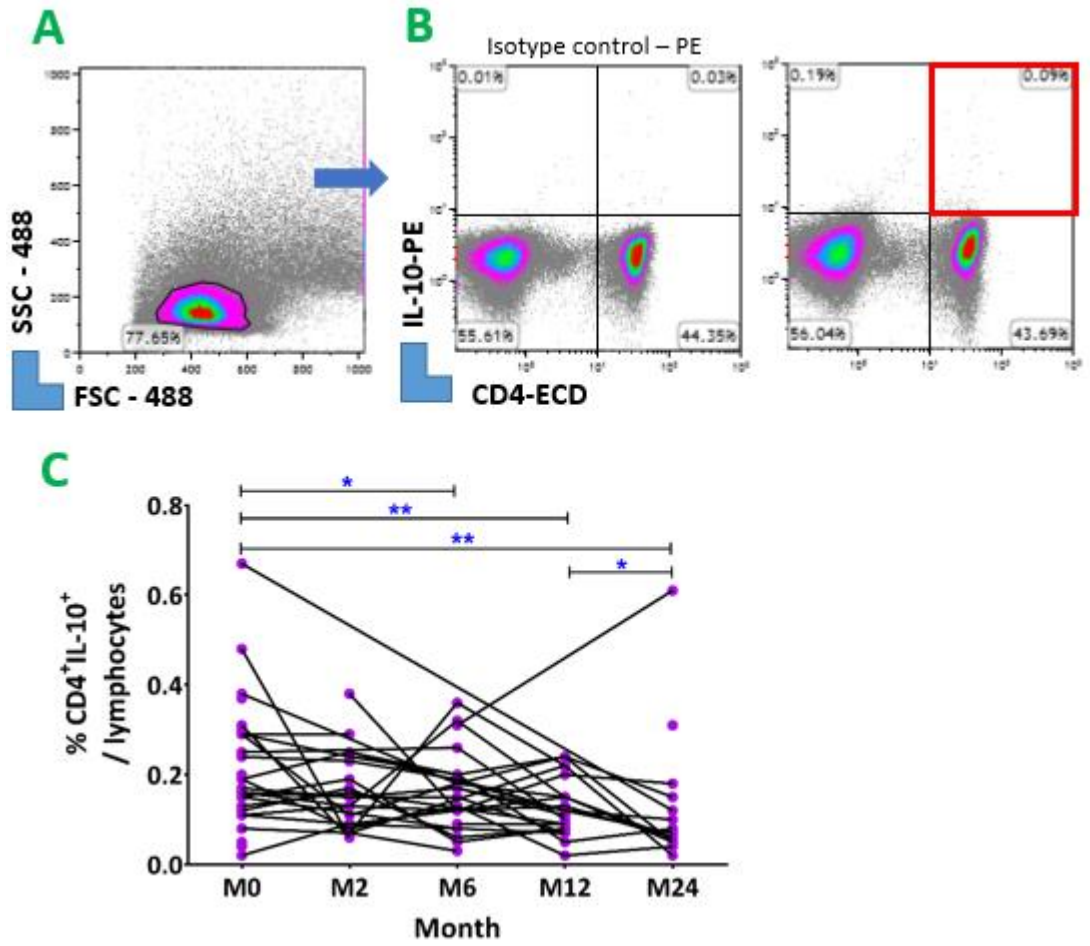



**Figure 2.6:** Representative flow cytometry plots, gating strategy, and subsequent analysis of $CD4^{+}IL\text{-}10^{+}$ T lymphocytes. Human PBMCs were stimulated with a mixed strain *H. pylori* lysate for 16 hours and stained with mouse and rat fluorochrome-conjugated antibodies. (A) Lymphocyte population gated by forward (FSC) and side (SSC) scatter under the 488nm laser. (B) Representative CD4-IL-10 flow cytometry plot and corresponding isotype control from the lymphocyte gated population. (C) Proportions of $CD4^{+}IL\text{-}10^{+}$ events from patients treated for *H. pylori* infection. After diagnosis and treatment at Month 0, patients donated further blood samples at Months 2, 6, 12 and 24. The linked lines represent samples donated by the same patient over time. Statistical analysis between Month 0 and Months 2-24 was carried out using a Wilcoxon signed rank test. The asterisks indicate the level of statistical significance, where * represents $p < 0.05$, and ** represents $p < 0.01$.

The frequency of $CD4^+IL\text{-}10^+$ T cells decreased after *H. pylori* eradication. $IL\text{-}10^+$ events accounted for less than 1% of $CD4^+$ lymphocytes after stimulation with *H. pylori* lysate (**Figure 2.7**). The frequency of these cells decreased suggesting that the proportion of IL-10 production by $CD4^+$ T cells also declined with time after eradication. Although the proportion of these cells statistically decreased after one year compared to during infection (medians: 0.25 and 0.34 respectively; $p = 0.0024$), there was a further significant decline after 2 years (median: 0.14, $p = 0.0313$).

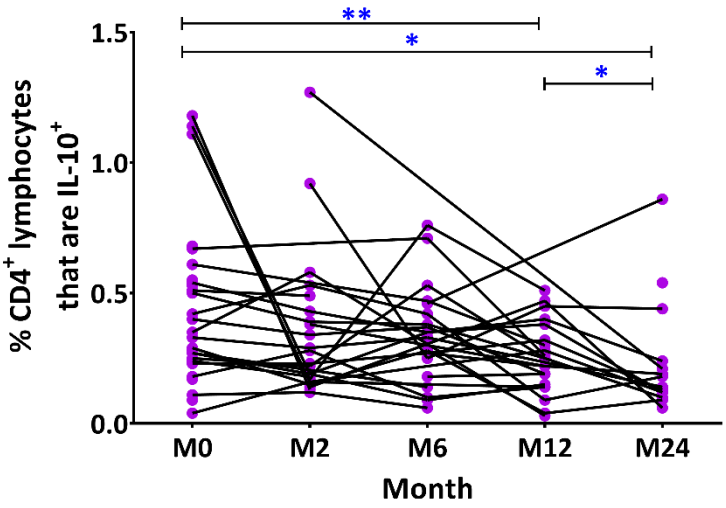



**Figure 2.7:** Proportions of $CD4^+$ lymphocytes that are $IL\text{-}10^+$ in PBMCs from patients treated for *H. pylori* infection. Cells were stimulated with a mixed strain *H. pylori* lysate for 16 hours. The linked lines represent samples donated by the same patient at set time points after diagnosis. Statistical analysis between Month 0 (infected state) and Months 2-24 (eradicated state) was carried out using a Wilcoxon signed rank test. The asterisks indicate the level of statistical significance, where * represents $p < 0.05$, and ** represents $p < 0.01$.

The frequency of $CD4^+CD25^{hi}$ lymphocytes producing IL-10 decreased two months after *H. pylori* eradication at Month 0 (medians 0.02 and 0.05 respectively; $p$ = 0.0415) (**Figure 2.8**). This trend continued after 1 year (median: 0.03, $p$ = 0.0159), and after 2 years, although this did not achieve statistical significance (median: 0.02).

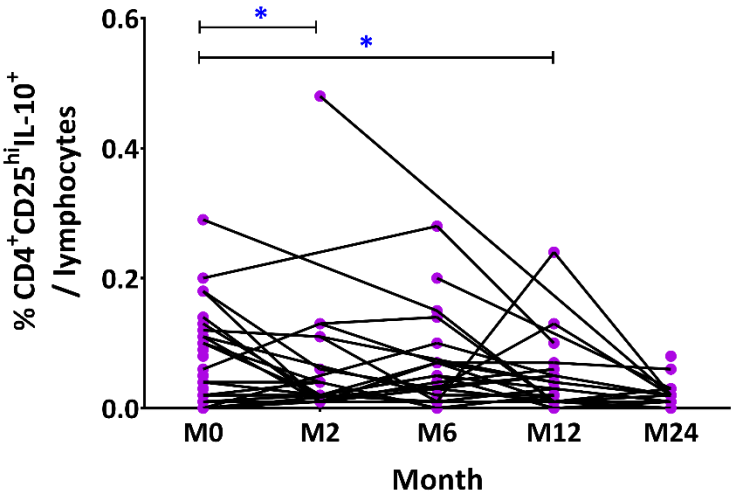



**Figure 2.8:** Proportions of $CD4^+CD25^{hi}IL\text{-}10^+$ lymphocytes in the peripheral blood of patients treated for *H. pylori* infection. Cells were stimulated with a mixed strain *H. pylori* lysate for 16 hours. The linked lines represent samples donated by the same patient at set time points after diagnosis. Statistical analysis between Month 0 (infected state) and Months 2-24 (eradicated state) was carried out using a Wilcoxon signed rank test. The asterisks indicate the level of statistical significance, where * represents $p < 0.05$.

For those who failed eradication, frequencies of $CD4^+IL\text{-}10^+$ lymphocytes were quantified (**Figure 2.9**). These cell frequencies remained consistent until *H. pylori* infection was successfully cleared (shown in purple).

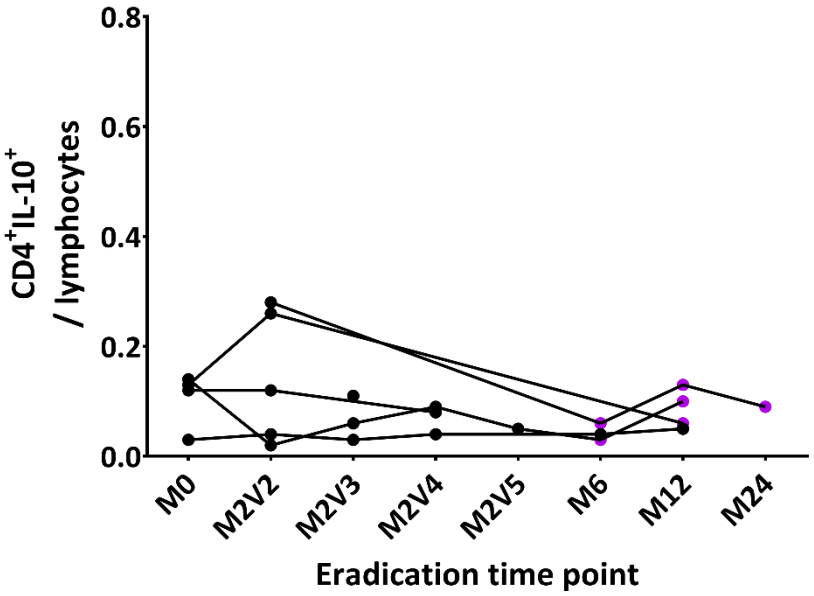



**Figure 2.9:** Proportions of $CD4^+IL\text{-}10^+$ lymphocytes in the peripheral blood of patients who failed eradication treatment for *H. pylori* infection. Cells were stimulated with a mixed strain *H. pylori* lysate for 16 hours. The linked lines represent *H. pylori*-positive samples (black points) donated by the same patient at set time points after diagnosis. Purple points describe samples which are *H. pylori* negative after successful eradication.

Treg frequencies in this eradication failure group were then analysed (**Figure 2.10**). Despite fluctuations at M2V2, Treg frequencies remained consisted with that seen during infection at Month 0.

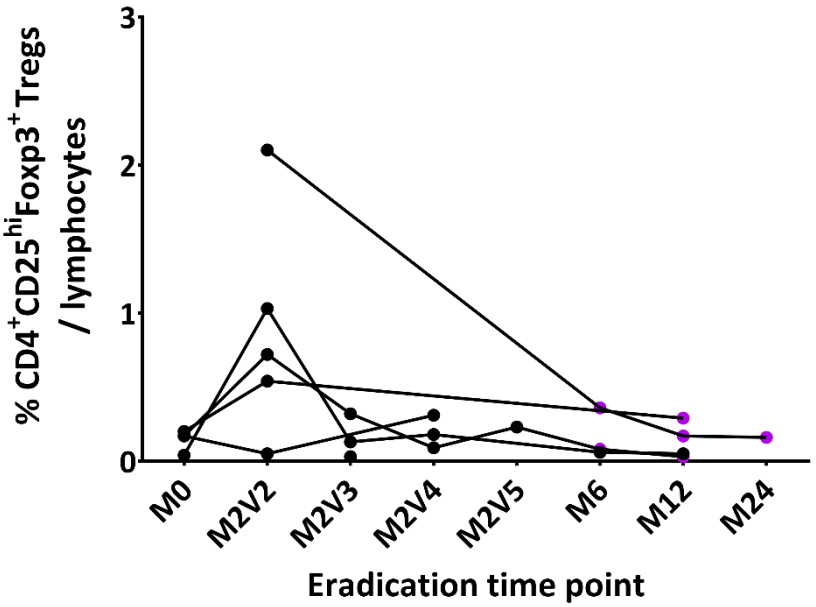



**Figure 2.10:** Proportion of $CD4^{+}CD25^{hi}Foxp3^{+}$ lymphocytes in the peripheral blood of patients who failed treatment for *H. pylori* infection. Cells were stimulated with a mixed strain *H. pylori* lysate for 16 hours. The linked lines represent *H. pylori*-positive samples (black points) donated by the same patient at set time points after diagnosis. Purple points describe samples which are *H. pylori* negative after successful eradication.

## 2.6 Discussion

### 2.6.1 Statement of principal findings

This interventional cohort study aimed to investigate the effect of *H. pylori* eradication therapy on peripheral blood Treg frequencies and their IL-10 production in a patient cohort. 50 *H. pylori* positive individuals donated blood samples after their diagnosis, and at set time points for 2 years after taking the eradication therapy. Results showed that $CD4^+CD25^{hi}$, $CD4^+Foxp3^+$ and $CD4^+CD25^{hi}Foxp3^+$ triple positive Treg frequencies did not differ significantly. The proportion of IL-10-producing $CD4^+$ T cells decreased significantly within six months of successful eradication, and this trend continued for two years. Further analysis described a 1.7 fold reduction in IL-10 production by $CD4^+CD25^{hi}$ events one year after successful *H. pylori* eradication, compared to during infection. For those patients who failed multiple rounds of eradication therapy, the frequencies of Tregs and IL-$10^+$ T cells remained consistent with the pre-treatment blood sample.

### 2.6.2 Biological relevance of the findings

This study was novel for its follow-up of the regulatory immune response in patients over two years after *H. pylori* eradication and it provides some important new findings. Patients who successfully cleared *H. pylori* infection were previously assumed to have levels of circulating anti-inflammatory cells similar to uninfected individuals, as the primary stimulus of *H. pylori* had been removed. The results revealed a great variation in the immune cell profile of individuals over time, and that this assumption cannot be made. Previous work has concentrated on comparing the immune cell profile of infected and uninfected individuals. This preliminary work was expanded on in the present study to show that while frequencies of Tregs did not decline statistically, their IL-10 production declined significantly at Month 6 in response to stimulation from the successful clearance of *H. pylori*.

An increased Treg and Th1 response in infected mucosa, and an increased $Foxp3^+$ Treg frequency has been noted previously in the literature, with infected individuals

expressing low frequencies of Tregs being more likely to have PUD[37 119]. Foxp3 is a marker of nTregs. An increase in Foxp3$^+$ Tregs has been noted in the infected mucosa, but was not observed previously in blood samples[188], which is consistent with the results of this study. While studying lymphocytes from the infected stomach would be ideal to observe the anti-inflammatory response in the mucosa, characterising peripheral Treg populations allows for the use of multiple markers to further identify Treg population phenotypes[149].

The variety of Treg cell subtypes could help explain why there were no differences in Treg frequencies observed in this study. It is possible that the Treg population in human peripheral blood is Foxp3$^-$. Multivariate analysis of multiple Treg markers (IL-10, Foxp3, and CD25) yielded results that were in line with prior work suggesting that IL-10 was being produced from Foxp3$^-$ Tregs[95 258].

Previous work in the research group identified an increased proportion of CD4$^+$CD25$^{hi}$IL-10$^+$ regulatory lymphocytes in the gastric mucosa and peripheral blood of infected individuals[119 149 188 189]. In this study, it was observed that IL-10 producing Treg subsets of the CD4$^+$ population decrease after eradication. This decreasing trend in IL-10 production was also confirmed at the transcriptional level, using real-time quantitative PCR (RT-qPCR) to quantify *IL-10* mRNA expression in patient PBMCs[117]. IL-10 is an important functional mediator of Treg activity. This is especially important in *H. pylori* research, because Treg frequencies and their IL-10 production are crucial in preventing immunopathological damage caused by infection[119]. While a pro-inflammatory Th1-skewed response occurs in the mucosa, the presence of Tregs dampens this response, and indirectly allows for the persistence of *H. pylori* survival in the stomach. While the study is still ongoing, Month 12 samples were shown to be the current most useful time point to compare IL-10-producing lymphocytes against infection (Month 0). The frequency of IL-10-producing CD4$^+$CD25$^{hi}$ lymphocytes tended towards a decrease at Month 24, but there were perhaps not enough paired samples to reveal a statistically significant difference.

The use of *H. pylori* lysate was to stimulate IL-10 production from PBMCs. The idea is to replicate the stimulation of *H. pylori* in the mucosa, in order to identify IL-10 lymphocyte populations which have expanded due to infection *in vivo*. This technique has been used previously by the research group[37 119], and shows a difference in IL-10$^+$ Treg responses between *H. pylori*-infected and uninfected patients. Results in this study appear to agree with this finding, as samples from patients taken 24 months after successful *H. pylori* eradication showed a decreased IL-10 response after *in vitro* stimulation with *H. pylori* lysate antigen. However, *in vitro* stimulation induced decreased IL-10$^+$ lymphocyte frequencies compared to previous work[95].

While undisputed evidence of *H. pylori* mediated protection in humans has not yet been published, the association between *H. pylori* infection and extra-gastric protection was first noted in neonatal mice in 2011[39]. The authors showed that while allergen-challenged *H. pylori* infected mice were protected from asthma, depleting Tregs from these mice ablated this effect. Furthermore, injecting CD4$^+$CD25$^+$ Tregs into uninfected mice also transferred this allergy protection, showing the protection to be Treg-dependent. Incidentally, this protection was strongest in mice infected with CagA-expressing *H. pylori* strains, and this trend has also been observed in human studies[42]. This suggests that virulence factors may play a role in inducing different regulatory immune responses in the *H. pylori*-infected host.

### 2.6.4 Clinical relevance of the findings

The global incidence of *H. pylori* infection is declining with each new generation[13]. However, parallel to this is an observed rise in gastric pathologies such as IBD, GORD, oesophageal cancer, and extra-gastric pathologies such as MS[34]. The immunological consequences following *H. pylori* eradication discussed in this study, such as the decline of IL-10 production, require further illumination. Current UK guidelines require the eradication of *H. pylori* when present in an individual presenting with dyspepsia or IDA. *H. pylori* colonisation is a normal part of human life; co-existing within our stomach for thousands of years[5]. Clearance could result in the unwanted increase in a patient's likelihood of developing oesophageal cancer, or other

conditions that colonisation with *H. pylori* has been providing immunological protection against[36]. Weighing the risk between oesophageal cancer (and other pathologies) and the likelihood of GA associated with *H. pylori* infection is an ethically difficult conundrum.

### 2.6.5 Critique of the experimental design

Preliminary data in the research group powered a calculation to determine how much data was required to demonstrate a significant difference in the regulatory immune response between *H. pylori* infection and eradication patient cohorts. Despite recruiting 50 patients, there was a dropout rate of 36% before the Month 12 sample collection. This is in line with work on another eradication study in Malaysia, which only managed to recruit 17 positive patients from a cohort of 57 *H. pylori* infected individuals, and observed a dropout rate of 41% by Month 12[259].

People aged 70 and over were excluded from this study. While this is a crucial group who are at an increased risk of *H. pylori*-mediated disease, it would be contraindicative for this study. Ageing is associated with immune senescence, which is an altered immune response favouring an elevated memory Treg frequency with a decreased proliferative capacity[260]. Due to the lifelong colonisation of the mucosa with *H. pylori*, infected ageing patients are also more likely to have gastric atrophy present[5]. Because of this, eradication would not ensure the resolution of active gastritis, because atrophy can lead to pre-cancerous dysplasia and may not be reversible. Furthermore, gastric atrophy is not an optimal environment to detect the *H. pylori* bacterium, which could result in a false negative result in a diagnostic test. Patients under 18 were excluded because they are less likely to be referred to gastroenterology clinics with symptoms of *H. pylori*-mediated disease. The peripheral blood Treg frequency could also be different to those observed in adults, and could mask trends observed within the data. Furthermore, the collection of 50ml blood from this age group would bring up ethical and practical considerations. Patients who were prescribed NSAIDS, PPIs or other immunomodulating medication, and those with co-morbidities such as cancer were also excluded. This is because disease and/or

medication can reduce the successful detection of *H. pylori* in diagnostic tests, and can potentially influence the host response to *H. pylori* infection, which would modify the immune parameters observed in this study. This exclusion criterion has been used previously in human *H. pylori* studies, and in work by the research group[37 259].

In this cohort study, *H. pylori* status and other risk factors for colonisation and disease were measured. Data was collected on parameters such as age, sex, ethnicity, CagA status, smoking status, indication for endoscopy referral, and atopic conditions such as allergies and asthma. This has been analysed in other studies, as it is useful in finding trends in populations who may be at an increased risk of disease. Another study used this detailed questionnaire to note that there is a uniform decline in *H. pylori* colonisation across generations in 9 ethnicities in the Netherlands[32]. Unfortunately, the number of *H. pylori*-positive patients with asthma/allergies in this cohort was too low to be analysed further as a separate study group.

CagA status was determined from serum collected from donated blood samples. Around 60-70% of *H. pylori* strains are CagPAI$^+$, and its presence is associated with the development of gastric cancer[261]. The research group previously found that CagPAI can induce CCL20 in infected mucosa, which then acts as a chemoattractant ligand for CCR6 on peripheral blood Tregs[149]. CagPAI$^+$ strains also induce higher levels of IL-10 expression in the infected mucosa. However, no differences in IL-10-producing CD4$^+$ lymphocyte frequencies were found in blood between infected and uninfected patients (data not shown), and no significant differences could be observed regarding CagA status, which is in accordance with previous work[37 149].

Contrary to a prior study, all patients who had multiple rounds of eradication failure were infected with CagA positive *H. pylori* strains[262]. Smoking status and eradication failure could not be studied further because only one smoker had eradication failure, although they did have PUD. This is important in understanding the causes of eradication failure, and developing strategies to prevent this occurrence further[63]. Alcohol intake was also listed as a reason for eradication failure, because it competes with metronidazole efficacy, but patients were expressly told not to drink.

What is yet unknown is whether it is the eradication of *H. pylori*, the use of PPIs, and/or the mechanism of antibiotics which drives a decline in IL-10 production by Tregs after eradication. PPIs are known to lower the acidity of the stomach, and combined with antibiotic use may alter the composition of microbiota. While the clearance of *H. pylori* before the development of atrophy may prevent the development of cancer, atrophy appears to be the crucial step for carcinogenesis[5]. In a study following up on adverse clinical events 5 years post-eradication therapy, all new cases of gastric cancer had occurred in patients with pre-existing pre-cancerous lesions in the gastric mucosa[256].

Observing the effect of eradication therapy on the Treg frequencies within blood from an uninfected patient cohort (who would be treated with antibiotics, and donated blood over time) was originally included in the study design. This would have also served as a control group to observe whether eradication drove the decline of IL-10 production in previously infected individuals to a level comparable to uninfected individuals. However, there are ethical difficulties in administering unnecessary antibiotics, which could trigger adverse clinical events[263]. This element of the study design was therefore abandoned.

### 2.6.6 Unanswered questions and future work

The data in this study showed that while there is a distinctive decline in IL-10 production by $CD4^+$ T and Treg lymphocytes, there is a variation in the regulatory immune response after *H. pylori* eradication. This variation, combined with issues such as patient compliance, antibiotic resistance, differences in gastric pH, host polymorphisms and a variance in bacterial load, suggests that it is unlikely that there will be a one-size-fits-all approach to treatment, even with fresh hopes for a *H. pylori* vaccine[16]. It is not yet known whether all *H. pylori*-infected individuals should be treated with the same therapy, given that that there might be consequences to eradicating a bacterium that has colonised the gastric mucosa for thousands of years.

The discussion of *H. pylori* eradication is also important because of rising antibiotic resistance cases globally. While the 12% eradication failure in this study is consistent with the European Maastricht findings[263] and reported failure rates for therapy[63], patient T048's persistent *H. pylori* infection is a troubling foreshadowing of a post-antibiotic future. This patient will require close monitoring to ensure no adverse outcomes result from her current PUD diagnosis, or any development of pre-clinical oncology[42].

As a potent immunomodulatory cytokine, IL-10 has been thought to be an important functional mediator of Treg activity. A weakness of this study is that it has only examined the frequencies of certain Treg subtypes, and not the suppressive capabilities of IL-10-producing $CD4^{+}CD25^{hi}$ Tregs[117]. Future functional assays of suppression should be done to determine whether $CD4^{+}CD25^{hi}IL\text{-}10^{+}$ cells in PBMCs can indeed be described as 'regulatory T cells'. Data on whether these cells can inhibit the proliferation and activity of effector T cells would also provide more information on the immunosuppressive effects of the infection. As this requires many cells, and Tregs are not plentiful in blood, a larger blood sample could be taken and cells could be sorted using a flow cytometer.

In addition to Tregs, IL-10 is also produced by many different cell types such as B cells, DCs, mast cells, macrophages, NK cells and neutrophils[168]. Recently, reports of an IL-10-producing subset of B cells (Bregs) has been described as playing a role in *H. pylori* infection in mice. One paper goes further to suggest that a decreased Breg function in human blood is indicative of an increased risk of gastric cancer development[225]. Observing the proportion of IL-10-producing B cells to T cells would also further elucidate the immune responses involved in the infected mucosa. IL-10 promotes the differentiation of IL-10-producing Tregs in a positive feedback loop[168], and it is yet to be studied if this is the case with other IL-10-producing cells. Furthermore, any correlation between Breg and $IL\text{-}10^{+}$ Breg frequencies and the incidence of *H. pylori*-mediated disease could potentially be identified as a risk factor.

Using stored extra cells and serum, this flow cytometry panel should be repeated to ensure that technical errors can be identified. Samples in this study were processed by different researchers. Therefore, once the study is completed, all samples from a single patient could be analysed together to ensure that there is no difference in the way the samples were processed. This repeat panel could be expanded to include other lymphocytes which may produce IL-10 *e.g.* B cells and NKT cells. Inflammatory markers such as IFN-γ could be used to identify differences in pro-inflammatory host responses to *H. pylori* infection. Furthermore, other Treg markers (such as CD127, Helios, TIGIT, FCRL3 and CD226) could be added to the panel to further investigate IL-10$^{+}$ T cell subsets[157 264].

The use of multiple fluorochromes in an antibody panel requires a balance of expression levels and fluorochrome brightness to prevent falsely positive populations being analysed. This is particularly important when studying small, rare populations such as regulatory cell frequencies in human blood. Further work in expanding this panel could include more internal controls. Although there were stimulation and isotype controls, unstained and single stain controls would provide a baseline of cellular autofluorescence and prevent batch-to-batch variations of fluorochrome-conjugated antibodies.

The wealth of information generated from the data on each patient in this study means that while this study is ongoing, various parameters can be linked with observed trends in disease. Sex, age and smoking are already known factors linked to an increased risk of disease, but future work could also describe the VacA type of colonised strains. The VacA i1 variant has already been described as an independent risk factor for disease[84]. This could also be linked to CagA types which are also linked to disease patterns. Using PCR, the presence of multiple EPIYA-C motifs (Western strains), or the presence of a single EPIYA-D motif (East Asian strains) could also model predictions for disease risk[261]. This can also be linked to race, as it has been reported that Japanese patients with Western strains are less likely to develop disease, than Japanese patients with East Asian colonising strains[265]. It is interesting

that while being associated with the most virulent forms of *H. pylori*-mediated disease, CagPAI is both selected for and lost from strains colonising the mucosa[68].

A final follow-up of this patient cohort after 5 years from eradication could provide a lot of information on the eradicated stomach. This includes information such as whether any adverse symptoms/effects have been linked to *H. pylori* clearance or the use of antibiotics, whether their initial GI complaint was resolved after treatment, the frequency of Tregs and IL-10$^{+}$ Tregs in their blood compared to during *H. pylori* infection, and whether this decreases or plateaus after 5 years.

Eradicated patients are a useful group that should be tapped into further for research projects. This could help further analysis of the mechanisms of protection against disease that *H. pylori* infection has been linked to[34]. There are no known studies on the direct effect of *H. pylori* infection on MS in humans[34] in the literature. Studying *H. pylori* infection in humans is difficult, but there have been published vaccine studies which have deliberately infected adults with *H. pylori* infection[266-268]. This has involved infecting adults with CagA$^{-}$ strains, and concluding the study with eradication therapy to prevent adverse consequences in the volunteers[266 267]. It has not been described whether infection from childhood is protective, or purposeful infection as an adult is enough for extra-gastric protection[34]. As *H. pylori* infection is linked with MS, and both conditions require Treg immunomodulatory activity, it would be useful clinically to understand any exacerbations as a consequence of eradication. Furthermore, this would further the work on childhood asthma, an arising condition in the UK[39 269]. Connection in research may determine whether children with *H. pylori* infection should or should not be eradicated if at an increased risk of developing asthma, or if eradication could be delayed until the patient is older to attain potential extra-gastric protection.

The role of microbiota in the infected stomach is not yet fully understood, and the effects of *H. pylori* eradication on microbial populations was not investigated in this study. One study that sequenced gut microbiota populations after *H. pylori*

eradication did not show any major permanent disruption to the mean relative abundance of various bacterial species in human microbiota[259].

The use of clarithromycin in front-line therapy means that clarithromycin resistance could be tested via PCR in this project. Kits for testing clarithromycin susceptibility are now commercially available[270]. Using this would provide insight into the reasons for eradication failure in this study, and to compare results against the reported growing resistance rates in Europe.

While it might not be ethical to leave *H. pylori* infection untreated if found to be protective for another condition, the administration of components of *H. pylori* in a therapy could help to continue conferring this protection. Such components may include modified GGT or VacA as Treg-inducing components that could be used to treat autoimmune conditions. Transplants of Tregs in mice have been shown to alleviate allergen-induced asthma[39], and this transfer of Tregs could potentially be used as a therapy for certain auto-immune conditions in humans[271].

### 2.6.7 Conclusions

- 50 patients were followed up after a successful (or unsuccessful) *H. pylori* eradication therapy regime.

- After 2 years of being uninfected, frequencies of $CD4^+CD25^{hi}$ and $CD4^+Foxp3^+$ Treg frequencies in the blood did not change significantly from infection.

- IL-10 production by $CD4^+$ T-helper cells, and the subset $CD4^+CD25^{hi}$ Tregs decreased significantly from infection at Month 6, and this trend continued until Month 24.

- Frequencies of $CD4^+IL\text{-}10^+$ and Tregs did not differ significantly in patients who had eradication failure, but sample numbers were very low.

## Chapter 3: Pilot study characterising IL-10-producing B cells in mice

### 3.1 Introduction

Identifying whether certain individuals are more likely to develop *H. pylori*-mediated disease is important so that they are treated before irreversible pre-malignant pathology develops, which can often be asymptomatic. Previously, the role of Tregs as a marker for disease has been studied in depth. Infected individuals who have a poor Treg response to *H. pylori* infection are more likely to develop PUD and pre-malignant pathology[87 119]. Levels of the immunomodulatory cytokine IL-10 is a good measure of Treg activity in suppressing the pro-inflammatory response to the infection. A reduced IL-10 response has also been observed in infected patients who are smokers, and this group are also more likely to have PUD[59].

Recent papers have identified B cells as another lymphocytic cell source of IL-10 production[209]. This 'regulatory' B cell (Breg) type could play a role in the *H. pylori*-infected mucosa, and may contribute to disease outcomes in a manner not observed previously. Upon *in vitro* stimulation, it has been suggested that in mice these IL-10-producing Bregs have a specific $CD1d^{hi}CD5^{+}$ phenotype[218]. Additionally, it has been shown that Bregs can also modulate and promote Treg differentiation in humans[193].

The importance of the immune response in *H. pylori* infection has long been established. Host genetic polymorphisms leading to an increased expression of pro-inflammatory cytokine genes such as IL-8, and the low frequency of Tregs has already been linked to an increased risk of disease (**Section 1.6.2.3**). Bregs may limit the development of peptic ulceration or gastric cancer by controlling mucosal inflammation. Conversely, they may also contribute to *H. pylori*-induced MALT lymphoma. Analysis of the existence and function of Bregs is important for many reasons. Firstly, it would provide a more complete picture of the infected mucosa, and provide an understanding of the ways in which IL-10 production, and other mechanisms of immunoregulation, protect us from disease. The frequency of Bregs and IL-10 production has yet to be studied after the successful eradication of *H. pylori*.

In addition, Bregs may also contribute to potential mechanisms of *H. pylori*-mediated protection against extra-gastric diseases. The role of IL-10-producing Bregs in this context has not yet been described in the literature.

## 3.2 Hypotheses

Upon *H. pylori* infection, B and $CD4^+$ T cell populations expand, and there are increased frequencies of IL-$10^+$ B and T cells, to limit the tissue damage caused by inflammation in the gastric mucosa. Splenic Breg and Treg populations also expand significantly and produce IL-10.

## 3.3 Aims

The aim of this pilot study was to characterise and compare the size of splenic regulatory B and T lymphocyte populations in mice during *H. pylori* infection. The level of IL-10-secreting lymphocytes was assessed, and the balance of IL-$10^+$ B cells and IL-$10^+$ $CD4^+$ T cells was compared.

## 3.4 Materials and methods

### 3.4.1 Study management

This experiment was conducted under the Home Office Licence 40/3399 by Dr. Karen Robinson, Dr. Darren Letley and Dr. Kazuyo Kaneko (Nottingham, UK) in Queen's Medical Centre, Nottingham. I analysed the data from this experiment. This experiment was approved by the University of Nottingham Animal Welfare and Ethical Review Body. Reagents were obtained from Sigma-Aldrich, unless otherwise stated.

### 3.4.2 Animals

Female Foxp3-Green Fluorescent Protein (GFP) transgenic C57BL/6 mice were bred in the Biomedical Services Unit at the University of Nottingham, and housed in individually ventilated cages.

### 3.4.3 *H. pylori* infection

*H. pylori* strain SS1 was thawed from stocks and cultured on 5% horse blood agar plates (Oxoid) at 37°C in a microaerophilic incubator. After 24 hours, *H. pylori* growth was collected and suspended in 1ml Brucella broth to obtain a desired optical density (O.D.) of 1 at a wavelength of 600nm.

Groups of four female 6-week-old Foxp3-GFP C57BL/6 mice were infected with *H. pylori* SS1 in 100µl Brucella broth via oral gavage, or given 100µl plain Brucella broth as a control. *H. pylori* viability was measured by plating serial dilutions onto agar plates and incubating for 72 hours. The mice were inoculated with a 1 x $10^9$ dose on three alternative days, and their body weights were recorded on a weekly basis. After three weeks, the mice were killed, and their spleens were removed and collected individually in sterile PBS. These tubes were stored on ice until further processing. A urease test was performed on extracted gastric tissue to confirm infection status.

### 3.4.4 Isolation of lymphocytes from mouse spleen

After being collected in PBS, individual murine spleen tissue was rubbed through a sterile disposable 100µM cell strainer (BD Biosciences), then pipetted into tubes, and washed twice in 25ml culture medium. Red Blood Cell lysing buffer was added for 20 seconds to eliminate erythrocytes before the cells were then washed, counted and resuspended as described previously (**Section 2.4.6.1**).

### 3.4.5 *In vitro* stimulation

At a concentration of 1 x $10^6$/ml, half the splenocytes were stimulated to induce IL-10 production. The cells were stimulated for six hours at 37°C with a combination of *E. coli* LPS (10µg/ml), phorbol myristate acetate (PMA) (50ng/ml), and ionomycin (1µg/ml). The remaining splenocytes were left unstimulated. BFA (10µg/ml) was added to all tubes after one hour of stimulation. After the six hours, all cells were then stored at 4°C prior to cell staining.

### 3.4.6 Flow cytometry analysis

#### 3.4.6.1 Fluorochromes

The properties of the fluorochrome dyes used for the MoFlo Astrios flow cytometer (Beckman Coulter) are described below (**Table 3.1**).

**Table 3.1:** The properties of fluorochromes used in the flow cytometry panel for the pilot study.

| Fluorophore | Abbreviation | Excitation laser nm | Emission filter | Emission bandwidth nm |
|---|---|---|---|---|
| Alexa Fluor 647 | AF647 | 642 | 671/30 | 656-686 |
| Phycoerythrin | PE | 488 | 576/21 | 565.5-586.5 |
| Phycoerythrin-Cyanin 7 | PE/Cy7 | 561 | 795/70 | 760-830 |
| Phycoerythrin-Texas Red | PE/TxR | 488 | 513/26 | 500-526 |

### 3.4.6.2 Antibody panels for Bregs and Tregs

Cells were stained using rat fluorochrome-conjugated antibodies in the following combinations detecting Bregs (**Table 3.2**) or Tregs (**Table 3.3**).

**Table 3.2:** Panel of antibodies used to identify mouse splenic populations of regulatory B cells.

| Marker/ Isotype | Fluorochrome | Species subtype | Company | Catalogue no. | Clone | Concentration | Volume |
|---|---|---|---|---|---|---|---|
| CD1d | PE | rat IgG2b | eBioscience | 12-0011-81 | 1B1 | 0.2 mg/ml | 1µl |
| iso-CD1d | PE | rat IgG2b | BioLegend | 400608 | RTK4530 | 0.2 mg/ml | 0.5µl |
| CD5 | PE/Cy7 | rat IgG2a | BioLegend | 100621 | 53-7.3 | 0.2 mg/ml | 1µl |
| iso-CD5 | PE/Cy7 | rat IgG1 | BioLegend | 400416 | RTK2071 | 0.2 mg/ml | 0.5µl |
| CD19 | PE/Texas Red | rat IgG2a | Invitrogen | RM7717 | 6D5 | 0.05 mg/ml | 1µl |
| IL-10 | AF647 | rat IgG2b | BioLegend | 505016 | JES5-16E3 | 0.5 mg/ml | 1µl |
| iso-IL-10 | AF647 | rat IgG2b | BioLegend | 400628 | RTK4530 | 0.5 mg/ml | 0.5µl |

**Table 3.3:** Panel of antibodies used to identify mouse splenic populations of regulatory T cells.

| Marker/ Isotype | Fluorochrome | Species subtype | Company | Catalogue no. | Clone | Concentration | Volume |
|---|---|---|---|---|---|---|---|
| CD4 | PE/Texas Red | rat IgG2a | Invitrogen | MCD0417 | RM4-5 | 0.2 mg/ml | 1µl |
| IL-10 | AF647 | rat IgG2b | BioLegend | 505016 | JES5-16E3 | 0.5 mg/ml | 1µl |
| iso-IL-10 | AF647 | rat IgG2b | BioLegend | 400628 | RTK4530 | 0.5 mg/ml | 0.5µl |

#### 3.4.6.3 Cell staining

The lymphocytes were centrifuged briefly at 1100 RPM for 5 minutes, before the fluorochrome-conjugated antibodies for surface markers were added to the cell pellets. These were gently mixed by pipette and incubated on ice in the dark for 30 minutes, with occasional mixing. All incubations described took place in the dark. The cells were then washed twice with 1ml PBA/2% FCS before being fixed in 500µl Fixation Buffer containing 4% paraformaldehyde (BioLegend).

After fixation, the cells were washed with 1ml PBA. Tubes not requiring permeabilisation for IL-10 were then stored overnight at 4°C in the dark. Other tubes were then washed once with 1ml PBA containing 1% saponin, and then with 1ml PBA with 1% saponin and 10% FCS. The anti-IL-10 antibody and corresponding isotype control were then added to the permeabilised cells, before they were kept incubated on a shaker at 4°C for 2 hours. The cells were then washed 3 times with PBA, before being resuspended in 0.5ml PBA for flow cytometry analysis.

#### 3.4.6.4 Flow cytometry

Multi-colour flow cytometry analysis was completed using a MoFlo Astrios flow cytometer (Beckman Coulter). Using a predetermined lymphocyte gate, data on 200,000 events was collected and analysed using Kaluza software (Beckman Coulter), with respect to appropriate isotype and single-stain controls. Samples were gated on forward and side scatter under the 488nm laser to exclude dead cells and debris.

## 3.5 Results

Following analysis on Kaluza software, a gating strategy was developed to ensure the consistent identification of positive and negative populations of each B cell, Breg, helper T cell and Treg markers individually, and in combination with each other. The gating strategy was applied to all mouse spleen samples. $CD4^+IL\text{-}10^+$ and $CD4^+CD25^{hi}$ events were gated according to previous work by the research group[95 119]. Samples were excluded from final analysis when there were fewer than 50,000 events per tube.

Firstly, mouse $CD19^+$ and $CD4^+$ splenic lymphocyte frequencies were compared to determine whether these populations had expanded during *H. pylori* infection. The frequencies of B cells amongst gated lymphocytes increased by an average of 34% after infection ($p = 0.0091$) (**Figure 3.1C**).

$CD4^+$ T cell frequencies accounted for a mean of 16% of the gated lymphocyte population in the spleen of uninfected mice (**Figure 3.2B**). This increased marginally to 19% when the mice were infected ($p = 0.0294$) (**Figure 3.2C**).

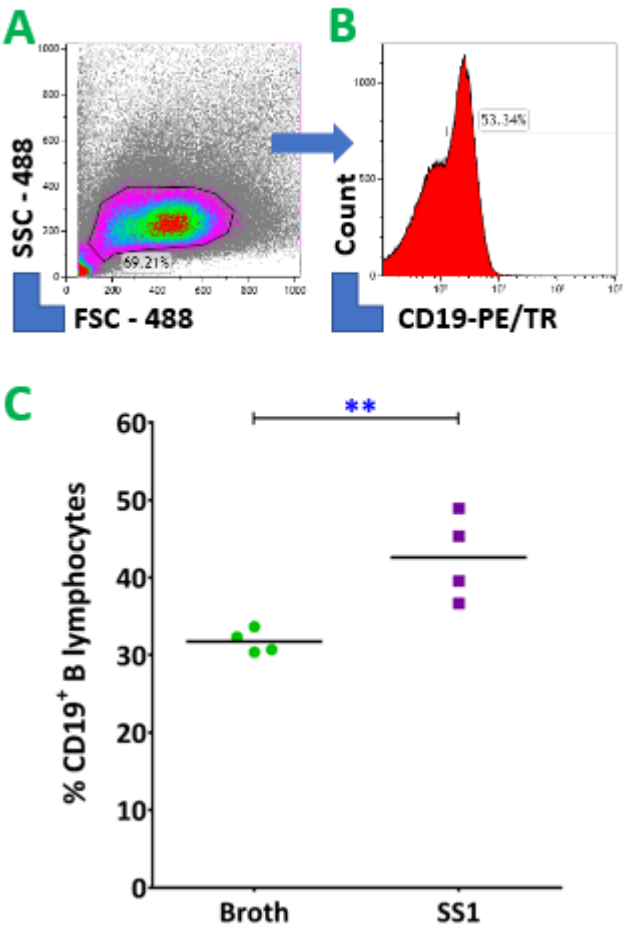



**Figure 3.1:** Representative flow cytometry plots, the gating scheme, and analysis of splenic CD19$^+$ lymphocytes. Mouse spleen cells were stained with rat fluorochrome-conjugated antibodies to identify CD19$^+$ B lymphocytes. (A) Lymphocyte population gated by forward (FSC) and side (SSC) scatter under the 488nm laser. (B) Histogram showing CD19$^+$ events amongst gated lymphocytes. (C) Proportions of splenic CD19$^+$ lymphocytes in mice orally dosed with *H. pylori* SS1 strain (SS1), compared to mice given Brucella broth only (Broth). The horizontal lines depict the mean value. Statistical analysis was performed using an unpaired T-test. The asterisks indicate the level of statistical significance, where ** represents $p < 0.01$.

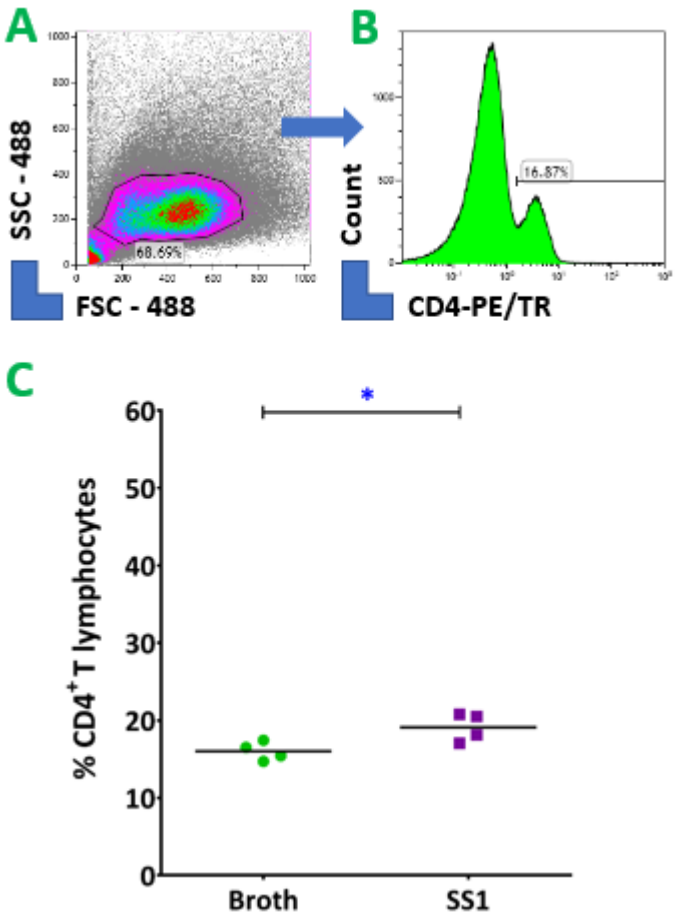



**Figure 3.2:** Representative flow cytometry plots, the gating scheme, and analysis of splenic $CD4^+$ lymphocytes. Mouse spleen cells were stained with rat fluorochrome-conjugated antibodies to identify $CD4^+$ B lymphocytes. (A) Lymphocyte population gated by forward (FSC) and side (SSC) scatter under the 488nm laser. (B) Histogram showing $CD4^+$ events amongst gated lymphocytes. (C) Proportions of splenic $CD4^+$ lymphocytes in mice orally dosed with *H. pylori* SS1 strain (SS1), compared to mice given Brucella broth only (Broth). The horizontal lines depict the mean value. Statistical analysis was performed using an unpaired T-test. The asterisks indicate the level of statistical significance, where * represents $p < 0.05$.

Studies have shown that regulatory B and T lymphocytes express IL-10 when stimulated. Therefore, the proportions of IL-10$^{+}$ lymphocytes were then analysed using the B cell and T cell antibody panels shown in **Tables 3.2** and **3.3**. CD4$^{+}$IL-10$^{+}$ events were gated according to previous work by the research group[95 119]. The PMA/ionomycin/LPS stimulation of cells was effective in inducing IL-10, with a four-fold increase in the frequency of IL-10$^{+}$ lymphocytes in splenocytes from both infected and uninfected mice (**Figures 3.3** and **3.4**). Both antibody staining panels demonstrated a slightly increased frequency of IL-10$^{+}$ lymphocytes during *H. pylori* infection, but this did not achieve statistical significance.

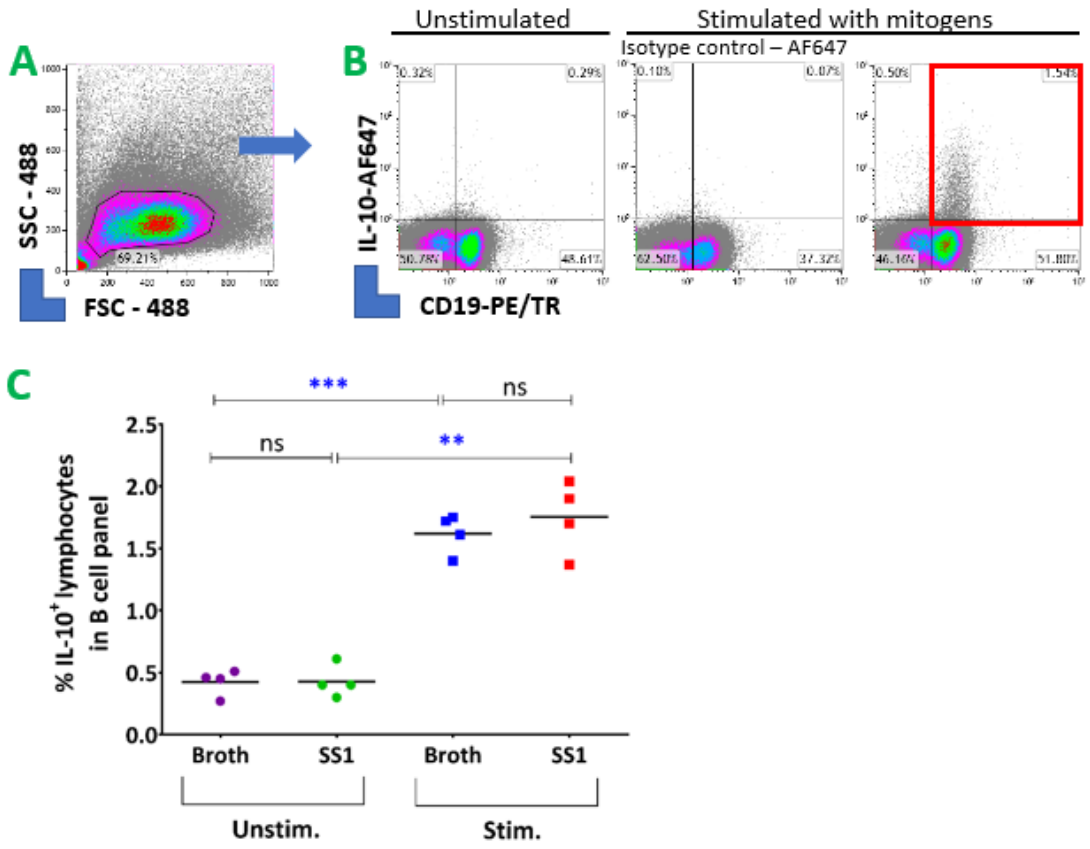



**Figure 3.3:** Representative flow cytometry plots, the gating scheme, and analysis of the proportions of IL-10$^+$ lymphocytes in groups of mice orally dosed with *H. pylori* strain SS1 (SS1) or given plain Brucella broth (Broth). Cells were stimulated (Stim.) with a combination of PMA, ionomycin and *E. coli* LPS for 6 hours, or left unstimulated (Unstim.). Mouse spleen cells were stained with rat fluorochrome-conjugated antibodies to identify IL-10$^+$ B lymphocytes. (A) Lymphocyte population gated by forward (FSC) and side (SSC) scatter under the 488nm laser. (B) Representative CD19-IL-10 plots from gated lymphocytes (left to right) anti-IL-10 stained and unstimulated cells, and anti-IL-10-stained and stimulated cells with its corresponding isotype control. (C) Cells were analysed using the B cell antibody panel. The horizontal lines depict the mean value. Statistical analysis of differences between stimulated and unstimulated cells was carried out using a paired T-test, while differences between the two groups of mice were analysed with an unpaired T-test. The asterisks indicate the level of statistical significance, where *** represents $p < 0.001$. ns = not statistically significant.

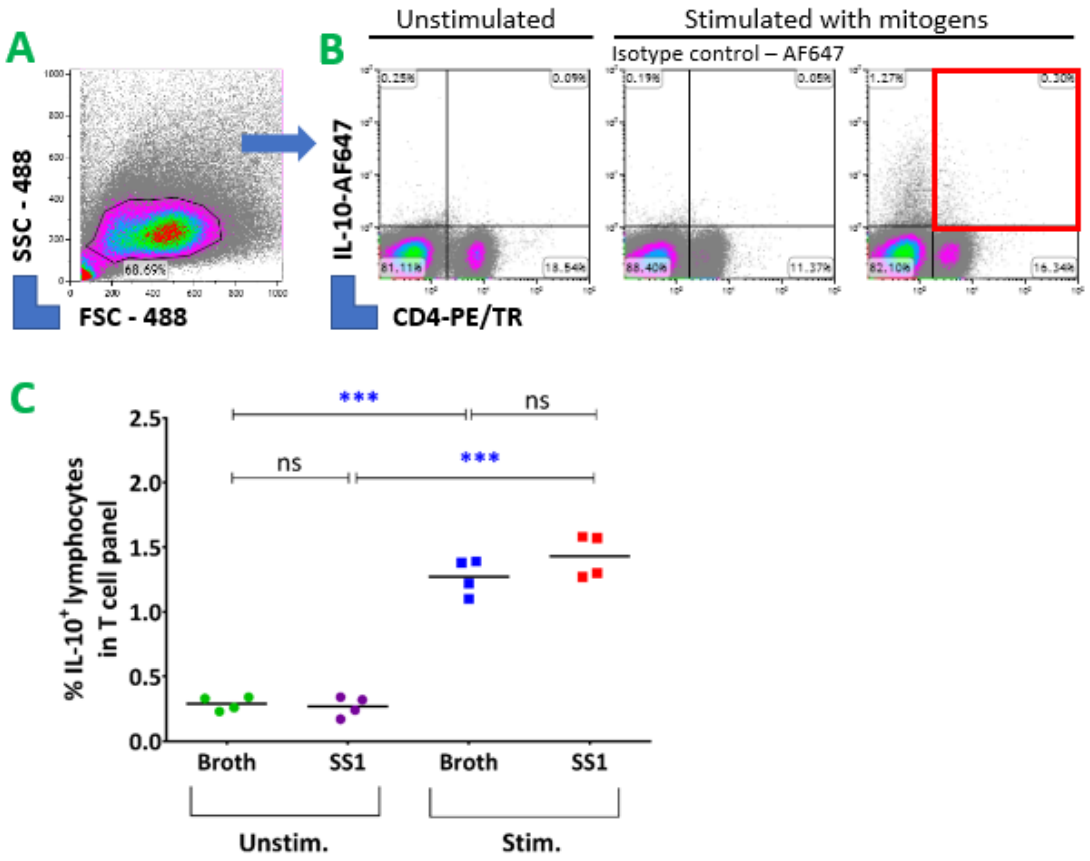



**Figure 3.4:** Representative flow cytometry plots, the gating scheme, and analysis of the proportions of IL-10$^+$ lymphocytes in groups of mice orally dosed with *H. pylori* strain SS1 (SS1) or given plain Brucella broth (Broth). Cells were stimulated (Stim.) with a combination of PMA, ionomycin and *E. coli* LPS for 6 hours, or left unstimulated (Unstim.). Mouse spleen cells were stained with rat fluorochrome-conjugated antibodies to identify IL-10$^+$ T lymphocytes. (A) Lymphocyte population gated by forward (FSC) and side (SSC) scatter under the 488nm laser. (B) Representative CD4-IL-10 plots from gated lymphocytes (left to right) anti-IL-10 stained and unstimulated cells, and anti-IL-10-stained and stimulated cells with its corresponding isotype control. (C) Cells were analysed using the T cell antibody panel. The horizontal lines depict the mean value. Statistical analysis of differences between stimulated and unstimulated cells was carried out using a paired T-test, while differences between the two groups of mice were analysed with an unpaired T-test. The asterisks indicate the level of statistical significance, where *** represents $p < 0.001$. ns = not statistically significant.

Several published studies have reported that *H. pylori* infection results in an increased IL-10$^+$ CD4$^+$ cell response[110 119]. Many different lymphocytic cell types are also known to secrete IL-10, including B cells, CD4$^+$ and CD8$^+$ T cells, NK cells, and invariant lymphoid cells[168]. The presence of these IL-10$^+$ cell types may mask differences in the frequencies of certain IL-10-producing lymphocyte subsets. Therefore, the gated splenocytes were then analysed to compare the relative proportions of IL-10$^+$ events amongst B and CD4$^+$ T lymphocytes (**Figure 3.5**).

An average of 74% of the IL-10$^+$ lymphocyte frequencies were CD19$^+$ cells, suggesting that B cells are the primary source of IL-10 in the lymphocyte population. This proportion was similar in both groups of mice, although as shown in (**Figure 3.1**), there was a 34% expansion of B cells following *H. pylori* infection. This suggests that the total number of IL-10$^+$ B cells would also be increasing accordingly. CD4$^+$ T cells accounted for a mean of 12% of the IL-10$^+$ lymphocytes. This was raised to 19% during *H. pylori* infection ($p$ = 0.0256).

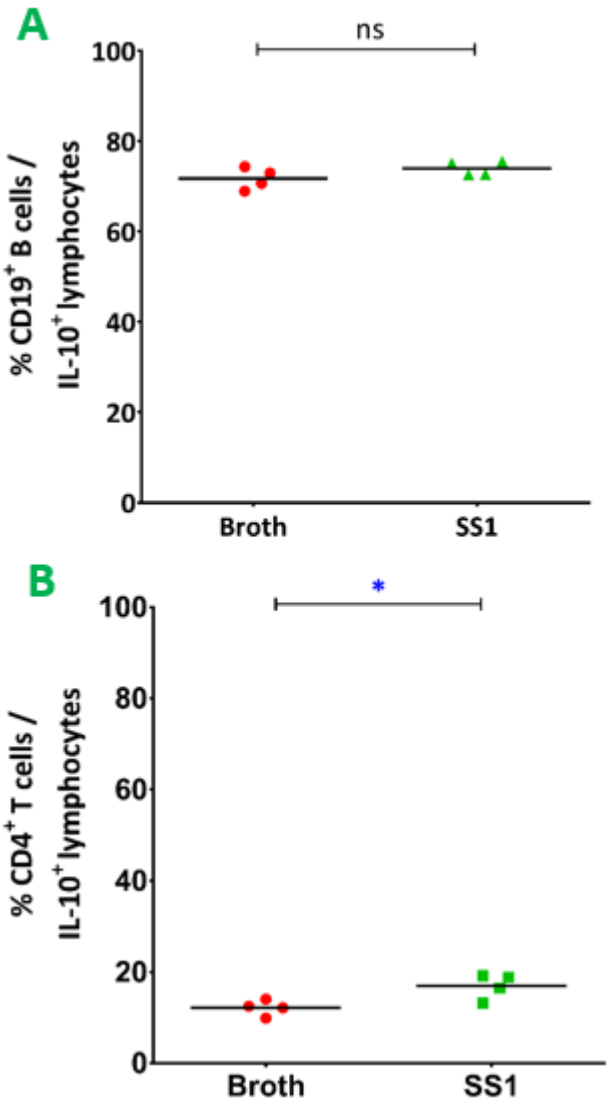



**Figure 3.5:** Proportion of splenic IL-10$^+$ lymphocytes in groups of mice orally dosed with *H. pylori* strain SS1 (SS1), or given plain Brucella broth (Broth). Mouse spleen cells were stained with rat fluorochrome-conjugated antibodies to identify IL-10$^+$ T lymphocytes. Cells were stimulated with a combination of PMA, ionomycin and *E. coli* LPS for 6 hours. (A) Proportion of IL-10$^+$ lymphocytes which are CD19$^+$ B cells. (B) Proportion of IL-10$^+$ lymphocytes which are CD4$^+$ T cells. The horizontal lines depict the mean value. Statistical analysis was carried out using an unpaired T-test. The asterisks indicate the level of statistical significance, where * represents $p < 0.05$. ns = not statistically significant.

Within this expanded B cell population, it was hypothesised that there would be Bregs present during *H. pylori* infection. As a subset of the CD19$^{+}$ B cell population, Bregs require more than one marker to identify them. Further analysis was therefore carried out to quantify the CD1d$^{hi}$CD5$^{+}$ Bregs amongst the total CD19$^{+}$ B cell population (**Figure 3.6**). *H. pylori* infection induced a significant increase for increased proportions of CD1d$^{hi}$CD5$^{+}$ cells; with a 30% increase in Breg proportions following stimulation (**Figure 3.7**).

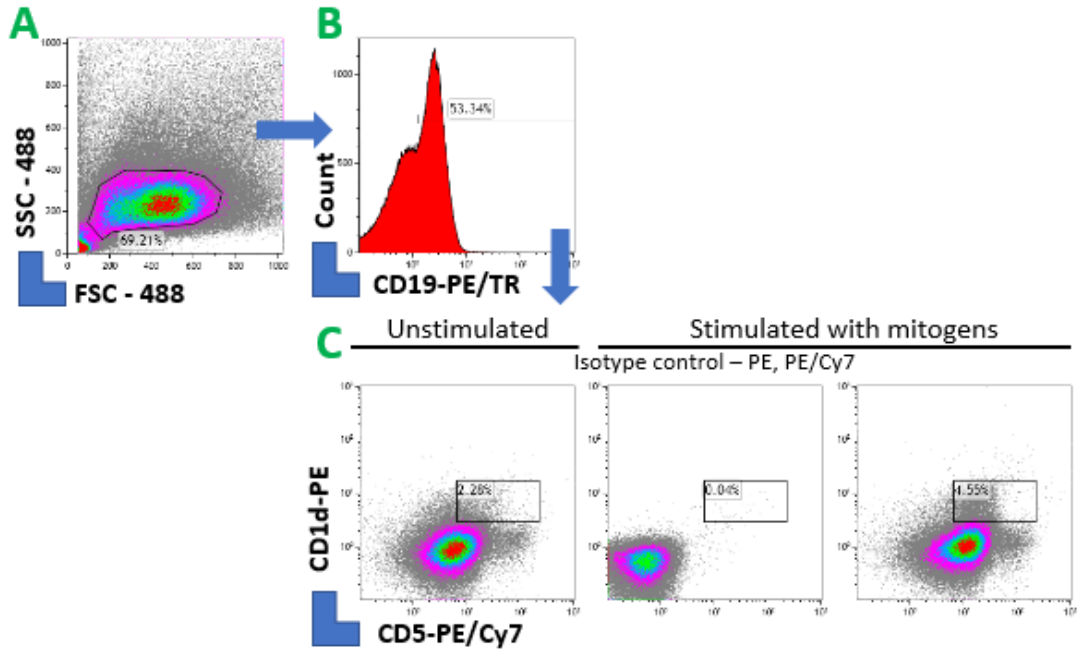



**Figure 3.6:** Representative flow cytometry plots and the gating analysis scheme for splenic CD1d$^{hi}$CD5$^{+}$ Bregs from mice orally dosed with *H. pylori* strain SS1 (SS1), or given plain Brucella broth (Broth). Cells were either stimulated (Stim.) with a combination of PMA, ionomycin and *E. coli* LPS for 6 hours, or left unstimulated (Unstim.). Mouse spleen cells were stained with rat fluorochrome-conjugated antibodies to identify CD1d$^{hi}$CD5$^{+}$ Bregs. (A) Lymphocyte population gated by forward (FSC) and side (SSC) scatter under the 488nm laser. (B) Histogram showing CD19$^{+}$ events amongst gated lymphocytes. (C) Representative CD1d-CD5 plots from CD19$^{+}$ gated lymphocytes (left to right) unstimulated cells, and stimulated cells with its corresponding isotype control.

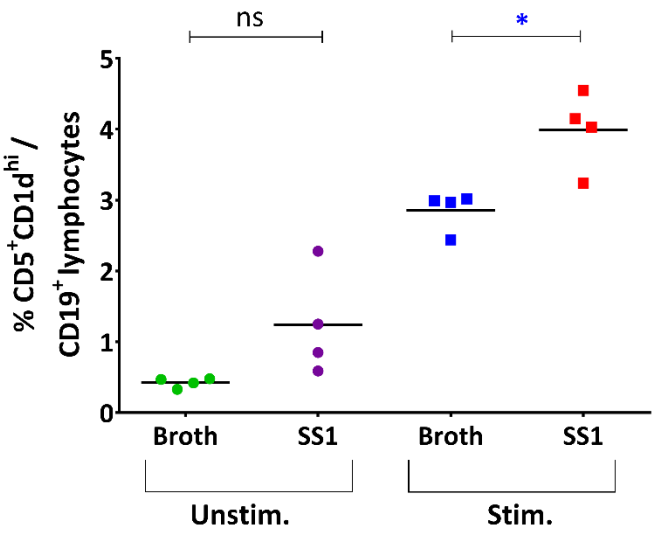



**Figure 3.7:** Proportion of splenic CD1d$^{hi}$CD5$^{+}$ Bregs within the CD19$^{+}$ B cell population from mice orally dosed with *H. pylori* strain SS1 (SS1), or given plain Brucella broth (Broth). Mouse spleen cells were stained with rat fluorochrome-conjugated antibodies to identify CD1d$^{hi}$CD5$^{+}$ Bregs. The horizontal lines depict the mean value. Statistical analysis of differences between stimulated and unstimulated cells was carried out using a paired T-test, while differences between the two groups of mice were analysed with an unpaired T-test. The asterisks indicate the level of statistical significance, where * represents $p < 0.05$. ns = not statistically significant.

Because B cells were identified as the primary lymphocytic source of IL-10 (**Figure 3.5A**), and IL-10 is thought to be a major Breg factor, proportions of IL-10$^{+}$ CD19$^{+}$CD1d$^{hi}$CD5$^{+}$ events were then analysed (**Figure 3.8**). The proportion of CD19$^{+}$CD1d$^{hi}$CD5$^{+}$ events producing IL-10 appeared to show an increased trend after *H. pylori* infection, but this did not achieve statistical significance.

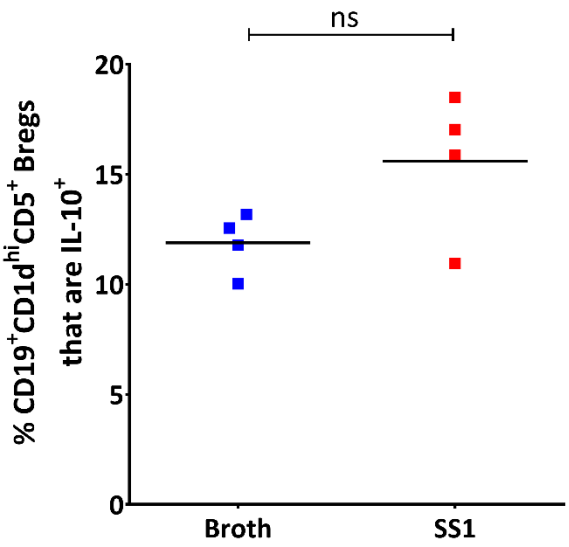



**Figure 3.8:** Proportion of splenic IL-10-producing CD19$^{+}$CD1d$^{hi}$CD5$^{+}$ Bregs in mice orally dosed with *H. pylori* strain SS1 (SS1), or given plain Brucella broth (Broth). Cells were stimulated with a combination of PMA, ionomycin and *E. coli* LPS for 6 hours. Mouse spleen cells were stained with rat fluorochrome-conjugated antibodies to identify IL-10-producing CD1d$^{hi}$CD5$^{+}$ Bregs. The horizontal lines depict the mean value. Statistical analysis was carried out using an unpaired T-test. ns = not statistically significant.

During analysis of spleen cells stained with the T cell antibody panel (**Table 3.3**), it was possible to assess $Foxp3^+$ events by the detection of GFP in these Foxp3-GFP transgenic mice. The Foxp3-GFP marker was used to quantify the frequency of regulatory T cells amongst the $CD4^+$ T cell population (**Figure 3.9B**).

The proportion of Tregs was found to be a little higher during *H. pylori* infection ($p$ = 0.0040) (**Figure 3.9C)**. Since Foxp3 is reported to be transiently upregulated on T cell activation, it was interesting to observe that there was a 25-30% increase in the frequency of $Foxp3^+CD4^+$ events after PMA/ionomycin/LPS stimulation.

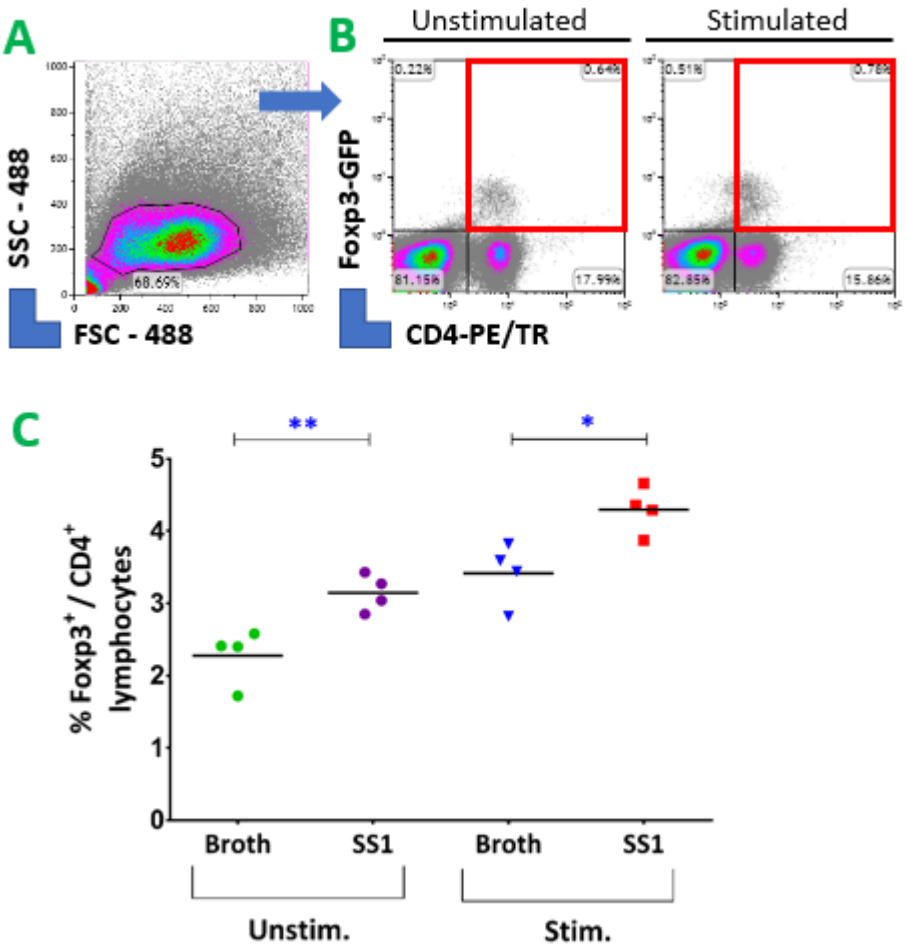



**Figure 3.9:** Representative flow cytometry plots, gating strategy and analysis of the proportion of splenic $CD4^+Foxp3^+$ Tregs from Foxp3-GFP-transgenic mice orally dosed with *H. pylori* strain SS1 (SS1), or given plain Brucella broth (Broth). Cells were either stimulated (Stim.) with a combination of PMA, ionomycin and *E. coli* LPS for 6 hours, or left unstimulated (Unstim.). Mouse spleen cells were stained with rat fluorochrome-conjugated antibodies to identify $CD4^+Foxp3^+$ Tregs. (A) Lymphocyte population gated by forward (FSC) and side (SSC) scatter under the 488nm laser. (B) Representative CD4-Foxp3 plots from gated lymphocytes (left to right) unstimulated cells, and stimulated cells. (C) Proportion of splenic $Foxp3^+$ lymphocytes from the $CD4^+$ T cell population. The horizontal lines depict the mean value. Statistical analysis of differences between the two groups of mice were analysed with an unpaired T-test. The asterisks indicate the level of statistical significance, where * represents $p < 0.05$ and ** represents $p < 0.01$.

Since IL-10 is an established marker for Tregs, proportions of IL-10-producing $CD4^+Foxp3^+$ events were then analysed (**Figure 3.10**). $IL\text{-}10^+$ Tregs were 4% of the Treg lymphocyte population following stimulation. This increased slightly during *H. pylori* infection ($p = 0.00346$).

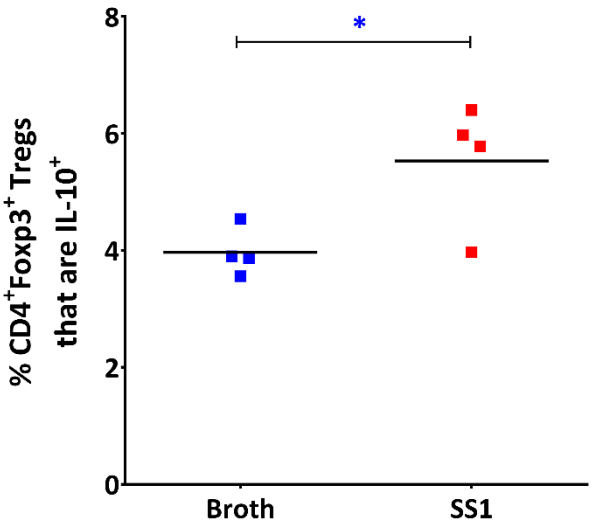



**Figure 3.10:** Proportion of splenic $IL\text{-}10^+$ $CD4^+Foxp3^+$ regulatory T cells in mice orally dosed with *H. pylori* strain SS1 (SS1), or given plain Brucella broth (Broth). Cells were stimulated with a combination of PMA, ionomycin and *E. coli* LPS for 6 hours. Mouse spleen cells were stained with rat fluorochrome-conjugated antibodies to identify IL-10-producing $CD4^+Foxp3^+$ Tregs. The horizontal lines depict the mean value. Statistical analysis was carried out using an unpaired T-test.

## 3.6 Discussion

### 3.6.1 Statement of principal findings

In this pilot study, it was observed that the populations of B and T lymphocytes expanded when mice were infected with *H. pylori*. Further analyses demonstrated that most IL-10-producing lymphocytes were B cells, and not Tregs. In response to infection, there was an expansion of the IL-10-producing Breg population, although this was not statistically significant. This indicates that the number of IL-10$^+$ B cells has increased accordingly. Foxp3$^+$ T cells expanded significantly upon infection, as did the IL-10$^+$ Treg population. Although it is acknowledged that experimental numbers in each group (n=4) were too low to draw conclusions from this pilot study, there were significant trends in the data showing the expansion of B and T cell frequencies after *H. pylori* infection.

### 3.6.2 Biological relevance of the findings

The observation that T cell populations expand after *H. pylori* infection is in line with previous work that has described a prolific T cell subset Treg expansion to infection[39 74 119 188 243]. Earlier work in the research group demonstrated that a decreased human Treg response to *H. pylori* contributed to the increased likelihood of PUD[119]. Foxp3 is a transcription factor which is permanently expressed by natural Tregs and is crucial for their immunosuppressive function. Results in the present study are comparable to other work demonstrating an increased Foxp3 expression in Tregs after *H. pylori* infection[39]. As this experiment used Foxp3-GFP transgenic mice, Foxp3 and GFP were co-expressed by Tregs. The GFP expression was then identified and analysed in a flow cytometer. Because Foxp3 and GFP were co-expressed, there were no antibody staining difficulties, or any non-specific expression, and therefore, the transgenic mouse model made Foxp3 frequency a more accurate representation.

There are few papers which suggest a role for Bregs in the immune response to *H. pylori* infection[225 243]. One study described IL-10-producing B cells which contributed to the induction of Treg responses. Results from that paper agree with the data here

describing an expansion of $CD19^+IL\text{-}10^+$ cells after *H. pylori* infection. The authors demonstrated larger frequencies of $CD19^+IL\text{-}10^+$ events (2.72%) after 2 weeks, compared to this study (1.54%) after 3 weeks[243]. However, this could be due to differences in inoculation. Wei *et al* described a five-time dose regimen of $1 \times 10^9$ *H. pylori* in Brain-Heart Infusion (BHI) broth. When compared to other established models commonly used throughout the world, the large dosage given may represent a different infection model for *H. pylori* in the gastric mucosa. Moreover, a triple dose of the suggested concentration given on alternative days has been established previously in the research group and in other studies[33 272]. It has been shown to be sufficient for colonisation in mice and provides consistent colony-forming units (CFU) counts[87]. A simple urease test, used on extracted gastric tissue, was used to confirm infection here, as a quantitative culture from gastric tissue was not required.

Wei *et al.* also found $IL\text{-}10^+$ lymphocyte responses in the stomach, small intestine, colon, mesenteric lymph nodes as well as the spleen. However, because the murine spleen is a convenient and major source of lymphocytes which shows an increased immune response after *H. pylori* infection[248], this organ was the focus of this study. The data in Wei's study agreed with the expansion of both regulatory subsets in response to *H. pylori* infection put forward in this paper. The authors found that IL-10-producing B cells also induced the production of Tregs. The present study identified a subset of $IL\text{-}10^+$ B cells, termed Bregs, and analysed the source of IL-10 production in Bregs and Tregs. The frequency of splenic Bregs identified here is consistent with another study, suggesting that Bregs form 1-3% of mouse splenocytes[218]. Li *et al.* also identified an increased Breg population in humans with *H. pylori* infection[225]. Although Li's findings agree with the data in the present study, the authors identified a $CD24^+CD38^+$ population which are not widely studied markers of Bregs in mice.

The use of multiple markers in this study was useful in highlighting populations of Bregs and assessing the proportion that produced IL-10. This study identified that splenic B cell expansion occurred in the early stages of the immune response to *H. pylori* infection. While recent published work has described a *H. pylori*-induced

expansion of the human Breg population in gastric cancer, little work has shown or quantified Breg presence in mice after *H. pylori* infection. This study has demonstrated that the most abundant IL-10-secreting splenic lymphocyte type was the B cell. This is crucial because of the central role IL-10 plays in immunoregulation. IL-10$^{+}$ Tregs are a crucial component in the prevention of immunopathology such as gastric ulcers[119]. The increasing frequencies of IL-10-secreting Foxp3$^{+}$ lymphocytes after *H. pylori* infection suggests that IL-10 could be inhibiting protective immunity; skewing the balance of immunity to favour bacterial colonisation to prevent immunopathology.

By comparing mice, both infected and uninfected by *H. pylori*, in a stimulated and unstimulated state, the influence of infection and mitogenic stimulation could be compared independently. PMA/ionomycin/LPS stimulation is an established technique used to mimic T cell activation through the activation of intracellular protein kinase C and $Ca^{2+}$ mobilisation[273]. Although this procedure is crucial for IL-10 production in lymphocytes, it also downregulates CD4 expression[274]. Studying unstimulated cell populations is important for assessing the effect of mitogens on the expression of extracellular markers. The impact of *in vitro* stimulation and *H. pylori* infection also determines the levels of cytokines expressed by PBMCs. Previous work in the research group has used *H. pylori* whole cell lysates *in vitro* cell stimulation to identify *H. pylori*-specific IL-10$^{+}$ Tregs[119 275]; whether this is identical to Bregs remains to be seen.

### 3.6.1 Critique of experimental design

C57BL/6 mice are a widely used model and the first mouse model to be genetically sequenced. They have a genetic background suited for transgenic purposes, such as those reported in this study. These mice breed well, and have a long life span[276], and so are conducive for *H. pylori* experiments. Female mice are generally preferred in *H. pylori* research as they exhibit a stronger Th1 host response against the infection[277], and so are a translatable model for human *H. pylori* infection.

Most animal research is conducted using mice[278]. This is because the mouse genome is very similar to humans[278 279]. Using a mouse model develops the understanding of the immune responses that are triggered after *H. pylori* infection, which has no substitute when trying, as in this study, to further understand host-pathogen interactions, and how this may prevent or aid the onset of pre-malignant pathology[278 279]. The mice in this study were inbred, equalising the variations seen in human populations such as age, race, diet, lifestyle, and the presence of any concurrent disease which could mask the regulatory immune response of *H. pylori* infection[280]. Differences found after *H. pylori* infection in this study provides a justification to further study Bregs and Tregs during *H. pylori* infection in humans.

*H. pylori* infection occurs primarily in the gastric mucosa. The stomach would therefore be the ideal organ to isolate and characterise Bregs and Tregs. However, there are many limits in the viability of such a plan. Primarily, this is due to a lack of lymphocytes for multiple experiments. Using a precise methodology, the stomach may yield 4 million lymphocytes[281]. This has not been the case in previous experiments in the research group. Finding definitive counts of lymphocytes in the murine mucosa in the literature has been difficult. One study found that B and T lymphocytes made up 2% and 4% of the gastric lymphocytes[282]. These small frequencies would make studying regulatory sub-populations of these two lymphocytes very difficult using flow cytometry protocols. Studying the effect of *H. pylori* infection on the frequencies of regulatory cells was the aim of this study, and so this would not be feasible using gastric tissue. Currently, histopathological data from the stomach detailing inflammation scores complements the flow cytometry analysis. Potentially, immunohistochemical techniques could also be used to identify B and T cells in the stomach. This could also be used to identify whether both populations are within close proximity to each other, and how Bregs may induce Tregs after *H. pylori* infection, as noted previously[243]. In mice, the spleen is the largest secondary immune organ. It samples antigens through the blood, and is involved in antigen processing. It is a plentiful source of B lymphocytes and B cells expressing 'regulatory' markers, as the organ contains 25% of the body's lymphocytes[283]. It is therefore an acceptable organ for analysis of the immune response to *H. pylori*

infection in mice, and indeed, differences in regulatory B and T cell populations were observed.

A limit to this study comes from the conflicting information about useful markers to identify Breg subsets. Unlike Tregs, which usually express Foxp3 crucial to their function, Breg subsets do not have a unifying and universal marker. Though the most commonly used markers were employed in this study, a number of alternative markers for mouse Breg subsets were not included. These other minor Breg subsets could be within or outside the $CD1d^{hi}CD5^{+}$ B cell subset, which accounts for the vast majority of splenic B lymphocytes in infected mice. The stimulation protocol resulted in an increased frequency of $CD1d^{hi}CD5^{+}$ B cells. This is possibly due to cells being fixed with formaldehyde before fluorochrome-conjugated antibodies were added. Although this effect of stimulation has not been described in other studies analysing Breg frequencies, the studies did not stain cells with extracellular antibodies after fixation[218 220 284].

### 3.6.2 Unanswered questions and future research

Analysis of the functional suppressive activity of Bregs would help to elucidate their role during infection. Despite their abundant production of IL-10, these IL-10-producing B cells cannot be termed 'regulatory B cells' until it can be demonstrated that they are immunomodulatory. It has been shown that $IL\text{-}10^{+}$ B cells expand prior to Treg proliferation after *H. pylori* infection[243]. IL-10 also contributes to the induction of IL-10-producing Tregs in a positive feedback loop. Moreover, IL-10 is a B cell growth factor[171]. Developing a B cell-specific IL-10 knockout model might further elucidate Breg immunomodulatory mechanisms that are dependent and independent of IL-10 function in the context of *H. pylori* infection. Furthermore, this experiment may help to clarify the importance of B cell IL-10 against other immune cell sources of IL-10 in a *H. pylori* infection model. Understanding the complex role that Bregs may also have in relation to Treg induction would be a crucial element to understanding the regulatory immune response to infection.

Whether Bregs are involved in the tolerogenic response to *H. pylori* in the gastric mucosa has not been clarified. If Bregs contribute to tolerance, it is tempting to speculate that they may suppress gastritis and *H. pylori*-associated pathology, as Tregs do. Wei *et al.* described IL-10-producing B cells in the colon of infected mice[243]. If increased Bregs can be observed in extra-gastric tissue after infection, this may clarify how *H. pylori* infection protects against other conditions, such as IBD and MS, or even, a potential role in MALT lymphoma.

The protective effect of *H. pylori* infection (and Bregs) may be facilitated indirectly through the modification of the gastrointestinal microbiota[33]. One study showed that inflammation of the small and large intestine resulted in a shift in floral microorganisms to favour *E. coli*, *Bacteroides* and *Provotella* subspecies overgrowth[272]. This shift was also further identified within 8 weeks of *H. pylori* infection, and was absent in uninfected controls[285]. This overgrowth, and perhaps the disappearance of other species, may help upregulate Bregs through the production of IL-1β and IL-6[212]. This effect of other microbial species may have contributed to the expansion of IL-10-producing B cells identified in this study. Surprisingly, although *H. pylori* infection is causally linked with gastric immunopathology, it did not alter the microbial composition of the stomach. Rather, it was the shifts in the large intestinal microbial community which were evident. The authors suggested that this may help explain why patients suspected of *H. pylori* infection also presented with irregular bowel movements and unlocalised abdominal pain[272]. This could justify the analysis of Bregs within gastric biopsy tissue. IL-10 production was also observed in the colon of *H. pylori*-infected mice. This increase in regulatory phenotypes seen in extra-gastric tissue could demonstrate a function for IL-10-producing B cells outside the gastric mucosa[243].

The dosage given in this study is comparable to previous infections in the research group, and in other models[87 281]. Three weeks were enough to establish increased immune responses, which contrasts with a study observing IL-10$^{+}$ B cell frequencies after infection[243]. To look at strain-specific differences, perhaps a longer colonisation

period could be calculated. Histopathology scores would then be able to describe pathology consistent with *H. pylori*-induced metaplasia in humans.

While this pilot study was small, a clear trend after *H. pylori* infection was identified. *H. pylori* immunopathology in the host is a complex, multi-step inflammatory process. Here, differences in immune response components between mice and humans may not be translatable. This difference must be identified in humans to be clinically significant, before further mechanistic studies in mice can be performed.

Mice are not a natural reservoir for *H. pylori* colonisation. As a model, Non-*H. pylori Helicobacter* (NHPH) species were generally used to model effects of *H. pylori* infection in humans. SS1 was the first isolated strain that consistently colonised mice. *H. pylori* SS1 strain preferentially colonises the antrum of the stomach, and induces a Th1-skewed immune response in the host[286]. This is comparable to human infection. SS1 is a *vacA*$^{s2/m2}$ strain, a virulent, pathogenic strain, which was recently found to have a non-functional CagPAI[287]. PMSS1 could perhaps be used in future experiments, as it has an active CagPAI, so that CagA would be successfully translocated into host cells and induce cell signalling[194]. SS1 VacA mutant mice would also be a good model, as the presence of VacA i1-variant would induce host pathology[288], which would be a more relevant human disease model.

The role of Bregs and their function has not been fully evaluated in this field. Questions regarding their activity still remain. If, as the data suggests, there are more IL-10-producing B lymphocytes than T lymphocytes in the infected host, studying their function, if any, would clarify our knowledge of the infected host, and the adaptive immune response towards it. Studying Breg/Treg populations simultaneously will also reduce intra-assay variation within the data. Markers for Bregs such as CD5 and CD38 cannot be analysed individually, as these are also T cell markers. By developing a flow cytometry panel, it would be possible to analyse multiple cellular parameters simultaneously. Moreover, it has been observed that there is a connection between *H. pylori* PUD patients, and a reduced Treg

response[119]. Whether this relationship echoes that of Bregs and *H. pylori* positive individuals with disease remains to be seen.

Further research into the role of Bregs after *H. pylori* infection is therefore warranted. Because of the multiple subsets of Breg and Treg populations, more markers could be incorporated into flow cytometry analysis. This would clarify the subsets of regulatory cells which expand after infection, as only 16% of the IL-10$^{+}$ lymphocyte population in infected mice were positive for CD19$^{+}$CD1d$^{hi}$CD5$^{+}$ Breg markers following stimulation. By using 4 mice in each group, patterns for IL-10 production by B and T lymphocytes could be identified. The proportion of IL-10$^{+}$ lymphocytes in both the B cell and T cell panels demonstrate a similar trend. This similarity highlights the consistency and quality of the antibody staining process, and demonstrates the high level of reproducibility even within the experiment. These trends could be further analysed and become more accurate with more specimens in each group. Because humans and mice have been reported to express Bregs with differing phenotypes, further research could identify whether there is a difference between the subset populations expanding after the same stimulus, that of *H. pylori* infection.

## 3.6. Conclusions

- After *H. pylori* infection, this pilot study demonstrated that both $CD4^+$ and $CD19^+$ splenic lymphocyte populations expand significantly in mice.

- After *in vitro* stimulation, B cells were the largest source of IL-10 within the $IL\text{-}10^+$ lymphocyte population.

- Upon *H. pylori* infection, $CD1d^{hi}CD5^+$ Breg frequencies tended to increase, but non-significantly. This pattern was also observed in $IL\text{-}10^+$ Bregs.

- $Foxp3^+$ T cells expanded significantly upon *H. pylori* infection. This was also observed in $IL\text{-}10^+$ Tregs.

## Chapter 4: Quantifying human Bregs and Tregs in *H. pylori* infection

### 4.1 Introduction

A lot of research has been undertaken on Breg phenotypes and their function in mice (reviewed in **Section 1.6.4.2**). A role for Bregs has been described in mouse models for autoimmune diseases including MS. Recently, increased frequencies of Bregs during *H. pylori* infection have also been reported[219].

Mouse models are used to understand the mechanisms of the immune response in humans. However, there are wide differences in mouse and human immunology. The spleen is a lymphocyte rich organ consisting of approximately 50% B cells from total lymphocytes, but the frequency of B cells in mouse peripheral blood lymphocytes is 50%. Human blood is neutrophil rich with around 10% B cells[289], and this low frequency makes studying B cell subpopulations more difficult.

As well as differences in B cell frequencies, mice and humans have differences in the cellular markers used to identify Bregs (**Section 1.6.4.1**). An example is CD38, a marker for terminally differentiated plasma cells in humans, which is also a named marker for Bregs. In humans, CD38 is highly expressed on B cells originating from the germinal centre and is downregulated on cells in the periphery. In mice, however, this marker is expressed in low levels in germinal centre B cells[289 290].

### 4.2 Hypotheses

During *H. pylori* infection, active inflammation and gastritis develops with strong $CD4^+$ Th1, Th17 and Treg immune responses. Much less is known about the role of other mucosal lymphocyte populations. During infection, healthy gastric tissue is exposed to pro-inflammatory cytokine activity which then becomes damaged and starts to lose function. It is hypothesised that:

- Alongside $CD4^+$ T cells, B cells are more frequent in the peripheral blood of patients with *H. pylori* infection, compared to *H. pylori*-negative individuals.

- B cells also produce IL-10, and this is increased in patients with *H. pylori* infection, compared to *H. pylori*-negative individuals.

- Peripheral blood Bregs are more frequent in patients with *H. pylori* infection, compared to *H. pylori*-negative individuals.

- More peripheral blood Bregs and Tregs produce IL-10 in patients with *H. pylori* infection, compared to *H. pylori*-negative individuals.

- The frequencies of IL-10-producing B cells and Bregs in peripheral blood declines after antibiotic eradication of *H. pylori* infection.

## 4.3 Aims

- To develop and test a multi-parameter flow cytometry panel to identify Bregs and Tregs from human peripheral blood.

- To compare B cell and T cell frequencies, and the proportions of these lymphocytes which produce IL-10, in peripheral blood samples.

- To devise a strategy to consistently and reliably identify and quantify human Bregs and Tregs.

- To compare Breg and Treg frequencies in *H. pylori*-negative and *H. pylori*-positive individuals, and also those who underwent successful eradication of their *H. pylori* infection.

## 4.4 Materials and methods

### 4.4.1 Patient recruitment and clinical history

40 individuals were recruited from patients undergoing a routine upper GI endoscopy at Queen's Medical Centre (Nottingham, UK). This study was performed with informed written patient consent (see **Appendices C** and **D** for information given to patients and consent form). Ethical approval was obtained by Nottingham Ethical Committee 2 (reference 08/H0408/195).

*H. pylori* status was determined according to previous work (**Section 2.4.2**), and *H. pylori*-positive and *H. pylori*-negative individuals were then recruited to donate blood samples (**Table 4.1**). Patients who had successfully eradicated *H. pylori* infection within 6-24 months were recruited from a previous study (**Section 2.4.2**).

**Table 4.1:** Clinical characteristics of patients recruited to the Breg/Treg study.

| | |
|---|---|
| **Total donors*** | 40 |
| ***H. pylori* status** | Positive (9), Negative (14), Eradicated (17) |
| **Median age** | 56 |
| **Male: female ratio** | 1.86 |
| **Ethnicity** | Caucasian (22), Black (3), Asian (3), unknown (13) |
| **Indication for endoscopy** | Dyspepsia (11)<br>IDA (7)<br>Reflux (7)<br>Other (15) – e.g. weight loss, dysphagia, abnormal CT scan |
| **CagA status** | Negative (7), Positive (10), unknown (23) |
| **Peptic ulcer disease** | 4/40 |
| **Smoking status** | Non-smoker (25), current smoker (7), ex-smoker (5), unknown (3) |

*See **Appendix E** for complete patient information

### 4.4.2 Isolation of lymphocytes from human PBMCs

20ml samples were collected in EDTA-containing vacutainer tubes. The blood was diluted 1:2 in RPMI culture medium and added to pre-filled Leucosep™ 50ml tubes (GBO Bioscience) containing Histopaque separating solution, and centrifuged at 800 x *g* for 15 minutes to isolate PBMCs in an enriched interphase. Cells were then washed, counted, and resuspended according to previous work (**Section 2.4.6.1**) and stimulated *in vitro* (**Section 3.4.5**).

### 4.4.3 Flow cytometry analysis

#### 4.4.3.1 Compensation beads

The properties of the fluorochrome dyes used in this study for the MoFlo Astrios flow cytometer (Beckman Coulter) are described in (**Table 4.2**).

**Table 4.2:** The properties of fluorochromes used in the flow cytometry panel for this study.

| Fluorophore | Abbreviation | Emission bandwidth (nm) |
|---|---|---|
| Alexa Fluor 647 | AF647 | 656-686 |
| Brilliant Ultra Violet 395 | BUV395 | 390-420 |
| Brilliant Violet 421 | BV421 | 418-477.5 |
| Brilliant Violet 605 | BV605 | 604-624 |
| Brilliant Violet 711 | BV711 | 700-744 |
| Brilliant Violet 785 | BV785 | 760-830 |
| Fluorescein isothiocyanate | FITC | 500-526 |
| Phycoerythrin | PE | 565.5-586.5 |
| Phycoerythrin-Cyanin 7 | PE/Cy7 | 730-830 |
| Phycoerythrin-Dazzle 594 | PE/Dazzle | 604-624 |
| Peridinin Chlorophyll Protein Complex-Cyanin 5.5 | PerCP/Cy5.5 | 683-701 |

The antibodies against B cells, $CD4^+$ T cells, Bregs and Tregs were used according to the manufacturer's instructions and are described overleaf (**Table 4.3**). Isotype controls are described as 'iso', e.g. 'iso-IL-10' indicates the isotype control antibody for anti-IL-10 staining.

**Table 4.3:** Fluorochrome-conjugated antibodies used to detect markers expressed by human Bregs and Tregs.

| Marker/Isotype | Fluorochrome | Species subtype | Company | Catalogue no. | Clone | Concentration | Volume |
|---|---|---|---|---|---|---|---|
| CD4 | FITC | mouse IgG1 | BioLegend | 300505 | RPA-T4 | 0.4mg | 1µl |
| CD19 | BV605 | mouse IgG1 | BioLegend | 302243 | HIB19 | 0.08mg | 1µl |
| CD24 | PerCP/Cy5.5 | mouse IgG2a | BioLegend | 311115 | ML5 | 0.4mg | 5µl |
| iso-CD24 | PerCP/Cy5.5 | mouse IgG2a | BioLegend | 400251 | MOPC-173 | 0.4mg | 5µl |
| CD24 | PE | mouse IgG2a | BioLegend | 311105 | ML5 | 0.2mg | 2ul |
| iso-CD24 | PE | mouse IgG2a | BioLegend | 400211 | MOPC-173 | 0.2mg | 2ul |
| CD24 | PE/Dazzle | mouse IgG2a | BioLegend | 311133 | ML5 | 0.2mg | 2µl |
| iso-CD24 | PE/Dazzle | mouse IgG2a | BioLegend | 400275 | MOPC-173 | 0.2mg | 2µl |
| CD25 | BV421 | mouse IgG1 | BioLegend | 302629 | BC96 | 0.2mg | 2µl |
| iso-CD25 | BV421 | mouse IgG1 | BioLegend | 400157 | MOPC-21 | 0.2mg | 2µl |
| CD25 | BV785 | mouse IgG1 | BioLegend | 302638 | BC96 | 0.2mg | 2µl |
| iso-CD25 | BV785 | mouse IgG1 | BioLegend | 400170 | MOPC-21 | 0.2mg | 2µl |
| CD25 | PE/Cy7 | mouse IgG1 | BioLegend | 302612 | BC96 | 0.1 mg | 5µl |
| iso-CD25 | PE/Cy7 | mouse IgG1 | BioLegend | 400125 | MOPC-21 | 0.1 mg | 5µl |
| CD25 | PE | mouse IgG2b | Miltenyi Biotec | 130-091-024 | 4E3 | 0.1 mg | 1µl |
| iso-CD25 | PE | mouse IgG2b | BioLegend | 400311 | MPC-11 | 0.2mg | 1µl |
| CD25 | PE | mouse IgG1 | BioLegend | 356103 | M-A251 | 0.1mg | 2µl |
| iso-CD25 | PE | mouse IgG1 | BioLegend | 400112 | MOPC-21 | 0.2mg | 1µl |
| CD38 | BV711 | mouse IgG1 | BioLegend | 303527 | HIT2 | 0.2mg | 2µl |
| iso-CD38 | BV711 | mouse IgG1 | BioLegend | 400167 | MOPC-21 | 0.2mg | 2µl |
| CD38 | BV421 | mouse IgG1 | BioLegend | 303526 | HIT2 | 0.2mg | 1µl |
| iso-CD38 | BV421 | mouse IgG1 | BioLegend | 400158 | MOPC-21 | 0.1mg | 2µl |
| CD38 | PE/Cy7 | mouse IgG1 | BioLegend | 303515 | HIT2 | 0.05mg | 2µl |

| Marker/Isotype | Fluorochrome | Species subtype | Company | Catalogue no. | Clone | Concentration | Volume |
|---|---|---|---|---|---|---|---|
| CD38 | PE/Cy7 | mouse IgG1 | BioLegend | 356607 | HB-7 | 0.05mg | 1µl |
| iso-CD38 | PE/Cy7 | mouse IgG1 | BioLegend | 400125 | MOPC-21 | 0.2mg | 0.5µl |
| CD45 | BV785 | mouse IgG1 | BioLegend | 304047 | HI30 | 0.1mg | 2µl |
| CD45 | BUV395 | mouse IgG1 | BD Biosciences | 563791 | HI30 | 0.1mg | 1µl |
| CD127 | BV421 | mouse IgG1 | BioLegend | 351309 | A019D5 | 0.1mg | 2µl |
| IL-10 | AF647 | rat IgG1 | BioLegend | 501414 | JES3-9D7 | 0.05mg | 2µl |
| iso-IL-10 | AF647 | rat IgG1 | BioLegend | 400418 | RTK2071 | 0.05mg* | 2µl |

* Diluted 10X: 2µl antibody in 18µl PBA

#### 4.4.3.3 Flow cytometry

Cellular staining, fixing and permeabilisation have been described previously (**Section 3.4.6.3**). Multi-colour flow cytometry data acquisition and analysis were completed according to previous work (**Section 3.4.6.4**). Following analysis on Kaluza software, a gating strategy was developed according to previous work (**Section 3.4.6.5**).

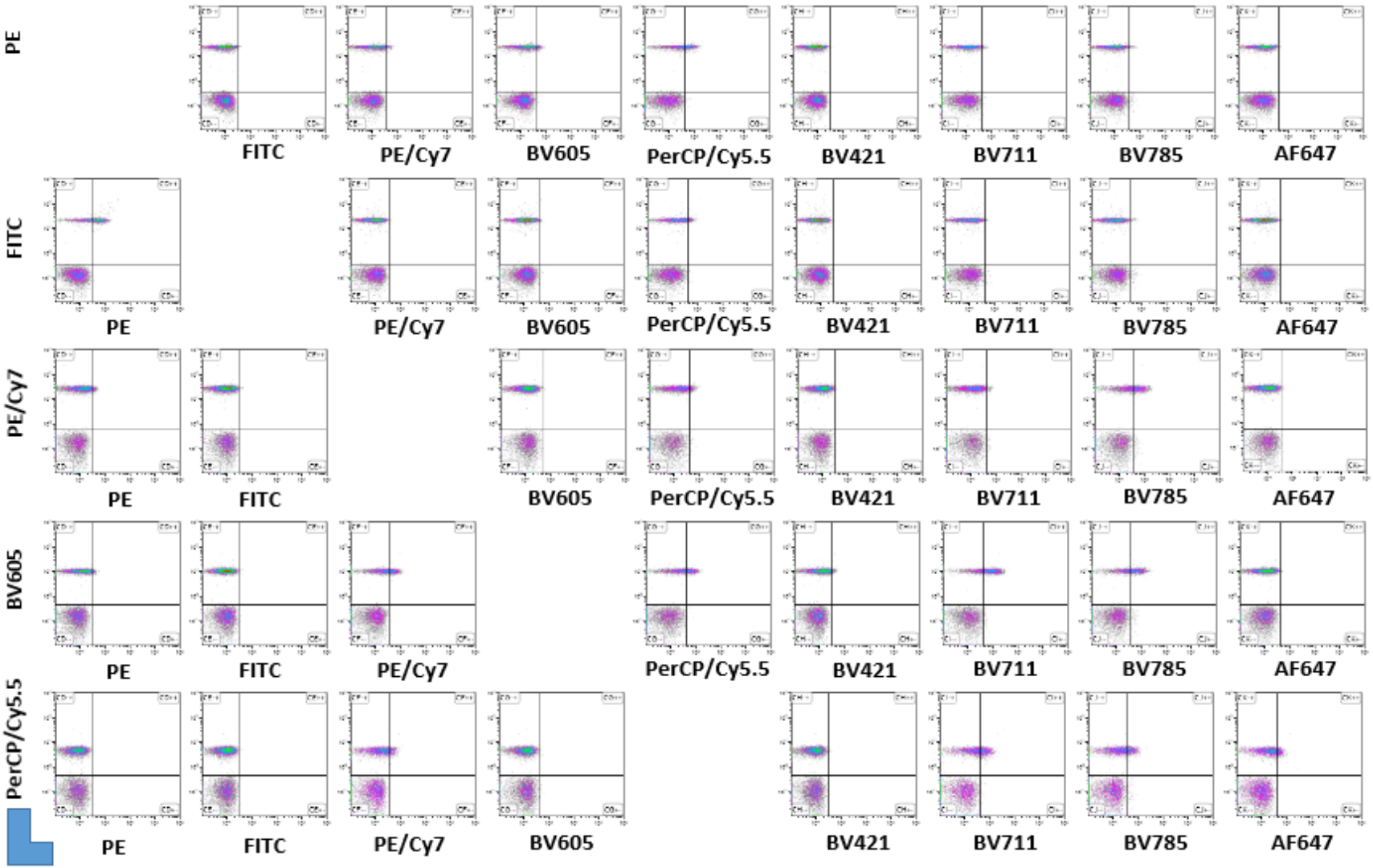
### 4.4.4 Statistical analysis

Statistical analysis and graphs were prepared using GraphPad Prism 6 software. The horizontal lines depict the median value. Statistical tests for unpaired data sets across all three groups was carried out using a 1-way Analysis of Variance (ANOVA) Kruskal-Wallis test. A statistical significant difference was taken at $p \leq 0.05$.

## 4.5 Results

### 4.5.1 Developing a multi-parameter panel

The development of the panel to identify Breg and Treg populations began with determining which combinations of fluorochromes could be used together effectively on the Astrios flow cytometer (**Figure 4.1**).


PE
FITC
PE/Cy7
BV605
PerCP/Cy5.5
BV421
BV711
BV785
AF647
FITC
PE
PE/Cy7
BV605
PerCP/Cy5.5
BV421
BV711
BV785
AF647
PE/Cy7
PE
FITC
BV605
PerCP/Cy5.5
BV421
BV711
BV785
AF647
BV605
PE
FITC
PE/Cy7
PerCP/Cy5.5
BV421
BV711
BV785
AF647
PerCP/Cy5.5
PE
FITC
PE/Cy7
BV605
BV421
BV711
BV785
AF647

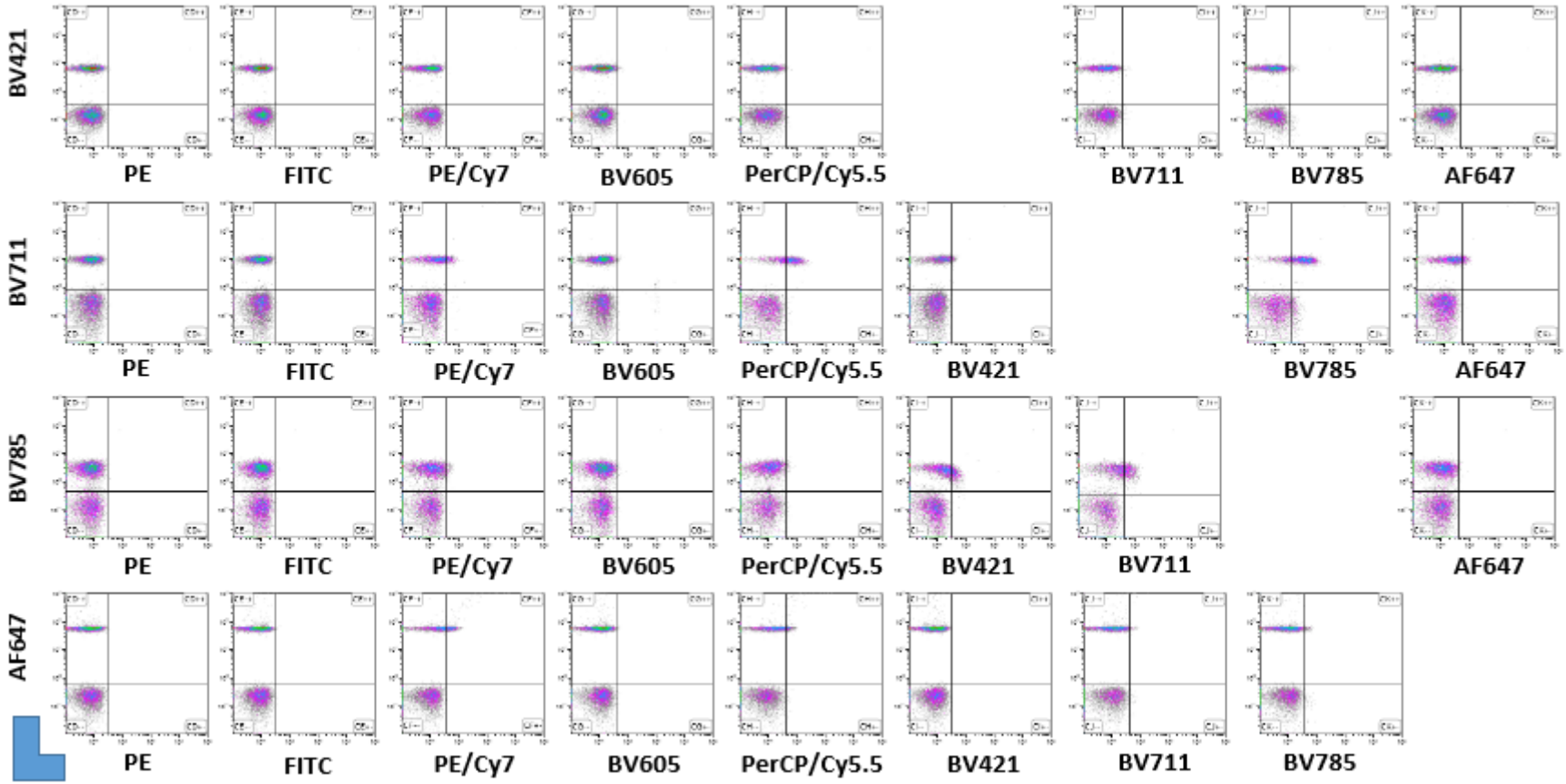



**Figure 4.1:** Anti-Rat and Anti-Hamster Ig CompBeads labelled with fluorophore-conjugated antibodies on the Astrios flow cytometer. (Top to bottom) PE, FITC, PE/Cy7, BV605, PerCP/Cy5.5, BV421, BV711, BV785 and AF647 conjugated antibodies were bound to CompBeads individually.

Fluorochromes BV711 and BV785 were removed from the panel optimisation, as spectral overlap between BV711 and BV785 could not be adequately compensated for in these channels. The next stage of development required the selection of cellular markers for Bregs and Tregs. These were chosen and matched with fluorochromes based on the brightness of the dye, and the expression level of the specific marker (**Table 4.4**). Brighter fluorochromes were matched with low level expressing cell markers, which required a clear discrimination between a dim positive signal and negative populations[291].

**Table 4.4**: The relative brightness index of various fluorophores where 1 represents the dimmest dyes, and 5 represents the brightest dyes.

| Fluorophore | Relative brightness index |
|---|---|
| AF647 | 4 |
| BUV395 | 3 |
| BV421 | 5 |
| BV605 | 4 |
| FITC | 2 |
| PE | 5 |
| PE/Cy7 | 4 |
| PE/Dazzle | 5 |
| PerCP/Cy5.5 | 2 |

After the brightness of the fluorophores was matched with the abundance of cellular markers, human PBMCs were stained with fluorochrome-conjugated antibodies in single stain controls (**Appendix F**). This was to determine if antibody-conjugated fluorochromes emitted detectable fluorescent signals, and whether positive and negative populations could be clearly observed. The data showed no compatibility issues between the fluorochrome-conjugated antibodies and the protocol used for cellular staining. The antibody anti-CD24-PerCP/Cy5.5 was replaced with a brighter PE/Dazzle fluorochrome conjugate because the PerCP/Cy5.5 fluorochrome was too dim for CD24 expression.

After determining that the other antibodies were effective in the singular staining of cells, a further experiment was required to identify whether these antibodies were compatible in combination. Fluorescence-minus-one (FMO) labelled samples, with all antibodies minus one, were set up (**Appendix G**). They served as a negative control to the single stain positive controls, and measured any fluorescence above background (unstained) levels[291 292].

Following further optimisation including antibody titration, a final panel was developed to identify and analyse Bregs and Tregs and their IL-10 production in peripheral blood samples in humans (**Table 4.5**).

**Table 4.5:** Optimised panel of fluorochrome-conjugated antibodies used to detect markers expressed by human Bregs and Tregs.

| Marker/ Isotype | Fluorochrome | Species subtype | Company | Catalogue no. | Clone | Concentration | Volume |
|---|---|---|---|---|---|---|---|
| CD4 | FITC | mouse IgG1 | BioLegend | 300505 | RPA-T4 | 0.4mg | 1µl |
| CD19 | BV605 | mouse IgG1 | BioLegend | 302243 | HIB19 | 0.08mg | 1µl |
| CD24 | PE/Dazzle | mouse IgG2a | BioLegend | 311133 | ML5 | 0.2mg | 2µl |
| iso-CD24 | PE/Dazzle | mouse IgG2a | BioLegend | 400275 | MOPC-173 | 0.2mg | 2µl |
| CD25 | PE | mouse IgG1 | BioLegend | 356103 | M-A251 | 0.1mg | 2µl |
| iso-CD25 | PE | mouse IgG1 | BioLegend | 400112 | MOPC-21 | 0.2mg | 1µl |
| CD38 | PE/Cy7 | mouse IgG1 | BioLegend | 356607 | HB-7 | 0.05mg | 1µl |
| iso-CD38 | PE/Cy7 | mouse IgG1 | BioLegend | 400125 | MOPC-21 | 0.2mg | 0.5µl |
| CD45 | BUV395 | mouse IgG1 | BD Biosciences | 563791 | HI30 | 0.1mg | 1µl |
| CD127 | BV421 | mouse IgG1 | BioLegend | 351309 | A019D5 | 0.1mg | 2µl |
| IL-10 | AF647 | rat IgG1 | BioLegend | 501414 | JES3-9D7 | 0.05mg | 2µl |
| iso-IL-10 | AF647 | rat IgG1 | BioLegend | 400418 | RTK2071 | 0.05mg* | 2µl |

* Diluted 10X: 2µl antibody in 18µl PBA

### 4.5.2 IL-10-producing B and T lymphocytes

Following analysis on Kaluza software, a gating strategy for identifying Bregs and Tregs was developed. Every blood sample analysis was tested with an unstained control, single stain controls, stimulated and unstimulated controls, and appropriate isotype controls.

The lymphocyte population was first gated by forward and side scatter plots. Then the gating of $CD45^+$ events was performed, before further analysis to quantify the frequencies of B and T lymphocyte populations in peripheral blood (**Figures 4.2** and **4.3**). In humans, approximately 50% of the $CD45^+$ lymphocytes in peripheral blood were identified as $CD4^+$ T cells (**Figure 4.3C**). B cells accounted for approximately 10% of lymphocytes. There were no significant differences in these lymphocyte populations between PBMCs from *H. pylori*-negative (Hp-), *H. pylori*-positive (Hp+) and *H. pylori*-eradicated patients (HpE).

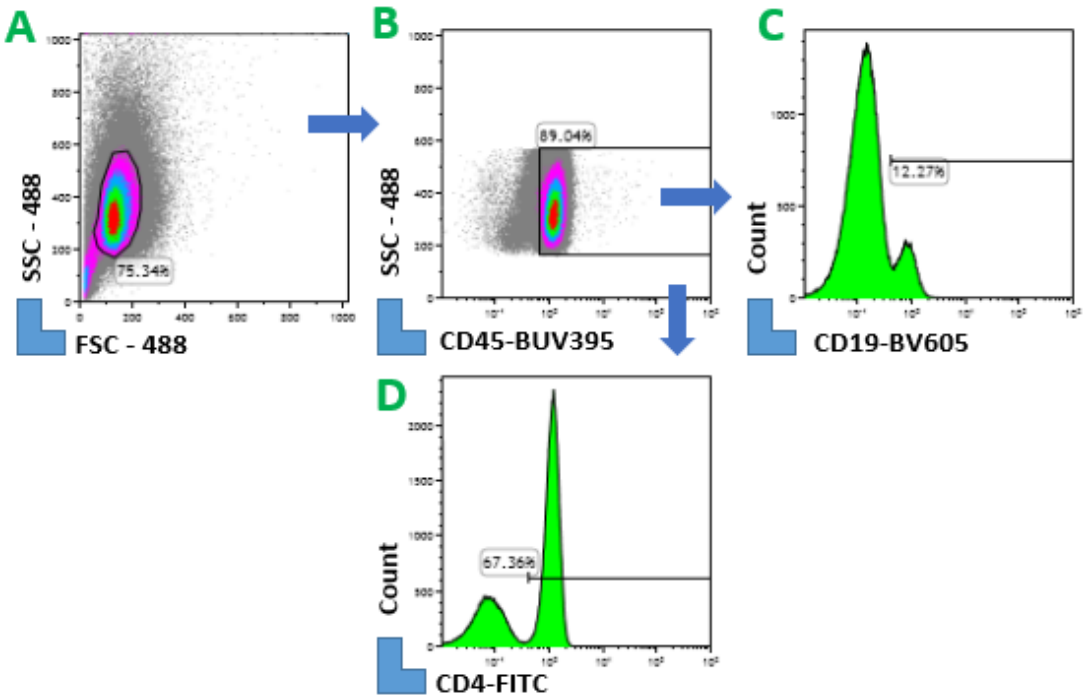



**Figure 4.2:** Representative flow cytometry plots and the gating analysis scheme for the identification of B and T lymphocytes. Human PBMCs were stained with mouse fluorochrome-conjugated antibodies to identify $CD19^+$ B and $CD4^+$ T cells within the lymphocyte population. (A) Lymphocyte population gated by forward (FSC) and side (SSC) scatter under the 488nm laser. (B) $CD45^+$ events from the lymphocyte gated population. (C) Histogram showing $CD19^+$ events amongst $CD45^+$ gated lymphocytes. (D) Histogram showing $CD4^+$ events amongst $CD45^+$ gated lymphocytes.

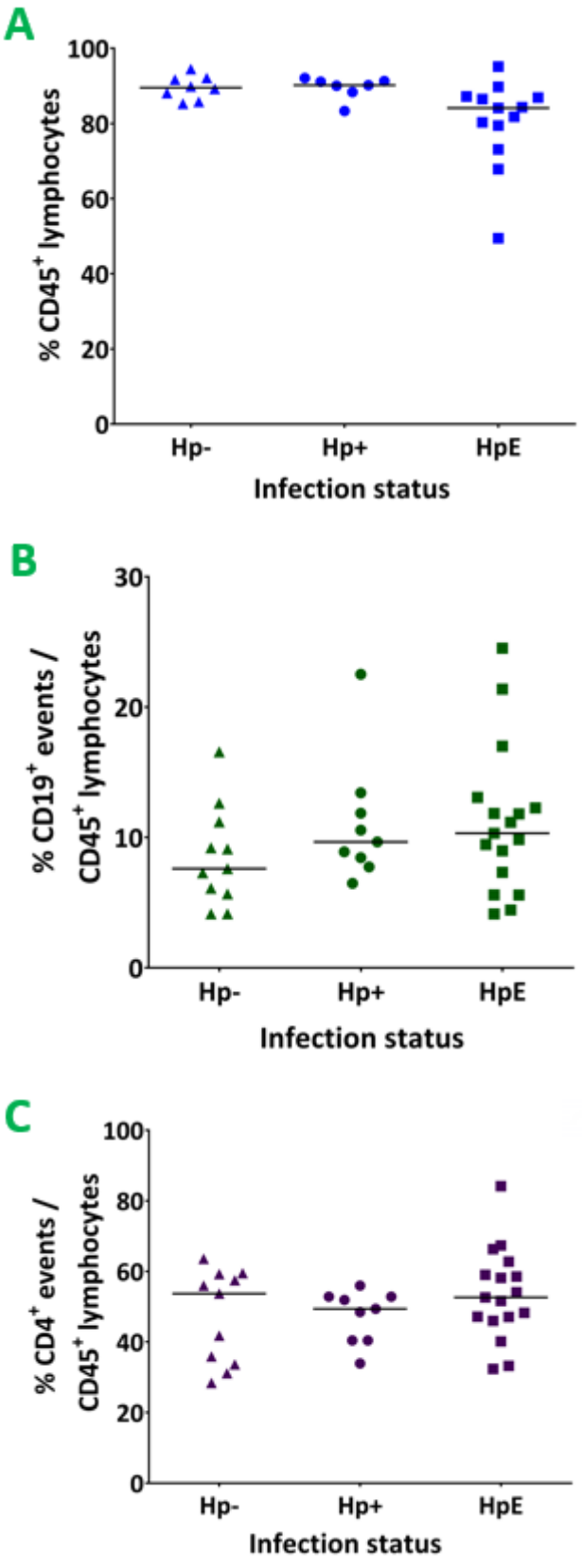

A
100
80
60
40
20
0
% CD45+ lymphocytes
Hp-
Hp+
HpE
Infection status
B
30
20
10
0
% CD19+ events / CD45+ lymphocytes
Hp-
Hp+
HpE
Infection status
C
100
80
60
40
20
0
% CD4+ events / CD45+ lymphocytes
Hp-
Hp+
HpE
Infection status

**Figure 4.3:** (Overleaf) Proportion of lymphocyte frequencies amongst PMBCs collected from patients who were *H. pylori*-negative (Hp-), *H. pylori*-positive (Hp+) or had successfully eradicated their *H. pylori* infection (HpE). (A) $CD45^+$ lymphocytes. Amongst the $CD45^+$ cells in the peripheral blood lymphocytes, (B) $CD19^+$ B and (C) $CD4^+$ T cells were quantified. The horizontal lines depict the median value.

Studies have shown that both B and T lymphocytes produce IL-10 when stimulated[220 293]. Therefore, the proportion of IL-10$^+$ lymphocytes that were CD19$^+$ or CD4$^+$ were analysed after *in vitro* stimulation with mitogens (**Figures 4.4** and **4.5**).

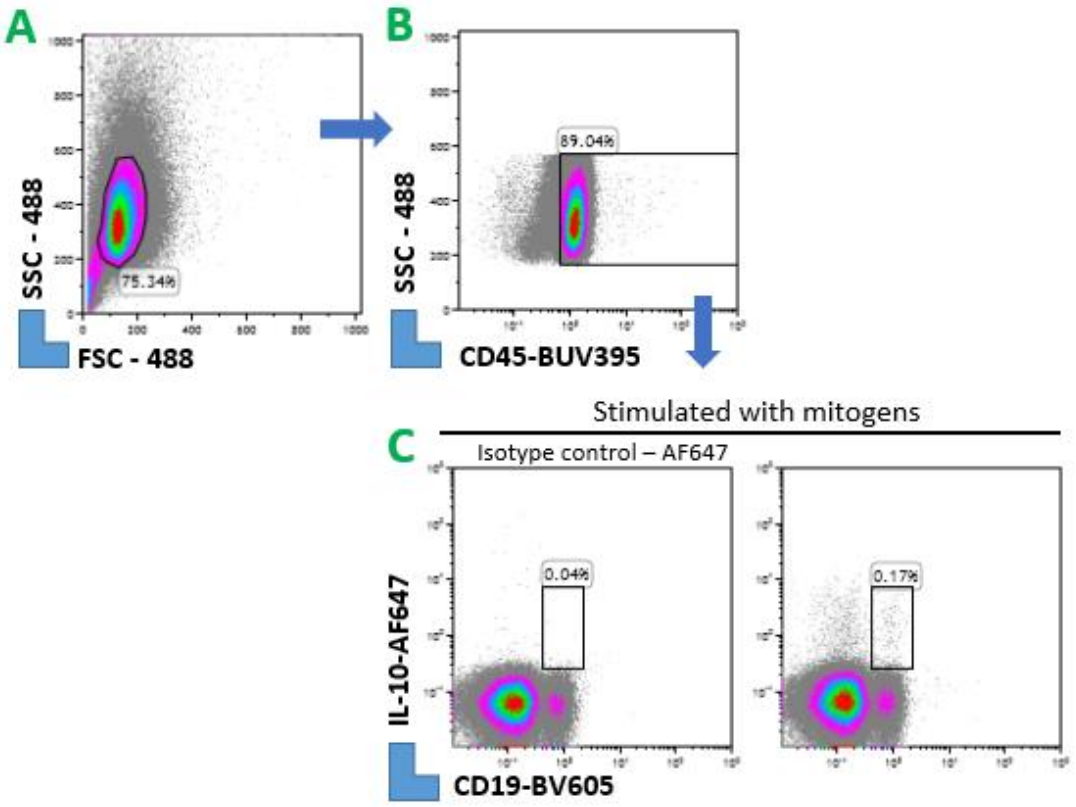



**Figure 4.4:** Representative flow cytometry plots and gating strategy analysis of the proportion of IL-10$^+$ lymphocytes that were CD19$^+$ B cells in PBMCs from patients. Patients were *H. pylori*-negative (Hp-), *H. pylori*-positive (Hp+) or had successfully eradicated their *H. pylori* infection (HpE). (A) Lymphocyte population gated by forward (FSC) and side (SSC) scatter under the 488nm laser. (B) CD45$^+$ events from the lymphocyte gated population. (C) Representative CD19-IL-10 plots from gated lymphocytes: anti-IL-10-stained and stimulated cells with its corresponding isotype control. Cells were stimulated with a combination of PMA, ionomycin and LPS for 6 hours. The horizontal lines depict the median value.

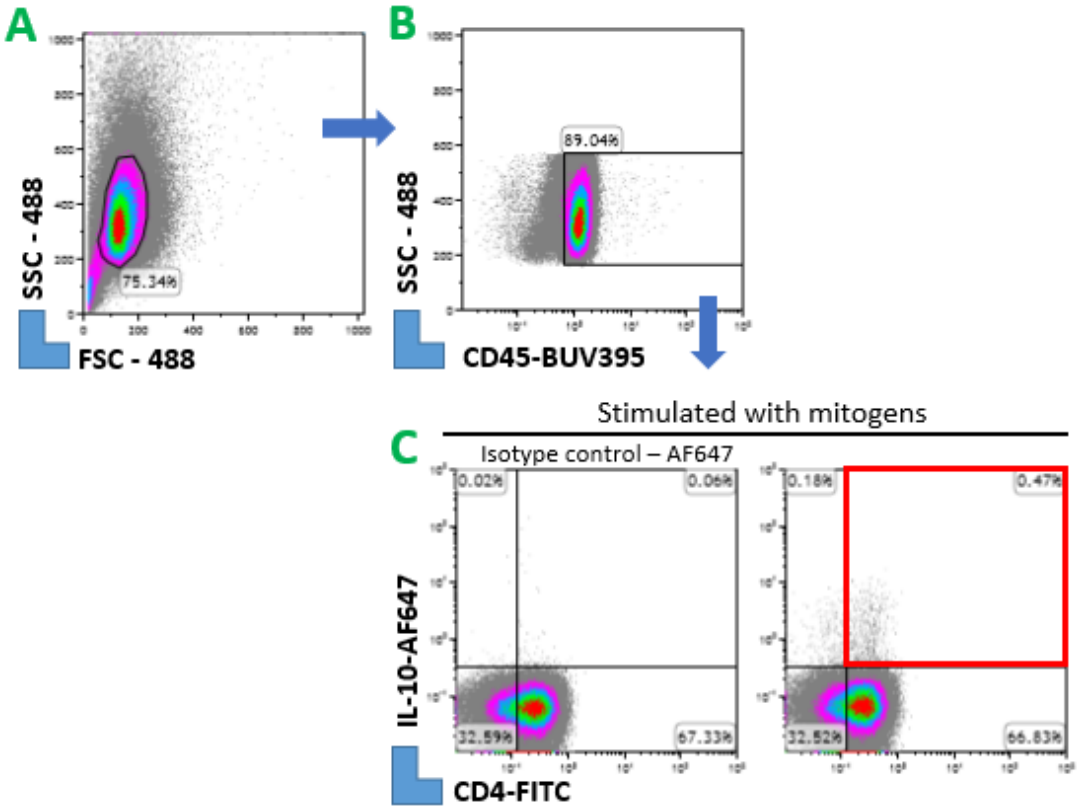



**Figure 4.5:** Representative flow cytometry plots and gating strategy analysis of the proportion of IL-10$^{+}$ lymphocytes that were CD4$^{+}$ T cells in PBMCs from patients. Patients were *H. pylori*-negative (Hp-), *H. pylori*-positive (Hp+) or had successfully eradicated their *H. pylori* infection (HpE). (A) Lymphocyte population gated by forward (FSC) and side (SSC) scatter under the 488nm laser. (B) CD45$^{+}$ events from the lymphocyte gated population. (C) Representative CD4-IL-10 plots from gated lymphocytes: anti-IL-10-stained and stimulated cells with its corresponding isotype control. Cells were stimulated with a combination of PMA, ionomycin and LPS for 6 hours. The horizontal lines depict the median value.

When comparing the relative proportions of $CD19^+$ and $CD4^+$ lymphocytes amongst IL-$10^+$ events (**Figure 4.6**), a median of 62% of the IL-$10^+$ lymphocytes were $CD4^+$ T cells, while 26% of them were $CD19^+$ B cells in *H. pylori*-negative individuals. This suggests that T cells are the primary source of IL-10 in the lymphocyte population in human PBMCs (**Figure 4.6B**). Similar proportions were observed regardless of *H. pylori* infection status.

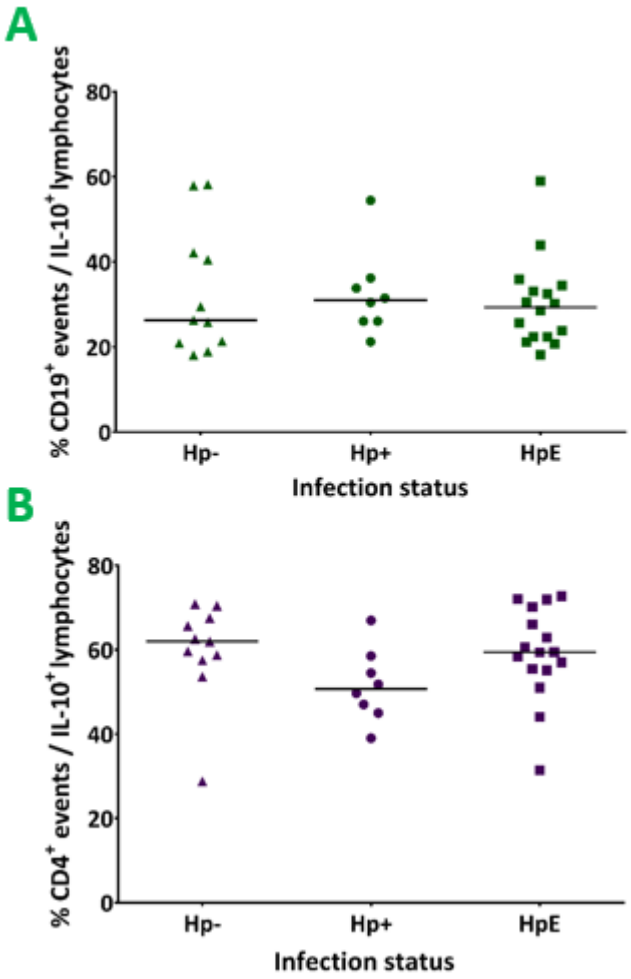



**Figure 4.6:** Proportions of peripheral blood IL-$10^+$ lymphocytes that were (A) $CD19^+$ B cells or (B) $CD4^+$ T cells. Patients were *H. pylori*-negative (Hp-), *H. pylori*-positive (Hp+) or had successfully eradicated their *H. pylori* infection (HpE).

However, there was a greater proportion of IL-10$^+$ B cells within the CD19$^+$ population (**Figure 4.7A**), compared to IL-10$^+$ T cells within the CD4$^+$ population. This suggested that while CD4$^+$ T cells were the primary source of IL-10, B cells were a more potent source of IL-10.

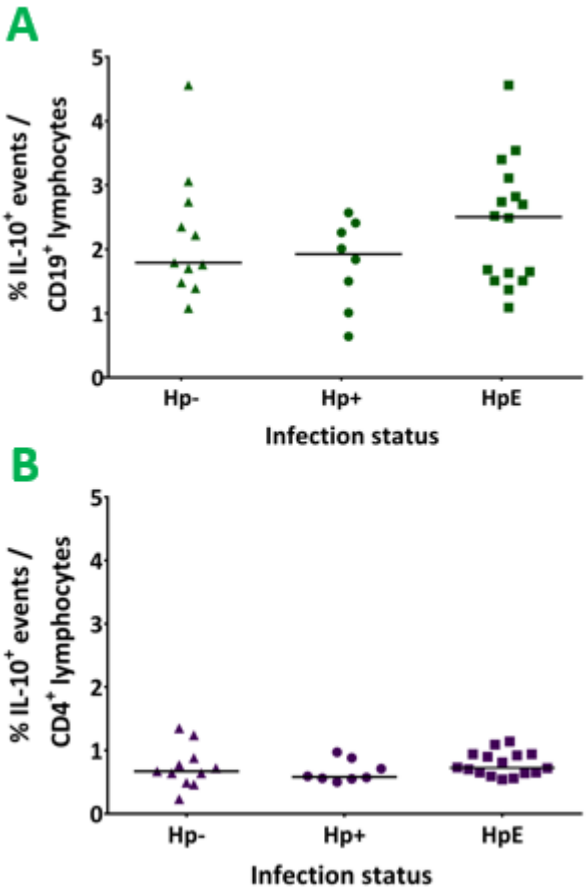



**Figure 4.7:** Proportion of (A) CD19$^+$ lymphocytes that were IL-10$^+$ or (B) CD4$^+$ lymphocytes that were IL-10$^+$ in PBMCs from patients undergoing an upper GI endoscopy. Patients were *H. pylori*-negative (Hp-), *H. pylori*-positive (Hp+) or had successfully eradicated their *H. pylori* infection (HpE). Cells were stimulated with a combination of PMA, ionomycin and *E. coli* LPS for 6 hours. The horizontal lines depict the median value.

Approximately 30% of IL-10-producing cells were B cells. To understand whether these IL-10 producing B cells were $CD24^{+}CD38^{hi}$ Bregs, further flow cytometry analyses were performed. A reproducible gating strategy to identify peripheral blood Bregs was developed (**Figure 4.8**). 3% of peripheral blood $CD19^{+}$ B cells were $CD24^{+}CD38^{hi}$ in *H. pylori*-negative patients, and this proportion was not significantly different amongst PBMCs from *H. pylori*-positive patients, or from those who had eradicated their *H. pylori* infection (**Figure 4.9**).

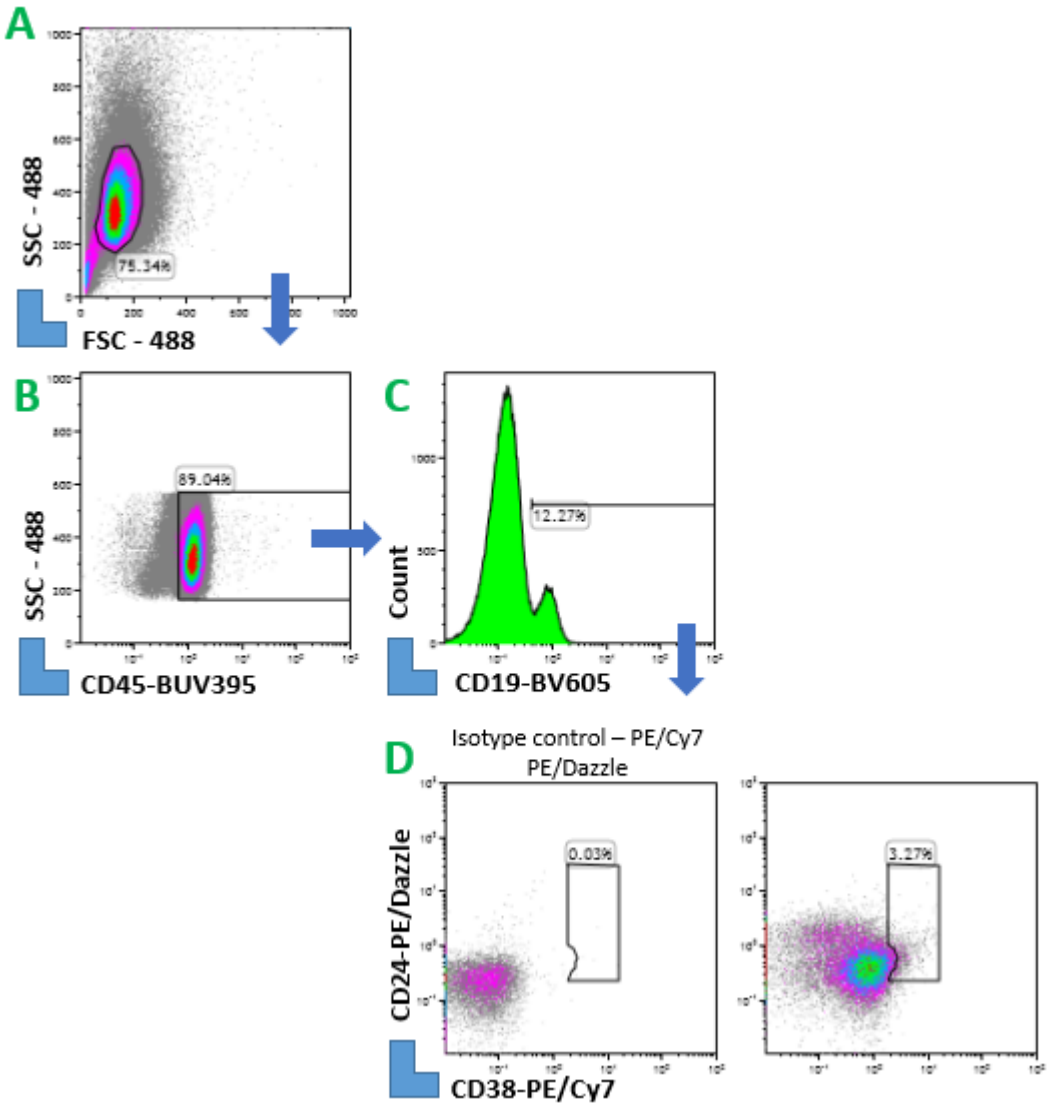



**Figure 4.8:** Representative flow cytometry plots and the gating analysis scheme for $CD19^{+}CD24^{+}CD38^{hi}$ Bregs from the peripheral blood of patients undergoing an endoscopy. (A) Lymphocyte population gated by forward (FSC) and side (SSC) scatter under the 488nm laser. (B) $CD45^{+}$ events from the lymphocyte gated population. (C) Histogram showing $CD19^{+}$ events amongst gated lymphocytes. (D) Representative CD24-CD38 plot from $CD19^{+}$ gated lymphocytes with its corresponding isotype control.

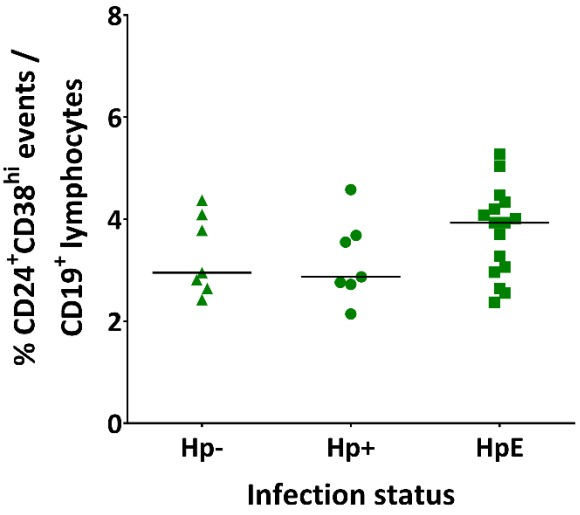



**Figure 4.9:** Proportion of peripheral blood $CD24^{+}CD38^{hi}$ Bregs within the $CD19^{+}$ B cell population. Patients were *H. pylori*-negative (Hp-), *H. pylori*-positive (Hp+) or had successfully eradicated their *H. pylori* infection (HpE). The horizontal lines depict the median value.

Bregs were a much higher proportion of their parent B cell population, compared to $CD25^{hi}$ cells from their $CD4^{+}$ T cell population. A reproducible gating strategy to identify peripheral blood Tregs was developed (**Figure 4.10**).

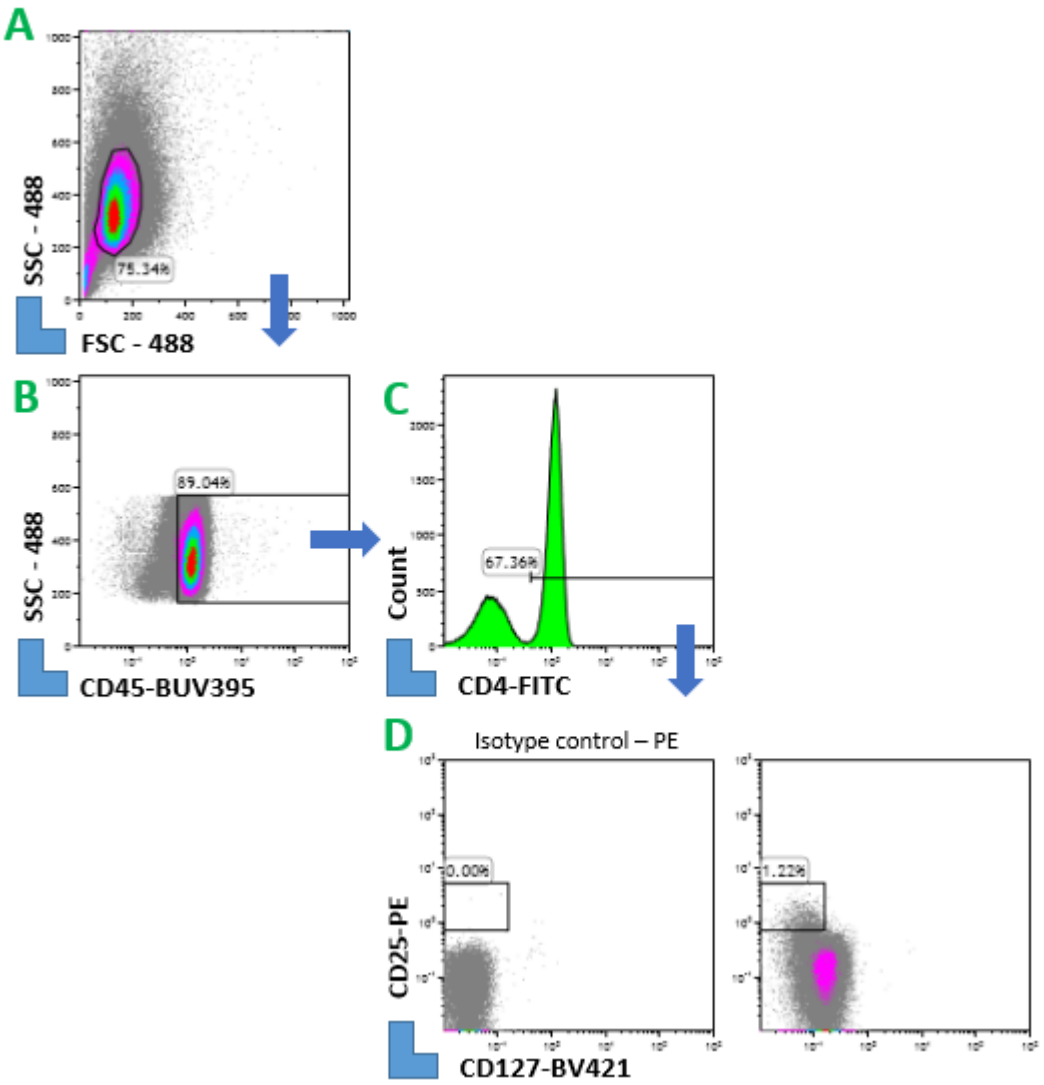



**Figure 4.10:** Representative flow cytometry plots and the gating analysis scheme for $CD4^{+}CD25^{hi}CD127^{lo}$ Tregs from peripheral blood samples in patients. (A) Lymphocyte population gated by forward (FSC) and side (SSC) scatter under the 488nm laser. (B) $CD45^{+}$ events from the lymphocyte gated population. (C) Histogram showing $CD4^{+}$ events amongst gated lymphocytes. (D) Representative CD25-CD127 plot from $CD4^{+}$ gated lymphocytes with its corresponding isotype control.

The size of the Treg ($CD4^{+}CD25^{hi}$) population was a third higher in PBMCs from *H. pylori*-positive patients compared to *H. pylori*-negative patients, but this trend was not statistically significant (**Figure 4.11**). This emerging trend was also observed in the frequencies of $CD4^{+}CD25^{hi}$ Tregs from all lymphocytes (**Figure 4.12**).

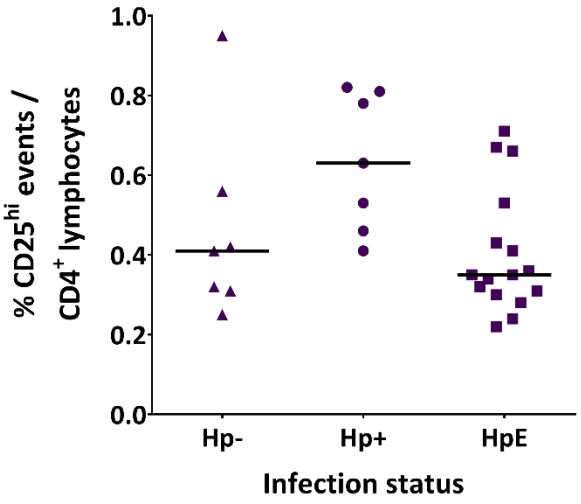



**Figure 4.11:** Proportion of $CD25^{hi}$ events from the total $CD4^+$ T cell population in blood samples donated by patients undergoing an upper GI endoscopy. Patients were *H. pylori*-negative (Hp-), *H. pylori*-positive (Hp+) or had successfully eradicated their *H. pylori* infection (HpE). The horizontal lines depict the median value.

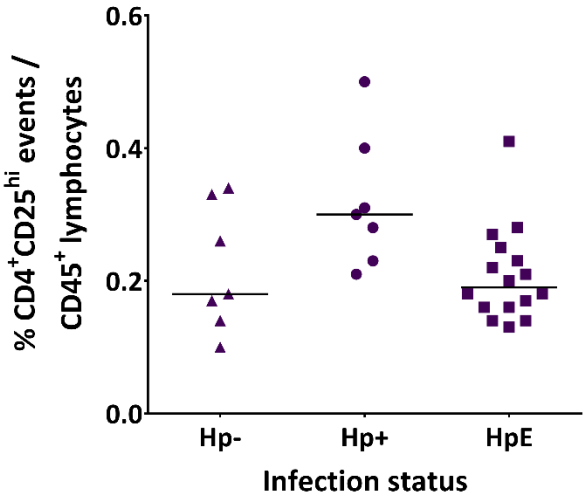



**Figure 4.12:** Proportion of $CD4^+CD25^{hi}$ Tregs from the total $CD45^+$ lymphocyte population in blood samples donated by patients. Patients were *H. pylori*-negative (Hp-), *H. pylori*-positive (Hp+) or had successfully eradicated their *H. pylori* infection (HpE). The horizontal lines depict the median value.

IL-10-producing Bregs and Tregs were then quantified. Only 2% of Bregs and Tregs produced IL-10, and this was a similar proportion across all three patient groups (**Figure 4.13**).

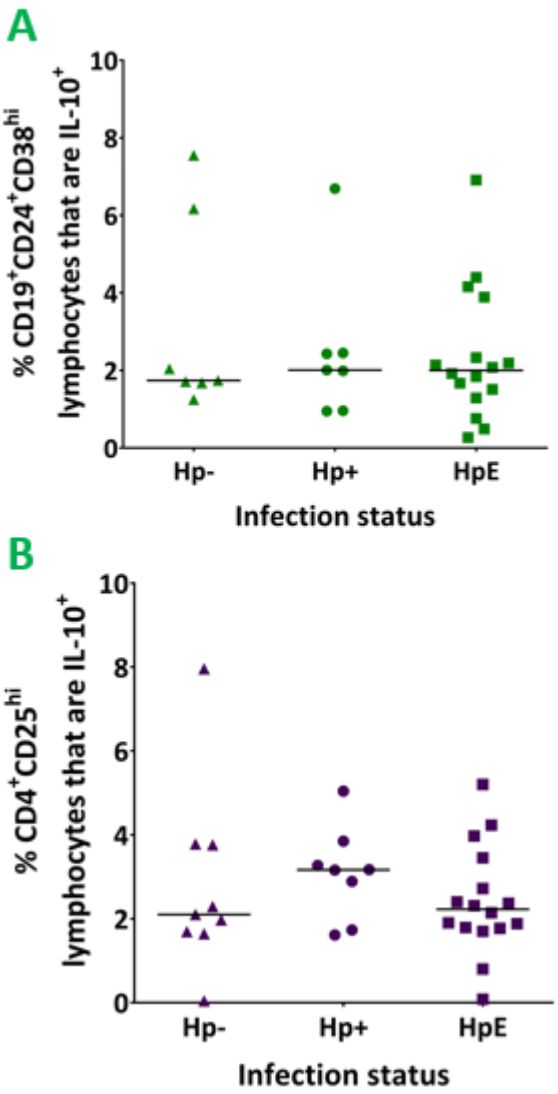



**Figure 4.13:** Proportion of IL-10-producing Bregs and Tregs in blood samples donated by patients undergoing an upper GI endoscopy. Patients were *H. pylori*-negative (Hp-), *H. pylori*-positive (Hp+) or had successfully eradicated their *H. pylori* infection (HpE). (A) Proportion of IL-10-producing $CD24^{+}CD38^{hi}$ Bregs from the total $CD19^{+}$ B cell population. (B) Proportion of IL-10-producing $CD25^{hi}$ Tregs from the total $CD4^{+}$ T cell population. The horizontal lines depict the median value.

## 4.6 Discussion

### 4.6.1 Statement of principal findings

This study aimed to investigate regulatory B and T lymphocyte subsets in human peripheral blood. During the development and optimisation of the panel of antibodies to quantify these cells using flow cytometry, peripheral blood samples were collected from 40 patients. These included *H. pylori*-negative controls, *H. pylori*-positive patients, and those who had successfully eradicated their *H. pylori* infection within the previous 3-24 months. B cells made up approximately 10% and $CD4^+$ T cells made up 25-60% of $CD45^+$ lymphocytes respectively. Further analysis after stimulation of the cells found that the majority of IL-10-producing lymphocytes were T cells. $CD19^+CD24^+CD38^{hi}$ Bregs accounted for approximately 3% of peripheral blood B cells. This proportion did not change significantly upon infection, or after eradication. Approximately 2% of Bregs produced IL-10, and this frequency did not change significantly after infection, or after eradication. $CD4^+CD25^{hi}$ Tregs showed an increased trend in *H. pylori*-positive patients, compared to *H. pylori*-negative and *H. pylori*-eradicated patients. $CD127^{lo}$ expression was used to confirm that the $CD25^{hi}$ population from $CD4^+$ T cells were Tregs.

### 4.6.2 Panel development

An eight-colour multi-parameter flow cytometry panel was developed and optimised to identify Bregs and Tregs in human blood. Careful development of this panel was important because $CD24^+CD38^{hi}$ Bregs had to be clearly and reproducibly identified to plausibly show a distinct population within B cells, as $CD24^+CD38^{hi}$ human Bregs share markers with differentiated B cells. The only phenotypic marker for all Bregs is IL-10, and it is possible that there may be multiple B cell subsets which have the capacity to produce IL-10. Furthermore, Bregs and Tregs are rare populations that are only defined by combinations of extracellular and intracellular markers. As the likelihood of counting errors increases with the number of fluorochromes in a panel[294], and the subsequent shift of marker expression, compensation was required to ensure that false positive populations were not identified.

Fluorochrome availability and flow cytometry compatibility were considered in the development of this panel. Each flow cytometer protocol has different configurations (including filters and lasers and differential pressure) which were found to have an important impact on the results. Therefore, this panel for quantifying Breg and Treg frequencies had to be developed from scratch, and could not follow on from previous Treg flow cytometry work from this group.

### 4.6.3 Biological relevance of the findings

Within the *H. pylori* field, there has been one paper in the literature to identify Bregs in human PBMCs[225]. Because the authors' gating strategy (**Section 1.6.4.3**) differs from other $CD24^{+}CD38^{hi}$ Breg gating in the literature, there are observed differences in the authors' Breg frequencies to the present study. Li *et al*. suggested that normal healthy individuals have almost no Breg cells in their blood, but that the frequency of Bregs was elevated in those with an asymptomatic *H. pylori* infection. These conclusions do not agree with the obtained results, or with other published papers on Bregs, which cite a 2-6% instance of Bregs from B cells in PBMCs from healthy human controls[193 224 253 284 295].

Bregs were studied to further clarify the source of IL-10 in lymphocytes during *H. pylori* infection in humans. In the mucosa for the majority of *H. pylori*-positive individuals, there is a lifetime of mild asymptomatic gastritis[5]. Here, the balance of pro-inflammatory and anti-inflammatory mechanisms of the immune response has been maintained. IL-10 production by various immune cells contributes to the anti-inflammatory mechanisms preventing the escalation of damage to host gastric tissue. The variation in the host response to *H. pylori* has identified ways in which individuals can be at an increased risk of disease. Mutations propelling the pro-inflammatory response (e.g. IL-1β and IL-8) increase the likelihood of gastric cancer[296]. On the other side, a low Treg response in *H. pylori*-positive individuals has been linked to an increased risk of peptic ulcer disease and pre-clinical gastric pathology[87 119].

There is a trend of an increased $CD4^+CD25^{hi}$ response in the peripheral blood of *H. pylori*-positive individuals, compared to *H. pylori*-negative patients. This result corroborates previous work in the research group and other studies showing an increased Treg response in the peripheral blood and gastric mucosa of *H. pylori*-positive patients[119 183-185]. The variation in $CD4^+CD25^{hi}$ response from the peripheral blood of patients with a previously eradicated infection is consistent with data analysed previously (**Section 2.5**). Further optimisation of the antibody panel showed that this $CD25^{hi}$ population, a subset of $CD4^+$ T cells, was also $CD127^{lo}$, showing that this population was likely to be Tregs.

There was no significant difference between Breg frequencies from *H. pylori*-negative, *H. pylori*-positive and *H. pylori*-eradicated patients. A curious result is that while the B cell population was 20% of the $CD4^+$ T cell population frequency, almost every blood sample indicated a higher proportion of Bregs from B cells compared to Tregs from $CD4^+$ T cells. However, similar proportions of these regulatory populations produced IL-10 after *in vitro* stimulation, regardless of infection status. This was not observed in Li's study[225].

There is also evidence to suggest that Bregs induce Treg differentiation in *H. pylori* infected mice, and that this process is IL-10-dependent[243]. New evidence highlights a similar phenomenon in humans, but one that is TGF-β dependent[193], which may explain why $IL\text{-}10^+$ cell frequencies did not change.

The correlation between Bregs and Tregs did not reflect the positive correlation identified in the PBMCs of gastric cancer patients ($R = 0.4352$, $p < 0.01$)[193]. This may be due to the infiltration of B cells in gastric cancer[193]. Therefore, the ratio of these cells could be modified in a disease state.

There were no differences in the frequencies of Bregs or IL-10-producing B cells according to age, sex, or smoking status, which is contrary to what was observed by Li *et al*[225]. When studying the patients' clinical histories, it became apparent that two *H. pylori*-negative individuals had previously completed a *H. pylori* eradication regime

within the last two years. Therefore, these samples were moved to the eradication cohort. Studying Bregs during antibiotic eradication is interesting because of the potential immune effects antibiotics have on colonising microbiota populations. Changes in the intestinal microbiota have been reported to induce Bregs in mice through IL-1β and IL-6 production[212]. While there were no differences in peripheral blood Breg frequencies between *H. pylori*-positive patients and the *H. pylori*-eradicated cohort, there is a decline in IL-10 producing B and T lymphocytes from patients donating blood after eradication at Month 6, to Month 12 and 24 samples (data not shown). This agrees with previous work (**Section 2.5**), and suggests a diminished capacity to produce IL-10 after stimulation over time. Whether this trend is due to antibiotics affecting the commensal microbiota, or the removal of *H. pylori*, or both, remains to be seen.

B cells have long been studied as antibody-producing cells in the host adaptive immune response. Recent findings on the plastic and flexible nature of immune cells means that different Treg subsets, and different IL-10-producing lymphocytes (such as B cells), are being investigated[168]. There is a defined role for regulatory T cells in immunomodulation. However, evidence suggests that through TGF-β and/or IL-10 production, Bregs can influence Treg numbers and function[193 211 244]. Because Treg frequencies and activity can be a marker for disease, B cell subsets which modulate Tregs could also become a marker.

Further analysis showed a small trend in which eradicated patients with a previous $CagA^+$ colonising *H. pylori* strain had increased $IL\text{-}10^+$ peripheral blood Bregs and Tregs, compared to patients with an eradicated $CagA^-$ strain (data not shown). $CagA^+$ *H. pylori* strains are associated with protection against extra-gastric diseases such as asthma[42]. This protection has been linked to Tregs and is IL-10-dependent[39]. If, after 2 years from eradication, patients previously infected with $CagA^+$ strains have Tregs which produce more IL-10 after stimulation, it may further suggest extra-gastric protection continues even after *H. pylori* eradication. Furthermore, within the eradication cohort, there was also a reduced $CD4^+IL\text{-}10^+$ response in smokers, compared to non-smokers (data not shown). To note that even 24 months after

eradication, there is a marked difference in IL-$10^+$ $CD4^+$ T cell frequencies suggests that there may be long term immunological consequences to smoking. *In vitro* challenge by mitogens was also not enough to reverse the smoke-induced inhibition of IL-5 and IL-13 production by mouse innate lymphoid cells[297]. *H. pylori*-positive smokers have ulcers that may be problematic to heal[62]. There is also a reduced trend of IL-10 concentration in the serum samples of *H. pylori*-positive smokers, compared to *H. pylori*-positive non-smokers[298].

### 4.6.4 Critique of experimental design

Developing this panel meant that issues such as poor compensation, dim fluorochromes matched with low level expressing markers, ineffective combinations and unspecific antibody staining were addressed and resolved. This was important as these can impact the data. On the basis of practical limitations such as the optical configurations of the Astrios flow cytometer, certain fluorochromes were eliminated before testing with beads. By further eliminating fluorochromes that could not be adequately compensated for using beads, eliminating fluorochromes which produced fluorescence above background level in FMO experiments, and using isotype controls to prevent non-specific binding, the likelihood of analysing false positive signals decreased substantially. Furthermore, the use of beads allowed for compensation to be finely tuned on the cytometer, so that compensated data could be reproducibly analysed for each experiment[299]. For the sake of brevity, a lot of the optimisation process involved has been shortened in this thesis.

The controls run in each experiment were crucial to differentiating positive and negative populations, and for observing if any non-specific binding occurred. Isotype controls have been suggested to be not only the identical light and heavy chain as its corresponding antibody, but also have the same fluorophore per IgG ratio[292]. Moreover, an unstained sample control is emphasised because the emission spectrum of cellular autofluorescence can spill over into channels detecting FITC and PE, two common fluorophores used in flow cytometry, and in this study[291].

Furthermore, the panel was necessary to adjust for effects from the cell staining protocol. $CD4^+$ events can be downregulated upon stimulation with PMA/ionomycin[274], and this was observed in this study. As the expression shifted, the CD4 gate had to be adjusted accordingly. This highlighted the importance of unstimulated and stimulated experiments. Also, as a tandem dye, PE/Cy7 is sensitive to cell fixation[300]. Tandem dye degradation would mean light emission being detected in the parent channel, PE, which may have led to a false positive population for CD25. This was accounted for when organising the collection of blood samples, so that stained samples were analysed in the flow cytometer within 2 days of fixation.

Developing and optimising this panel was crucial because the data generated from using this panel was the basis for identifying host immune differences between *H. pylori*-negative individuals, *H. pylori*-positive individuals and individuals with a successfully eradicated *H. pylori* infection. While the optimisation of flow cytometry panels is not generally emphasised in Breg literature, efforts to ensure its specificity and reproducibility must be described to highlight an adherence to good flow cytometry practice, and is the basis for valid representative dot plots. The protocol and data presented in this chapter has followed peer-recommended guidelines for panel optimisation and data presentation, including a consistent gating strategy for cell markers and the use of density plots to highlight the spread of fluorescence in cell populations[299].

The sole paper identifying human Bregs in *H. pylori* literature does not adhere to these principles of flow cytometry. There is no clear distinction between CD24 and CD38 positive and negative populations for Breg quantification[225]. While there are no axis marks on the dot plot to identify the logicle or logarithmic display, the pooled events concentrated at the bottom left corner of the dot plot suggests that the gated events in the middle are neither CD24 positive, nor CD38 high in expression. The authors' use of monochrome dot plots mask the intensity of the fluorescence signals by Breg markers, and cannot be relied upon to identify Breg populations. The authors' identification of a CD27 sub-population of B cells is also based upon an inconsistent gating strategy[225]. Furthermore, the Bregs identified by the authors in the

aforementioned study bear no similarity in pattern to Bregs identified by groups currently working on the role of Bregs in disease (**Section 1.6.4.3**). Bregs were also shown to produce large proportions of IL-10 after no stimulation, which has not been in this study, or in published Breg literature[210 225].

### 4.6.5 Future work

A panel of flow cytometry antibodies was optimised using PBMCs for subsequent use on *H. pylori*-positive and *H. pylori*-negative human gastric tissue. While PBMCs are not *H. pylori*-infected tissue, they are a current measure of pro and anti-inflammatory cells present within the stomach. Blood has been commonly used in *H. pylori* diagnoses, and in *H. pylori* clinical research, since it is a good source of lymphocytes and is not as invasive as gastric biopsies. This panel consistently and accurately identified $CD45^+$ lymphocytes, B and T lymphocytes and their regulatory subset phenotypes. This could be further expanded in gastric tissue to include advances in novel Breg and Treg markers, including CD27, TIM-1, TIGIT, LAG3, IFN-γ, CD3, IgM and TGF-β.

Bregs in humans have been reported to express different cell markers, with different expression levels and identified using different gating strategies, so the role of Bregs remains unclear in translational research. Clinical research is therefore crucial to examine the potential role for Bregs in human diseases. Bregs have been implicated in diseases such as MS, SLE and for patients undergoing a renal transplantation[211]. Bregs have also been shown to modulate Treg production and $CD4^+$ T cell suppression in humans, therefore decreasing T cell driven immunopathology[171]. When the phenotype, function and mechanism of action of Bregs are clearly established, they could be tested for use in potential therapeutics for autoimmune conditions.

The role of Bregs is still not universally acknowledged, but may play a crucial role in *H. pylori*-mediated disease. There was no significant difference between peripheral blood Breg responses in *H. pylori*-negative and asymptomatic *H. pylori*-positive patients. However, not only is an infiltration of Bregs described in gastric cancer[193]

and oesophageal cancer[249], but Bregs may also play a role in MALT lymphoma, an uncontrolled proliferation of B cell lymphocytes. This would clarify the role of Bregs in human *H. pylori* infection.

There are a rising number of cases of immunopathological disorders worldwide. The aetiology implicates an excessive antibiotic use in children, a highly sterile environment, diet, and changes to the host microbiota. Evidence from mouse studies discusses a role for Bregs in diseases such as MS, IBD, Type 1 diabetes, allergic diseases, and collagen-induced arthritis[210 211 301]. The role of *H. pylori*-induced Tregs in asthma and allergies has already been identified[37 39]. *H. pylori* infection has been observed to be partially protective against MS in mice and humans[33 38]. IL-10-producing B cells are also less frequent in the peripheral blood of MS patients compared to healthy controls[301]. The advent of next-generation sequencing has also brought about many studies on the effect of microbiota on gastric conditions ranging from obesity to IBD. Bregs have been shown to be induced by microbiota population, through IL-1β and IL-6 cytokine release[212].

While Bregs were identified phenotypically in this study, further suppression assays are required to demonstrate that they have suppressive function. As this requires many cells and B cells only account for approximately 10% of PBMCs, a number of patients could be asked to provide a larger blood sample. A recent report suggests that Bregs may induce Treg proliferation through TGF-β, not IL-10 in gastric cancer[193]. Further studies could include a TGF-β assay with B cells and $CD4^+$ T lymphocytes in cell co-culture, or blocking TGF-β and/or IL-10 with antibodies to study Breg and Treg suppressive function and activity.

Virulence factors in *H. pylori* such as CagA and VacA are risk factors for *H. pylori*-mediated disease, but their connection to Bregs has not been studied in mice or humans. Further work could determine any role for virulence factors in Breg frequency, activity in disease or asymptomatic gastritis, and connection with Treg activity. The presence of VacA i1-variant, CagA, and various pro-inflammatory immune responses has been correlated with the presence of immunopathology[30].

Indeed, the reduced number of Tregs has been causally linked to peptic ulcer disease[119], and the presence of the i1 variant of VacA has been independently listed as a risk factor for *H. pylori*-mediated disease[84].

The ability of VacA to promote DCs to induce Tregs and promote *H. pylori* persistence has been documented[191]. The role of VacA in inducing Bregs, and the role of i-region variants in inducing a Breg/Treg response is not known. Comparing the size and number of Breg populations to gastric histopathology scores and colonisation density may provide clues into how Bregs may suppress inflammation-associated pathology in the mucosa of the *H. pylori*-positive host. Furthermore, studying strain-specific differences in VacA and CagA could identify nuances in the immune response that the infection induces in its host. This may be in the level of response evoked, or in the time it takes for the adaptive immune response to develop.

Older people, who are at an increased risk of *H. pylori*-mediated disease, undergo an immune senescence in which regulatory T cells proliferate over time[260]. Within the eradication cohort, there were trends of declining IL-10 production by peripheral blood lymphocytes shown over 6-24 months after successful eradication (data not shown). It is not yet known whether *H. pylori* infection can induce an increased Breg proliferation over a time course, or with age.

### 4.6.6 Conclusions

- A multi-parameter flow cytometry panel was developed to reproducibly and reliably identify Bregs and Tregs, and their IL-10 production in human peripheral blood.

- B cells produced IL-10 upon mitogenic stimulation, but this proportion was not increased in patients with *H. pylori* infection.

- Tregs were more frequent than Bregs, but only 2% of both these populations produced IL-10, regardless of *H. pylori* infection status.

- Breg frequencies were not significantly different during *H. pylori* infection or in patients with a previously eradicated *H. pylori* infection.

- There was a trend of an increased frequency of $CD4^{+}CD25^{hi}$ Tregs in *H. pylori*-positive patients, compared to *H. pylori*-negative and *H. pylori*-eradicated patients. This is in agreement with previous findings from this group, and in the *H. pylori* Treg literature.

## Chapter 5: Characterising the effect of VacA on Bregs and Tregs in mice

### 5.1 Introduction

$CD19^+$ B and $CD4^+$ T cells are the largest IL-$10^+$ lymphocyte population in mouse spleen and peripheral blood. IL-10 is a crucial function of Treg activity. The presence of VacA in *H. pylori* can also promote the induction of Tregs through its effects on immature dendritic cells[191 192]. This promotes the regulatory response in the gastric mucosa, and prevents the successful clearance of the bacterium from the stomach. It is not known whether different types of VacA can affect Treg frequencies or function, or whether *H. pylori* infection has a direct effect on Treg function. There is also no data in the literature on the effect of VacA, or VacA variants on Breg frequencies in *H. pylori*-infected mouse models.

### 5.2 Hypotheses

- There is an expansion in B and $CD4^+$ T cell populations in murine spleen after *H. pylori* infection.
- There is an increase in IL-$10^+$ lymphocyte frequency after *H. pylori* infection.
- The frequencies of Bregs and Tregs in mouse spleen and blood are at similar levels, and there is an increased proportion of these populations after *H. pylori* infection.
- *H. pylori* expressing $VacA^{i1}$ induces a greater Treg IL-10 response in mice, compared to those infected with a *H. pylori* $VacA^{i2}$ strain or uninfected mice.
- *H. pylori* expressing $VacA^{i1}$ induces a greater Breg IL-10 response in mice, compared to those infected with a *H. pylori* $VacA^{i2}$ strain or uninfected mice.
- The splenic and peripheral blood Breg population expands earlier than Tregs after *H. pylori* infection.

- Infection with *H. pylori* induces a greater suppressive activity by Tregs in mice compared to uninfected mice.

## 5.3 Aims

- To compare B cell and T cell frequencies, and the proportions of these lymphocytes producing IL-10 in the peripheral blood samples and spleens of uninfected and infected mice at 3, 6 and 9 weeks after *H. pylori* infection.

- To compare Breg and Treg frequencies in the peripheral blood samples and spleens of uninfected and infected mice at 3, 6 and 9 weeks after *H. pylori* infection.

- To compare the effect of VacA variants on Breg and Treg frequencies from mice infected with different *H. pylori* strains.

- To compare the suppressive function of Tregs from uninfected mice with mice infected with *H. pylori* infection.

## 5.4 Materials and methods

### 5.4.1 Study management

This experiment was conducted by Dr. Kazuyo Kaneko, Mr. Ekene Ogbodu, Dr. Darren Letley, Mrs. Jo Rhead, Dr. Karen Robinson and myself under Home Office Project licence 30/3298 and approval from the local Animal Welfare and Ethical Review Body committee (as stated previously in **Section 3.4.1**). Six-week-old female C57BL/6 mice were obtained by Charles River and housed in previously described conditions.

### 5.4.2 *H. pylori* infection

After one week of acclimatisation, the mice (6 per group) were infected with *H. pylori* SS1$^{s2/i2}$ wild-type or mutant SS1$^{s1/i1}$ strains (**Table 5.1**), or given Brucella broth via oral gavage as previously described (**Section 3.4.3**). The mice were infected for 3, 6 or 9 weeks. 1/6 mice was colonised with SS1$^{s1/i1}$ after 9 weeks, compared to 5/6 mice infected with wild-type *H. pylori* SS1$^{s2/i2}$.

**Table 5.1**: Virulence factor properties in *H. pylori* SS1 wild-type and mutant strains.

| Strain | CagPAI status | VacA type | Reference |
|---|---|---|---|
| SS1 wild-type | Defective CagA translocation | s2/i2 | [87] |
| SS1 mutant | | s1/i1 | |

### 5.4.3 Isolation and stimulation of lymphocytes from mouse spleen

Splenic lymphocytes were isolated (**Section 3.4.4**), counted using 3% acetic acid with methylene blue (StemCell Research), and stimulated with PMA/ionomycin/LPS mitogens, as previously described (**Section 3.4.5**). Lymphocytes were stained with fluorochrome-conjugated antibodies (**Table 5.2**), with permeabilisation using Foxp3 perm buffer (BioLegend). Data on 200,000 events was collected using an Astrios flow cytometer (Beckman Coulter) as stated previously (**Section 3.4.6.4**).

**Table 5.2**: Fluorochrome-conjugated antibodies used to detect markers expressed by mouse regulatory B and T lymphocytes in spleen.

| Marker/Isotype | Fluorochrome | Species subtype | Company | Catalogue no. | Clone | Concentration | Volume |
|---|---|---|---|---|---|---|---|
| CD1d | PE | rat IgG2b | BioLegend | 123509 | 1B1 | 0.2mg/ml | 0.5µl |
| iso-CD1d | PE | rat IgG2b | BioLegend | 400608 | RTK4530 | 0.2mg/ml | 0.5µl |
| CD4 | PE/Dazzle | rat IgG2a | BioLegend | 100566 | RM4-5 | 0.2mg/ml | 1µl |
| CD5 | PE/Cy7 | rat IgG2a | BioLegend | 100621 | 53-7.3 | 0.2mg/ml | 0.5µl |
| iso-CD5 | PE/Cy7 | rat IgG2a | BioLegend | 400521 | RTK2758 | 0.2mg/ml | 0.5µl |
| CD19 | BV605 | rat IgG2a | BioLegend | 115540 | 6D5 | 0.2mg/ml | 0.5µl |
| CD25 | BV421 | rat IgG1 | BioLegend | 102043 | PC61 | 0.2mg/ml | 0.5µl |
| iso-CD25 | BV421 | rat IgG1 | BioLegend | 401911 | G0114F7 | 0.2mg/ml | 0.5µl |
| Foxp3 | FITC | rat IgG2a | e-Bioscience | 11-5773-82 | FJK-16s | 0.5mg/ml | 1µl |
| iso-Foxp3 | FITC | rat IgG2a | BioLegend | 400505 | RTK2758 | 0.5mg/ml | 1µl |
| IL-10 | AF647 | rat IgG2b | BioLegend | 505016 | JES5-16E3 | 0.5mg/ml | 0.5µl |
| iso-IL-10 | AF647 | rat IgG2b | BioLegend | 400626 | RTK4530 | 0.5mg/ml | 0.5µl |

### 5.4.4 Preparation of leukocytes from mouse blood

0.5ml blood was collected via cardiac puncture and pooled from two treatment-matched mice into a 15ml tube. Red Blood Cell lysing buffer was added for 1 minute to eliminate erythrocytes before 10ml culture media was added. This suspension was then centrifuged twice at 1500 RPM for 3 minutes before being washed with RPMI culture medium, counted, and resuspended in culture medium at 1 x $10^6$/ml. The leukocytes were stimulated with the previously described mix of LPS, PMA and ionomycin (**Section 3.4.5**), or left unstimulated for 6 hours.

Following incubation, the lymphocytes were stained with the following fluorochrome-conjugated antibodies (**Tables 5.2 and 5.3**). Data on 200,000 events was collected on the Astrios flow cytometer (Beckman Coulter) as previously described (**Section 3.4.6.4**).

**Table 5.3**: Fluorochrome-conjugated antibodies used to detect markers expressed by mouse B and T lymphocytes in blood.

| Marker/Isotype | Fluorochrome | Species subtype | Company | Catalogue no. | Clone | Concentration | Volume |
|---|---|---|---|---|---|---|---|
| CD3 | FITC | rat IgG2b | BioLegend | 100203 | 17A2 | 0.5mg/ml | 2µl |
| CD4 | PE | rat IgG1 | BioLegend | 102043 | PC61 | 0.2mg/ml | 0.5µl |
| CD8 | PE/Cy7 | rat IgG2a | BioLegend | 100722 | 53-6.7 | 0.2mg/ml | 1µl |

A gating strategy was developed to identify B cells, $CD3^+$, $CD4^+$, and $CD8^+$ T cells, Tregs, Bregs and IL-10-producing lymphocytes in peripheral blood samples and is shown overleaf (**Figures 5.3-5.5**).

### 5.4.5 Suppression assay

$CD4^+CD25^-$ T responder (Tresp) cells and $CD4^+CD25^+$ Treg splenic cells from uninfected mice and mice infected with *H. pylori* $SS1^{s2/i2}$ strain were isolated by MACS (Miltenyi Biotech) at 3, 6 and 9 weeks after infection, according to the manufacturer's instructions. 4.5ml of 1 x $10^6$/ml Tresp $CD4^+CD25^-$ cells was then centrifuged at 1500 RPM for 3 min. The supernatant was removed. 10 µl carboxyfluorescein succinimidyl ester (CFSE) stock solution (5mM) was diluted in 5ml 0.1% Bovine Serum Albumin (BSA) with PBS and mixed. The cells were resuspended in 4.5ml of this solution and incubated for 10 minutes. 20ml RPMI culture medium was then added to the cells and incubated on ice for 5 minutes. This was then centrifuged at 1500 RPM for 3 minutes, before being resuspended in culture medium and washed 3 times, before being resuspended in 4.5ml culture medium.

To create a dilution series, 200µl culture medium was added to 3 Eppendorf tubes. 200µl of 1 x $10^6$/ml $CD4^+CD25^+$ Tregs was added into the first tube and mixed. 200µl of the cell suspension from the first tube was transferred to the second tube and mixed. 200µl of the cell suspension from the second tube was then transferred to the third tube and mixed. 50µl of 1 x $10^6$/ml CFSE labelled $CD4^+CD25^-$ Tresp cells was then added into a 96 well plate. 50µl $CD4^+CD25^+$ Tregs from uninfected mice or *H. pylori* $SS1^{s2/i2}$ infected mice was then added into triplicate wells in a dilution series. Unlabelled Tresp, labelled Tresp only and labelled Tresp with 100µl CD3/CD28 beads were added as internal controls. This plate was then incubated at 37°C for 4 days.

Cells were then collected into a fluorescence and cell sorting (FACS) tube and centrifuged before being resuspended in fixation buffer. This was then incubated for 10 minutes at room temperature before being spun at 300 x *g* for 5 minutes. The supernatant was then removed and the cells were washed with 1ml PBA. Afterwards, the cells were resuspended in 0.5ml PBA before being stored in a cold room before flow cytometry analysis.

## 5.5 Results

### 5.5.1 IL-10-producing B and T lymphocytes in mouse spleen

Following analysis on Kaluza software, a gating strategy for identifying splenic lymphocytes was developed. The lymphocyte population was first gated by forward and side scatter, before being gated and analysed further (**Figures 5.1 and 5.2**) to quantify the $CD19^+$ B and $CD4^+$ T cell populations.

In uninfected mice, approximately 75% of the lymphocytes in the spleen were identified as $CD19^+$ B cells (**Figure 5.1C**). B cell frequencies declined over time in all mouse groups, irrespective of *H. pylori* infection status. *H. pylori* infection did not affect B cell frequencies at 3 or 9 weeks post infection, however at 6 weeks, there was a small significance between $SS1^{s1/i1}$ infected mice and uninfected mice ($p$ = 0.0316). $CD4^+$ T cells accounted for approximately 16% of splenic lymphocytes (**Figure 5.2C**). This population did not differ upon infection, or with time.

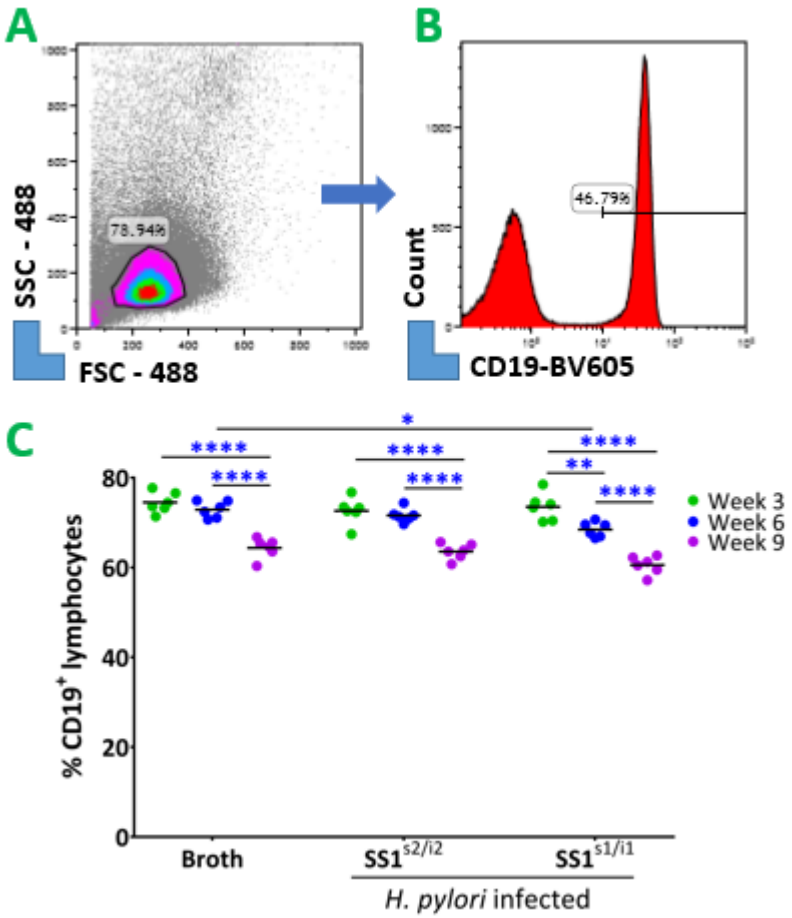



**Figure 5.1:** Representative flow cytometry plots, the gating scheme, and subsequent analysis of splenic $CD19^+$ lymphocytes. Mouse spleen cells were stained with rat fluorochrome-conjugated antibodies to identify $CD19^+$ B lymphocytes. (A) Lymphocyte population gated by forward (FSC) and side (SSC) scatter under the 488nm laser. (B) Histogram showing $CD19^+$ events amongst gated lymphocytes. (C) The proportion of $CD19^+$ B lymphocytes. Female C57BL/6 mice were orally dosed with Brucella broth (Broth), infected with *H. pylori* SS1 wild-type strain ($SS1^{s2/i2}$), or with *H. pylori* mutant SS1 strain ($SS1^{s1/i1}$) for 3, 6 or 9 weeks. The horizontal lines depict the mean value. Statistical analysis was performed across all groups using a 2-way ANOVA. If significant, a post-hoc Tukey's test was performed. The asterisks indicate the level of statistical significance, where * represents $p < 0.05$, ** represents $p < 0.01$, *** represents $p < 0.001$ and **** represents $p < 0.0001$.

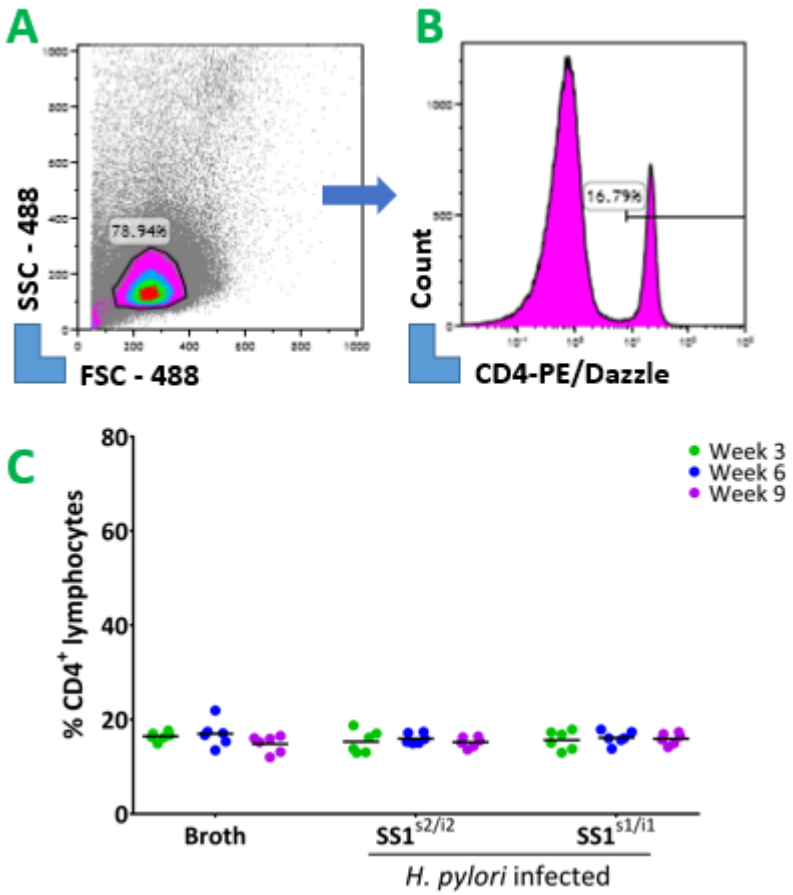



**Figure 5.2:** Representative flow cytometry plots, the gating scheme, and subsequent analysis of splenic $CD4^+$ lymphocytes. Mouse spleen cells were stained with rat fluorochrome-conjugated antibodies to identify $CD4^+$ T lymphocytes. (A) Lymphocyte population gated by forward (FSC) and side (SSC) scatter under the 488nm laser. (B) Histogram showing $CD4^+$ events amongst gated lymphocytes. (C) The proportion of $CD4^+$ T lymphocytes. Female C57BL/6 mice were orally dosed with Brucella broth (Broth), infected with *H. pylori* SS1 wild-type strain ($SS1^{s2/i2}$), or with *H. pylori* mutant SS1 strain ($SS1^{s1/i1}$) for 3, 6 or 9 weeks. The horizontal lines depict the mean value.

A gating strategy was used to consistently identify IL-10-producing B and T lymphocytes. Upon stimulation, the proportion of B cells producing IL-10 did not change significantly 3 weeks after infection with either strain, or after 9 weeks (**Figure 5.3**). However, between 3 weeks and 9 weeks after infection with the mutant *H. pylori* $SS1^{s1/i1}$ strain, there was a significant 2-fold expansion in the frequency of $CD4^+$ T cells producing IL-10 ($p = 0.0129$) (**Figure 5.4**).

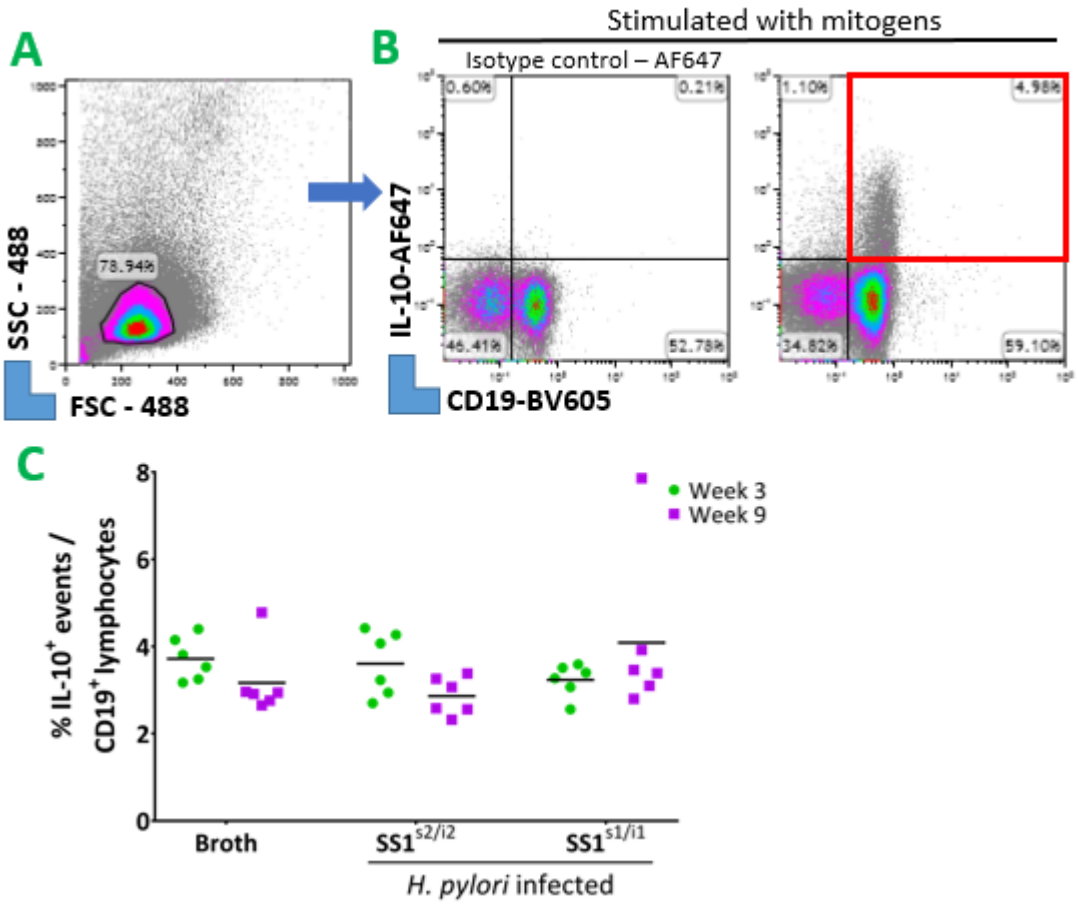



**Figure 5.3:** Representative flow cytometry plots, the gating scheme, and subsequent analysis of the proportions of IL-10$^{+}$ lymphocytes in uninfected and *H. pylori*-infected groups of mice. Mouse spleen cells were stained with rat fluorochrome-conjugated antibodies to identify IL-10$^{+}$ CD19$^{+}$ B lymphocytes. Cells were stimulated with a combination of PMA, ionomycin and *E. coli* LPS mitogens for 6 hours. (A) Lymphocyte population gated by forward (FSC) and side (SSC) scatter under the 488nm laser. (B) Representative CD19-IL-10 plot and corresponding isotype control. (C) Proportion of CD19$^{+}$ B lymphocytes which are IL-10-producing. Female C57BL/6 mice were orally dosed with Brucella broth (Broth), infected with *H. pylori* SS1 wild-type strain (SS1$^{s2/i2}$), or with *H. pylori* mutant SS1 strain (SS1$^{s1/i1}$) for 3 or 9 weeks. The horizontal lines depict the mean value.

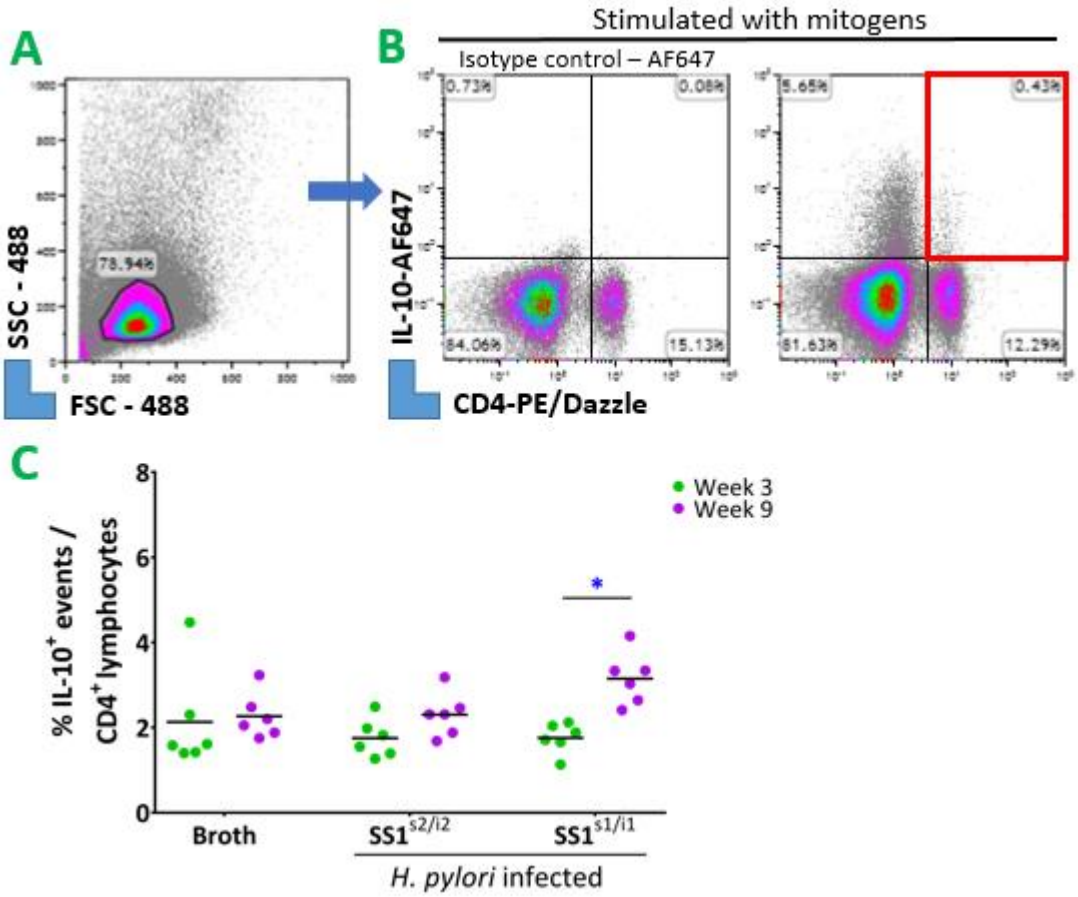



**Figure 5.4:** Representative flow cytometry plots, the gating scheme, and subsequent analysis of the proportions of IL-10$^+$ lymphocytes in uninfected and *H. pylori*-infected groups of mice. Mouse spleen cells were stained with rat fluorochrome-conjugated antibodies to identify IL-10$^+$ CD4$^+$ T lymphocytes. Cells were stimulated with a combination of PMA, ionomycin and *E. coli* LPS mitogens for 6 hours. (A) Lymphocyte population gated by forward (FSC) and side (SSC) scatter under the 488nm laser. (B) Representative CD4-IL-10 plot and corresponding isotype control. (C) Proportion of CD4$^+$ T lymphocytes which are IL-10-producing. Female C57BL/6 mice were orally dosed with Brucella broth (Broth), infected with *H. pylori* SS1 wild-type strain (SS1$^{s2/i2}$), or with *H. pylori* mutant SS1 strain (SS1$^{s1/i1}$) for 3 or 9 weeks. The horizontal lines depict the mean value. Statistical analysis was performed using a 2-way ANOVA, with a post-hoc Tukey's test. The asterisk indicates the level of statistical significance, where * represents $p < 0.05$.

An average of 64% of the gated IL-10$^{+}$ lymphocyte frequencies were CD19$^{+}$ cells (data not shown), suggesting that B cells are the primary source of IL-10 in the lymphocyte population of the spleen. This did not change significantly upon infection. The splenic B cell population of the infected groups tended to decline slightly over the 9-week time course (**Figure 5.1C**), and this may mask an increase in the frequency of Bregs after *H. pylori* infection. A gating strategy was developed to consistently identify CD1d$^{hi}$CD5$^{+}$ Bregs (**Figure 5.5**). The frequency of Bregs was also studied from all mouse groups (**Figure 5.6**). Between 3 weeks and 9 weeks after infection with the mutant *H. pylori* SS1$^{s1/i1}$ strain, there was a significant 2-fold expansion in the frequency of Bregs ($p$ = 0.0006), but was not statistically different compared to uninfected mice.

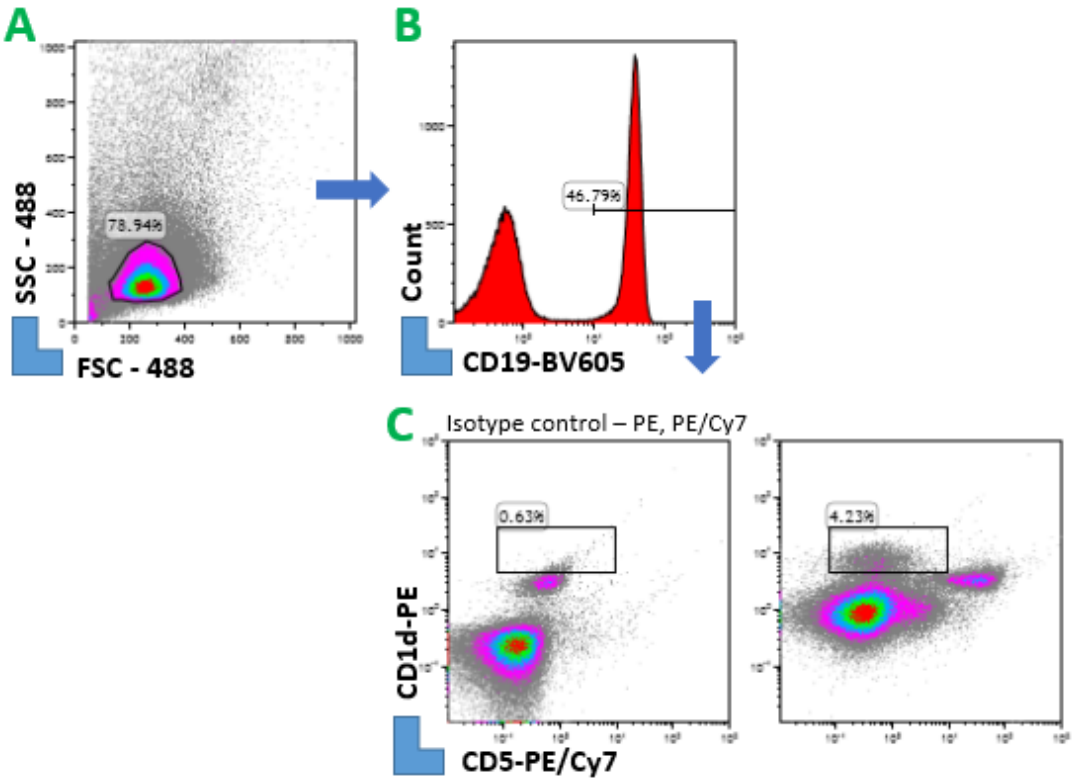



**Figure 5.5:** Representative flow cytometry plots and the gating analysis scheme for splenic CD1d$^{hi}$CD5$^{+}$ Bregs from mice orally dosed with *H. pylori*. Mouse spleen cells were stained with rat fluorochrome-conjugated antibodies to identify Bregs. (A) Lymphocyte population gated by forward (FSC) and side (SSC) scatter under the 488nm laser. (B) Histogram showing CD19$^{+}$ events amongst gated lymphocytes. (C) Representative CD1d-CD5 plot from CD19$^{+}$ gated events with its corresponding isotype control.

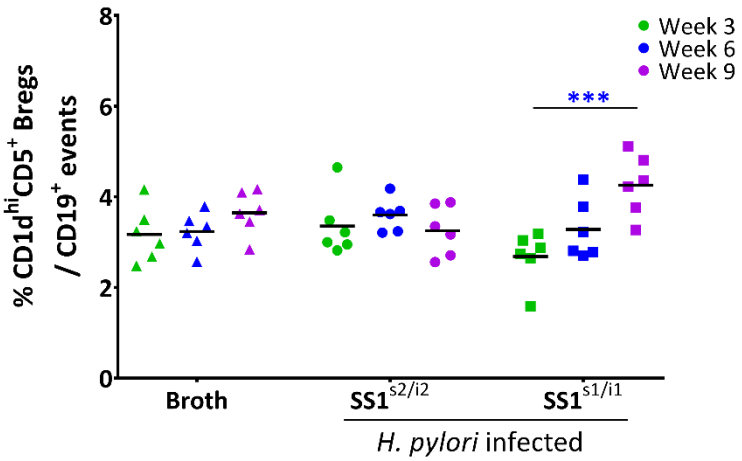



**Figure 5.6:** Proportion of splenic CD1d$^{hi}$CD5$^{+}$ Bregs within the CD19$^{+}$ B cell population in mice. C57BL/6 mice were orally dosed with Brucella broth (Broth), infected with *H. pylori* SS1 wild-type strain (SS1$^{s2/i2}$), or with *H. pylori* mutant SS1 strain (SS1$^{s1/i1}$) for 3, 6, or 9 weeks. Mouse spleen cells were stained with rat fluorochrome-conjugated antibodies to identify Bregs. The horizontal lines depict the mean value. Statistical analysis was performed using a 2-way ANOVA, with a post-hoc Tukey's test. The asterisk indicates the level of statistical significance, where *** represents $p < 0.001$.

At 9 weeks after infection, IL-10 production by these Bregs was then analysed (**Figure 5.7**). While mice infected with the mutant *H. pylori* SS1$^{s1/i1}$ strain had an increased CD1d$^{hi}$CD5$^{+}$ Breg frequency after 9 weeks of infection, there was no statistical difference in the proportions of IL-10-producing Bregs compared to uninfected mice.

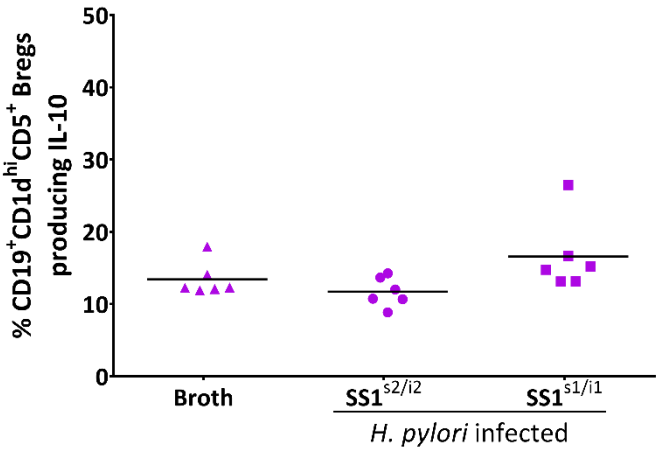



**Figure 5.7:** Proportion of splenic IL-10-producing CD1d$^{hi}$CD5$^{+}$ Bregs within the CD19$^{+}$ B cell population in mice. C57BL/6 mice were orally dosed with Brucella broth (Broth), infected with *H. pylori* SS1 wild-type strain (SS1$^{s2/i2}$), or with *H. pylori* mutant SS1 strain (SS1$^{s1/i1}$) for 9 weeks. Mouse spleen cells were stained with rat fluorochrome-conjugated antibodies to identify IL-10$^{+}$ Bregs. Cells were stimulated with a combination of PMA, ionomycin and *E. coli* LPS mitogens for 6 hours. The horizontal lines depict the mean value.

A gating strategy was developed to consistently identify Tregs (**Figure 5.8**). Since the proportion of IL-10-producing $CD4^+$ T cells expanded in response to infection with the *H. pylori* $SS1^{s1/i1}$ mutant strain, the size of the $CD4^+CD25^{hi}Foxp3^+$ Treg population was quantified and compared between all groups (**Figure 5.9**). However, Treg frequencies did not change significantly after infection with either *H. pylori* strain or with time.

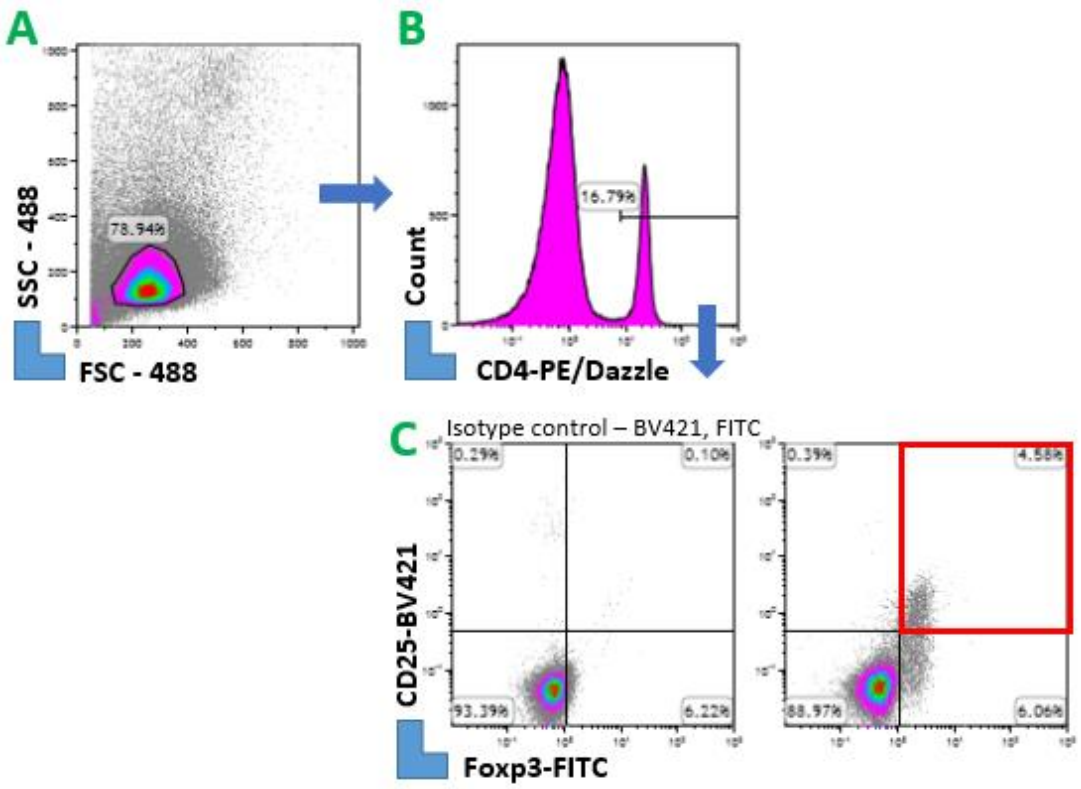



**Figure 5.8:** Representative flow cytometry plots and the gating analysis scheme for splenic $CD25^{hi}Foxp3^+$ Tregs from mice orally dosed with *H. pylori*. Mouse spleen cells were stained with rat fluorochrome-conjugated antibodies to identify Tregs. (A) Lymphocyte population gated by forward (FSC) and side (SSC) scatter under the 488nm laser. (B) Histogram showing $CD4^+$ events amongst gated lymphocytes. Representative CD25-Foxp3 plot from $CD4^+$ gated events with its corresponding isotype control.

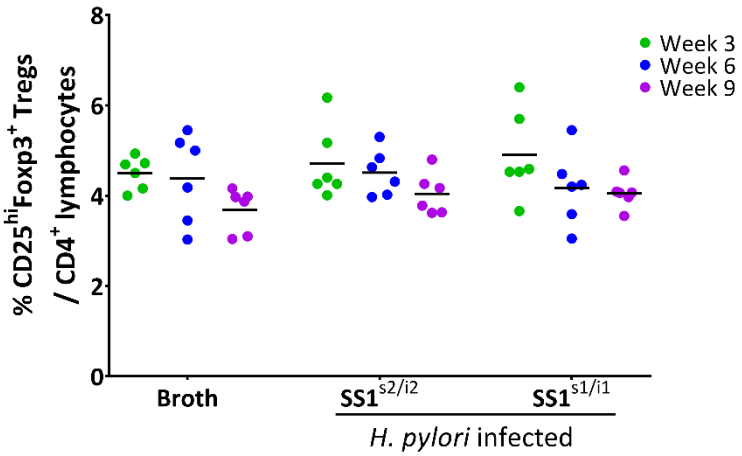



**Figure 5.9:** Proportion of splenic $CD25^{hi}Foxp3^{+}$ Tregs within the $CD4^{+}$ T cell population in mice. C57BL/6 mice were orally dosed with Brucella broth (Broth), infected with *H. pylori* SS1 wild-type strain ($SS1^{s2/i2}$), or with *H. pylori* mutant SS1 strain ($SS1^{s1/i1}$) for 3, 6 or 9 weeks. Mouse spleen cells were stained with rat fluorochrome-conjugated antibodies to identify Tregs. The horizontal lines depict the mean value.

At 9 weeks after infection, changes in IL-10-producing Treg frequencies were analysed (**Figure 5.10**). There was a trend in the increased proportion of Tregs producing IL-10 from the spleens of mice infected with the mutant *H. pylori* SS1$^{s1/i1}$ strain, compared to uninfected mice.

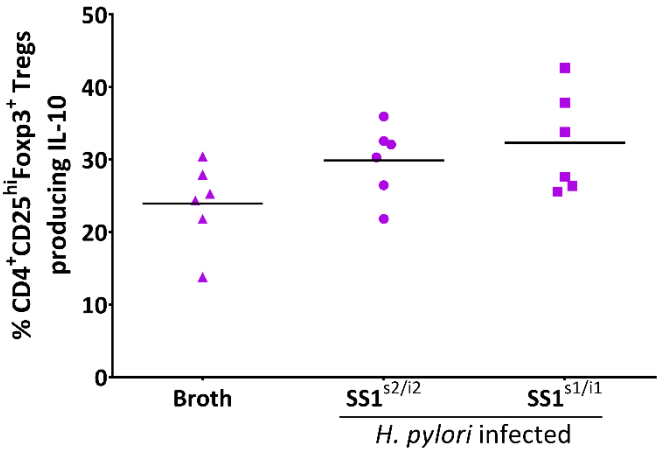



**Figure 5.10:** Proportion of splenic IL-10-producing CD25$^{hi}$Foxp3$^{+}$ Tregs within the CD4$^{+}$ T cell population in mice. C57BL/6 mice were orally dosed with Brucella broth (Broth), infected with *H. pylori* SS1 wild-type strain (SS1$^{s2/i2}$), or with *H. pylori* mutant SS1 strain (SS1$^{s1/i1}$) for 9 weeks. Mouse spleen cells were stained with rat fluorochrome-conjugated antibodies to identify IL-10$^{+}$ Tregs. Cells were stimulated with a combination of PMA, ionomycin and *E. coli* LPS mitogens for 6 hours. The horizontal lines depict the mean value.

### 5.5.2 Bregs and Tregs in mouse blood after *H. pylori* infection

The spleen is a widely used model for *H. pylori* infection in mice. In mice, the spleen is the largest secondary immune organ. It samples antigens through the blood, and is involved in antigen processing. It is a plentiful source of B lymphocytes and B cells expressing 'regulatory' markers, as the organ contains 25% of the body's lymphocytes[283]. Blood is used in human *H. pylori* diagnostic tools and research. By comparing lymphocyte populations in spleen and blood in a mouse model, a greater picture is formed of the lymphocyte responses after *H. pylori* infection. So far in this thesis, only B and $CD4^+$ T lymphocytes and their IL-10 production have been studied. The proportions of other potentially IL-10-producing T cells ($CD3^+$ and $CD8^+$) were included in the blood sample analysis. B lymphocytes were first analysed by light and side scatter under the 488nm laser, and according to the gating strategy described (**Figure 5.11**).

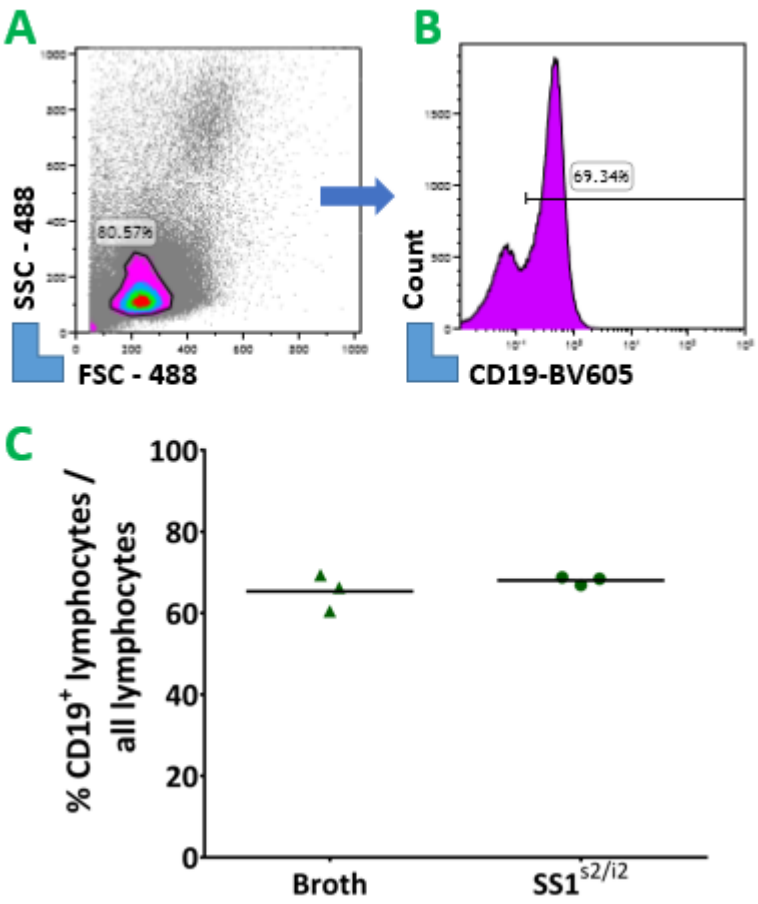



**Figure 5.11:** Representative flow cytometry plots, the gating scheme, and subsequent analysis of $CD19^+$ lymphocytes in mouse blood. Mouse leukocytes were stained with rat fluorochrome-conjugated antibodies to identify B lymphocytes. (A) Lymphocyte population gated by forward (FSC) and side (SSC) scatter under the 488nm laser. (B) Histogram showing $CD19^+$ events amongst gated lymphocytes. (C) Proportions of $CD19^+$ B lymphocytes. Female C57BL/6 mice were orally dosed with Brucella broth (Broth), or infected with *H. pylori* SS1 wild-type strain ($SS1^{s2/i2}$) for 9 weeks. The horizontal lines depict the mean value.

As with splenic populations, B cells in blood were more abundant than T cells, at an average of 65% of gated lymphocytes, but this did not change upon *H. pylori* infection (**Figure 5.11**). A gating strategy was developed to consistently identify $CD3^+$, $CD4^+$ and $CD8^+$ T lymphocytes (**Figure 5.12**). $CD3^+$ T cell frequencies accounted for a mean of 22% of the gated lymphocyte population in the peripheral blood lymphocytes of uninfected mice (**Figure 5.13A**). While this population did not change significantly upon infection, the $CD8^+$ subpopulation increased by 9% after *H. pylori* infection ($p$ = 0.0050). The $CD4^+$ subpopulation did not increase upon infection, consistent with $CD4^+$ lymphocytes in the spleen of uninfected and *H. pylori* infected mice.

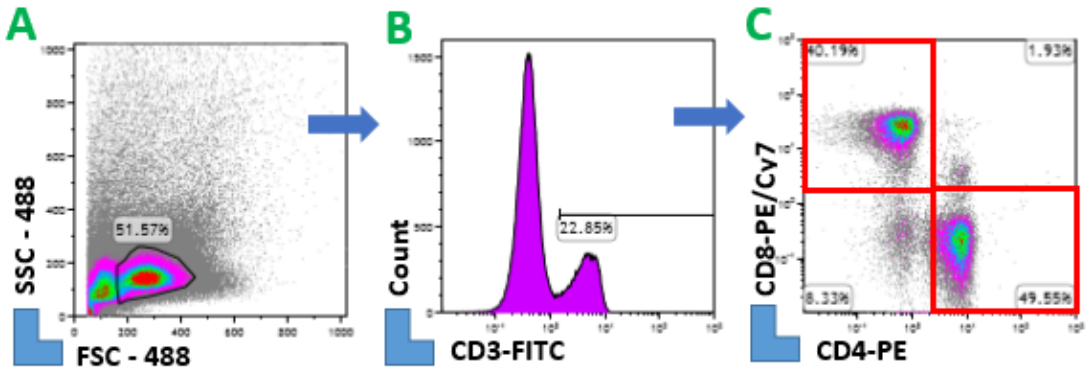



**Figure 5.12:** Representative flow cytometry plots and the gating analysis scheme for $CD3^+$, $CD4^+$ and $CD8^+$ lymphocytes in mouse blood. Mouse leukocytes were stained with rat fluorochrome-conjugated antibodies to identify T lymphocytes. (A) Lymphocyte population gated by forward (FSC) and side (SSC) scatter under the 488nm laser. (B) Histogram showing $CD3^+$ events amongst gated lymphocytes. (C) $CD4^+$ and $CD8^+$ events gated from $CD3^+$ lymphocytes.

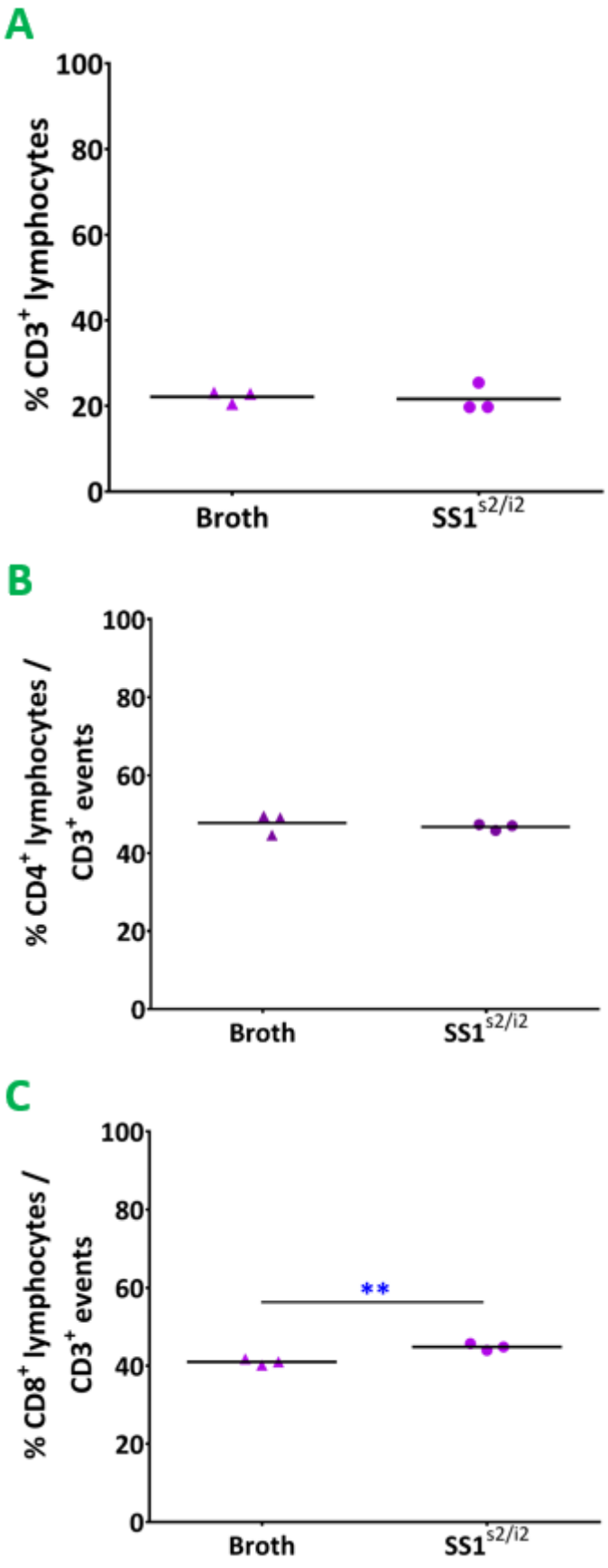

A
100
80
60
40
20
0
% CD3+ lymphocytes
Broth
SS1s2/i2
B
100
80
60
40
20
0
% CD4+ lymphocytes / CD3+ events
Broth
SS1s2/i2
C
100
80
60
40
20
0
% CD8+ lymphocytes / CD3+ events
**
Broth
SS1s2/i2

**Figure 5.13:** (Overleaf) Proportion of T cells amongst peripheral blood lymphocytes in mice. C57BL/6 mice were orally dosed with Brucella broth (Broth) or infected with *H. pylori* SS1 wild-type strain ($SS1^{s2/i2}$) for 9 weeks. (A) $CD3^+$ T cells. (B) $CD4^+$ T cells from the $CD3^+$ population. (C) $CD8^+$ T cells from the $CD3^+$ population. The horizontal lines depict the mean value. Statistical analysis was carried out using an unpaired T-test. The asterisks indicate the level of statistical significance, where ** represents $p \leq 0.01$.

The relative proportions of IL-$10^+$ events amongst B lymphocytes were then analysed in mouse blood (**Figure 5.14**). An average of 88% of the IL-$10^+$ lymphocyte frequencies were $CD19^+$ cells, suggesting that peripheral blood B cells are a major potential source of IL-10.

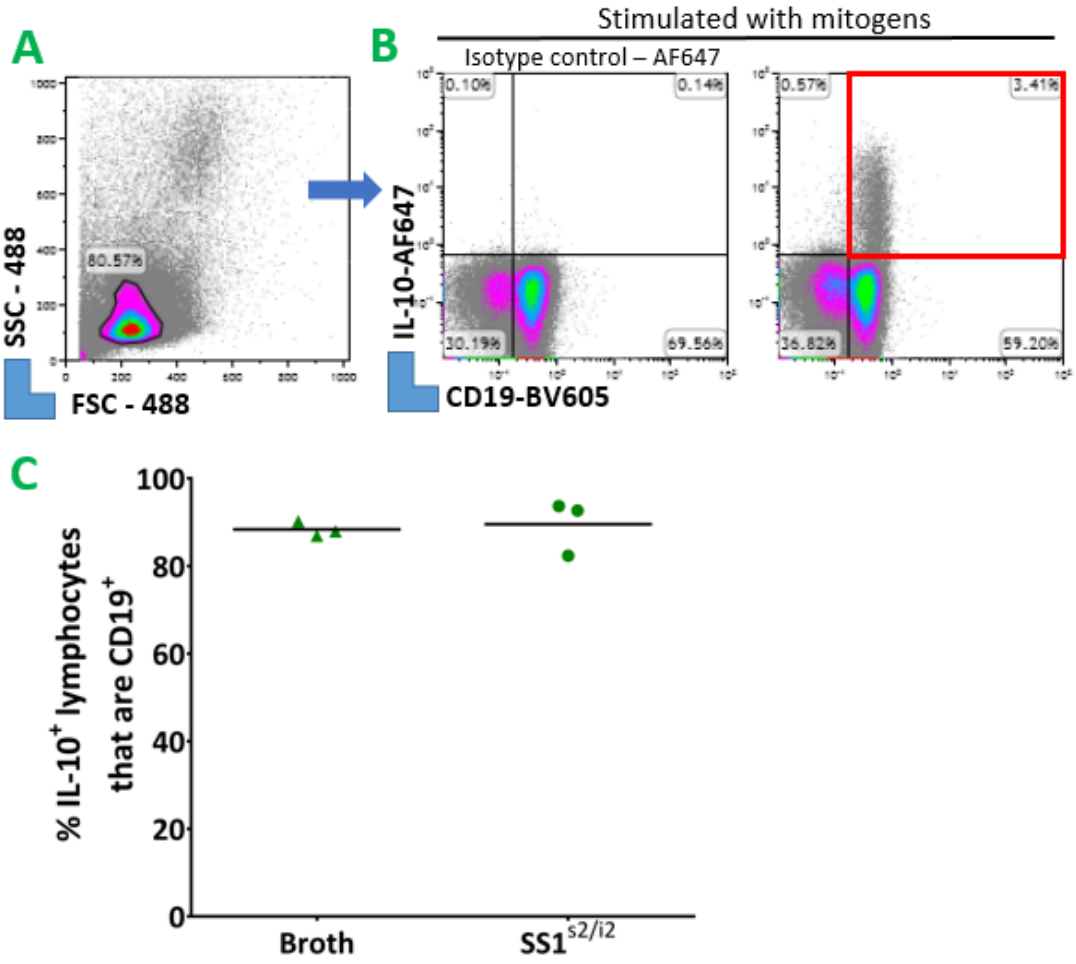



**Figure 5.14:** Representative flow cytometry plots, the gating scheme, and subsequent proportions of IL-10$^+$ lymphocytes in uninfected and *H. pylori*-infected groups of mice. Mouse blood was stained with rat fluorochrome-conjugated antibodies to identify IL-10$^+$ CD19$^+$ B lymphocytes. Cells were stimulated with a combination of PMA, ionomycin and *E. coli* LPS mitogens for 6 hours. (A) Lymphocyte population gated by forward (FSC) and side (SSC) scatter under the 488nm laser. (B) Representative CD19-IL-10 plot and corresponding isotype control. (C) Proportion of IL-10$^+$ lymphocytes that are CD19$^+$ B cells in mouse blood. Female C57BL/6 mice were orally dosed with Brucella broth (Broth) or infected with *H. pylori* SS1 wild-type strain (SS1$^{s2/i2}$) for 9 weeks. The horizontal lines depict the mean value.

By further analysing the IL-10-producing $CD3^+$ population, different subpopulations of IL-10-producing cells were identified. This was important to understand the phenotype of cells which are capable of producing IL-10. A gating strategy was developed to consistently identify these $IL\text{-}10^+$ population. Both $CD4^+$ and $CD8^+$ T cells produced IL-10 at similar frequencies, and the populations tended to expand upon *H. pylori* infection (**Figures 5.15-5.18**).

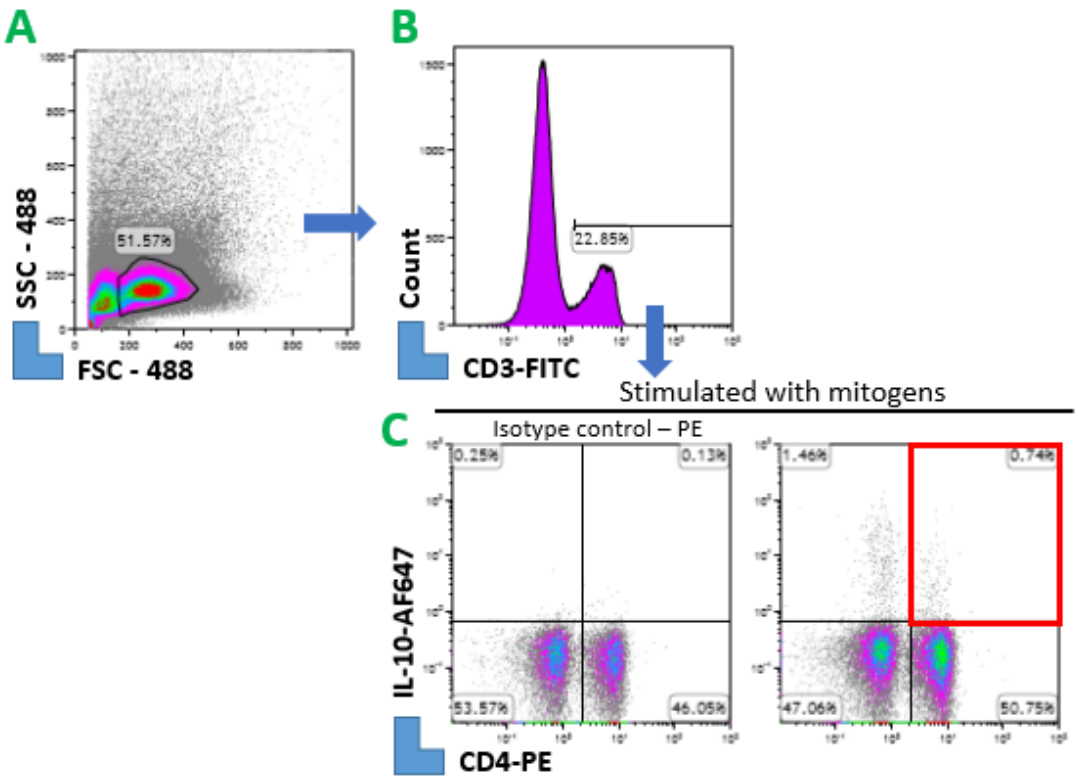



**Figure 5.15:** Representative flow cytometry plots and the gating analysis scheme for proportions of $IL\text{-}10^+$ T lymphocytes in uninfected and *H. pylori*-infected groups of mice. Mouse blood was stained with rat fluorochrome-conjugated antibodies to identify $IL\text{-}10^+$ $CD4^+$ T lymphocytes. Cells were stimulated with a combination of PMA, ionomycin and *E. coli* LPS mitogens for 6 hours. (A) Lymphocyte population gated by forward (FSC) and side (SSC) scatter under the 488nm laser. (B) $CD3^+$ events gated from the lymphocyte population. (C) Representative CD4-IL-10 plot and corresponding isotype control.

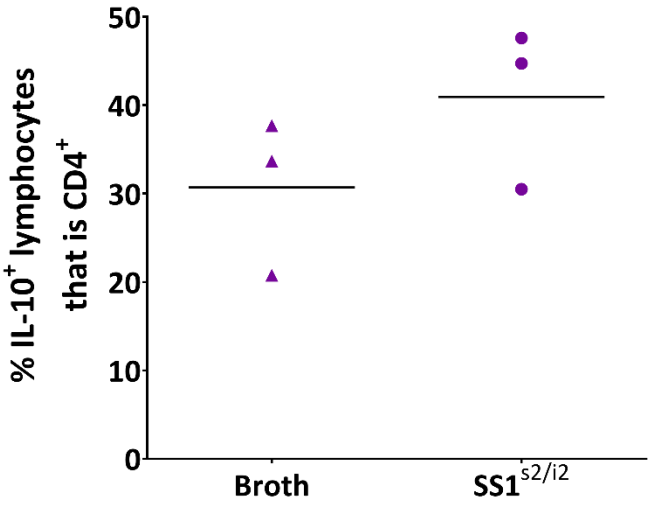



**Figure 5.16:** Proportion of IL-10$^+$ lymphocytes that are CD4$^+$ T cells in mouse blood. Female C57BL/6 mice were orally dosed with Brucella broth (Broth) or infected with *H. pylori* SS1 wild-type strain (SS1$^{s2/i2}$) for 9 weeks. Mouse blood was stained with rat fluorochrome-conjugated antibodies to identify IL-10$^+$ CD4$^+$ T lymphocytes. Cells were stimulated with a combination of PMA, ionomycin and *E. coli* LPS mitogens for 6 hours. The horizontal lines depict the mean value.

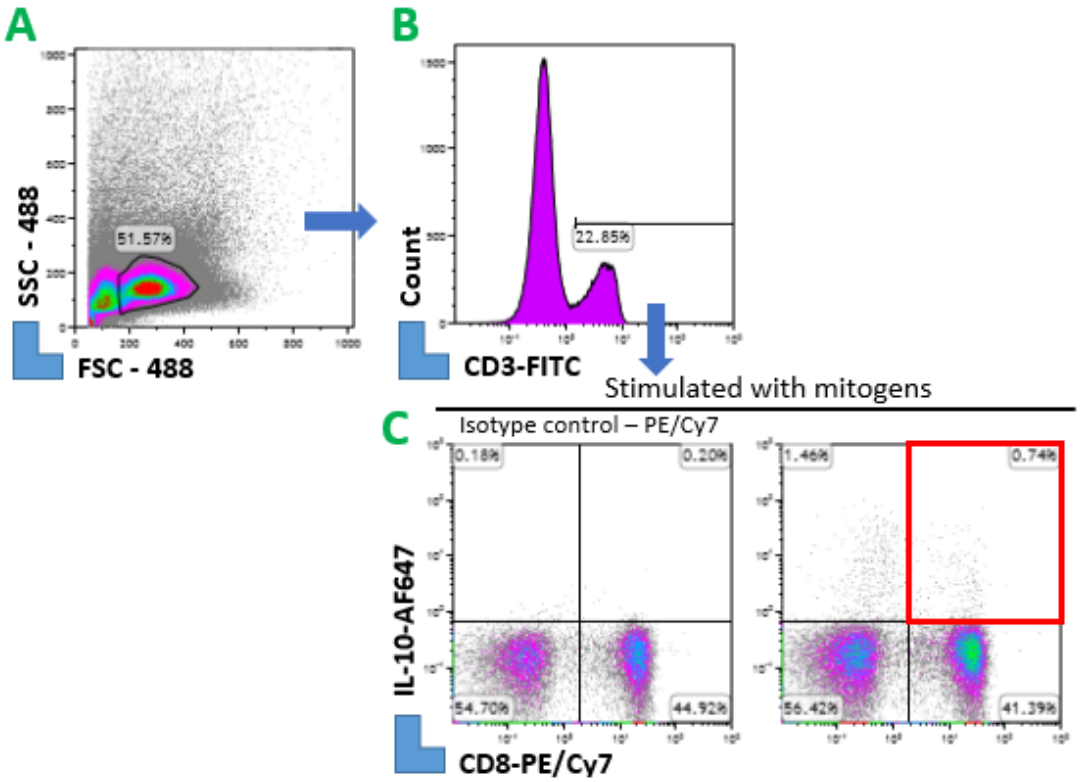



**Figure 5.17:** Representative flow cytometry plots and the gating analysis scheme for proportions of peripheral blood IL-10$^+$ T lymphocytes in uninfected and *H. pylori*-infected groups of mice. Mouse blood was stained with rat fluorochrome-conjugated antibodies to identify IL-10$^+$ CD8$^+$ T lymphocytes. Cells were stimulated with a combination of PMA, ionomycin and *E. coli* LPS mitogens for 6 hours. (A) Lymphocyte population gated by forward (FSC) and side (SSC) scatter under the 488nm laser. (B) CD3$^+$ events gated from the lymphocyte population. (C) Representative CD8-IL-10 plot and corresponding isotype control.

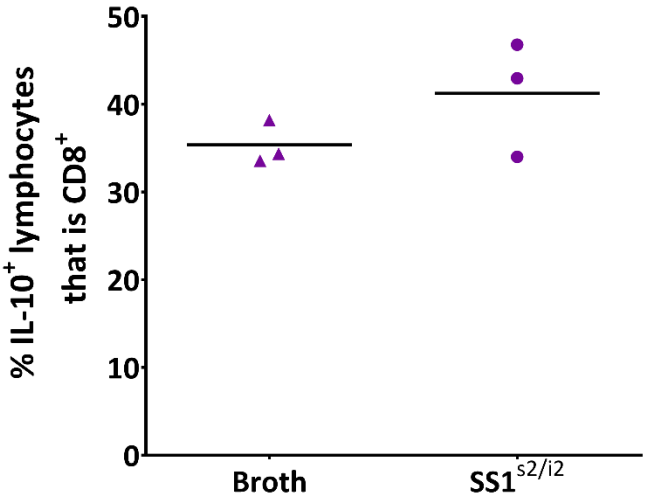



**Figure 5.18:** Proportion of IL-10-producing $CD8^+$ T cells in peripheral blood lymphocytes from mice. C57BL/6 mice were orally dosed with Brucella broth (Broth), or infected with *H. pylori* SS1 wild-type strain ($SS1^{s2/i2}$) for 9 weeks. Mouse blood was stained with rat fluorochrome-conjugated antibodies to identify $IL\text{-}10^+$ $CD8^+$ T lymphocytes. Cells were stimulated with a combination of PMA, ionomycin and *E. coli* LPS mitogens for 6 hours. The horizontal lines depict the mean value.

Because B cells were identified as a major source of IL-10, and IL-10 is thought to be a major Breg marker, proportions of $CD19^{+}CD1d^{hi}CD5^{+}$ events were then analysed from amongst the $IL\text{-}10^{+}$ lymphocyte population. Surprisingly, $CD1d^{hi}CD5^{+}$ Bregs could not be detected in mouse blood (**Figure 5.19**).

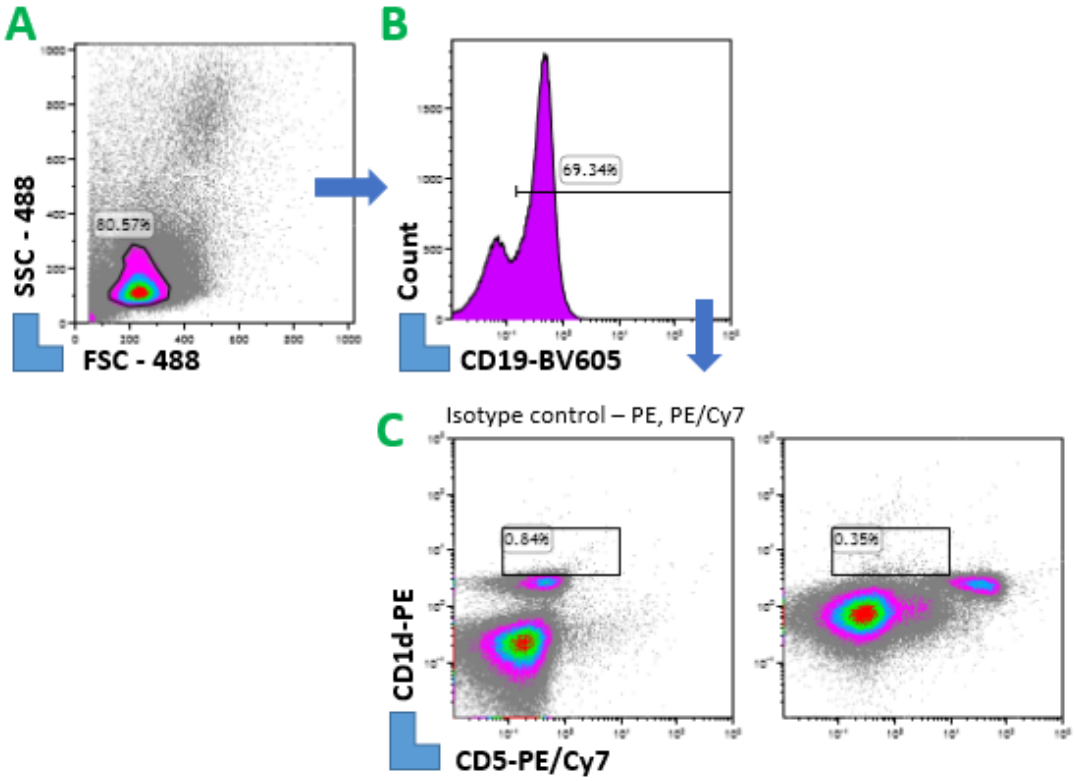



**Figure 5.19:** Representative flow cytometry plots and the gating analysis scheme for peripheral blood $CD1d^{hi}CD5^{+}$ Bregs in mice. Mouse blood was stained with rat fluorochrome-conjugated antibodies to identify Bregs. (A) Lymphocyte population gated by forward (FSC) and side (SSC) scatter under the 488nm laser. (B) Histogram showing $CD19^{+}$ events amongst gated lymphocytes. (C) Representative CD1d-CD5 plot from $CD19^{+}$ gated events with its corresponding isotype control.

There were also no significant differences in the frequencies of $CD4^+Foxp3^+$ Treg frequencies in the blood of infected and uninfected mice (**Figure 5.20**), or in the proportion of IL-10-producing Tregs (**Figure 5.21**).

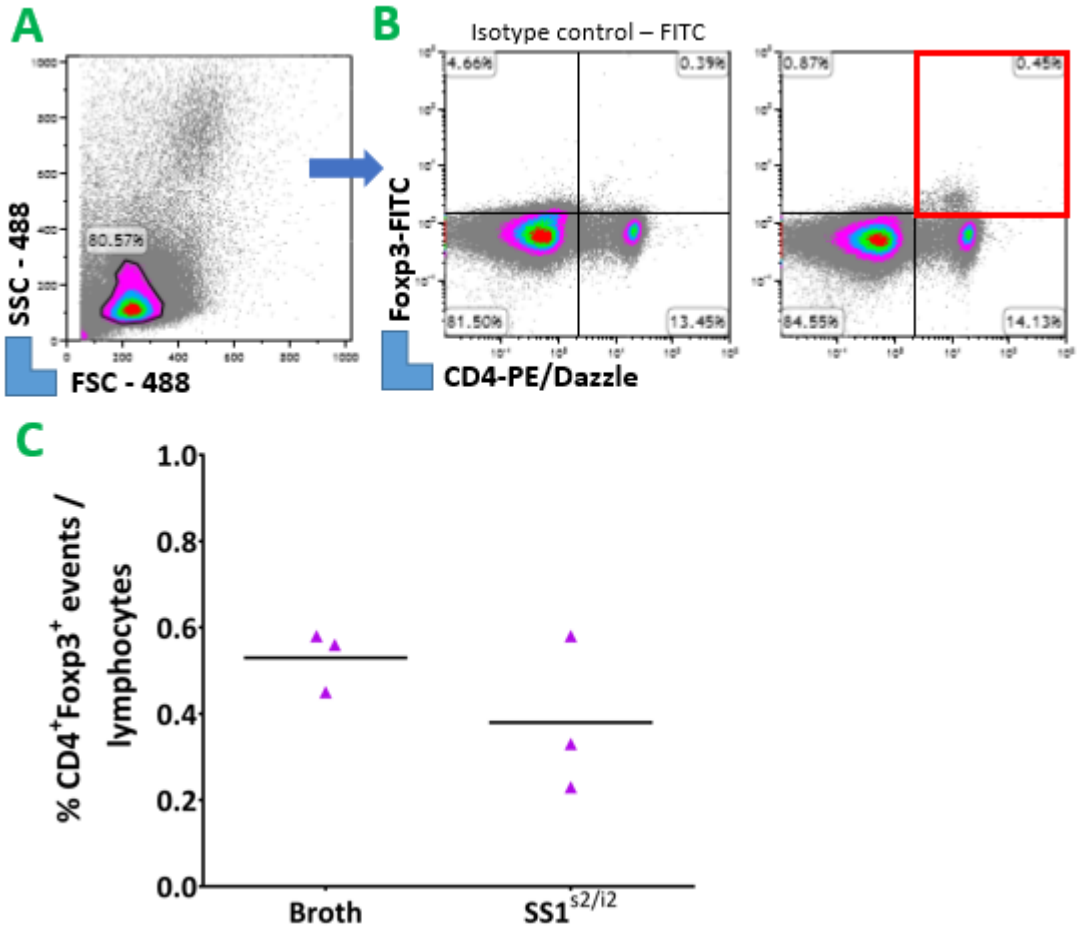



**Figure 5.20:** Representative flow cytometry plots, the gating scheme, and the analysis of the proportion of $Foxp3^+$ peripheral blood Tregs in mice. Mouse blood was stained with rat fluorochrome-conjugated antibodies to identify Tregs. (A) Lymphocyte population gated by forward (FSC) and side (SSC) scatter under the 488nm laser. (B) Representative CD4-Foxp3 plot from gated lymphocytes with its corresponding isotype control. (C) Proportions of $CD4^+Foxp3^+$ Tregs in mice. C57BL/6 mice were orally dosed with Brucella broth (Broth) or infected with *H. pylori* SS1 wild-type strain ($SS1^{s2/i2}$) for 9 weeks. The horizontal lines depict the mean value.

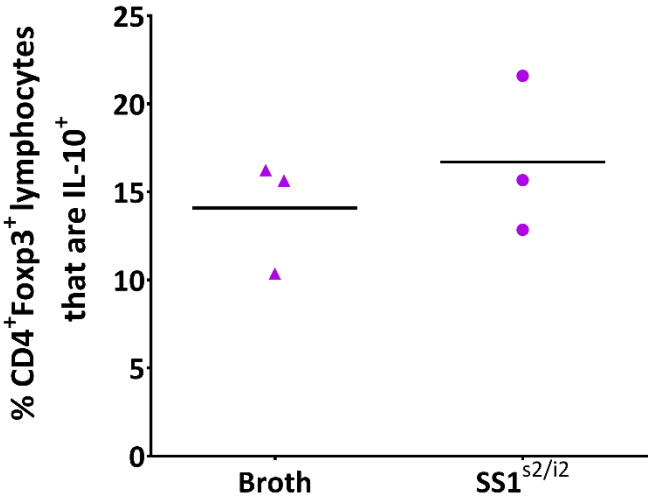



**Figure 5.21**: Proportion of $CD4^+Foxp3^+$ Tregs producing IL-10 within the peripheral blood lymphocyte population in mice. C57BL/6 mice were orally dosed with Brucella broth (Broth), or infected with *H. pylori* SS1 wild-type strain ($SS1^{s2/i2}$) for 9 weeks. Mouse blood was stained with rat fluorochrome-conjugated antibodies to identify $IL\text{-}10^+$ $CD8^+$ T lymphocytes. Cells were stimulated with a combination of PMA, ionomycin and *E. coli* LPS mitogens for 6 hours. The horizontal lines depict the mean value.

### 5.5.3 Studying splenic Treg function in *H. pylori*-infected mice

To investigate whether *H. pylori* infection induced differences in Treg functional activity, $CD4^+CD25^+$ Tregs were purified from the spleens of mice at 6 and 9 weeks after infection with wildtype *H. pylori* $SS1^{s2/i2}$ strain, or given Brucella broth. $CD4^+CD25^-$ responder (Tresp) cells were purified from naïve mice, labelled with the fluorescent dye CFSE, activated with anti-CD3/CD28 beads and cultured with a range of concentrations of $CD4^+CD25^+$ Tregs for four days. The expansion of $CFSE^+$ Tresp cells was then assessed by flow cytometry analysis. A gating strategy was developed to identify peaks in cell division in $CD4^+CD25^-$ CFSE-labelled and unlabelled spleen cells (**Appendix H**).

While Tregs were able to suppress Tresp cell division even at a 1:8 Treg:Tresp ratio, there was no significant difference in Treg suppression capacity between the uninfected or *H. pylori*-infected mice at 6 and 9 weeks after infection (**Figure 5.22**).

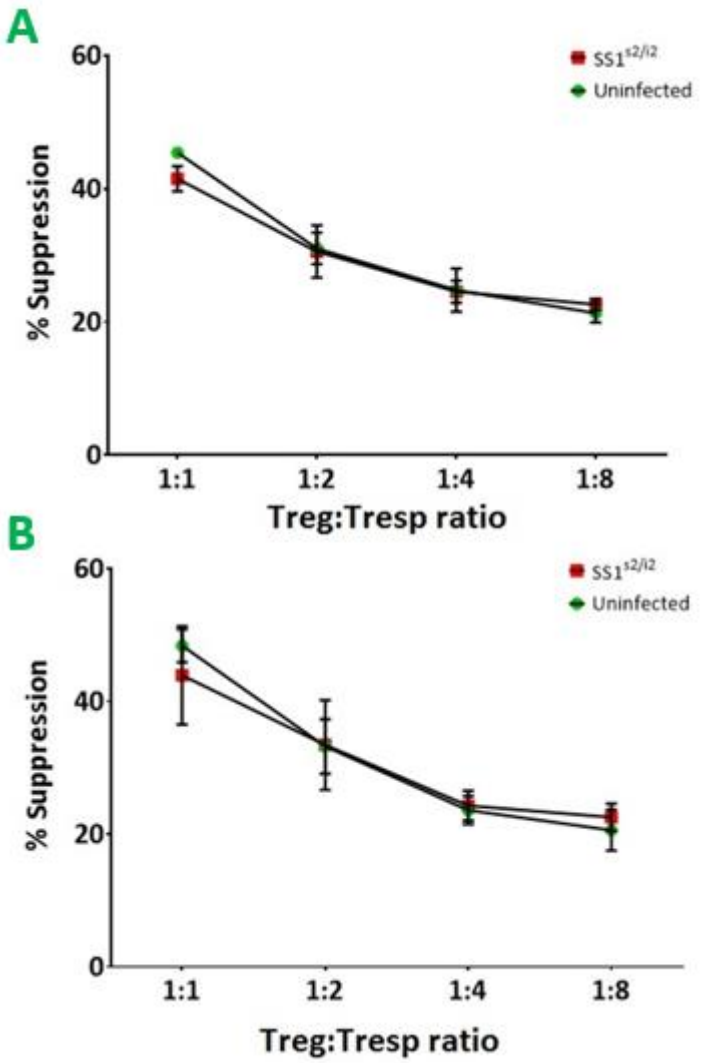



**Figure 5.22:** The *ex vivo* suppression capacity of splenic Tregs after *H. pylori* infection in mice. $CD4^+CD25^-$ Tresp cells from naïve C57BL/6 mice were labelled with CFSE and co-cultured with $CD4^+CD25^+$ Tregs from C57BL/6 mice orally dosed with Brucella broth (Uninfected), or infected with *H. pylori* SS1 wild-type strain ($SS1^{s2/i2}$) at different ratios for 4 days. (A) 6 weeks after infection (C) 9 weeks after infection. The error bars depict the mean and standard deviation.

## 5.6 Discussion

### 5.6.1 Statement of principal findings

This study aimed to investigate regulatory B and T lymphocyte responses in the blood and spleen of *H. pylori* infected and uninfected mice over a time course of 9 weeks. C57BL/6 mice were infected with wild-type *H. pylori* SS1$^{s2/i2}$ or mutant *H. pylori* SS1$^{s1/i1}$, or given Brucella broth. While CD19$^{+}$ B cells declined over time in all groups, there was no significant difference in the spleen of infected and uninfected mice. Although the CD1d$^{hi}$CD5$^{+}$ Breg response to mutant *H. pylori* SS1$^{s1/i1}$ increased over 9 weeks, this was not significantly different from uninfected mice. Splenic CD4$^{+}$ T cell and CD4$^{+}$CD25$^{hi}$Foxp3$^{+}$ Treg frequencies stayed consistent after 9 weeks, irrespective of *H. pylori* infection status. There was a trend of increased IL-10$^{+}$ splenic Tregs from mice infected with the *H. pylori* SS1$^{s1/i1}$ mutant strain compared to uninfected mice, but no difference was observed in IL-10$^{+}$ B, T or Breg cell frequencies in murine spleen after *H. pylori* infection.

There was no detectable CD1d$^{hi}$CD5$^{+}$ Breg population in murine blood. As observed in the spleen, CD19$^{+}$ B cells were the major lymphocyte type in blood. While there was a small increase in the proportion of CD8$^{+}$ T cells after *H. pylori* infection, there was no significant difference in CD3$^{+}$ or CD4$^{+}$ T and B cell frequencies up to 9 weeks after *H. pylori* infection. 88% of IL-10$^{+}$ lymphocytes were also CD19$^{+}$ B cells, and this did not change upon infection. 11% of IL-10$^{+}$ lymphocytes were CD3$^{+}$ T cells, and this did not change with infection. 30-40% of CD3$^{+}$IL-10$^{+}$ lymphocytes were from CD4$^{+}$ and CD8$^{+}$ subset populations. CD4$^{+}$Foxp3$^{+}$ Treg frequencies in peripheral blood did not increase 9 weeks after *H. pylori* infection. There was also no significant difference in the function of CD4$^{+}$CD25$^{+}$ regulatory cells in the suppression of CD4$^{+}$CD25$^{-}$ effector cells after 9 weeks, or after *H. pylori* infection.

### 5.6.2 Importance of the findings

This is a novel study identifying the frequencies of regulatory B and T cells in mouse models after infection with the bacterium *H. pylori*. Previous work in this field showed that *H. pylori* VacA induces a tolerisation of DCs in mice, promoting a Treg response from the host and indirectly, its own persistent colonisation[192]. In this group, the VacA$^{i1}$ variant was identified as a risk factor for *H. pylori*-induced intestinal metaplasia in mice[87]. The role of the i1 variant in the induction of Bregs and Tregs was therefore an important subject to research further. It was crucial to perform this investigation in mice to prevent the influence of confounding factors on *H. pylori*-induced Breg and Treg responses such as age, sex, genetic differences, co-morbidities, and lifestyle choices such as smoking and diet. Mice in this study were inbred females, age-matched, housed in the same facility and with the same diet.

Findings show that Bregs accounted for approximately 3% of splenic B cells in uninfected mice. This agrees with data from other studies[221 302 303]. After *H. pylori* infection, the frequency of Bregs did not increase significantly compared to uninfected mice. However, there was an increasing trend of Bregs in mice infected with the *H. pylori* SS1$^{s1/i1}$ mutant strain over time. Approximately 4% of splenic CD4$^{+}$ T cells were Tregs. This is in agreement with results from published studies[192 243]. After 9 weeks with mutant or wild-type SS1 infection, there was no change in Treg frequency. This is a finding also shown in another study where the Treg population did not expand until after 10 weeks of *H. pylori* infection[243].

This experiment aimed to characterise the IL-10-producing lymphocytes after infection with *H. pylori*. IL-10 is an important immunomodulatory cytokine which has been cited as the major means of suppression by Bregs and Tregs. IL-10 knockout mice have been shown to have more gastric immunopathology than wild-type mice, but also, removed of Treg influence maintaining *H. pylori* persistence, promotes further host pro-inflammatory responses to eradicate the infection. In the present study, it was found that 3% of splenic B cells produced IL-10 after stimulation, and this did not change after 9 weeks. Upon stimulation with mitogens, 1-3% of B cells

are IL-10-producing[218 221]. After infection with *Helicobacter felis*, one study reported that there were no differences in IL-10$^+$ cell frequencies in splenic B cells[106]. The authors found that while there was an expansion of B cells in the stomach, there were no differences in the size of the IL-10$^+$ B cell population. Therefore, large numbers of B cells were recruited, but most did not produce IL-10.

IL-10-producing CD4$^+$ lymphocytes expanded by almost two-fold 9 weeks after *H. pylori* SS1$^{s1/i1}$ infection. There was also a higher proportion of IL-10$^+$ Tregs compared to IL-10$^+$ Bregs which was observed previously in an analysis of IL-10$^+$ events from CD4$^+$ T cell frequencies in the *Helicobacter*-infected stomach[106]. This IL-10$^+$ population expanded at 9 weeks after infection with mutant *H. pylori* SS1$^{s1/i1}$ infection. The non-significant expansion of IL-10-producing CD4$^+$ T cells and its subset Treg population after *H. pylori* infection suggests that the hypothesis was disproved.

Furthermore, a comparison of Breg and Treg frequencies in mouse spleen and peripheral blood in uninfected and *H. pylori*-infected mice has not previously been published. This is important because there are known differences between the consequences of *H. pylori* infection in mice and humans. *H. pylori* research in humans usually includes analysis of PBMCs, but in mice, splenic tissue is often used. While mouse spleen is a convenient source of lymphocytes, also studying blood from infected mice provided a bigger picture of the effects of *H. pylori* infection on the host immune response, and an insight into regulatory cells which may have been recruited to the gastric mucosa during infection. In this study, CD1d$^{hi}$CD5$^+$ Bregs were identified in splenic tissue, but not in blood. This Breg population has not been observed previously in mouse blood[218]. B cells were the largest lymphocyte population in both blood and spleen, and most IL-10$^+$ lymphocytes were B cells. This did not change significantly upon infection. Regardless of infection status, the proportion of CD19$^+$CD1d$^{hi}$CD5$^+$ Bregs in mouse spleen from the parent B cell population were much less frequent than Tregs. This is surprising, given that B cells are several fold more frequent than T cells in mouse spleen, and by far the largest IL-10$^+$ population.

This is also the first study to look at the effect of different VacA types on immunomodulatory Breg and Treg frequencies, and suppressive function. This is important because VacA is a cytotoxin expressed by virtually all *H. pylori* strains. The i1 variant form of VacA is an independent risk factor for *H. pylori*-mediated disease[84]. Furthermore, recent evidence suggests that VacA promotes *H. pylori* persistence by modulating DCs to skew a Treg immune response via GGT[192]. The study used mice infected with a *H. pylori vacA*$^{-/-}$ strain to observe Treg frequencies, but the effect of different VacA variants on Bregs and Tregs has not yet been reported in the literature. While there was a slight increase in Breg frequencies in mice infected with mutant SS1$^{s1/i1}$ *H. pylori*, this was not significantly more than in uninfected mice. However, at week 9 post infection, mice infected with *H. pylori* SS1$^{s1/i1}$ had the largest frequency of IL-10-producing CD4$^{+}$ T cells. Infection with either *H. pylori* strain did not appear to modulate Treg frequency but both infections had increased IL-10$^{+}$ Tregs at week 9. An increased infiltration of Foxp3$^{+}$ Tregs in the stomach was also only observed at the 9-week time point (Dr. Kazuyo Kaneko, unpublished data). Another study showed that mice infected with a *H. pylori* v*acA* null strain induced similar Treg frequencies to uninfected mice[192]. By further studying how Treg suppression of effector cells differed between strains, any effects of VacA types on Treg activity could be observed. In this study, *H. pylori* infection did not influence the frequencies or function of Tregs induced by *H. pylori* infection.

### 5.6.3 Biological relevance of the findings

There was no effect on Breg frequencies by different VacA variants within *H. pylori* infection after 9 weeks. The only published study to investigate IL-10-producing B cells in mice described a marked expansion two weeks after *H. pylori* infection[243]. This study also used the same mitogen stimulation as the present study. The difference in results may be accounted for in the larger and more frequent dose of *H. pylori* given to the mice in the published study. In this study, only ~15% of CD1d$^{hi}$CD5$^{+}$ Bregs were producing IL-10. Other work also suggests that most Bregs are not IL-10-producing lymphocytes[221], possibly suggesting another mechanism of suppression, such as TGF-β[106 193]. One study showed through three different experiments that IL-10-producing

B cells were dispensable for gastric cancer pathology in mice, but that IL-10 from $CD4^+$ T cells was not, implying a crucial protective role[106].

The hypothesis that there is an increased Treg response after *H. pylori* $SS1^{s1/i1}$ infection compared to Brucella broth was not proven. There was no difference in Treg frequencies in blood or spleen and no difference in Treg functional suppression in infected and uninfected mice. The data in the present study does not correspond to other *H. pylori* studies in the literature[191 192]. Other groups have observed an increased Treg frequency upon infection, but this may be due to a number of different factors, such as different mouse species, *H. pylori* strain differences, age and gender of mice when infected and differences in the gastric microbiota. Moreover, differences in the characterisation of Tregs in flow cytometry (use of $CD25^+$ expression and not $CD25^{hi}$ expression) mean that there are differences between published studies and the present study[192 243].

In the present study, only 1/6 mice were colonised with $SS1^{s1/i1}$ after 9 weeks, compared to 5/6 mice infected with wild-type *H. pylori* $SS1^{s2/i2}$. Few *H. pylori* strains are capable of infecting mice, and the common strain SS1 lacks a functional *cag*PAI, and expresses $VacA^{s2/i2}$. An alternative strain, used especially for mouse *H. pylori* investigations (PMSS1), has the same virulence factor variants[87]. The use of wild-type $SS1^{s2/i2}$ and the mutant $SS1^{s1/i1}$ *H. pylori* strains were developed specifically to observe the VacA-specific differences in gastric inflammation[87]. The authors described that *H. pylori* $VacA^{s2/i2}$ strains colonised mice more effectively than *H. pylori* $VacA^{s1/i1}$ strains, suggesting a selection advantage in the expression of the non-vacuolating $VacA^{s2}$ in *H. pylori* strains. However, although $VacA^{s1/i1}$ strains did not colonise as effectively, they induced higher grades of pathology in the mouse stomach, compared to strains expressing $VacA^{s2/i2}$. VacA and CagA are known determinants for *H. pylori*-mediated disease. The extensive metaplasia and inflammation observed after the mutant *H. pylori* infection in mice provided a translatable model for human *H. pylori* symptomatic disease. Even with a $CagA^+$ background, $VacA^{i1}$ was strongly associated with pre-clinical oncology in human biopsy samples. There was virtually no pre-clinical oncological pathology observed in biopsy tissues infected with a $CagA^+$

VacA$^{s1/i2}$ *H. pylori* strain[87]. As the VacA$^{i2}$ is also present in *H. pylori* wild-type SS1 strain, the *H. pylori* mutant SS1$^{s1/i1}$ strain was therefore used in this study, as the strain background is more relevant for studying human *H. pylori*-mediated disease.

Anne Muller's group investigated the effects of *H. pylori* infection on extra-gastric diseases using a lower dose of *H. pylori* inoculum (compared to the present study) on neonatal mice[110]. One study showed a visibly decreased cell count at 10 weeks post-infection, compared to weeks 2-5[243]. The study also described a 30% CD4$^+$ T cell population from the total lymphocyte population in spleen. Differences in the age of infection in mice may explain why this has not been observed in the present study, irrespective of infection status.

There are limitations for Breg study in translational work, due to differences in Breg markers between mice and humans. These Breg markers also correspond to different B cell markers on the B cell differentiation pathway, and are not of a separate lineage, such as Foxp3$^+$ Tregs[304]. It is known that Tregs play an important role in *H. pylori*-mediated disease: Treg frequencies have been inversely associated with PUD, pre-clinical pathological changes and gastric cancer[119 193]. One study described that after mice were infected with *H. pylori*, an increased population of regulatory T cells was observed in extra-gastric tissue such as the intestinal mucosa[243]. Studying this further may provide some answers as to how *H. pylori* infection may help protect individuals from extra-gastric immune conditions such as MS.

### 5.6.4 Future work

With new research and developments in technology to accompany them, it has become evident that lymphocytes are more plastic in their activity than previously thought. Effector T cells have been shown to show Treg-like functions; for example, in this study pro-inflammatory cytotoxic CD8$^+$ T cells can also produce IL-10 after stimulation. The role for B cells in *H. pylori* infection is still unclear. Further *in vitro* studies on B cell suppressive mechanisms in *H. pylori* infection, and not on reported Breg cell phenotypes, may provide a greater understanding in how they can interact

with T cells in patients. This could be further examined with anti-TGF-β and/or anti-IL-10 assays in B and T cell co-culture, or from observing stained mucosal tissue in infected and uninfected mouse models.

Although not found in this study, VacA is an important factor that promotes the differentiation of host Tregs in *H. pylori* infection[192]. The VacA$^{i1}$ variant is an independent risk factor for diseases and pre-clinical gastric pathology caused by *H. pylori* infection[84 87]. Detecting VacA types may therefore be useful in a non-invasive diagnostic tool to identify individuals who are at an increased risk of *H. pylori*-mediated disease. This would be of clinical relevance, as current *H. pylori* diagnostic tools such as upper GI endoscopy are expensive, require a hospital setting with trained staff, and may not be appropriate for use in children[305 306]. Relatively non-invasive techniques such as blood tests also require the use of a needle. The use of stool is a cheap, non-invasive resource which, if optimised, could be used in PCR to identify VacA types in *H. pylori*-positive patients.

### 5.6.5 Conclusions

- The frequency of Bregs and Tregs in mouse spleen did not change significantly upon *H. pylori* infection compared to uninfected mice.

- *H. pylori* VacA type did not influence Breg or Treg frequency in mouse spleen or blood after infection with *H. pylori* for 9 weeks.

- $CD19^{+}CD1d^{hi}CD5^{+}$ Bregs were not detected in mouse blood, irrespective of infection status.

- The functional suppression of $CD4^{+}CD25^{+}$ splenic Tregs did not differ significantly between uninfected and *H. pylori*-infected mice.

# Chapter 6: Developing a *H. pylori vacA* type stool-based PCR test

## 6.1 Introduction

### 6.1.1 Invasive testing for *H. pylori* infection

*H. pylori* infection is most commonly diagnosed during an endoscopy of the upper GI tract. While scanning for gross abnormalities such as ulcers, small biopsies are usually collected from the stomach lining for histopathology and *H. pylori* diagnostic tests. These are taken from both the corpal and antral regions of the stomach[51]. The endoscopic procedure required to collect these stomach biopsies is expensive, invasive and requires multiple trained personnel in a hospital setting. However, the most commonly used and accurate diagnostic tests for *H. pylori* infection utilise these gastric mucosal biopsies.

A Rapid Urease Test (RUT), also known as the *Campylobacter*-Like Organism (CLO) test, is used in the endoscopy clinic to determine the presence of *H. pylori*. This is typically a commercial kit with an agar gel containing urea and a pH indicator solution (usually phenol red). A biopsy sample taken during the endoscopy procedure is pressed into the agar. If *H. pylori* is present, a colour change reflects the increased pH arising from *H. pylori* urease-mediated hydrolysis of urea into ammonia[307]. Although this test can be rapid, with a result in as little as 5 minutes, and reliable (>95% specificity, 85-95% sensitivity), there are some specific issues with its use. The sensitivity of this test can be decreased in certain conditions, such as the presence of bleeding peptic ulcers[308]. The ability of the test to detect the presence of *H. pylori* may also be affected by the site where the biopsy was obtained. Colonisation, and therefore damage to the gastric epithelium, is often patchy; so it is possible to miss an area of colonisation with *H. pylori*. Any atrophic or metaplastic tissue is also less optimal for *H. pylori* colonisation, and so there is a decreased likelihood of detecting *H. pylori* infection. Moreover, the routine use of PPIs in dyspepsia management creates a less acidic environment in the stomach; conditions which are less favourable for *H. pylori* colonisation. There is also evidence to suggest that PPIs have

some anti-bacterial properties[309], which may reduce the sensitivity of the test in some patients.

Biopsies may also be sent to a histopathologist for study and confirmation of *H. pylori* infection by histological staining. This method is largely used to assess the presence of pre-malignant pathology in gastric tissue, but stains such as Rapid Romanowsky, Modified Giemsa, Genta and silver stains can also be used to detect the presence of the *H. pylori* bacterium[51]. *H. pylori* is found at lower densities in areas of atrophy and inflammation of the stomach[310]. However, mucosal samples in close proximity to these regions are more likely to test positive for *H. pylori*. The specificity and sensitivity of this method of *H. pylori* infection diagnosis can be over 95%, when more than one biopsy is analysed[51]. Although this is beneficial, due to the subjective nature of the process, the accuracy of the test is largely dictated by quality of the biopsy sample, the precision of the staining process, and the experience of the histopathologist concerned.

Gastric biopsy samples may also be applied to bacteriological solid media for the isolation and culture of *H. pylori*. This method of diagnosis is usually used when eradication therapy has failed, to determine the antibiotic resistance and sensitivity profile of the isolate. *H. pylori* is a highly fastidious bacterium, which grows only in particular conditions. This includes a microaerophilic environment akin to that of the human stomach (3-7% oxygen)[311]. *H. pylori* requires rich media containing blood, or blood-derived products[311]. The presence of antibiotics and anti-fungal reagents within the culture media hinders the overgrowth of other more rapidly growing organisms, allowing for the easier isolation of *H. pylori*. An example of this is DENT *Helicobacter pylori* selective supplement, which contains vancomycin, trimethoprim, cefsulodin and amphotericin B. However, any sample which appears to be negative for the presence of *H. pylori* may be a true negative, or a positive sample which has failed to culture. This can be a common occurrence as the culture of *H. pylori* from biopsies may not be possible for all infected patients, and has a success rate near 50%[11].

### 6.1.2 Serological tests

Serological testing is another method used to determine *H. pylori* infection status. It is a form of commercial ELISA, where the plate is coated with *H. pylori* antigens. If an individual is positive for the infection, their serum contains IgG antibodies with paratropes to match epitopes seen on the antigens. After binding serum IgG to the antigens, a detection antibody tagged with horse-radish peroxidase (HRP) is added. When a substrate for HRP is added, a colour change occurs if a sample is sero-positive. This provides an absorbance value from which one can calculate the concentration of IgG antibodies present in the serum sample. This can then determine *H. pylori* status, with respect to appropriate standards and controls, according to the manufacturer's instructions for each commercial kit.

While this diagnostic tool has many advantages, including a high specificity and sensitivity, no cross-reactivity with other bacteria, and is less invasive than endoscopy, there are some drawbacks. IgG antibodies may be detectable for at least 2-6 months after *H. pylori* eradication. Therefore, serological testing is not effective for determining eradication success, as it may yield a positive result due to persistent immunological memory[8]. It also does not fully overcome the problem of being an invasive procedure, particularly for children[312]. Moreover, using serology collectively across the world brings problems as there is antigenic variability between isolates. However, this can be overcome by using antigens from local strains of *H. pylori*[313 314]. Malnutrition in developing countries also has a direct influence on the immune response. Consequently, IgG concentrations raised against a *H. pylori* infection may not be within a reference range used in diagnostic kits, limiting sensitivity.

### 6.1.3 Non-invasive tests

One of the most widely-used non-invasive diagnostic tools for determining *H. pylori* infection status is the Urease Breath Test (UBT). It is used clinically to check whether eradication therapy has been successful[315]. This test exploits the hydrolytic activity of *H. pylori*'s urease enzyme. There are other urease-positive organisms, but *H. pylori*

expresses very abundant quantities. In addition, all *H. pylori* strains are urease-positive, and this, combined with the large quantity produced[6], makes urease a reliable marker for *H. pylori* testing.

In the highly acidic environment of the stomach, the bacterium gains access to urea from tissue as a waste product of aerobic respiration. Urease then hydrolyses this into carbon dioxide ($CO_2$) and ammonia ($NH_3$). Ammonium ions buffer the bacterial surface, protecting *H. pylori* from gastric acid corrosion[315]. The test itself involves orally dosing patients with an aqueous solution containing urea labelled with a non-radioactive carbon isotope $^{13}C$. When urea is converted into $NH_3$ and $CO_2$, this is exhaled from the lungs and collected. The presence of *H. pylori* urease is detected, by quantifying how much $^{13}C$ or $^{14}C$ labelled $CO_2$ is exhaled[315]. If the individual is negative for the infection, urea remains unmodified, and no labelled $CO_2$ is detected.

This is a reliable test which detects a current infection, and consistently provides a >95% sensitivity and specificity[316]. Unfortunately, because of the requirement for a hospital setting and mass spectrometer to measure the labelled carbon dioxide, this test is expensive[51]. It is also of limited use because it only provides information on *H. pylori* infection status. Endoscopy-based tests can also highlight other potential problems, such as the presence of gastritis, tumours or ulcers.

Another non-invasive tool is the *H. pylori* Stool Antigen test (HpSA). It is convenient for patients, and especially applicable for young children, for whom endoscopy requires special equipment, and serology is invasive. It is a cheap test which contains an antibody complementary to *H. pylori* attached to microwells. It has a sensitivity and specificity of 94%[317] and reflects a current infection as it is a real-time product of the body. Although it provides few false positives[318], it can be affected by recent PPI use[195]. Unfortunately, like UBT, it is also a qualitative test which serves only to detect a *H. pylori* infection, and does not provide any data on other factors such as virulence factor type.

### 6.1.4 Testing for antibiotic resistance in *H. pylori* infection

The antibiotic sensitivities of a colonising strain can be evaluated using PCR. The bacterial resistance of antibiotics is the leading cause of *H. pylori* eradication therapy failure[319]. Identifying resistance is especially important for a patient with MALT-lymphoma, in areas of high resistance, or with adverse consequences from *H. pylori* infection[13], as delayed effective treatment may result in a declining prognosis.

This antibiotic resistance has been associated with the presence of polymorphisms within the *H. pylori* genome (**Table 6.1**), but there are differences in how these mutations link to resistance; mutations in the *rdxA* sequence did not necessarily translate into metronidazole resistance[320]. Antibiotic resistance can be tested with PCR, and is the basis of commercial kits, such as those detecting clarithromycin resistance[321 322]. PCR typing can determine which line of therapy should be given to the patient considering this, and so the infection can successfully be eradicated.

**Table 6.1:** Types of antibiotics used in eradication therapy for *H. pylori* infection, and the bacterial polymorphisms associated with resistance. Adapted from Mégraud[319]. Gene information was obtained from UniProt[323].

| Antibiotic group | Gene containing polymorphism |
|---|---|
| Amoxicillin | *pbp-1A* (encoding Penicillin-binding protein 1A) |
| Macrolides (*e.g.* Clarithromycin) | *23S* rRNA<br>Nucleotide positions 2142 and 2143<br>(2142) A modified to C<br>(2142) A modified to G<br>(2143) A modified to G |
| Metronidazole | *rdxA* and *frxA* (encoding an oxygen-insensitive nicotinamide adenine dinucleotide phosphate (NADPH) nitroreductase enzyme)[320] |
| Quinolones | *gyrA* (encoding DNA gyrase subunit A) |
| Rifamycins | *rpoB* (encoding DNA-directed RNA polymerase subunit B) |
| Streptomycin | *rpsL* (encoding 30S ribosomal protein S12) |
| Tetracycline | *16S* rRNA<br>Nucleotide positions 926-928<br>Arginine (AGA) modified to Phenylalanine (TTC) |

### 6.1.5 Testing for *H. pylori* virulence factors in clinical samples

As well as testing for *H. pylori* infection, specific tests for the presence of bacterial virulence factors have been developed. *H. pylori*-specific virulence factors include CagA, VacA and others which promote adhesion and immune evasion (**Section 1.4.2**). Because of the established links of East-Asian CagA$^{+}$, VacA$^{i1}$-variant infections with an increased risk of GA and PUD[84 261 324], these virulent types could be included in future prognostic tests.

#### 6.1.5.1 Serology

CagA-expressing *H. pylori* strains are likely to cause more severe inflammation than CagA$^{-}$ strains[73]. Their presence can be detected using an anti-CagA IgG antibody ELISA[325], or a western-blot based immunoblot, of which the latter is more sensitive[326 327]. The number of TPMs are variable, and can affect the phenotype of CagA[328], but there is no serological test to distinguish between the different CagA types. CagA is an immunogenic protein, and can maintain a constant response to antibody presence in a host for 20 years after eradication[65]. Because there are many commercially available kits to detect CagA presence, each with a varying degree of sensitivity and specificity, it has been recommended that scientific publications note which kit they have used for their research[329]. Virulence factor serotyping tests are not currently used clinically[263], because of the unreliable nature of the tests; some kits are reported to yield inconclusive results at a rate up to 19%[330]. There is also a likelihood of false positives[329]. However, developments in CagA serological tests have improved accuracy and provided rapid results. A combination of ELISA and western blot protocols produced a sensitivity of 94%, and a specificity of 81%, compared to the specificity of ELISA alone at 75% [331].

There are no commercially available VacA serology kits, and one study suggested that immunoblot assays should not be recommended for determining VacA status in *H. pylori* infected individuals[329] due to the variation observed in the immune response to VacA.

#### 6.1.5.2 PCR

PCR can be used to identify and classify virulence genotypes from different *H. pylori* strains. It is a technique which can amplify bacterial genes directly and indirectly (through DNA extraction) from clinical samples such as biopsies, saliva and stool. One study determined that performing PCR directly from biopsy samples recorded the highest sensitivity compared to histology, culture and CLO-testing[83]. It has been successfully used to determine associations of virulence types with disease outcomes. The level of specificity and sensitivity of PCR can be compared to that of culture[332], and PCR can detect as few as 10 *H. pylori* cells present in a clinical sample[333].

The *cagA* gene may be present, but a positive PCR result does not provide evidence that the 30-gene *cag*PAI is intact within the genome. Consequently, it cannot be determined whether an active T4SS is expressed and assembled to translocate CagA into the host cell. Furthermore, *cagA* itself has variation within strains from different populations around the world[65]. In PCR, a seemingly *cagA*-negative result may be a true negative, or a consequence of PCR failure due to small changes in the gene sequence at primer-binding regions. Therefore, *cagA*-PCR alone is a limited marker for determining an individual's increased risk of developing future disease.

Almost all *H. pylori* strains have a *vacA* gene[81], and there are several important allelic regions (signal, intermediate and mid) which have been used for PCR typing[84]. Because of the link between the expression of s1 and i1 variants in *vacA* and an increased risk of disease [81] [84], this is a more effective marker compared to *cagA*. Certain primers can bind and amplify different *vacA* variants. As *vacA* is ubiquitous in *H. pylori* infection, this eliminates a negative PCR result due to PCR failure.

#### 6.1.5.3 Stool PCR

The idea of using stool to identify a *H. pylori* infection has always been a desired aid for diagnosis. It is non-invasive and convenient for the patient, does not require a hospital setting, does not require specific growth conditions, and is inexpensive. *H. pylori* DNA can be derived from stool using a variety of commercial bacterial DNA purification kits. The purified DNA is then tested via PCR for the presence and typing of virulence *vacA* and *cagA* genes as accurate and sensitive markers for an increased disease risk in the future. However, there are many challenges to overcome PCR detection failure. Firstly, *H. pylori* grows optimally in gastric conditions and is shed with mucus into the intestine. The bacterium is unable to multiply within the (alkaline) intestine, and may be present in low numbers in stool – except in diarrhoea[334].

*H. pylori* DNA was first cultured from stool in African children[335]. This was potentially due to children having a faster stool transit time through the gut. Detecting *H. pylori* DNA has proved difficult to use in PCR-based stool testing because of the contaminated nature of stool. As *H. pylori* passes through the intestine, it is exposed to other micro-organisms, mucus, partially digested food remains, and various proteolytic enzymes[336] [337]. These are capable of degrading biological material, including *H. pylori* cells. A high vegetable diet also leads to the presence of complex carbohydrates in the stool. Such material contaminates stool DNA and can inhibit the successful amplification of *H. pylori* genes[337]. Abstention of vegetables in a patient's diet for two days prior to the collection of the stool sample removed much of these inhibitors. Another study by the same group described using DNA embedded in agarose to successfully decrease the concentration of inhibitors after DNA extraction[338] [339].

While numbers of *H. pylori* are potentially low in stool-extracted DNA[340], the potential resourcefulness of stool, combined with the simplicity of the PCR technique, meant that many attempts have been made to make a viable stool test. Efforts to amplify them have often included further PCR processing conditions. The sensitivity and specificity of this method of *H. pylori* testing has proved to be wide-ranging.

Different groups have modified traditional PCR techniques to detect *H. pylori* genes. Longer PCR conditions of 60-80 cycles were used because of a failure to detect *H. pylori* genes in traditional 30-40 cycling conditions[270 305 306 322 341-345]. The use of real-time and nested-PCR techniques over conventional PCR methods have also been used in various studies to increase the likelihood of detecting small concentrations of amplified DNA[341 306 270 312 346-348]. One study used radioactive primers to detect *H. pylori cagA* and *vacA* s-variant genes[340].

## 6.2 Rationale

Non-invasive tests for *H. pylori* infection used currently, such as the UBT and the stool antigen test, are limited because they can only confirm the presence of the *H. pylori* organism, and are unable to provide further information on virulence types. Endoscopy-based tests are invasive, expensive, and technically difficult for use in paediatric patients.

Stool tests to detect clarithromycin resistance have been developed[321 322]. They have also been developed to detect *vacA*$^{s1 \text{ or } s2}$ regions with varying degrees of success[305 343 346 349]. However, there are currently no developed tests to detect *vacA*$^{i1 \text{ or } i2}$ gene variants in the literature.

Infection with a *H. pylori* strain expressing *vacA*$^{i1}$ is an independent risk factor for an increased likelihood of disease outcome, such as GA. This project sought to develop a reproducible stool sample DNA extraction protocol, and develop a test for detecting the *vacA* i-region.

## 6.3 Aims

- To assess which commercial stool DNA extraction kit produced the highest concentration and best quality of DNA from human stool samples. Other practical parameters such as the applicability of the kit, and the length of time required to extract purified DNA were taken into consideration to develop a protocol which was easy to reproduce.

- To evaluate the level of chemicals acting as PCR inhibitors in eluted DNA, and to determine to what extent this prevents the successful detection and amplification of the *H. pylori 16S* rRNA gene.

- To optimise PCR primers and thermo-cycling conditions to successfully amplify *H. pylori* genes *16S* rRNA and *vacA* s-region variant genes, before using these conditions on DNA purified from stool samples.

- To use sequencing to firstly confirm the presence of *H. pylori 16S* rRNA and *vacA* PCR products in bands detected on agarose gels, then to match PCR product sequences from stool DNA with the *H. pylori* isolate recovered from the biopsies of the corresponding infected patients.

## 6.4 Materials and methods

### 6.4.1 Patient recruitment

Stool samples were donated by 16 patients undergoing a routine upper gastrointestinal endoscopy procedure at the Queen's Medical Centre in Nottingham, UK. The samples were collected under ethical approval from Nottingham Research Ethics Committee 2, and with informed written patient consent (**Appendix D**).

Patients (age range 35-77 years; 8 men and 8 women) were referred for a routine endoscopy to investigate a variety of symptoms (**Appendix I** for complete patient history). *H. pylori* positive and negative individuals were identified by diagnostic test results (**Table 6.2**). The patient's *H. pylori* status was determined by the results of a RUT, histological examination and by culture from gastric biopsies collected during an upper GI endoscopy procedure. Patients were excluded from participating in the study if they were regularly taking NSAIDs, or had consumed antibiotics or PPIs four weeks prior to the endoscopy.

When patients consented to participate in the study, they were provided with a stool sample collection pot and a gel pack, which was to be frozen overnight (**Appendix J** for information provided to patients). The following morning, the freshly filled stool pot was to be placed in the gel pack and mailed directly to the QMC for next day delivery. On arrival, the sample was snap frozen, and stored at -20°C.

**Table 6.2:** The results of *H. pylori* tests and the *H. pylori* status of patients undergoing an endoscopy at QMC, who consented to contribute to this *H. pylori* stool study.

| Patient no. | Histology | Serology | Culture | RUT | *H. pylori* status |
|---|---|---|---|---|---|
| 755 | Positive | Not done | Positive | Positive | Positive |
| 764 | Positive | Not done | Positive | Positive | Positive |
| 775 | Positive | Not done | Not done | Positive | Positive |
| 779 | Positive | Not done | Positive | Positive | Positive |
| 784 | Positive | Not done | Positive | Positive | Positive |
| 803 | Positive | Not done | Positive | Positive | Positive |
| 810 | Positive | Not done | Negative | Positive | Positive |
| 812 | Positive | Not done | Negative | Negative | Positive |
| 813 | Positive | Not done | Positive | Positive | Positive |
| 849 | Not done | Negative | Not done | Negative | Negative |
| 850 | Mild chronic inflammation | Not done | Negative | Negative | Negative |
| 856 | Normal | Not done | Not done | Negative | Negative |
| 857 | Not done | Negative | Not done | Negative | Negative |
| 858 | Mild chronic gastritis | Negative | Not done | Negative | Negative |
| 861 | Mild chronic inflammation | Negative | Not done | Negative | Negative |
| 862 | Normal | Not done | Not done | Negative | Negative |

### 6.4.2 *H. pylori* DNA extraction from stool

The stool samples were partially thawed, and a small piece (approx. 0.2-0.5g) was used with different commercial kits to purify DNA. The PowerSoil DNA Isolation Kit (Mo Bio) and Fecal DNA Miniprep kit (Zymo Research) were used according to the manufacturer's instructions. The *H. pylori* DNA Stool Extraction Kit (Ingenetix) was used according to the manufacturer's instructions, with the following modifications; 0.5g stool was added to Wash Buffer II and centrifuged at 800 x *g* for 8 minutes. This was then placed on a heating block at 95°C for 10 minutes, and vortexed every 2-3 minutes. The QIAamp DNA Stool Mini Kit (QIAGEN) was used according to the manufacturer's instructions, with modifications from a previous study[340].

The modifications in the QIAGEN kit method included the following; the bacterial lysis stage was increased to 95°C for 10 minutes. After centrifugation with the Inhibitex tablet, the supernatant was equally distributed into two or three tubes with 15µl Proteinase K, which were then heated at 70°C for 10 minutes. 200µl of 100% ethanol was added to all tubes for precipitation of DNA, and the three lysates were applied to the same spin column. An increased incubation time prior to the final elution (5 minutes) aided in increasing the yield of DNA purified from stool samples.

The eluted DNA concentration was determined using a NanoDrop spectrophotometer. The 260/280 wavelength O.D. ratios were used to determine the quality of DNA, with an ideal score of 1.8-2.2.

### 6.4.3 Culture of *H. pylori* and purification of genomic DNA

*H. pylori* strains 60190 and Tx30a (described in **Table 6.3**) were grown overnight on 5% horse blood agar plates (Oxoid) at 37°C in a microaerophilic incubator. Genomic DNA (one plate per strain) was purified using a Bacterial Genomic DNA Kit (Sigma-Aldrich) according to the manufacturer's instructions. The DNA concentration of eluted DNA was determined using a NanoDrop spectrophotometer, with respect to an elution buffer blank.

**Table 6.3:** *H. pylori* strains used as genomic DNA positive controls for stool-based PCR.

| *H. pylori* strain | Strain properties | ATCC ID* | Reference |
|---|---|---|---|
| 60190 | *vacA*$^{s1/m1}$, *cag*PAI$^{+}$ | 49503 | [80] |
| Tx30a | *vacA*$^{s2/m2}$, *cag*PAI$^{-}$ | 51932 | |

*ATCC ID; American Type Culture Collection identification number

### 6.4.4 Amplification of *H. pylori* genes

40-300ng purified DNA from stool samples was added to 12.5µl 2X DreamTaq MasterMix containing 4mM $MgCl_2$ and dNTPs (Thermo Scientific) and 0.5µM of each set of primers (Sigma-Aldrich) (**Table 6.4**), made up to a total volume of 25µl with

distilled water. Each PCR run contained tubes with 60190 and Tx30a *H. pylori* genomic DNA as positive controls, and with an equivalent volume of sterile deionised water as a no-template negative control.

10μl of each completed PCR experiment was run on a 2% agarose gel with 6μl of 500 μg/ml Low Molecular Weight DNA marker (New England Biolabs). The gel was supplemented with 5μg/ml ethidium bromide, to observe DNA bands under ultra-violet light. The gel was run at 65V for 80 minutes.

### 6.4.5 Sequencing *H. pylori* stool PCR products

Patients also consented for biopsies to be taken for *H. pylori* culture. If these were positive, the GenElute Bacterial Genomic DNA kit (Sigma-Aldrich) was used to extract genomic DNA – completed by Jo Rhead (Nottingham, UK). A GenElute PCR Clean-Up kit (Sigma-Aldrich) was used to purify amplified PCR products prior to sequencing, which was completed by Source Bioscience GeneService (Nottingham, UK). The sequencing primers were those used for PCR runs (**Table 6.4**).

**Table 6.4:** Primers used to amplify *H. pylori* specific genes in stool-based PCR, and their corresponding thermo-cycling conditions.

| Primer name | Amplified gene | Sequence (5' to 3') | Primer length (bp) | Melting temp (°C) | Expected product size (bp) | Cycling conditions | Reference |
|---|---|---|---|---|---|---|---|
| 16S_F<br>16S_R | *16S* rRNA | CGATGAAGCTTCTAGCTTGC<br>ATAGGACATAGGCTGATCTC | 20<br>20 | 58.4<br>56.4 | 164 | 95°C for 3 min<br>60-80 cycles:<br>1 min at 95°C,<br>30s at 56°C, 1 min at 72°C<br>Final extension:<br>3 min at 72°C | [350] |
| GAPDH_F<br>GAPDH_R | Human *GAPDH* | GGTCCGAGTCACCGCCT<br>TGGCGACGAAAAAGAAGATG | 17<br>20 | 59.8<br>56.4 | 118 | 95°C for 3 min<br>35 cycles:<br>30s at 95°C, 30s at 56°C, 30s at 72°C<br>Final extension:<br>10 min at 72°C | [351] |

| Primer name | Amplified gene | Sequence (5’ to 3’) | Primer length (bp) | Melting temp (°C) | Expected product size (bp) | Cycling conditions | Reference |
|---|---|---|---|---|---|---|---|
| VA1_F<br>VA1_R | *vacA* s-region | ATGGAAATACAACAAACACAC<br>CTGCTTGAATGCGCCAAAC | 21<br>19 | 53.4<br>57.5 | 259 (s1)<br>286 (s2) | 95°C for 1 min 30s<br>60 cycles: 30s at 95°C, 1 min at 56°C, 45s at 72°C<br>Final extension: 5 min at 72°C | 81 |
| VA1_F<br>VA136_R | *vacA* s-region | ATGGAAATACAACAAACACAC<br>CAACAATGGCTGGAATGAT | 21<br>19 | 53.4<br>53 | 136 (s1)<br>163 (s2) | 94°C for 3 min<br>60 cycles: 1 min at 94°C, 30s at 53°C, 1 min at 72°C<br>Final extension: 3 min at 72°C | 81<br>305 |

## 6.5 Results

### 6.5.1 Comparison of stool DNA extraction methods

Purifying DNA from stool samples provides a current-infection diagnosis, is non-invasive and cheap to complete. Human stool contains numerous micro-organisms, and chemical constituents, including indigestible plant material[337]. A high quantity and quality of DNA should be extracted from stool samples to detect *H. pylori* DNA. Therefore, an extraction kit needed to provide rapid, consistent and reproducible results, while being user-friendly.

The Powersoil DNA Isolation kit (Mo Bio) and Fecal DNA Miniprep kit (Zymo Research) were compared to the QIAamp DNA Stool Mini kit (QIAGEN) in initial experiments. A *H. pylori* DNA Stool Extraction Kit (Ingenetix) was also included, because it was a newly available commercial kit designed to be used with a *H. pylori* PCR test.

The QIAGEN kit was chosen because it yielded higher quantities and qualities of purified DNA from 2 repeat samples (**Table 6.5**). With modifications, the yield improved from 9μg to 35μg, and it produced the highest quality DNA. The Ingenetix kit contained steps which were difficult to accommodate; the manufacturer's instructions included an incubation stage at 95°C on a rotating shaker. This was not possible in this laboratory. Instead, the sample was placed on a heating block at 95°C for 10 minutes, and vortexed every 2-3 minutes. Moreover, the suggested centrifugation speed of 200 x *g* was too low to obtain a sufficient supernatant to proceed with the protocol.

**Table 6.5:** A comparison of tested stool DNA extraction kits and the average quality and quantity of purified DNA.

| | | | NanoDrop results | |
|---|---|---|---|---|
| Kit | Modifications | Time taken | DNA eluted | 260/280 ratio[a] |
| Ingenetix *H. pylori* DNA Stool Extraction kit | 800 x *g* for 8 minutes<br>Shaking at 95°C:<br>10 mins on heating block<br>Vortex every 2-3 mins | > 3 hours | 1.2µg | 1.75 |
| Mo Bio PowerSoil DNA Isolation kit | None | 1.5 hours | 2.7µg | 1.52 |
| QIAGEN QIAamp DNA Stool Mini Kit | None | 2 hours | 9µg | 1.31 |
| | Bacterial lysis stage was increased to 95°C for 10 minutes. After centrifugation with Inhibitex, the supernatant was distributed into 2-3 tubes with 15µl Proteinase K, which were then heated at 70°C for 10 minutes. 200µl of 100% ethanol was added to all tubes for precipitation of DNA, and the three lysates were applied to the same spin column. 5 additional minutes of incubation time was added prior to the final elution. | 1.5 hours | 35µg | 2.09 |
| Zymo Research Fecal DNA MiniPrep kit | None | 1.5 hours | 2.6µg | 1.18 |

[a] Ratio refers to quality of DNA (expected values ~1.8)

### 6.5.2 Stool DNA extraction from clinical samples

The modified QIAGEN protocol was then used to purify DNA from 16 stool samples (**Table 6.6**). There was a broad range of DNA concentrations eluted (39.71-299.4 ng/µl). Although there was also a range in the quality of DNA, all 260/280 absorbance readings were acceptable.

**Table 6.6:** The *H. pylori* status of patients in this study, and the concentrations of DNA extracted from 0.2-0.5g of their donated stool samples.

| Patient number | *H. pylori* status | DNA eluted (ng/µl) | 260/280 ratio[a] | 260/230 ratio[b] |
|---|---|---|---|---|
| 755 | Positive | 279.9 | 1.99 | 2.14 |
| 764 | Positive | 40.1 | 2.08 | 1.37 |
| 775 | Positive | 287.3 | 2.14 | 2.4 |
| 779 | Positive | 299.4 | 2.09 | 2.26 |
| 784 | Positive | 260.4 | 2.04 | 2.1 |
| 803 | Positive | 136.1 | 2.04 | 2.12 |
| 810 | Positive | 47.01 | 1.87 | 2.33 |
| 812 | Positive | 114.7 | 1.97 | 2.3 |
| 813 | Positive | 90.91 | 2.01 | 2.38 |
| 849 | Negative | 196.31 | 2.02 | 2.05 |
| 850 | Negative | 172.75 | 2.01 | 2.11 |
| 856 | Negative | 39.71 | 1.97 | 2.4 |
| 857 | Negative | 82.57 | 1.96 | 1.84 |
| 858 | Negative | 171.5 | 2.07 | 2.2 |
| 861 | Negative | 103.14 | 2.1 | 1.97 |
| 862 | Negative | 240.5 | 2.09 | 2.14 |

[a] Ratio refers to quality of DNA (expected values ~1.8)
[b] Ratio refers to secondary quality measure of DNA (expected values ~2.0-2.4)

### 6.5.3 Human *GAPDH* PCR on stool DNA samples

In addition to bacteria and undigested food waste, stool usually contains human cells that are sloughed off during transit through the length of the gut[352]. It should therefore be possible to detect the presence of human DNA by PCR.

Human Glyceraldehyde 3-Phosphate Dehydrogenase (*GAPDH*) is a well-characterised housekeeping gene in qRT-PCR assays[353]. Since human DNA was likely to be abundantly present in stool, the *GAPDH* gene, which has multiple copies per cell[354], was tested as a preliminary step in optimising conditions for the stool *H. pylori* PCR test. *GAPDH* could not be detected using recommended cycling conditions in PCR (data not shown). This highlighted the difficulty of developing a stool test.

### 6.5.4 Comparison of PCR enzymes

As human *GAPDH* could not be detected in DNA extracted from stool sample #779, further measures to combat possible effects from PCR inhibitors were taken. This included changing from the DreamTaq Mastermix polymerase (Thermo Scientific), to increase the sensitivity of PCR. A specialist PCR enzyme, designed to work in the presence of common PCR inhibitors, was tested for this purpose. The Human Specimen Direct PCR kit (Phusion, Thermo-Scientific) was used according to the cycling conditions for VA1_F and VA1_R *vacA* signal region primers (**Table 6.4**), for 35 cycles. Unfortunately, no PCR products could be detected on an agarose gel (data not shown). Therefore, a different approach was used for optimising stool PCR conditions.

### 6.5.5 Adding *H. pylori* genomic DNA to extracted stool DNA to test PCR inhibition

The presence of complex carbohydrates, such as undigested plant material[337] and other PCR inhibitors, decreases the likelihood of observing amplified target genes using PCR techniques. To test whether inhibitors prevented the PCR amplification of *H. pylori* genes from stool, and to check the ability of the *16S* rRNA primers to detect *H. pylori*, an experiment was devised where *H. pylori* genomic DNA was added to stool DNA.

A dilution series of genomic DNA from *H. pylori* strain 60190 (described in **Table 6.3**) was added to 100ng of DNA extracted from stool sample #779 (a *H. pylori* positive sample). These samples were then tested by PCR, including positive and negative controls, amplify the *16S* rRNA gene. *H. pylori 16S* rRNA was detected at all serial dilutions, down to picogram concentrations (**Figure 6.1**). This suggested that a *H. pylori* stool PCR should be plausible, so long as the template DNA had not become too degraded during its transit through the intestines.

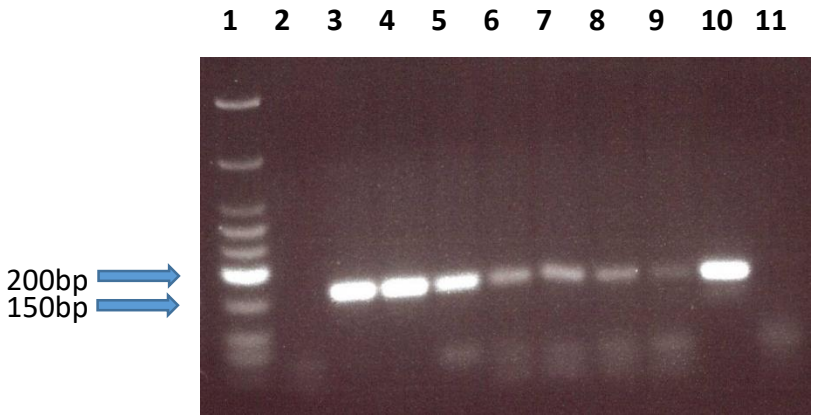



**Figure 6.1:** Agarose gel of *H. pylori 16S* rRNA gene PCR products from a dilution series of DNA extracted from stool sample 779. (Left to right) Lane 1 contains a 0.05μg DNA marker (NEB) Lanes 2 and 11 contain PCR products from two no template negative controls, while Lane 10 contains products amplified from 40ng *H. pylori* 60190 strain genomic DNA as a positive control. Lanes 3-9 contain products from ten-fold dilutions ($10^{-4}$ – $10^{-9}$) of genomic DNA (7.1ng – 0.71pg) added to 100ng of stool DNA, with a product size of 164bp. The lower bands observed in Lanes 2-9, and 11 are likely to be primer dimers.

### 6.5.6 Testing for the presence of *16S* rRNA gene in stool samples via PCR

#### 6.5.6.1 Optimisation

In order to increase the sensitivity of the PCR reaction and compensate for the degraded template, the amount of stool DNA template was increased from 100ng to 300ng DNA. Furthermore, the number of PCR cycles was reduced from 80 to 60, to reduce the likelihood of non-specific products being amplified. This would potentially also produce a cleaner agarose gel. The detection of amplified *H. pylori 16S* rRNA gene PCR products, extracted from stool sample #764 (**Figure 6.2**). This is because this *16S* rRNA gene PCR result was consistent. This demonstrates the presence of *H. pylori* in a patient identified as positive for *H. pylori* infection.

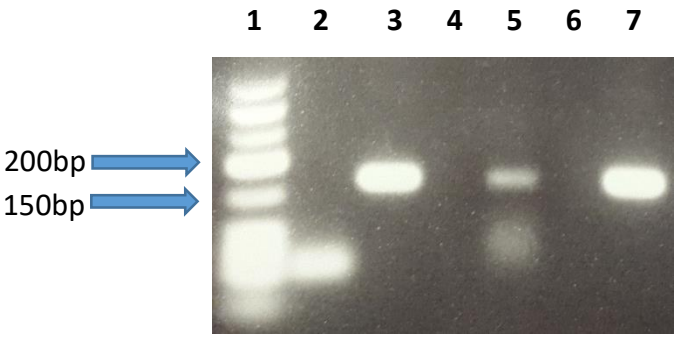



**Figure 6.2:** Agarose gel separation of *H. pylori 16S* rRNA gene PCR products from DNA extracted from stool sample #764. (Left to right) Lane 1 contains 0.05μg DNA marker (NEB). Lane 2 contains a no-template PCR negative control. Lane 3 contains a PCR product from amplified DNA extracted from *H. pylori* genomic DNA sample #764, with a corresponding product size of 164bp. Lanes 4 and 6 are empty. Lane 5 contains a PCR product from amplified DNA extracted from stool DNA sample #764, with a corresponding product size of 164bp. Lane 7 contains a PCR product resulting from *H. pylori* 60190 strain genomic DNA as a positive control. The lower bands observed in Lanes 2 and 5 are likely to be primer dimers.

#### 6.5.6.2 Detecting *H. pylori 16S* rRNA in stool and genomic DNA PCR

The modified protocol for *16S* rRNA gene detection described above was applied to all available DNA stool samples (**Figures 6.3-6.5**). Stool samples 755-810, 856 and 861 were PCR positive for *H. pylori 16S* rRNA gene, while samples 812-861 were PCR negative. The match between a positive or negative PCR result with the patient's *H. pylori* status is shown below (**Table 6.7**).

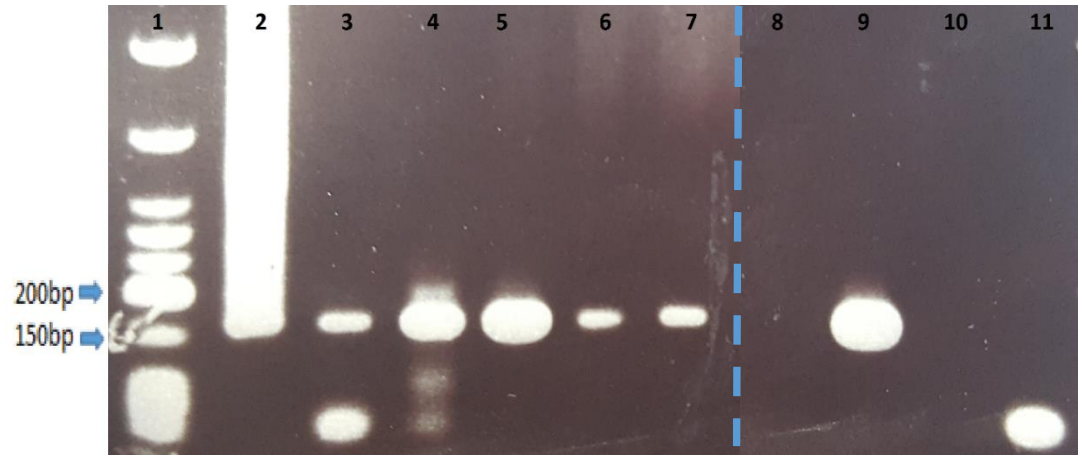



**Figure 6.3:** Agarose gel separation of *H. pylori 16S* rRNA gene PCR products from DNA extracted from stool samples. (Left to right) Lane 1 contains 0.05µg DNA ladder (NEB). Lanes 2-7 contain PCR products from stool DNA samples (775-784), with a corresponding product size of 164bp for *H. pylori* positive samples. Lanes 8 and 10 are empty. Lane 9 contains PCR product from *H. pylori* strain 60190 as a positive control, while Lane 11 contains PCR products from a no-template PCR negative control. The lower bands observed in Lanes 3, 4 and 11 are likely to be primer dimers.

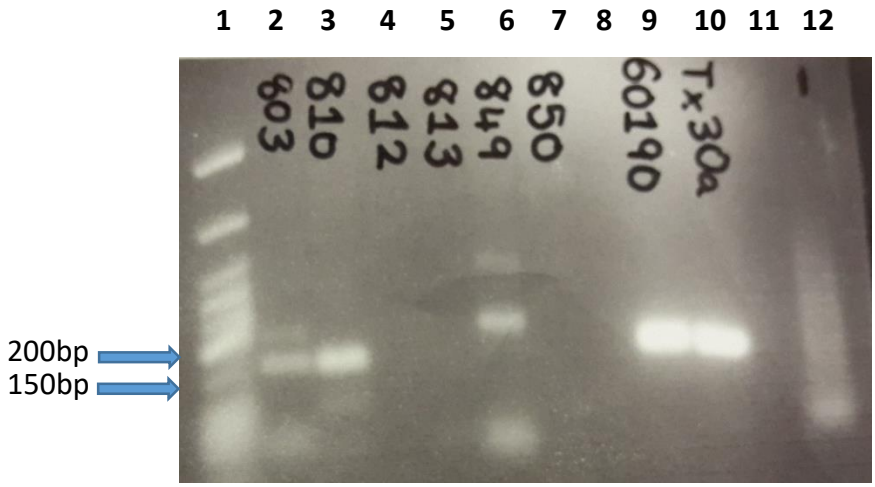



**Figure 6.4:** Agarose gel separation of *H. pylori 16S* rRNA gene PCR products from DNA extracted from stool samples. The detection of *H. pylori 16S* rRNA DNA from 6 stool DNA samples (803-850). (Left to right) Lane 1 contains 0.05μg DNA ladder (NEB). Lanes 2-7 contain PCR products from stool DNA, with a corresponding product size of 164bp for *H. pylori* positive samples. Lanes 8 and 11 were empty. Lanes 9 and 10 contain PCR products from *H. pylori* 60190 and Tx30a strains genomic DNA as positive controls, while Lane 12 contains PCR products from a no-template PCR negative control. The lower bands observed in Lanes 2, 3, 6 and 12 are likely to be primer dimers.

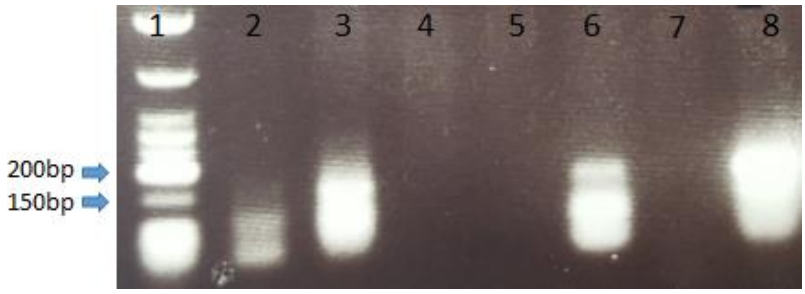



**Figure 6.5:** Agarose gel separation of *H. pylori 16S* rRNA gene PCR products from DNA extracted from *H. pylori*-negative stool samples. The detection of *H. pylori 16S* rRNA gene DNA from 5 *H. pylori*-negative stool DNA samples (856-862). (Left to right) Lane 1 contains 0.05µg DNA ladder (NEB). Lane 2 contains PCR products from a no-template PCR negative control. Lanes 3-7 contain PCR products from stool DNA, with a corresponding product size of 164bp for *H. pylori* negative samples. Lanes 8 contains a PCR product from *H. pylori* strain 60190 as a positive control. The lower band observed in Lane 2 is likely to be primer dimers.

**Table 6.7:** Matching patients' *H. pylori* status with the resulting *H. pylori 16S* rRNA gene stool PCR result to determine the accuracy of the typing method.

| Patient number | *H. pylori* status | *16S* PCR result | Match |
|---|---|---|---|
| 755 | Positive | Positive | √ |
| 764 | Positive | Positive | √ |
| 775 | Positive | Positive | √ |
| 779 | Positive | Positive | √ |
| 784 | Positive | Positive | √ |
| 803 | Positive | Positive | √ |
| 810 | Positive | Positive | √ |
| 812 | Positive | Negative | X |
| 813 | Positive | Negative | X |
| 849 | Negative | Negative | √ |
| 850 | Negative | Negative | √ |
| 856 | Negative | Positive | X |
| 857 | Negative | Negative | √ |
| 858 | Negative | Negative | √ |
| 861 | Negative | Positive | X |
| 862 | Negative | Negative | √ |

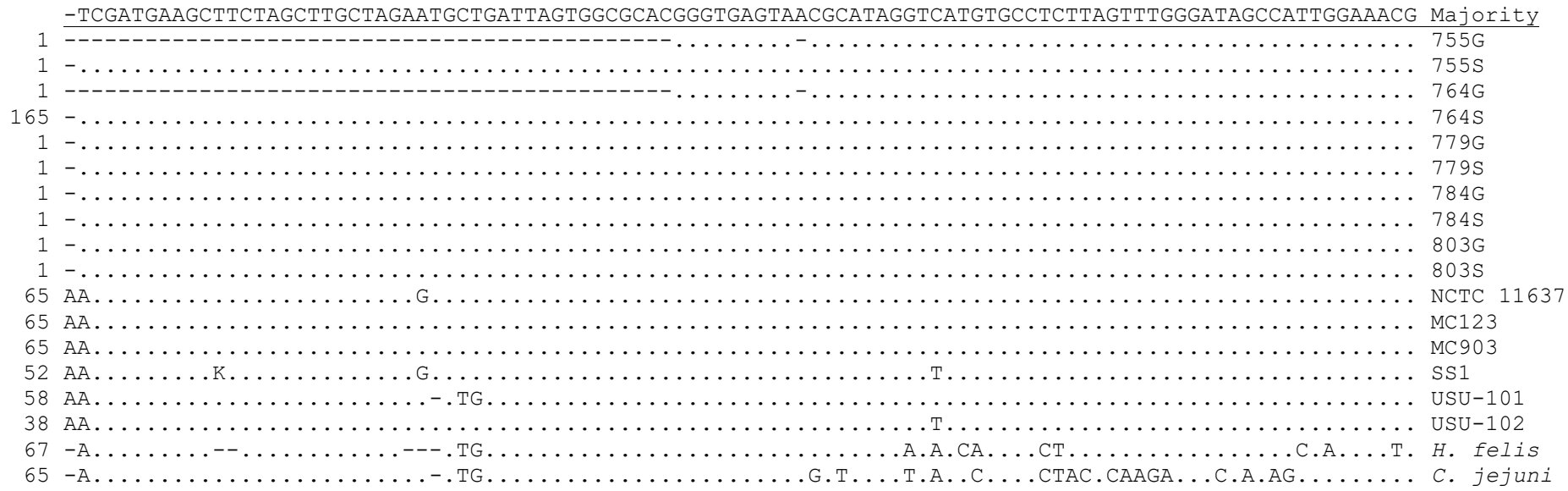
Seven samples were correctly identified as *H. pylori*-positive, and five samples were correctly identified as *H. pylori*-negative. There were two false negative results, and two false positive results. This showed a sensitivity of 78%, and a specificity of 71%.

#### 6.5.6.3 Comparison of sequencing data

DNA extraction was then performed on genomic DNA from the corresponding *H. pylori* isolate from these patients. This was to compare the *H. pylori 16S* rRNA sequence from stool DNA, with that amplified from the patient's isolate (data not shown).

PCR products from the *16S* rRNA PCR from both genomic and corresponding stool DNA sample were sent for sequence analysis (Source Bioscience, Nottingham). These samples (#755, #764, #779, #784 and #803) were from *H. pylori* positive patients. This was to confirm that the expected *16S* rRNA amplicon was indeed amplified, and to compare the sequence of *16S* rRNA from the stomach and stool. This would help confirm that these were products from the same *H. pylori* strain. Because the *16S* rRNA sequence proved to be highly conserved, there was little genetic difference between the *H. pylori* strains. Therefore, the products could not be confirmed as being from the matching strain to the stomach, because two different strains would also be genetically similar within their *16S* rRNA region.

Because of the presence of other micro-organisms in the stool, it is feasible that non-specific PCR products of the expected amplicon size were from a different micro-organism. **Figure 6.6** shows that there were noticeable nucleotide differences in *16S* rRNA between *H. pylori* strains (NCTC 11637, MC123, MC903, SS1, USU-101, USU-102) and other similar micro-organisms present in the gut, such as *H. felis* and *C. jejuni*. Therefore, it is highly likely that the amplified product was indeed *H. pylori 16S* rRNA. Analysis was performed with supervision by Dr. Darren Letley.


-TCGATGAAGCTTCTAGCTTGCTAGAATGCTGATTAGTGGCGCACGGGTGAGTAACGCATAGGTCATGTGCCTCTTAGTTTGGGATAGCCATTGGAAACG Majority
1 ---------- 755G
1 - 755S
1 ---------- 764G
165 - 764S
1 - 779G
1 - 779S
1 - 784G
1 - 784S
1 - 803G
1 - 803S
65 AA G NCTC 11637
65 AA MC123
65 AA MC903
52 AA K G T SS1
58 AA -TG USU-101
38 AA T USU-102
67 -A --- TG A.A.CA CT C.A T. H. felis
65 -A -TG G.T T.A..C CTAC.CAAGA C.A.AG C. jejuni

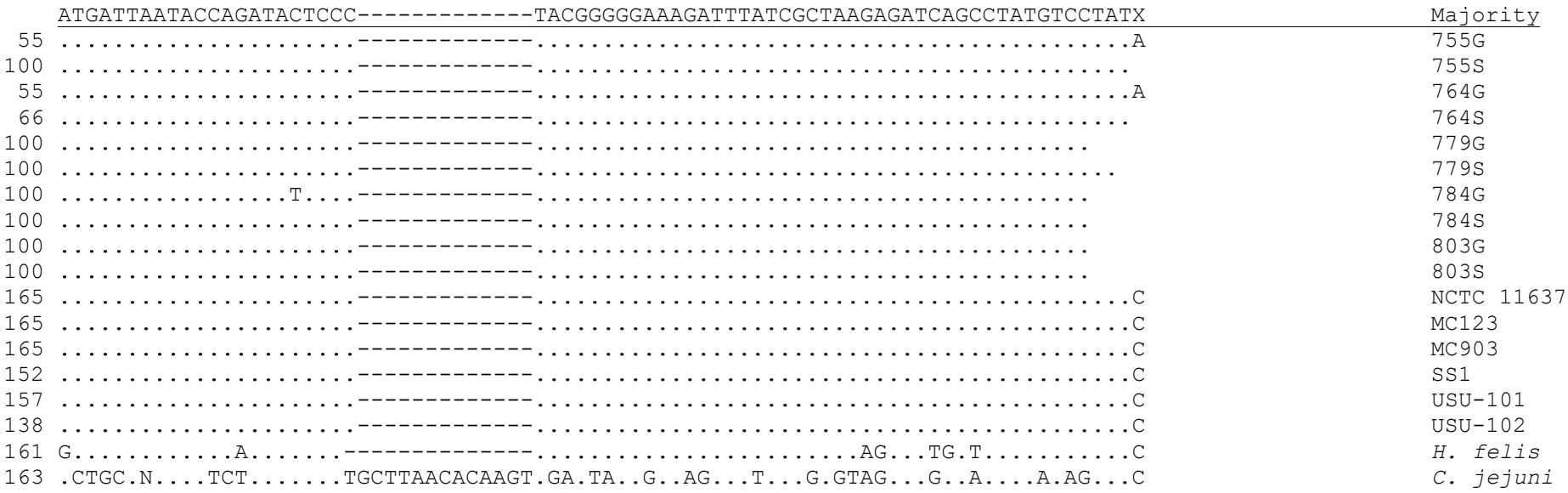

ATGATTAATACCAGATACTCCC----------TACGGGGGAAAGATTTATCGCTAAGAGATCAGCCTATGTCCTATX Majority
55 .....----------.....A 755G
100 .....----------..... 755S
55 .....----------.....A 764G
66 .....----------..... 764S
100 .....----------..... 779G
100 .....----------..... 779S
100 .....T....----------..... 784G
100 .....----------..... 784S
100 .....----------..... 803G
100 .....----------..... 803S
165 .....----------.....C NCTC 11637
165 .....----------.....C MC123
165 .....----------.....C MC903
152 .....----------.....C SS1
157 .....----------.....C USU-101
138 .....----------.....C USU-102
161 G.....A.....----------.....AG...TG.T.....C H. felis
163 .CTGC.N....TCT.....TGCTTAACACAAGT.GA.TA..G..AG...T...G.GTAG...G..A....A.AG...C C. jejuni

**Figure 6.6:** *H. pylori 16S* rRNA gene sequence analysis, comparing stool DNA to those from the corresponding *H. pylori* isolate genomic DNA. PCR products for *16S* rRNA were purified and sent for nucleotide identification. The majority describes the nucleotides identified in all the samples listed on the right. The dots (.) refer to a match between the majority nucleotide listed and the sample's nucleotide sequence. Dashes (-) refer to gaps in the alignment. Letters A, T, C and G denote nucleotide differences between strains and the majority nucleotide sequence. The letter N denotes a nucleotide which could not be identified as a specific base. This diagram shows (on the right), five stool samples ('S') with their corresponding *H. pylori* stomach genomic DNA sample (designated 'G'). Below these are sequence data from several *H. pylori* typed strains used in comparison (NCTC 11637, MC123, MC903, SS1, USU-101, USU-102). *H. felis* and *C. jejuni* are gastrointestinal pathogens, used to confirm a difference in this *16S* rRNA region, and therefore confirming the PCR product to most likely be *H. pylori 16S*.

### 6.5.7 Testing for the presence of *vacA* s-region DNA in stool samples via PCR

The optimisation of conditions for the *H. pylori 16S* rRNA PCR and validating the amplified products were completed. Afterwards, a PCR protocol was designed for detecting *vacA* s-region type, using primers employed previously in the research group's internationally adopted *H. pylori* strain *vacA* genotyping system **(Table 6.4**).

#### 6.5.7.1 Optimisation

As with *16S* rRNA PCR, the number of cycles was reduced from 80 to 60, to decrease the likelihood of non-specific binding amplicons in PCR. Using VA1_F and VA1_R primers (**Table 6.4**), the expected PCR product sizes were 259-286 bp. *H. pylori* DNA can degrade upon contact with faeces[338]. A smaller amplicon increased the likelihood of successful PCR, because this would be more likely to be intact. Therefore, a modified reverse primer VA136_R (**Table 6.4**) was used, providing a smaller amplicon (136-163 bp) size. The suggested annealing temperature[340] was further modified from 52°C to 53°C to detect the s1-region in *vacA* in sample #764 (**Figure 6.7**), with respect to appropriate controls.

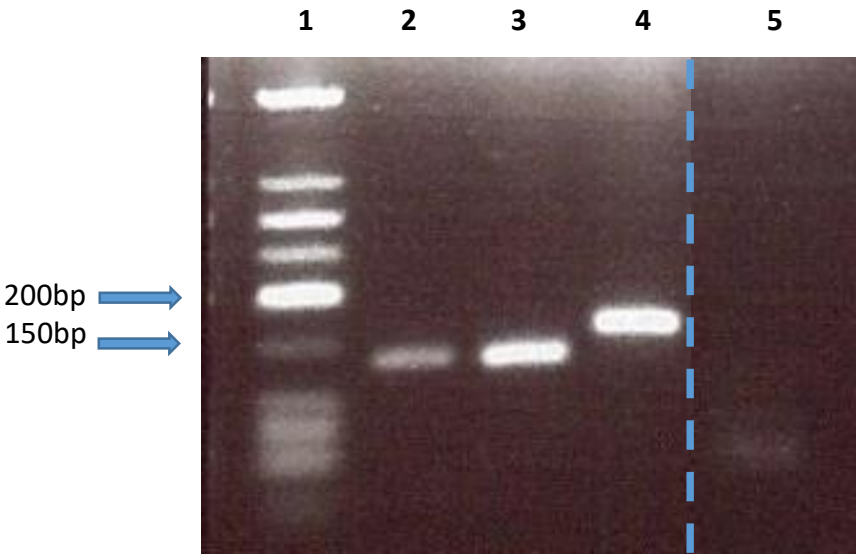



**Figure 6.7:** Agarose gel separation of *H. pylori vacA* s-region gene PCR products from DNA extracted from stool sample #764. (Left to right) Lane 1 contains 0.05µg DNA marker (NEB). Lane 2 contains PCR products from stool DNA sample #764, with a corresponding product size of 136bp. Lane 3 contains *H. pylori* 60190 strain genomic DNA as a positive control, while Lane 4 contains *H. pylori* Tx30a strain genomic DNA as a positive control. Lane 5 contains PCR products from a no-template PCR negative control. The lower band observed in Lane 5 is likely to be a primer dimer.

#### 6.5.7.2 Touchdown PCR

Efforts to amplify *vacA* s-region sequences from stool samples proved to be inconsistent. To reproduce the results, touchdown PCR techniques were used. As this technique uses a range of annealing temperatures, it was more likely that a product would be successfully amplified. With VA1_F and VA136_R primers (**Table 6.4**) and an annealing temperature decreasing in increments of 1.5°C, this technique was used by Jo Rhead on samples 764 and 779 (known *H. pylori*-positive samples). Although this was initially successful, with appropriate size amplicon bands on agarose gel, it was ultimately rejected because *H. pylori*-negative samples repeatedly tested PCR-positive for *vacA* s-region gene (data not shown).

## 6.6 Discussion

### 6.6.1 Statement of principal findings

The aim of this study was to identify *H. pylori*-infected individuals, and simultaneously determine the *vacA* genotype of the colonising strain, using a stool-based PCR test. 16 *H. pylori*-positive and negative patients donated stool samples, which were frozen upon arrival. A user-friendly, reproducible, and reliable method for DNA extraction from stool was chosen and optimised. Following DNA extraction from all stool samples, the stool DNA was subjected to attempts to PCR amplify the human *GAPDH* gene, but this could not be detected. To determine if this negative result was due to a degraded DNA template in the stool samples, or arose from the presence of PCR inhibitors, purified *H. pylori* genomic DNA was added to stool extracted DNA at different concentrations. After the *H. pylori 16S* rRNA gene was successfully detected at low concentrations in PCR, PCR inhibitors were shown not to be the problem. Following further modification of PCR cycle conditions, *H. pylori 16S* rRNA was successfully tested in stool samples donated from all patients (sensitivity 78%, specificity 71%). By sequencing the amplicon, this was confirmed to be *H. pylori 16S* rRNA. While initial attempts to test *vacA*$^{s1 \text{ or } s2}$ type by PCR were promising, repeated attempts failed to provide results from samples and contamination problems were a common occurrence. At this point, a decision was taken to discontinue the work.

### 6.6.2 Biological relevance of the findings

Stool is a crude mixture which contains other micro-organisms, complex polysaccharides, bile salts, blood products, polyphenolic compounds and heavy metals[336 337]. Obtaining purified *H. pylori* DNA from stool, in the presence of these potential contaminants is a more challenging task compared to other tissues such as gastric biopsies[11]. Contamination of *H. pylori* in stool PCR procedures is also a concern[346]. Additionally, there are low amounts of *H. pylori* present in stool which are also subject to enzymatic and mechanical degradation[11 341 344 345 355].

PCR based tests require reliable methods that readily provide reproducible results: an adequate quality and quantity of DNA recovered, conserved target sequences, and an appropriate form of the amplification process[312]. Preparation, handling and storage of human faeces are critical processes that alter the outcomes of downstream DNA-based bacterial community analyses via qPCR[356]. In the process of assessing the presence of *H. pylori* virulence factors in stool samples, an efficient DNA extraction kit was required. The most important factor in selection was the yield and quality of DNA obtained from the kit, as well as the removal of PCR inhibitors prior to elution. However, in the development of a practical prognostic test for clinical use, other factors for practical use were taken into consideration. These included the time taken to extract purified DNA, and the user-friendly nature of the protocol.

Each kit in this study used a different mechanism to ensure the removal of these chemical inhibitors before the final elution of DNA. The Ingenetix *H. pylori* DNA Stool Extraction kit contained a wash buffer step prior to the lysis of the stool sample, the Mo Bio PowerSoil DNA Isolation kit included an inhibitor removal solution during lysis, the Zymo Research Fecal DNA MiniPrep kit provided a filtration step to remove inhibitors from the sample, and the QIAGEN QIAamp DNA Stool Mini kit contained an Inhibitex tablet incubation period with the stool sample to remove inhibitors.

The Ingenetix kit was initially thought likely to be the best kit for the purification of DNA from stool. This *H. pylori* stool kit is marketed and used commercially specifically for the extraction of *H. pylori* DNA (as opposed to the general extraction of bacterial DNA using the other kits). Also, the accompanying ClariRes RT-PCR kit simultaneously detecting *H. pylori* infection and clarithromycin resistance has been cited previously[321 322]. This did not prove to be the case in this study, and low DNA concentrations and quality were yielded. This was perhaps due to technical difficulties faced in following the manufacturer's instructions exactly.

Following incubation of the stool with reconstituted wash buffer, the low centrifugation speed (400 x *g*) did not produce enough supernatant to continue onto the next step of the protocol. This step was repeated multiple times, with an

increased time and speed, but still resulted in a sludgy consistency that proved difficult to pipette. Furthermore, a step recommending an incubation of 95°C on a rotating shaker proved difficult to accommodate. This was modified to incubate the sample at 95°C on a heating block for 10 minutes, and vortexed every 2-3 minutes to ensure the sufficient mixing of reagents. From these concerns, it was excluded as an impractical kit.

The three other kits chosen in this analysis had been assessed in previous stool PCR studies[259 336]. During the current study, kits from Zymo Research and Mo Bio proved to be user-friendly and yielded 2.6μg and 2.7μg of DNA respectively from 0.2-0.5g stool. Although the QIAGEN kit provided a similar quality of eluted DNA to these kits, there was a three-fold increase in yield. The QIAGEN kit passed all the criteria needed for a reliable kit. The optimal amount of stool for testing was as the manufacturer recommended, a finding agreed in another study[322]. Because this kit had been cited numerous times by groups working on *H. pylori* stool PCR [270 306 321 322 338 340 341 344 345 357], some modifications recommended by one of the groups was investigated[305]. DNA extraction from stool sample #779 was repeated with these modifications and this protocol was then used for the remaining stool samples, with further modifications including a 5-minute incubation period with buffer on the spin column prior to the final elution. The DNA eluted was comparable in yield to DNA extracted from stool in another study[321].

After the protocol was optimised and completed on 16 samples, some differences in stool DNA yield, concentration and quality were observed. A higher yield was not an absolute indicator of the template stability/suitability for PCR amplification. Samples #810 and #856 were incubated with the Inhibitex tablet for 4-5 minutes longer than for the other samples. This was due to the visible presence of partially-digested plant material in the samples taken for extraction, which is known to contain inhibitors for PCR. Although this appeared to have no impact on the quality of the eluted sample, the yield dropped significantly (four-fold less than the mean). This may be attributed to DNA binding to the Inhibitex tablet. Purity of DNA did not translate into a good

PCR sensitivity[336]. Sample #764 provided a lower yield in extraction, but was the first sample to consistently amplify *H. pylori 16S* rRNA and *vacA* s-region genes.

Human *GAPDH* could not be detected via PCR in stool-extracted DNA. This was surprising as stool usually contains plenty of human cells that are sloughed off during passage through the gut[352].

The cause of this PCR failure was attributed to two possibilities. Firstly, the degradation of cells through the gut by various nucleases and basic conditions, and the subsequent delay of the stool sample being returned to the hospital, meant that the DNA template may have been degraded, and was too poor to amplify from. Secondly, it was possible that the presence of PCR inhibitor chemicals in the eluted sample were impeding the amplification of *GAPDH*. To evaluate the second possibility, genomic *H. pylori* 60190 DNA was added to purified stool DNA and this was tested for the *16S* rRNA gene by PCR. Similar spiking experiments have been described previously in the *H. pylori* stool literature[338 341 344 345].

*H. pylori* genomic DNA added to DNA eluted from stool sample #779 was successfully detected by PCR. A serial dilution allowed for the detection of *H. pylori* strain 60190 at low concentrations; concentrations consistent with the possible levels of *H. pylori* present in stool. The successful detection of *H. pylori* strain 60190 at picogram concentrations showed a good sensitivity of the PCR test, and that the presence of PCR inhibitors in the eluted DNA did not drastically impede the amplification of *H. pylori 16S* rRNA gene. This finding has been observed in another study[321], and demonstrated that a degraded DNA template was most likely a key reason for PCR failure, which is consistent with the high level of endonucleases expected in stool.

The nucleotide sequencing data confirmed that the PCR products were likely to be from the *H. pylori 16S* rRNA gene, as published *H. pylori* sequences were almost identical. There were some differences in the sequence from that of similar bacteria such as *H. felis* and *C. jejuni* and more diverse bacteria in the human gut should have

more nucleotide differences in this region. Sequencing is an important process after qPCR to identify that the resulting amplicon is the target gene[322].

Sequencing compared PCR products from the genomic DNA of the colonising strains in 5 patients, to those in corresponding stool samples. Because of the highly conserved nature of the nucleotides within this region, there were very few differences. Other regions in *16S* were analysed to observe if there were any variable regions by which to make a comparison. There were none. This was a finding described in another study[343]. It could not be concluded that stool DNA PCR results matched the corresponding strain from the stomach, because contamination could not be ruled out definitively. However, the *16S* rRNA PCR test compared well with a commercial serology test for detecting *H. pylori* infection, because it could detect a real-time infection and showed no cross-reactivity with *C. jejuni* infection. Moreover, the reproducibility of *16S* rRNA PCR typing showed that stability of the gene was important for the protocol. This consistency is important as in a previous study, 25% of samples were positive in only 1 out of 2 runs[306].

Sample #812 was shown to provide a false negative result in the *16S* rRNA gene PCR. This may have been due to the low abundance of *H. pylori* organisms observed in histological examination of biopsies from this patient. However, this negative stool test result was comparable to negative results from culture and RUT. As the most reliable *H. pylori* diagnostic test with a qualified histopathologist and specific staining techniques, it is unlikely that the positive *H. pylori* result identified from the histological test was a false negative. A mega analysis of stool PCR literature showed that 11% of papers analysed did not have a comparison against a reference standard[312]. The sensitivity of this test was comparable to other studies [312 341 358 11].

VA1_F and VA1_R primers were primarily used to prevent the possibility of a negative PCR result being due to PCR failure. This was because *vacA* s1 or s2 types would theoretically be identified from this one test. However, this could not be detected consistently in PCR.

Further attempts to optimise this PCR test after changing primers were attempted. Touchdown PCR was used to obtain more sensitive and consistent data for the presence of *vacA* s-region genes. It is a technique that is recommended for difficult templates, like degraded templates as in this study. This did not prove successful by myself, and further, by an independent researcher in the research group. Nested PCR has been recommended in the literature for improving stool PCR accuracy[312 346], but ultimately, the increased probability of contamination would not allow for a feasible PCR test in this laboratory.

While other researchers have developed *vacA* stool PCR tests, no one has yet developed a *vacA* i-region typing test[305 349 358]. While it was disappointing that the *vacA* PCR was unsuccessful, this difficulty has been noted previously[321 336 346]. A stool PCR test has yet to be recommended for diagnostic use. One group added BSA to the PCR master mix to improve PCR sensitivity, to no avail[321]. While *16S* rRNA could be detected consistently, there are two copies of the *16S* rRNA gene in the *H. pylori* genome, but only one copy of the *vacA* gene, making the latter harder to amplify from degraded stool[84 322].

### 6.6.3 Clinical relevance of the findings

The aim to produce a real-time diagnosis of *H. pylori* infection and strain virulence type without invasive procedures and specialist equipment is yet unrealised. *H. pylori* infection is usually diagnosed using techniques that are dependent on biopsies obtained from an endoscopy procedure. This procedure has limitations, particularly for children. This is because there is a limited access for paediatric endoscopy equipment and a low patient compliance means that non-invasive *H. pylori* diagnostic tools are generally preferred for clinical use[305 306].

*H. pylori* acquisition in developed countries such as the UK has been declining over the last few decades[13]. This has been associated with socioeconomic developments, improved hygienic practices and the widespread use of antibiotics, leading to long-term changes in the human microbiota[259]. However, *H. pylori* incidence in developing

countries is on the rise, and with it, an increased disease burden. Fairly non-invasive tests such as UBT and the stool antigen test have excellent sensitivity and specificity (**Section 6.1.3**), and may be used for children, but have limitations concerning their clinical use. Because only a small percentage of *H. pylori*-infected individuals develop disease, it is important to understand why particular people are at risk (and indeed, how others are protected from it).

Stool testing has the potential to reduce healthcare costs. Unsuccessful *H. pylori* treatment requires the patient to return for endoscopy and the collection of more gastric biopsy samples. PCR testing could reduce the need for biopsies for culture and sensitivity (C+S) testing[322]. A diagnostic test should provide a quick result: culture is time-consuming and it is difficult to maintain anaerobic conditions in developing countries, while histopathology involves extensive staining and visualisation requiring trained expertise[355]. Another advantage of stool testing is that it does not require patients to fast before their clinic appointment[321].

If a non-invasive protocol could be developed to test for the presence of the *vacA* i1-form in infected individuals, community-based screenings could then identify those most likely at risk to be given eradication therapy, preventing their risk of future disease. In one study, *H. pylori* presence in stool decreased significantly at 12 months post eradication, but were not significantly different at Month 18[259]. This correlates with Treg eradication study findings showing that Month 12 after eradication is the most significant time point for a reduced *H. pylori*-induced regulatory T cell IL-10 response (**Section 2.5**). This could be due to a reduced pro-inflammatory response after the removal of *H. pylori* as an active stimulus. Furthermore, due to alarming levels of increased antibiotic resistance worldwide, this targeted screening process would also help identify those who are infected with an antibiotic-resistant strain. In this study, 5/16 patients had failed eradication therapy, consistent with the level of resistance previously noted in European countries[319].

There are commercially available serological tests which go further in diagnosing infections with particular strain virulence types (such as the presence of CagA), but

there are no commercially available tests which show differences within the *cagA* genotypes. For example, CagA expressed by East Asian strains has differences in the number and types of TPMs, and these are linked to more severe disease outcomes[5]. Although stool PCR testing for *H. pylori* has been described in several previous studies[11 259 270 305 306 312 317 318 321 322 327 332 333 335 338 340-349 355 357-361], the focus has mostly been on detecting *16S* rRNA, *ureA*, clarithromycin resistance (*23S*), and also *vacA* s-region types. The stool PCR *H. pylori* typing test aimed for in this project was to advance the field in *H. pylori* diagnostics, but this was not successful.

To determine *H. pylori* status, each patient underwent diagnostic testing including a CLO-test (RUT), *H. pylori* culture from biopsies and/or histological examination. For patients #849 and #857, a serological test for anti-*H. pylori* IgG was performed. Culture of *H. pylori* from biopsies may not be possible for all infected patients, and has a success rate near 50%[11]. However, if culture is positive, it is certain that a patient is currently infected with the micro-organism. Patient #812 was positive by histology, but negative by both CLO and culture. Histology for *H. pylori* may be as sensitive as culture, depending on the type of stain used. This patient was infected with *H. pylori*, but presented with a low load of *H. pylori* colonisation. However, as culture and CLO-tests were negative, this negative stool test result for *16S* rRNA is comparable to current clinically used diagnostic tools.

Stool is a convenient sample to test for current host infections. One gram of stool can contain approximately one trillion bacterial cells[360], and bacteria accounts for one third of stool composition[362]. Clinical microbiology laboratories take advantage of this in the widespread use of stool-based tests to detect enteric pathogens. These include tests for various intestinal viruses and parasites, as well as for enteric pathogens such as *C. difficile*. These microorganisms are often easier to detect in stool, because they are diarrhoeal. Diarrhoea is a rapid excretion from the gut which can be collected as a fresh sample (especially in a hospital setting); and with a shorter transit time, microbial DNA is more likely to be preserved[11]. Viral infections often include a high viral load present in stool samples. Moreover, it is likely that diarrhoea, in its semi-watery state, contains fewer chemicals which can act as inhibitors, and so bacterial

genes are more likely to be detected in PCR. Other tests, such as the FAO test used to diagnose colorectal cancer, detect the presence of occult blood within stool. However, because the test identifies any bleeding along the GI tract, blood is likely to be present in sufficient amounts for detection, even if hidden. This is not the case with *H. pylori* in stool.

### 6.6.4 Critique of the experimental design

#### 6.6.4.1 Patient recruitment

To obtain a stool sample, patients undergoing an endoscopy were provided with the means to collect and post their stool samples to the lab in cool packs, which were immediately frozen upon arrival. This protocol was developed to maximise patient compliance in the study. It is unlikely that fresh stool could be supplied for immediate diagnostic testing in a primary care setting, such as G.P. surgeries, because of the lack of resources. For this study, it was impossible to obtain fresh samples. This is because written consent needed to be obtained before the endoscopy procedure, which also required a minimum of six hours prior fasting. Unfortunately, the unfeasibility of fresh samples meant that DNA degradation would automatically become a problem. This actually aided in creating a realistic scenario for stool test research. There is a practical delay of a few days before samples are processed. Therefore, if a stool PCR typing test could be developed to work under these conditions, it would be highly reproducible and effective around the world, and in less well-resourced labs.

However, problems were encountered with this approach. It was difficult to recruit patients to contribute to this study; in fact, only 16 were recruited over two years after 25 pots were given to consenting patients. This was also shown in another stool study, where 32/59 participants gave their consent for the study, but only 17 individuals actually provided a stool sample. This number reduced to 6 participants at further time points[259].

Even if it were theoretically possible to ask for a fresh stool sample, there are a number of issues which impede compliance from patients. Firstly, people have

different bowel movements in their daily routine. Asking for a fresh stool sample for their appointment may not be possible for them to provide. Providing stool is not something the human body can provide upon demand, and may trigger some anxiety. Secondly, stool and gut movements are a taboo topic within society[362]. Some people cannot defecate in toilets other than their own, for comfort, hygienic and personal reasons. The taboos relating to faeces and bowel movements seemed to affect the willingness of patients to volunteer samples to the study. These reasons may seem trivial, but may realistically impact patient compliance to a stool study.

This study was not blinded because of the decreasing prevalence of *H. pylori* infection in the local community, so *H. pylori*-infected individuals had to be clearly identified. To develop a test for stool PCR sensitivity, many *H. pylori* positive individuals were also needed[322]. This is comparable with a meta-analysis of *H. pylori* studies which confirmed that 50% of studies did not have blind testing either[312].

It is noted that the selection of *H. pylori*-diagnostic tests or the combination of tests without identifying any one as a reference standard can introduce bias[355]. However, this was not feasible during patient recruitment as matching the same diagnostic test and result would have proven unfeasible.

#### 6.6.4.2 Stool applicability

The use of stool as a model for detecting a real-time *H. pylori* infection is fraught with difficulties. Stool is a crude mixture which contains other micro-organisms, complex polysaccharides, bile salts, blood products, polyphenolic compounds and heavy metals[336 337]. There is also a large variation in different species[336 344]. In humans alone, there is such a large variation because of diet and the presence of any co-morbidities[336]. This variation extends to the stool itself; subsampling has shown that different bacteria are present in the inner and outer microenvironments of the stool[356].

There are many factors which affect how much *H. pylori* is present in stool. These include how quickly gastric epithelial cells are sloughed off, how much bile enters the stool, alimentary factors, and how long it takes for stool to pass through the bowel[341].

However, it is generally agreed that with a low density of colonisation in the stomach, the amount of *H. pylori* in stool will be in low quantities[11 341 344 345 355]. This may be due to the fastidious nature of *H. pylori*, and its niche in the acidic gastric mucosa. The precise conditions needed to culture *H. pylori in vitro* and its lack of regulatory genes suggests that it does not thrive in abnormal environments[11]. It has been suggested that this low CFU per mg of *H. pylori* in stool means that it cannot be detected by QIAamp DNA kit, as it may be outside its means of detection[344].

In an attempt to make stool samples viable for *H. pylori* testing, many groups have tested additional (strenuous) protocols to extract *H. pylori* DNA prior to PCR testing. This has included requiring patients to have a vegetable-free diet for 1-2 days before providing a stool sample[338 358], embedding DNA preparations with agarose[339], providing a laxative to patients before collecting stool[11], and using streptavidin-coated magnetic beads[344]. Another recommendation to reduce intra-sample variation suggests homogenising the entire stool sample with liquid nitrogen[356]. Admirable as these efforts are, they only serve to make the test less feasible in a clinical setting.

#### 6.6.4.3 Storage of stool

The storage of the stool samples may have also contributed to the degradation of *H. pylori* cells. In this study, stool samples returned to QMC were exposed to room temperature for a minimum of 30 hours in transportation. Previous work in this field showed that exposure to room temperature affected the effectiveness of the PCR stool test[306]. Given that *H. pylori* is present in small numbers in stool, the subsequent exposure to room temperature may have contributed to the variation in yielded DNA. Other groups resuspended the stool in cold phosphate buffer and returned the stool to the laboratory within 2 hours, or transported the sample on dry ice to mitigate this exposure[343 345].

Upon arrival to QMC, stool samples were stored at -20°C. This has been used by other stool studies [322] [345], and a review indicated that samples stored at -20 instead of -70 improved the accuracy of PCR 6-fold[312].

This may have been acceptable for short-term storage, but the samples were kept, without preservation media, for months. Differences in microbial populations has been observed in frozen stool samples after 30 days. The authors also demonstrated that bacterial populations in stool changed after a mere 15 minutes in room temperature after defecation, or after storage in a domestic freezer for over three days[356]. Using frozen stool samples for *H. pylori* extraction has also been suggested as a reason for the lack of intact DNA after extraction[321]. This highlights the enormity of the DNA degradation problem faced in this study.

Stool samples in this study were partially thawed and refrozen to obtain a small quantity for DNA extraction analyses. Reviews of *H. pylori* stool studies suggested that inadequate or repeated thawing events of stool samples and DNA extracts explained the poor results obtained in some studies[345] [312]. One study suggested that freeze-thawing only had consequences after 4 cycles, but this was tested with liquid nitrogen. Most studies do not describe such measures, and are assumed to use domestic freezers, as used in this study. This meant that freeze-thawing cycles were longer, and so samples were more exposed to milder conditions over time, compared to quick freezing procedures such as liquid nitrogen. This hypothesis was supported by the same study, which commented that there was a greater variation in data seen when freeze-thawing cycles lasted more than 10 minutes[356].

Storage conditions of stool samples should be optimised to slow DNA degradation, which is an already prevalent issue in stool studies[345] [356]. However, this is not often prioritised by researchers, and efforts to transport and store stool samples to avoid degradation are sometimes not mentioned[322]. To promote microbiome data reproducibility from stool, it is recommended that stool is frozen within 15 minutes of defecation, stored in a freezer for less than 3 days, and homogenised in liquid nitrogen prior to DNA extraction[356]. This is not feasible for a clinical setting.

#### 6.6.4.4 Stool PCR

PCR testing for detecting *H. pylori* infection in stool would be useful for those whom endoscopy may not be possible; children and clinical settings in developing countries. It avoids the need for invasive procedures such as endoscopy, or the use of needles in drawing blood. Furthermore, it does not require the active participation of children, such as in UBT[312]. The sensitivity of PCR has also been described as being able to detect as few as 10 *H. pylori* cells in a sample[333].

*H. pylori* stool testing in the literature has involved different PCR techniques in attempts to make an appropriate diagnostic tool: nested[341 347], quantitative[305 343], real-time[270 322 341 342 344], Fluorescence *in Situ* Hybridization (FISH)[355], digital droplet[361] and microfluidic single-cell PCR[354]. By developing a PCR test, there are important parameters to be checked and vetted – DNA preparation, primer selection, appropriate internal controls, the detection of amplicons, and the constant look out for inhibitors and contamination. These factors were thoroughly vetted in this study, to optimise the likelihood of detecting *H. pylori* infection in stool DNA[346].

Multiple precautions were taken to prevent contamination, because positive control *H. pylori* genomic DNA frequently contaminated the no-template negative controls in PCR. Pipettes were cleaned in disinfectant and separate pieces of equipment were used for stool DNA extraction protocols and the PCR work. The PCR reagent mastermix and stool-extracted DNA were added in a sterile hood, filter pipette tips were used, and nuclease-free water and primer stocks were aliquoted into 0.2ml tubes and disposed of after a single use. Gloves were exchanged multiple times during each PCR set up, and a separate washed lab coat was stored away for PCR work, because of the possibility of contamination from the sleeve cuffs. A new extraction of a *H. pylori*-negative sample was undertaken to overcome the false positive of touchdown PCR, but this also tested *H. pylori*-positive. These unsuccessful attempts at preventing contamination demonstrate the difficulty of this test.

Increasing the number of PCR cycles from 35-40 to 80 made the assays longer to complete, and increased the risk of contamination. Because of the small quantity and quality of the DNA extracted, it was a necessary step to detect *H. pylori* in PCR. This has been observed in multiple studies[270 305 306 322 341-345]. The problem was that the results yielded multiple PCR products due to non-specific binding. Adjusting the annealing temperature and reducing the cycle number to 60 addressed this issue. However, the increased number of cycles is the most likely reason for the increased intensity of primer dimer bands observed in agarose gel[341].

The main weakness of *H. pylori* stool PCR is that the test cannot distinguish between live and dead *H. pylori* cells, which could create a false positive result, and noted when other gold standard tests test negative[11 259 341 346 358].

Another disadvantage of using conventional PCR techniques is the reliance on agarose gels to detect the presence of amplified DNA. This is a semi-quantitative result which is often open to post-PCR cross-contamination[333]. The sensitivity of this method is questionable because some PCR products may not be present in a high enough concentration to appear on a gel. This may be a problem for samples containing mixed strains of *H. pylori*, if products from only one strain are visible on an agarose gel[341]. To combat this, real-time PCR techniques could be optimised after conventional conditions are developed for *vacA* i-region typing. This would decrease the time taken to attain a positive or negative result, provide a quantitative measure of the DNA amplified from stool, and be a more sensitive test for *H. pylori* gene detection. Another weakness of PCR is that inter-observer variability can become a concern when a result is weakly positive[312 337 346].

It remains to be seen whether stool PCR is a technique which can be feasibly used in a *H. pylori* clinical setting. It requires a specialised (and non-contaminated) laboratory and trained professionals, which may not be available in diagnostic facilities in developing countries[312]. Furthermore, a lower density of *H. pylori* DNA in stool samples of children may be below the sensitivity threshold of stool PCR. Differences

in the microbiota, and the reduced passage of stool through the bowel may be a reason for why diagnostic results vary between children and adults[312 321].

Furthermore, even when *H. pylori* stool PCR can be optimised for sensitivity and specificity, there is a potential for a falsely positive result. *H. pylori* DNA was detected at 18 months post eradication in one stool study. The PCR product was confirmed to be *H. pylori* by sequencing[259] and was accompanied by a negative UBT result. Sequencing is also not a fool-proof addition to qPCR – one study showed that 27 samples were excluded from analysis because sequencing showed a failed sequencing, or was unreadable at the nucleotides of interest[322].

### 6.6.5 Future work

Further work on developing this stool test will require major modifications, and extensive measures to avoid contamination. However, *vacA* is a good marker for prognostic testing for *H. pylori* infection because it is almost ubiquitously present in all strains. The *vacA* i1-form is a known independent risk factor for an increased likelihood of *H. pylori*-related disease[84]. As an alternative to stool-based PCR for *vacA* typing, another future project will be the development and optimisation of a serology-based test for anti-VacA IgG. There are currently no commercial serology kits available for the detection of VacA in *H. pylori*. This may be partially because the mid-region of VacA is not highly immunogenic[363]. There have been previously attempts to develop this within the research group, but this has met with limited success as there is too much cross-reactivity between serum and the different VacA forms; the O.D. values of sera from infected individuals overlapped with the sera of uninfected individuals[364]. Recent work has been done to improve this; immunoblotting techniques has been shown to be more specific than ELISAs, and this can be tested using the research group's considerable serum collection from patients.

### 6.6.6 Conclusions

While the *H. pylori 16S* rRNA gene was successfully detected in stool sample donated by *H. pylori*-uninfected and infected patients, the test itself was found to be insufficiently sensitive and specific, and the aim to develop a *vacA* PCR typing test was not achieved. Stool PCR testing has been optimistically described in length in the literature by many groups, due to the potential ease of stool donations. However, it has been repeatedly concluded that PCR testing is a difficult technique which has heterogeneous results in different studies, is not comparable to current gold standard techniques, has no clinical value in determining *H. pylori* presence in human stool, cannot replace other techniques, is not recommended for use in children, and cannot be used in clinical settings until further work can increase its sensitivity and specificity[355] [312] [321] [346]. Unfortunately, the variation observed in *H. pylori* concentrations, stool sample collection procedures, stool storage, processing and DNA amplification in labs worldwide mean that this is unlikely to occur.

## 7.1 General findings and conclusions

### 7.1.1 Tregs in *H. pylori* infection

During *H. pylori* infection, Tregs serve to prevent tissue damage to the host stomach from excessive pro-inflammatory T cell responses. The failure of the immune response to clear *H. pylori* infection, and the subsequent chronic inflammation is also linked to the Treg response. Previous work in the field has identified that *H. pylori*-positive individuals have an increased $CD4^+CD25^{hi}$ Treg response in their peripheral blood and infected mucosa[119 183-185]. Furthermore, *H. pylori*-positive individuals with low frequencies of Treg are an increased risk of PUD and pre-clinical pathology[87 119]. IL-10 is an important mediator of Treg activity, and IL-$10^+$ Treg frequencies are also increased in *H. pylori*-positive individuals, compared to *H. pylori*-negative individuals[188].

$CD4^+CD25^{hi}Foxp3^+$ Treg frequencies did not decline 2 years after successful *H. pylori* eradication therapy (**Chapter 2**). This provides a unique insight into the long-term re-programming of the host immune response after a decades-long chronic *H. pylori* infection. That this population does not decline after the active stimulus has been removed suggests the possibility that extra-gastric protection may be maintained after *H. pylori* infection has been cleared.

$CD4^+$ T splenic lymphocytes expanded in response to *H. pylori* infection in mice (**Chapter 3**). In this population, the proportion of $Foxp3^+$ Tregs also increased after infection. Likewise, there was an increase in the proportion of $CD4^+Foxp3^+$ lymphocytes that were IL-$10^+$. This agreed with previous work in the research group and from other studies[119 188 190].

In humans, $CD4^+CD25^{hi}$ lymphocytes were on an increasing trend compared to uninfected patients (**Chapter 4**). The scarcity of *H. pylori*-positive patients most likely limited the significance of this. Previous work in the research group has consistently

identified an increased Treg response in the peripheral blood and gastric mucosa of *H. pylori*-positive individuals[119 149 188]. $CD127^{lo}$ gating also helped confirm that the $CD25^{hi}$ events from the $CD4^+$ T cell population were Tregs.

### 7.1.2 Bregs in *H. pylori* infection

As well as IL-$10^+$ Tregs, IL-10-producing B cells, namely Bregs, were studied. The pilot study in mice (**Chapter 3**) demonstrated that splenic B cells expanded significantly in response to *H. pylori* infection. Furthermore, they were major sources of IL-10, when compared to T cells, in uninfected and *H. pylori*-infected mice. While not significant, there were trends of increased $CD1d^{hi}CD5^+$ Breg proportions after *H. pylori* infection, which also led to an increase in IL-$10^+$ Bregs.

These trends were the basis for studying Bregs and IL-10-producing-Bregs in *H. pylori*-positive and *H. pylori*-negative patients (**Chapter 4**). A flow cytometry panel was developed and optimised to ensure that Breg populations could be reproducibly identified and gated in each blood sample analysis. An additional novel aspect of this study was that it also analysed Breg frequencies and IL-$10^+$ Bregs in *H. pylori*-eradicated patients.

Despite B cells accounting for 10% of lymphocytes in human PBMCs, they were the source of 30% of IL-$10^+$ lymphocytes, irrespective of *H. pylori* infection status. This agrees with previous literature describing B cells as another potential source of IL-10[169 235 284 365]. However, neither *H. pylori* infection nor eradication affected Breg frequencies, or IL-$10^+$ Breg frequencies, which stayed consistent with levels found in the peripheral blood of *H. pylori*-negative individuals. The sole published study on Bregs in human *H. pylori* infection described a significant increase of Bregs in patients with asymptomatic *H. pylori* infection[225]. This proportion was lower in *H. pylori*-positive smokers and obese patients. In the present study, *H. pylori* infection and smoking did not affect the frequencies of peripheral blood Bregs. The difference between the studies may have been due to variations in the gating strategy and flow cytometry protocols to identify Bregs.

### 7.1.3 Effect of VacA types on the immune response and in diagnostic tools

The frequencies of Tregs have shown to be increased in *H. pylori*-positive individuals. A previous study in mice identified the expansion of IL-10-producing B cells at 2 weeks after *H. pylori* infection, and an expansion of Tregs 10 weeks after *H. pylori* infection[243]. It is important to understand early responses to *H. pylori* infection, and whether B cells may play a role in modulating Tregs in response to infection. VacA has recently been shown to influence Treg frequencies[192], but the effect of VacA i-region variants on Bregs and Tregs were previously unknown.

After 9 weeks of *H. pylori* infection, there were no differences in Treg frequency or function (**Chapter 5**). Comparing models for mouse spleen and blood provided a bigger picture to the context of *H. pylori* infection studies in mice. In mouse spleen there were slight non-significant differences in IL-10$^{+}$ Tregs in both groups of *H. pylori*-infected mice compared to uninfected mice. However, there were no significant differences in peripheral blood Tregs, or in the function of CD4$^{+}$CD25$^{+}$ Tregs.

There were differences between the Breg and Treg frequency in the pilot study (**Chapter 3**) and the VacA type mouse study (**Chapter 5**). The pilot study demonstrated small differences between *H. pylori*-infected and uninfected mice. The frequency of splenic Bregs was also non-significant with *H. pylori* infection, but both studies showed Breg frequencies in uninfected mice as consistent with another study[190]. Perhaps in a larger group (6 mice, over 4 mice per group in the pilot study), and over 9 weeks, rather than a single time point at 3 weeks post-infection, these small significant differences were lost with variation.

Mice infected with mutant *H. pylori* SS1$^{s1/i1}$ developed a significant Breg increase over 9 weeks. However, this was not significantly different from uninfected mice. Curiously, CD1d$^{hi}$CD5$^{+}$ Bregs were not detected in mouse blood, regardless of *H. pylori* infection status. This suggests that CD1d and CD5 may be markers for splenic Bregs in mice, and may help clarify why so many Breg subsets (**Section 1.6.4.1**) have been described previously in the literature.

It is a mark of VacA's importance to *H. pylori* that nearly all strains of *H. pylori* have the *vacA* gene in their genome, and protein expression is almost ubiquitous[56 78]. The presence of VacA i1-variant in a colonising *H. pylori* strain is an independent risk factor for an increased likelihood of gastric disease[84 85]. As *H. pylori* infection diagnoses with current techniques such as upper GI endoscopy are not practical for some people such as children, a *vacA* i-region PCR-based stool typing test was attempted (**Chapter 6**). While initial attempts with *16S* rRNA and *vacA* s-region gene PCR showed comparable sensitivity and specificity with current diagnostic tools, contamination issues compounded existing questions on the viability of stool-PCR in a clinical setting.

### 7.1.4 Conclusions

While this thesis validated previous studies in the significant increase of Treg during *H. pylori* infection in mice and humans, it was also novel for studying peripheral blood Treg frequencies in patients after *H. pylori* eradication. There was no change in Treg frequencies 2 years after *H. pylori* infection, but a significant decline in IL-10 production, suggesting that further study is necessary to better understand the long-term effects of *H. pylori* infection and eradication. As evidence suggests that the declining *H. pylori* colonisation within the gastric mucosa in humans is associated with the incidence of various extra-gastric conditions[34-36 42], this is an important finding. Although VacA type did not influence Treg frequency or function in the *H. pylori*-infected mouse model, the presence of VacA i1 variant in the *H. pylori* colonising strain and a decreased Treg frequency in the peripheral blood and mucosa of infected individuals remain independent risk factors for *H. pylori*-mediated disease in humans.

The frequencies of Bregs did not increase in *H. pylori* infection in two mouse experiments. They did not change upon *H. pylori* infection with a VacA i-region variant. Breg frequencies were not significantly different in *H. pylori*-negative, *H. pylori*-positive and *H. pylori*-eradicated patient cohorts.

Although a reproducible population which has been identified in mice and humans, Bregs are not yet a convincing regulatory population. Bregs in both species share markers with differentiating B cells. There are no unique markers which identify Bregs, as Foxp3 do for Tregs. Furthermore, the absence of $CD1d^{hi}CD5^{+}$ Bregs in mouse blood, regardless of *H. pylori* infection status, suggests that different Breg subsets may reside in different locations. This makes it harder to identify Bregs, and develop a suitable model for disease associations.

The universal Breg marker, IL-10, is also a cytokine which is expressed by different immune cells after mitogen stimulation – such as $CD4^{+}$ T cells, Tregs, IIC lymphoid-type cells and $CD8^{+}$ T cells. It is also an autocrine B cell growth factor. Studies in the literature have described Bregs as a sub-population of the $CD19^{+}$ B cell population which are an enriched set of IL-10-producing cells[220]. The majority of Bregs identified in this thesis in mice and humans were not $IL\text{-}10^{+}$ cells.

Suppression assays of Bregs were not completed to achieve the gold standard of identifying suppressive cells[171]. Bregs in mice and humans, which require multiple markers, are a small proportion of lymphocytes within blood and splenic tissue. Isolating this population would require an initial large sample size, and this is not always plausible. Although a suppression assay was attempted, it unfortunately failed to produce meaningful data and was left to be optimised for future experiments.

Many groups have made attempts to develop stool PCR testing[11 259 270 305 306 312 317 318 321 322 327 332 333 335 338 340-349 355 357-361], due to the potential ease and availability of stool donations, and the possibility of studying bacterial populations such as *H. pylori* in depth. Unfortunately, contamination issues prevented the feasibility of the stool *vacA* PCR test in this thesis. Further studies are still required to address the variation of sample collection procedures, stool sample storage, DNA extraction of degraded *H. pylori* template and PCR protocols in published studies before stool PCR testing can be made clinically relevant.

## 7.2 Critique of experimental design

The use of an infection time course was useful to describe the early immune responses to *H. pylori* infection, and how these developed over time. This methodology has been used previously in mouse *H. pylori* experiments[87 243]. Furthermore, they provided insight into when future *H. pylori* infection experiments should be terminated to observe optimum levels of inflammation and host immune response. In humans, 1 year after eradication was shown to be a major time point to identify a decline in IL-10$^{+}$ Tregs after successful *H. pylori* eradication. Months 2-6 after *H. pylori* eradication produced lots of flux in the regulatory immune response. The time course also showed incremental but significant differences in IL-10 decline over time which was not observed in *H. pylori*-positive and *H. pylori*-eradicated groups of patients. It was important to recruit patients for multiple time points to show this finding, but it was difficult maintaining patient consent to return for future blood donations. This difficulty has been observed in another *H. pylori* study with multiple time points[259].

Cytokines are potent mediators for cell functions. Without *in vitro* stimulation, B and T lymphocytes produce little or no IL-10, and therefore *in vitro* stimulation of cells is used to detect these cytokines. In this thesis, two stimulatory techniques were used; a mix of mitogenic chemicals PMA, ionomycin and LPS, and a lysate made from 6 clinical isolates of *H. pylori*. *H. pylori* lysate antigen has been used previously by the research group and in other studies to induce IFN-γ and IL-10 production from T cells for the quantification of cytokine-producing subsets[119 188]. Preliminary data showed that *H. pylori* lysate did not induce IL-10 production from B cells (data not shown). Instead, stimulation using a combination of PMA, ionomycin and LPS has been widely used in B cell and Breg studies in mice and humans[212 218 219 225 243 302]. These techniques were compared to understand the benefits and limits of each technique in IL-10 stimulation of peripheral blood lymphocytes, and the relevancy of each model in *H. pylori* research.

The induction of IL-10 by peripheral blood $CD4^+$ T lymphocytes in humans after stimulation with PMA/ionomycin/LPS or *H. pylori* lysate was compared (**Appendix K**). Blood was donated by patients who had successfully cleared their *H. pylori* infection, and PBMCs were stimulated with *H. pylori* lysate for 16 hours or PMA/ionomycin/LPS for 6 hours, or left unstimulated. *H. pylori*-stimulated cells were stained and analysed using a previous protocol (**Section 2.4.7.2**), and mitogen-stimulated cells were stained and analysed using a different protocol described earlier (**Section 4.4.3.3**). When cytokines are produced by cells in response to these stimulation protocols, they are secreted by the cell into the tissue culture medium. BFA was used an hour after both stimulation protocols to inhibit the secretion of these cytokines, so that Foxp3 and IL-10 intracellular expression could be quantified[366].

*H. pylori* lysate, made from clinical strains, is representative of a clinical and physiological response, and produces a *H. pylori*-specific immune response[119]. The antigens can induce *H. pylori*-specific responses, such as the production of IFN-γ[119]. When PBMCs from *H. pylori*-positive individuals are re-stimulated with *H. pylori*, effector memory cells can become re-stimulated with *H. pylori* antigens and induce IL-10. However, $IL\text{-}10^+$ lymphocytes are less frequent in peripheral blood after stimulation, as *H. pylori* lysate antigens are not as immunogenic as potent mitogens. This is also why *H. pylori* lysate is co-cultured with leukocytes for 16 hours. Data also showed that stimulated PBMCs from a *H. pylori*-negative patient with *H. pylori* lysate produced a $CD4^+IL\text{-}10^+$ response similar to unstimulated levels[119]. Therefore, it was not a feasible model to study the capacity of IL-10-producing lymphocytes in *H. pylori*-negative patient cohorts. Additionally, *H. pylori* lysate can show variance between each cultivated batch, and also demonstrate an inter-lab variability in chosen isolates, as it is a mixture of cultured lab strains.

PMA/ionomycin is a polyclonal stimulatory mix. Ionomycin is an ionophore produced by the bacterium *Streptomyces conglobatus* to increase the level of intracellular calcium ions. Ionomycin then induces protein kinase C (PKC) activation in resting T cells by phosphorylating CD4 and CD8 proteins. PMA furthers this activation by synergizing with ionomycin, and triggering T cell activation and subsequent

proliferation through NFAT nuclear transduction signalling[273 367]. LPS, produced by Gram-negative bacteria (in this case, *E. coli*), is a PAMP which induces the proliferation of B cells through TLR4 dimerisation and the MyD88 signalling cascade[368]. *H. pylori* LPS was not used because its lipid A component is less immunogenic compared to other Gram-negative bacteria[102]. Ultimately, this is a model which may require adaptation for studying *H. pylori* infection. This model did not show an increased Treg IL-10 production in *H. pylori*-positive individuals, which has been reported previously.

## 7.3 Future work and unanswered questions

The Treg eradication study is ongoing, with more patients due to donate blood at the 2-year time point. Once this is completed, there are many components of the study to help fully elucidate the immune response in humans after eradication.

Firstly, extra PBMCs and serum from all samples have been stored at -80$^{o}$C. The extra PBMCs can be thawed to repeat the findings discussed (**Section 2.5**). This can be used to test frequencies of other Treg markers, such as CD127$^{lo}$, LAG3$^{+}$ and Helios$^{+}$ Tregs. Furthermore, repeating the study removes the variation from different users processing the blood samples. The serum will be used to test how the *H. pylori* IgG response changes in time after successful eradication.

Ongoing work has identified a trend in declining *IL-10* mRNA expression over time after *H. pylori* eradication[117]. As this nears completion, further work on *IL-17* and *IFN-γ* mRNA PCR will also be completed to observe pro-inflammatory cytokine activity after *H. pylori* infection is eradicated. IFN-γ has been shown to be increased in *H. pylori* infection[119], while IL-17, a measure of Th17 activity, is also increased in *H. pylori* infection[124].

Pending ethical permission and patient consent, a 5 year follow up upper GI endoscopy/blood donation attached to the Eradication study could be useful to

understand long-term consequences to *H. pylori* eradication. Tregs did not decline after 2 years, suggesting a slow immunological change.

There is increasing evidence to support the hypothesis that *H. pylori* infection protects against extra-gastric diseases such as MS, asthma, allergy-induced asphyxia and oesophageal cancer[33-35 37 40 42 49 194 195]. However, mechanisms of this protection are mostly known from studying *H. pylori*-infected mouse models[33 39 40 194]. Future work could be expanded in human patient cohorts to determine a clinical relevance and promote further discussion about the benefits of eradication in these patients.

Identification of new environmental risk factors is also important in reducing stomach cancer incidences around the world. The demographic of smoking has shifted – as increasing measures are placed on UK tobacco companies to provide plain packaging on cigarette packets, more people are also using electronic cigarettes. Smoking increases the risk of recurring ulcers and eradication failure[62 63]. The equivalence of using electronic cigarettes and smoking nicotine cigarettes, in the context of *H. pylori* infection risk is yet unknown.

6/50 patients failed to eradicate their *H. pylori* infection with first line treatment in the eradication study. This is in line with reported treatment failure rates across Europe, and around the world[24]. 6/16 patients from the stool study had also previously failed eradication therapy, 3 of whom failed more than once. In this thesis, 1 patient remained *H. pylori*-positive despite one year of eradication therapy regimes. There is evidence to suggest a decline in successful *H. pylori* eradication rates and a rise in antibiotic resistance (particularly clarithromycin) worldwide[24]. The development of new antibiotics for *H. pylori* treatment to replace clarithromycin has been described as a high priority for member states by WHO[369]. Unfortunately, this increased antibiotic resistance is a disconcerting trend with all bacterial infections. There are already *N. gonorrhoeae* isolates that are resistant to last-line cephalosporins, along with 13+ isolates of vancomycin-resistant MRSA, and hypervirulent *C. difficile* strains which are multi-drug resistant[370-373].

## 7.4 Final summary

Overall, this thesis investigated markers for *H. pylori*-mediated disease. It was found that peripheral blood Tregs, which are upregulated in *H. pylori*-positive patients, remained consistent two years after successful eradication therapy, whereas IL-10$^{+}$ Tregs declined in frequency over time. Meanwhile, the frequencies of Bregs, which were described in the literature as an enriched population of IL-10-producing B cells, were not affected by *H. pylori* infection in mice or in patients. Furthermore, the presence of the VacA i1-variant, which is an independent risk factor for *H. pylori*-mediated disease, did not affect Treg frequency or function in a mouse model, and could not be used as the basis for a *H. pylori* stool PCR test.

It is hoped that current studies, or those being planned for the future, will provide a greater comprehension of the mechanisms of pathogenesis and immunoregulation that *H. pylori* infection induces in humans. This knowledge is crucial to understanding the consequences to eradicating this bacterium in the face of rising immunopathological diseases.

## Bibliography


1. Jones KR, Whitmire JM, Merrell DS. A Tale of Two Toxins: *Helicobacter pylori* CagA and VacA Modulate Host Pathways that Impact Disease. *Frontiers in microbiology* 2010;1:115. doi: 10.3389/fmicb.2010.00115
2. Maixner F, Krause-Kyora B, Turaev D, et al. The 5300-year-old *Helicobacter pylori* genome of the Iceman. *Science* 2016;351(6269):162-5. doi: 10.1126/science.aad2545
3. Moodley Y, Linz B, Bond RP, et al. Age of the association between *Helicobacter pylori* and man. *PLoS Pathogens* 2012;8(5):e1002693. doi: 10.1371/journal.ppat.1002693
4. Kuwahara H, Miyamoto Y, Akaike T, et al. *Helicobacter pylori* urease suppresses bactericidal activity of peroxynitrite via carbon dioxide production. *Infection and immunity* 2000;68(8):4378-83.
5. Atherton JC, Blaser MJ. Coadaptation of *Helicobacter pylori* and humans: ancient history, modern implications. *Journal of Clinical Investigation* 2009;119(9):2475-87. doi: 10.1172/JCI38605
6. Mobley HLT. In: Mobley HLT MG, Hazell SL, ed. *Helicobacter pylori*: Physiology and Genetics. Washington, DC: ASM Press 2001.
7. Cancer IAfRo. Agents classified by the IARC monographs, 2012.
8. Kusters JG, van Vliet AH, Kuipers EJ. Pathogenesis of *Helicobacter pylori* infection. *Clinical microbiology reviews* 2006;19(3):449-90. doi: 10.1128/CMR.00054-05
9. Berger J. *Helicobacter pylori* bacteria, SEM: Science Photo Library.
10. Hatakeyama M. Oncogenic mechanisms of the *Helicobacter pylori* CagA protein. *Nature Reviews Cancer* 2004;4(9):688-94. doi: 10.1038/nrc1433
11. Parsonnet J, Shmuely H, Haggerty T. Fecal and oral shedding of *Helicobacter pylori* from healthy infected adults. *Journal of the American Medical Association* 1999;282(23):2240-5.
12. J. R. Warren BM. Unidentified curved bacilli on gastric epithelium in active chronic gastritis. *Lancet* 1983;1(8336):1273-5.
13. O'Connor A, O'Morain CA, Ford AC. Population screening and treatment of *Helicobacter pylori* infection. *Nature Reviews Gastroenterology & Hepatology* 2017;14(4):230-40. doi: 10.1038/nrgastro.2016.195
14. Goddard AF, James MW, McIntyre AS, et al. Guidelines for the management of iron deficiency anaemia. *Gut* 2011;60(10):1309-16. doi: 10.1136/gut.2010.228874
15. NHS. Stomach ulcer - complications 2015 [Available from: http://www.nhs.uk/Conditions/Peptic-ulcer/Pages/Complications.aspx2016.
16. White JR, Winter, J.A., Robinson, K. Differential inflammatory response to *Helicobacter pylori* infection: etiology and clinical outcomes. *Journal of Inflammation Research* 2015;8:137-47.
17. Palmer K. Acute upper gastrointestinal haemorrhage. *British Medical Bulletin* 2007;83:307-24. doi: 10.1093/bmb/ldm023
18. Zucca E, Bertoni F, Roggero E, et al. The gastric marginal zone B-cell lymphoma of MALT type. *Blood* 2000;96(2):410-9.

19. Morgner A, Bayerdorffer E, Neubauer A, et al. *Helicobacter pylori* associated gastric B cell MALT lymphoma: predictive factors for regression. *Gut* 2001;48(3):290-2.
20. Zucca E, Bertoni F, Vannata B, et al. Emerging role of infectious etiologies in the pathogenesis of marginal zone B-cell lymphomas. *Clinical Cancer Research* 2014;20(20):5207-16. doi: 10.1158/1078-0432.CCR-14-0496
21. Ernst PB, Gold BD. The disease spectrum of *Helicobacter pylori*: the immunopathogenesis of gastroduodenal ulcer and gastric cancer. *Annual review of microbiology* 2000;54:615-40. doi: 10.1146/annurev.micro.54.1.615
22. Kumar P, Clark M. Kumar and Clark's Clinical Medicine. 8th ed: Saunders, Ltd. 2012:248-253.
23. Colquhoun A, Arnold M, Ferlay J, et al. Global patterns of cardia and non-cardia gastric cancer incidence in 2012. *Gut* 2015;64(12):1881-8. doi: 10.1136/gutjnl-2014-308915
24. Malfertheiner P, Megraud F, O'Morain CA, et al. Management of *Helicobacter pylori* infection-the Maastricht V/Florence Consensus Report. *Gut* 2017;66(1):6-30. doi: 10.1136/gutjnl-2016-312288
25. Blaser M. Missing Microbes. London: Oneworld 2014:115.
26. International WCRF. Stomach cancer statistics [Available from: http://www.wcrf.org/int/cancer-facts-figures/data-specific-cancers/stomach-cancer-statistics accessed 28/07/2017 2017.
27. UK CR. Worldwide cancer mortality statistics [Available from: http://www.cancerresearchuk.org/health-professional/cancer-statistics/worldwide-cancer/mortality#heading-One2017.
28. Statistics and outlook for stomach cancer: Cancer Research UK; [Available from: http://www.cancerresearchuk.org/about-cancer/type/stomach-cancer/treatment/statistics-and-outlook-for-stomach-cancer2015.
29. Stomach cancer statistics: World Cancer Research Fund International; [Available from: http://www.wcrf.org/int/cancer-facts-figures/data-specific-cancers/stomach-cancer-statistics accessed 08/10 2015.
30. Robinson K, Argent RH, Atherton JC. The inflammatory and immune response to *Helicobacter pylori* infection. *Best Practice & Research Clinical Gastroenterology* 2007;21(2):237-59. doi: 10.1016/j.bpg.2007.01.001
31. Correa P, Haenszel W, Cuello C, et al. A model for gastric cancer epidemiology. *Lancet* 1975;2(7924):58-60.
32. den Hollander WJ, Holster IL, van Gilst B, et al. Intergenerational reduction in *Helicobacter pylori* prevalence is similar between different ethnic groups living in a Western city. *Gut* 2015;64(8):1200-8. doi: 10.1136/gutjnl-2014-307689
33. Cook KW, Crooks J, Hussain K, et al. *Helicobacter pylori* infection reduces disease severity in an experimental model of multiple sclerosis. *Frontiers in microbiology* 2015;6:52. doi: 10.3389/fmicb.2015.00052
34. Robinson K. *Helicobacter pylori*-Mediated Protection against Extra-Gastric Immune and Inflammatory Disorders: The Evidence and Controversies. *Diseases* 2015;3(2):34-55.

35. Shah A, Talley NJ, Walker M, et al. Is There a Link Between *H. pylori* and the Epidemiology of Crohn's Disease? *Digestive diseases and sciences* 2017 doi: 10.1007/s10620-017-4496-z
36. Islami F, Kamangar F. *Helicobacter pylori* and esophageal cancer risk: a meta-analysis. *Cancer Prevention Research* 2008;1(5):329-38. doi: 10.1158/1940-6207.CAPR-08-0109
37. Hussain K, Letley DP, Greenaway AB, et al. *Helicobacter pylori*-Mediated Protection from Allergy Is Associated with IL-10-Secreting Peripheral Blood Regulatory T Cells. *Frontiers in Immunology* 2016;7:71. doi: 10.3389/fimmu.2016.00071
38. Pedrini MJ, Seewann A, Bennett KA, et al. *Helicobacter pylori* infection as a protective factor against multiple sclerosis risk in females. *Journal of Neurology, Neurosurgery, and Psychiatry* 2015;86(6):603-7. doi: 10.1136/jnnp-2014-309495
39. Arnold IC, Dehzad N, Reuter S, et al. *Helicobacter pylori* infection prevents allergic asthma in mouse models through the induction of regulatory T cells. *Journal of Clinical Investigation* 2011;121(8):3088-93. doi: 10.1172/JCI45041
40. Kyburz A, Urban S, Altobelli A, et al. *Helicobacter pylori* and its secreted immunomodulator VacA protect against anaphylaxis in experimental models of food allergy. *Clinical & Experimental Allergy* 2017 doi: 10.1111/cea.12996
41. Amberbir A, Medhin G, Abegaz WE, et al. Exposure to *Helicobacter pylori* infection in early childhood and the risk of allergic disease and atopic sensitization: a longitudinal birth cohort study. *Clinical & Experimental Allergy* 2014;44(4):563-71. doi: 10.1111/cea.12289
42. Chen Y, Blaser MJ. *Helicobacter pylori* colonization is inversely associated with childhood asthma. *Journal of Infectious Diseases* 2008;198(4):553-60. doi: 10.1086/590158
43. Kiselev I, Bashinskaya V, Kulakova O, et al. Variants of MicroRNA Genes: Gender-Specific Associations with Multiple Sclerosis Risk and Severity. *International Journal of Molecular Sciences* 2015;16(8):20067-81. doi: 10.3390/ijms160820067
44. Ramagopalan SV, Dobson R, Meier UC, et al. Multiple sclerosis: risk factors, prodromes, and potential causal pathways. *Lancet Neurology* 2010;9(7):727-39. doi: 10.1016/S1474-4422(10)70094-6
45. Li W, Minohara M, Su JJ, et al. *Helicobacter pylori* infection is a potential protective factor against conventional multiple sclerosis in the Japanese population. *Journal of Neuroimmunology* 2007;184(1-2):227-31. doi: 10.1016/j.jneuroim.2006.12.010
46. Mokry LE, Ross S, Ahmad OS, et al. Vitamin D and Risk of Multiple Sclerosis: A Mendelian Randomization Study. *PLoS Medicine* 2015;12(8):e1001866. doi: 10.1371/journal.pmed.1001866
47. Guo L, Chen W, Zhu H, et al. *Helicobacter pylori* induces increased expression of the vitamin d receptor in immune responses. *Helicobacter* 2014;19(1):37-47. doi: 10.1111/hel.12102
48. UK A. What is asthma? 2016 [updated November 2016. Available from: https://www.asthma.org.uk/advice/understanding-asthma/what-is-asthma/2017.

49. Lord AR, Simms LA, Hanigan K, et al. Protective effects of *Helicobacter pylori* for IBD are related to the *cagA*-positive strain. *Gut* 2017 doi: 10.1136/gutjnl-2017-313805
50. O'Connor HJ. Review article: *Helicobacter pylori* and gastro-oesophageal reflux disease-clinical implications and management. *Alimentary Pharmacology & Therapeutics* 1999;13(2):117-27.
51. Versalovic J. *Helicobacter pylori*. Pathology and diagnostic strategies. *American journal of clinical pathology* 2003;119(3):403-12.
52. Horn JR. How Do PPIs Work? Implications for Therapy. http://www.medscape.org/viewarticle/457393_4 (accessed January 2015).
53. Graham DY, Fischbach L. *Helicobacter pylori* treatment in the era of increasing antibiotic resistance. *Gut* 2010;59(8):1143-53. doi: 10.1136/gut.2009.192757
54. Fischer W, Breithaupt U, Kern B, et al. A comprehensive analysis of *Helicobacter pylori* plasticity zones reveals that they are integrating conjugative elements with intermediate integration specificity. *BMC genomics* 2014;15:310. doi: 10.1186/1471-2164-15-310
55. Megraud F, Lamouliatte H. Review article: the treatment of refractory *Helicobacter pylori* infection. *Alimentary Pharmacology & Therapeutics* 2003;17(11):1333-43.
56. Yamaoka Y, Graham DY. *Helicobacter pylori* virulence and cancer pathogenesis. *Future Oncology* 2014;10(8):1487-500. doi: 10.2217/fon.14.29
57. Replogle ML, Glaser SL, Hiatt RA, et al. Biologic sex as a risk factor for *Helicobacter pylori* infection in healthy young adults. *American journal of epidemiology* 1995;142(8):856-63.
58. Ogihara A, Kikuchi S, Hasegawa A, et al. Relationship between *Helicobacter pylori* infection and smoking and drinking habits. *Journal of gastroenterology and hepatology* 2000;15(3):271-6.
59. Parasher G, Eastwood GL. Smoking and peptic ulcer in the *Helicobacter pylori* era. *European journal of gastroenterology & hepatology* 2000;12(8):843-53.
60. Lee SA, Kang D, Shim KN, et al. Effect of diet and *Helicobacter pylori* infection to the risk of early gastric cancer. *Journal of Epidemiology* 2003;13(3):162-8.
61. Gaddy JA, Radin JN, Loh JT, et al. High dietary salt intake exacerbates *Helicobacter pylori*-induced gastric carcinogenesis. *Infection and immunity* 2013;81(6):2258-67. doi: 10.1128/IAI.01271-12
62. Brenner H, Rothenbacher D, Bode G, et al. Relation of smoking and alcohol and coffee consumption to active *Helicobacter pylori* infection: cross sectional study. *The BMJ* 1997;315(7121):1489-92.
63. Suzuki T, Matsuo K, Ito H, et al. Smoking increases the treatment failure for *Helicobacter pylori* eradication. *American Journal of Medicine* 2006;119(3):217-24. doi: 10.1016/j.amjmed.2005.10.003
64. Delahay RM, Rugge M. Pathogenesis of *Helicobacter pylori* infection. *Helicobacter* 2012;17 Suppl 1:9-15. doi: 10.1111/j.1523-5378.2012.00976.x
65. Blaser MJ, Atherton JC. *Helicobacter pylori* persistence: biology and disease. *Journal of Clinical Investigation* 2004;113(3):321-33. doi: 10.1172/JCI20925
66. Atherton JC. The pathogenesis of *Helicobacter pylori*-induced gastro-duodenal diseases. *Annual Review of Pathology* 2006;1:63-96. doi: 10.1146/annurev.pathol.1.110304.100125

67. Patel SR, Smith K, Letley DP, et al. *Helicobacter pylori* downregulates expression of human beta-defensin 1 in the gastric mucosa in a type IV secretion-dependent fashion. *Cellular microbiology* 2013;15(12):2080-92. doi: 10.1111/cmi.12174
68. Salama NR, Hartung ML, Muller A. Life in the human stomach: persistence strategies of the bacterial pathogen *Helicobacter pylori*. *Nature Reviews Microbiology* 2013;11(6):385-99. doi: 10.1038/nrmicro3016
69. Higashi H, Tsutsumi R, Fujita A, et al. Biological activity of the *Helicobacter pylori* virulence factor CagA is determined by variation in the tyrosine phosphorylation sites. *Proceedings of the National Academy of Sciences of the United States of America* 2002;99(22):14428-33. doi: 10.1073/pnas.222375399
70. Umehara S, Higashi H, Ohnishi N, et al. Effects of *Helicobacter pylori* CagA protein on the growth and survival of B lymphocytes, the origin of MALT lymphoma. *Oncogene* 2003;22(51):8337-42. doi: 10.1038/sj.onc.1207028
71. Blaser MJ, Perez-Perez GI, Kleanthous H, et al. Infection with *Helicobacter pylori* strains possessing *cagA* is associated with an increased risk of developing adenocarcinoma of the stomach. *Cancer research* 1995;55(10):2111-5.
72. Boquet P, Ricci V. Intoxication strategy of *Helicobacter pylori* VacA toxin. *Trends in microbiology* 2012;20(4):165-74. doi: 10.1016/j.tim.2012.01.008
73. Peek RM, Jr., Miller GG, Tham KT, et al. Heightened inflammatory response and cytokine expression in vivo to *cagA*+ *Helicobacter pylori* strains. *Laboratory Investigation* 1995;73(6):760-70.
74. Winter J, Letley D, Rhead J, et al. *Helicobacter pylori* membrane vesicles stimulate innate pro- and anti-inflammatory responses and induce apoptosis in Jurkat T cells. *Infection and immunity* 2014;82(4):1372-81. doi: 10.1128/IAI.01443-13
75. Utsch C, Haas R. VacA's Induction of VacA-Containing Vacuoles (VCVs) and Their Immunomodulatory Activities on Human T Cells. *Toxins* 2016;8(6) doi: 10.3390/toxins8060190
76. Kim IJ, Blanke SR. Remodeling the host environment: modulation of the gastric epithelium by the *Helicobacter pylori* vacuolating toxin (VacA). *Frontiers in cellular and infection microbiology* 2012;2:37. doi: 10.3389/fcimb.2012.00037
77. Tombola F, Morbiato L, Del Giudice G, et al. The *Helicobacter pylori* VacA toxin is a urea permease that promotes urea diffusion across epithelia. *Journal of Clinical Investigation* 2001;108(6):929-37. doi: 10.1172/JCI13045
78. Cover TL, Tummuru MK, Cao P, et al. Divergence of genetic sequences for the vacuolating cytotoxin among *Helicobacter pylori* strains. *Journal of Biological Chemistry* 1994;269(14):10566-73.
79. Atherton JC, Cover TL, Twells RJ, et al. Simple and accurate PCR-based system for typing vacuolating cytotoxin alleles of *Helicobacter pylori*. *Journal of clinical microbiology* 1999;37(9):2979-82.
80. Leunk RD, Johnson PT, David BC, et al. Cytotoxic activity in broth-culture filtrates of *Campylobacter pylori*. *Journal of Medical Microbiology* 1988;26(2):93-9.
81. Atherton JC, Cao P, Peek RM, Jr., et al. Mosaicism in vacuolating cytotoxin alleles of *Helicobacter pylori.* Association of specific *vacA* types with cytotoxin production and peptic ulceration. *Journal of Biological Chemistry* 1995;270(30):17771-7.

82. Letley DP, Rhead JL, Twells RJ, et al. Determinants of non-toxicity in the gastric pathogen *Helicobacter pylori*. *Journal of Biological Chemistry* 2003;278(29):26734-41. doi: 10.1074/jbc.M304071200
83. van Doorn LJ, Henskens Y, Nouhan N, et al. The efficacy of laboratory diagnosis of *Helicobacter pylori* infections in gastric biopsy specimens is related to bacterial density and *vacA*, *cagA*, and *iceA* genotypes. *Journal of clinical microbiology* 2000;38(1):13-7.
84. Rhead JL, Letley DP, Mohammadi M, et al. A new *Helicobacter pylori* vacuolating cytotoxin determinant, the intermediate region, is associated with gastric cancer. *Gastroenterology* 2007;133(3):926-36. doi: 10.1053/j.gastro.2007.06.056
85. Basso D, Zambon CF, Letley DP, et al. Clinical relevance of *Helicobacter pylori cagA* and *vacA* gene polymorphisms. *Gastroenterology* 2008;135(1):91-9. doi: 10.1053/j.gastro.2008.03.041
86. Hussein NR, Mohammadi M, Talebkhan Y, et al. Differences in virulence markers between *Helicobacter pylori* strains from Iraq and those from Iran: potential importance of regional differences in *H. pylori*-associated disease. *Journal of clinical microbiology* 2008;46(5):1774-9. doi: 10.1128/JCM.01737-07
87. Winter JA, Letley DP, Cook KW, et al. A role for the vacuolating cytotoxin, VacA, in colonization and *Helicobacter pylori*-induced metaplasia in the stomach. *Journal of Infectious Diseases* 2014;210(6):954-63. doi: 10.1093/infdis/jiu154
88. Chung C, Olivares A, Torres E, et al. Diversity of VacA intermediate region among *Helicobacter pylori* strains from several regions of the world. *Journal of clinical microbiology* 2010;48(3):690-6. doi: 10.1128/JCM.01815-09
89. Argent RH, Thomas RJ, Letley DP, et al. Functional association between the *Helicobacter pylori* virulence factors VacA and CagA. *Journal of Medical Microbiology* 2008;57(Pt 2):145-50. doi: 10.1099/jmm.0.47465-0
90. Cover TL, Blanke SR. *Helicobacter pylori* VacA, a paradigm for toxin multifunctionality. *Nature Reviews Microbiology* 2005;3(4):320-32. doi: 10.1038/nrmicro1095
91. Kalali B, Mejias-Luque R, Javaheri A, et al. *H. pylori* virulence factors: influence on immune system and pathology. *Mediators of inflammation* 2014;2014:426309. doi: 10.1155/2014/426309
92. Boren T, Falk P, Roth KA, et al. Attachment of *Helicobacter pylori* to human gastric epithelium mediated by blood group antigens. *Science* 1993;262(5141):1892-5.
93. Hage N, Howard T, Phillips C, et al. Structural basis of Lewis(b) antigen binding by the *Helicobacter pylori* adhesin BabA. *Science Advances* 2015;1(7):e1500315. doi: 10.1126/sciadv.1500315
94. Amieva MR, El-Omar EM. Host-bacterial interactions in *Helicobacter pylori* infection. *Gastroenterology* 2008;134(1):306-23. doi: 10.1053/j.gastro.2007.11.009
95. Hussein NR, Argent RH, Marx CK, et al. *Helicobacter pylori dupA* is polymorphic, and its active form induces proinflammatory cytokine secretion by mononuclear cells. *Journal of Infectious Diseases* 2010;202(2):261-9. doi: 10.1086/653587

96. Argent RH, Burette A, Miendje Deyi VY, et al. The presence of *dupA* in *Helicobacter pylori* is not significantly associated with duodenal ulceration in Belgium, South Africa, China, or North America. *Clinical Infectious Diseases* 2007;45(9):1204-6. doi: 10.1086/522177
97. Alandiyjany MN, Croxall NJ, Grove JI, et al. A role for the *tfs3* ICE-encoded type IV secretion system in pro-inflammatory signalling by the *Helicobacter pylori* Ser/Thr kinase, CtkA. *PLoS One* 2017;12(7):e0182144. doi: 10.1371/journal.pone.0182144
98. Wilson KT, Crabtree JE. Immunology of *Helicobacter pylori*: insights into the failure of the immune response and perspectives on vaccine studies. *Gastroenterology* 2007;133(1):288-308. doi: 10.1053/j.gastro.2007.05.008
99. Ohyauchi M, Imatani A, Yonechi M, et al. The polymorphism interleukin 8 -251 A/T influences the susceptibility of *Helicobacter pylori* related gastric diseases in the Japanese population. *Gut* 2005;54(3):330-5. doi: 10.1136/gut.2003.033050
100. Kawai T, Akira S. Toll-like receptor downstream signaling. *Arthritis research & therapy* 2005;7(1):12-9. doi: 10.1186/ar1469
101. Yarovinsky F. Innate immunity to *Toxoplasma gondii* infection. *Nature Reviews Immunology* 2014;14(2):109-21. doi: 10.1038/nri3598
102. Moran AP, Lindner B, Walsh EJ. Structural characterization of the lipid A component of *Helicobacter pylori* rough- and smooth-form lipopolysaccharides. *Journal of bacteriology* 1997;179(20):6453-63.
103. Andersen-Nissen E, Smith KD, Strobe KL, et al. Evasion of Toll-like receptor 5 by flagellated bacteria. *Proceedings of the National Academy of Sciences of the United States of America* 2005;102(26):9247-52. doi: 10.1073/pnas.0502040102
104. Su B, Ceponis PJ, Lebel S, et al. *Helicobacter pylori* activates Toll-like receptor 4 expression in gastrointestinal epithelial cells. *Infection and immunity* 2003;71(6):3496-502.
105. Lepper PM, Triantafilou M, Schumann C, et al. Lipopolysaccharides from *Helicobacter pylori* can act as antagonists for Toll-like receptor 4. *Cellular microbiology* 2005;7(4):519-28. doi: 10.1111/j.1462-5822.2005.00482.x
106. Sayi A, Kohler E, Toller IM, et al. TLR-2-activated B cells suppress *Helicobacter*-induced preneoplastic gastric immunopathology by inducing T regulatory-1 cells. *Journal of immunology* 2011;186(2):878-90. doi: 10.4049/jimmunol.1002269
107. Kawai T, Akira S. The role of pattern-recognition receptors in innate immunity: update on Toll-like receptors. *Nature Immunology* 2010;11(5):373-84. doi: 10.1038/ni.1863
108. Hemmi H, Takeuchi O, Kawai T, et al. A Toll-like receptor recognizes bacterial DNA. *Nature* 2000;408(6813):740-5. doi: 10.1038/35047123
109. Smith SM. Role of Toll-like receptors in *Helicobacter pylori* infection and immunity. *World journal of gastrointestinal pathophysiology* 2014;5(3):133-46. doi: 10.4291/wjgp.v5.i3.133
110. Muller A, Oertli M, Arnold IC. *H. pylori* exploits and manipulates innate and adaptive immune cell signaling pathways to establish persistent infection. *Cell Communication and Signaling* 2011;9(1):25. doi: 10.1186/1478-811X-9-25

111. Gringhuis SI, den Dunnen J, Litjens M, et al. Carbohydrate-specific signaling through the DC-SIGN signalosome tailors immunity to *Mycobacterium tuberculosis*, HIV-1 and *Helicobacter pylori*. *Nature Immunology* 2009;10(10):1081-8. doi: 10.1038/ni.1778
112. Leung SY, Yuen ST, Chu KM, et al. Expression profiling identifies chemokine (C-C motif) ligand 18 as an independent prognostic indicator in gastric cancer. *Gastroenterology* 2004;127(2):457-69.
113. Quiding-Jarbrink M, Raghavan S, Sundquist M. Enhanced M1 macrophage polarization in human *Helicobacter pylori*-associated atrophic gastritis and in vaccinated mice. *PLoS One* 2010;5(11):e15018. doi: 10.1371/journal.pone.0015018
114. Gobert AP, Verriere T, Asim M, et al. Heme oxygenase-1 dysregulates macrophage polarization and the immune response to *Helicobacter pylori*. *Journal of Immunology* 2014;193(6):3013-22. doi: 10.4049/jimmunol.1401075
115. Harris PR, Ernst PB, Kawabata S, et al. Recombinant *Helicobacter pylori* urease activates primary mucosal macrophages. *Journal of Infectious Diseases* 1998;178(5):1516-20.
116. Wunder C, Churin Y, Winau F, et al. Cholesterol glucosylation promotes immune evasion by *Helicobacter pylori*. *Nature Medicine* 2006;12(9):1030-8. doi: 10.1038/nm1480
117. White JR. Developing new predictors of *Helicobacter pylori* associated disease and its progression [PhD]. University of Nottingham, 2017.
118. Goll R, Gruber F, Olsen T, et al. *Helicobacter pylori* stimulates a mixed adaptive immune response with a strong T-regulatory component in human gastric mucosa. *Helicobacter* 2007;12(3):185-92. doi: 10.1111/j.1523-5378.2007.00495.x
119. Robinson K, Kenefeck R, Pidgeon EL, et al. *Helicobacter pylori*-induced peptic ulcer disease is associated with inadequate regulatory T cell responses. *Gut* 2008;57(10):1375-85. doi: 10.1136/gut.2007.137539
120. Garhart CA, Nedrud JG, Heinzel FP, et al. Vaccine-induced protection against *Helicobacter pylori* in mice lacking both antibodies and interleukin-4. *Infection and immunity* 2003;71(6):3628-33.
121. Robinson K, Argent RH, Atherton JC. The inflammatory and immune response to *Helicobacter pylori* infection. *Best Practice & Research: Clinical Gastroenterology* 2007;21(2):237-59. doi: 10.1016/j.bpg.2007.01.001
122. Robinson KA, J.C. *Helicobacter pylori*-induced Acquired Immunity and Immunoregulation. In: P. Sutton HM, ed. *Helicobacter pylori* in the 21st Century: CABI Publishing 2010:94-115.
123. Mizuno T, Ando T, Nobata K, et al. Interleukin-17 levels in *Helicobacter pylori*-infected gastric mucosa and pathologic sequelae of colonization. *World Journal of Gastroenterology* 2005;11(40):6305-11.
124. Shi Y, Liu XF, Zhuang Y, et al. *Helicobacter pylori*-induced Th17 responses modulate Th1 cell responses, benefit bacterial growth, and contribute to pathology in mice. *Journal of Immunology* 2010;184(9):5121-9. doi: 10.4049/jimmunol.0901115

125. Hernandez C, Serrano C, Einisman H, et al. Peptic ulcer disease in *Helicobacter pylori*-infected children: clinical findings and mucosal immune response. *Journal of Pediatric Gastroenterology and Nutrition* 2014;59(6):773-8. doi: 10.1097/MPG.0000000000000500
126. Zabaleta J, McGee DJ, Zea AH, et al. *Helicobacter pylori* arginase inhibits T cell proliferation and reduces the expression of the TCR zeta-chain (CD3zeta). *J Immunol* 2004;173(1):586-93.
127. Sakaguchi S, Yamaguchi T, Nomura T, et al. Regulatory T cells and immune tolerance. *Cell* 2008;133(5):775-87. doi: 10.1016/j.cell.2008.05.009
128. Gabrilovich DI, Nagaraj S. Myeloid-derived suppressor cells as regulators of the immune system. *Nature Reviews Immunology* 2009;9(3):162-74. doi: 10.1038/nri2506
129. Nau D, Altmayer N, Mattner J. Mechanisms of innate lymphoid cell and natural killer T cell activation during mucosal inflammation. *Journal of Immunology Research* 2014;2014:546596. doi: 10.1155/2014/546596
130. Wang P, Zheng SG. Regulatory T cells and B cells: implication on autoimmune diseases. *International Journal of Clinical and Experimental Pathology* 2013;6(12):2668-74.
131. Vignali DA, Collison LW, Workman CJ. How regulatory T cells work. *Nature Reviews Immunology* 2008;8(7):523-32. doi: 10.1038/nri2343
132. Zhang H, Kong H, Zeng X, et al. Subsets of regulatory T cells and their roles in allergy. *Journal of Translational Medicine* 2014;12:125. doi: 10.1186/1479-5876-12-125
133. Bluestone JA, Abbas AK. Natural versus adaptive regulatory T cells. *Nature Reviews Immunology* 2003;3(3):253-7. doi: 10.1038/nri1032
134. Gershon RK, Cohen P, Hencin R, et al. Suppressor T cells. *Journal of Immunology* 1972;108(3):586-90.
135. Weaver CT, Hatton RD. Interplay between the TH17 and TReg cell lineages: a (co-)evolutionary perspective. *Nature Reviews Immunology* 2009;9(12):883-9. doi: 10.1038/nri2660
136. Sakaguchi S, Sakaguchi N, Asano M, et al. Immunologic self-tolerance maintained by activated T cells expressing IL-2 receptor alpha-chains (CD25). Breakdown of a single mechanism of self-tolerance causes various autoimmune diseases. *Journal of Immunology* 1995;155(3):1151-64.
137. Campbell DJaK, M.A. Phenotypic and functional specialization of FOXP3+ regulatory T cells. *Nature Reviews Immunology* 2011;11(2):119–30.
138. Lu L, Barbi J, Pan F. The regulation of immune tolerance by FOXP3. *Nature Reviews Immunology* 2017 doi: 10.1038/nri.2017.75
139. Sakaguchi S, Wing K, Miyara M. Regulatory T cells - a brief history and perspective. *European Journal of Immunology* 2007;37 Suppl 1:S116-23. doi: 10.1002/eji.200737593
140. Ramsdell F, Ziegler SF. FOXP3 and scurfy: how it all began. *Nature Reviews Immunology* 2014;14(5):343-9. doi: 10.1038/nri3650
141. Godfrey VL, Wilkinson JE, Rinchik EM, et al. Fatal lymphoreticular disease in the scurfy (sf) mouse requires T cells that mature in a sf thymic environment: potential model for thymic education. *Proceedings of the National Academy of Sciences of the United States of America* 1991;88(13):5528-32.

142. Godfrey VL, Wilkinson JE, Russell LB. X-linked lymphoreticular disease in the scurfy (sf) mutant mouse. *American Journal of Pathology* 1991;138(6):1379-87.
143. Brunkow ME, Jeffery EW, Hjerrild KA, et al. Disruption of a new forkhead/winged-helix protein, scurfin, results in the fatal lymphoproliferative disorder of the scurfy mouse. *Nature Genetics* 2001;27(1):68-73. doi: 10.1038/83784
144. Beissert S, Schwarz A, Schwarz T. Regulatory T cells. *Journal of Investigative Dermatology* 2006;126(1):15-24. doi: 10.1038/sj.jid.5700004
145. Bennett CL, Christie J, Ramsdell F, et al. The immune dysregulation, polyendocrinopathy, enteropathy, X-linked syndrome (IPEX) is caused by mutations of FOXP3. *Nature Genetics* 2001;27(1):20-1. doi: 10.1038/83713
146. Polansky JK, Kretschmer K, Freyer J, et al. DNA methylation controls Foxp3 gene expression. *European Journal of Immunology* 2008;38(6):1654-63. doi: 10.1002/eji.200838105
147. Hori S, Nomura T, Sakaguchi S. Control of regulatory T cell development by the transcription factor Foxp3. *Science* 2003;299(5609):1057-61. doi: 10.1126/science.1079490
148. Fontenot JD, Gavin MA, Rudensky AY. Foxp3 programs the development and function of CD4+CD25+ regulatory T cells. *Nature Immunology* 2003;4(4):330-6. doi: 10.1038/ni904
149. Cook KW, Letley DP, Ingram RJ, et al. CCL20/CCR6-mediated migration of regulatory T cells to the *Helicobacter pylori*-infected human gastric mucosa. *Gut* 2014;63(10):1550-9. doi: 10.1136/gutjnl-2013-306253
150. Jonuleit H, Schmitt E. The regulatory T cell family: distinct subsets and their interrelations. *Journal of Immunology* 2003;171(12):6323-7.
151. Borsellino G, Kleinewietfeld M, Di Mitri D, et al. Expression of ectonucleotidase CD39 by Foxp3+ Treg cells: hydrolysis of extracellular ATP and immune suppression. *Blood* 2007;110(4):1225-32. doi: 10.1182/blood-2006-12-064527
152. Antonioli L, Pacher P, Vizi ES, et al. CD39 and CD73 in immunity and inflammation. *Trends in Molecular Medicine* 2013;19(6):355-67. doi: 10.1016/j.molmed.2013.03.005
153. Gagliani N, Magnani CF, Huber S, et al. Coexpression of CD49b and LAG-3 identifies human and mouse T regulatory type 1 cells. *Nature Medicine* 2013;19(6):739-46. doi: 10.1038/nm.3179
154. Kurtulus S, Sakuishi K, Ngiow SF, et al. TIGIT predominantly regulates the immune response via regulatory T cells. *Journal of Clinical Investigation* 2015;125(11):4053-62. doi: 10.1172/JCI81187
155. Nishikawa H, Sakaguchi S. Regulatory T cells in tumor immunity. *International Journal of Cancer* 2010;127(4):759-67. doi: 10.1002/ijc.25429
156. Tai X, Van Laethem F, Pobezinsky L, et al. Basis of CTLA-4 function in regulatory and conventional CD4(+) T cells. *Blood* 2012;119(22):5155-63. doi: 10.1182/blood-2011-11-388918
157. Bin Dhuban K, d'Hennezel E, Nashi E, et al. Coexpression of TIGIT and FCRL3 identifies Helios+ human memory regulatory T cells. *Journal of Immunology* 2015;194(8):3687-96. doi: 10.4049/jimmunol.1401803

158. Yamaguchi T, Hirota K, Nagahama K, et al. Control of immune responses by antigen-specific regulatory T cells expressing the folate receptor. *Immunity* 2007;27(1):145-59. doi: 10.1016/j.immuni.2007.04.017
159. Liu Y, Carlsson R, Comabella M, et al. FoxA1 directs the lineage and immunosuppressive properties of a novel regulatory T cell population in EAE and MS. *Nature Medicine* 2014;20(3):272-82. doi: 10.1038/nm.3485
160. van Olffen RW, Koning N, van Gisbergen KP, et al. GITR triggering induces expansion of both effector and regulatory CD4+ T cells in vivo. *Journal of Immunology* 2009;182(12):7490-500. doi: 10.4049/jimmunol.0802751
161. Ephrem A, Epstein AL, Stephens GL, et al. Modulation of Treg cells/T effector function by GITR signaling is context-dependent. *European Journal of Immunology* 2013;43(9):2421-9. doi: 10.1002/eji.201343451
162. Sugimoto N, Oida T, Hirota K, et al. Foxp3-dependent and -independent molecules specific for CD25+CD4+ natural regulatory T cells revealed by DNA microarray analysis. *International Immunology* 2006;18(8):1197-209. doi: 10.1093/intimm/dxl060
163. Yan Y, Zhang GX, Gran B, et al. IDO upregulates regulatory T cells via tryptophan catabolite and suppresses encephalitogenic T cell responses in experimental autoimmune encephalomyelitis. *Journal of Immunology* 2010;185(10):5953-61. doi: 10.4049/jimmunol.1001628
164. Baban B, Chandler PR, Sharma MD, et al. IDO activates regulatory T cells and blocks their conversion into Th17-like T cells. *Journal of Immunology* 2009;183(4):2475-83. doi: 10.4049/jimmunol.0900986
165. Sarris M, Andersen KG, Randow F, et al. Neuropilin-1 expression on regulatory T cells enhances their interactions with dendritic cells during antigen recognition. *Immunity* 2008;28(3):402-13. doi: 10.1016/j.immuni.2008.01.012
166. Moore KW, de Waal Malefyt R, Coffman RL, et al. Interleukin-10 and the interleukin-10 receptor. *Annual Review of Immunology* 2001;19:683-765. doi: 10.1146/annurev.immunol.19.1.683
167. Ouyang W, Rutz S, Crellin NK, et al. Regulation and functions of the IL-10 family of cytokines in inflammation and disease. *Annual Review of Immunology* 2011;29:71-109. doi: 10.1146/annurev-immunol-031210-101312
168. Saraiva M, O'Garra A. The regulation of IL-10 production by immune cells. *Nature Reviews Immunology* 2010;10(3):170-81. doi: 10.1038/nri2711
169. Kessel A, Haj T, Peri R, et al. Human CD19(+)CD25(high) B regulatory cells suppress proliferation of CD4(+) T cells and enhance Foxp3 and CTLA-4 expression in T-regulatory cells. *Autoimmunity Reviews* 2012;11(9):670-7. doi: 10.1016/j.autrev.2011.11.018
170. Cao X, Cai SF, Fehniger TA, et al. Granzyme B and perforin are important for regulatory T cell-mediated suppression of tumor clearance. *Immunity* 2007;27(4):635-46. doi: 10.1016/j.immuni.2007.08.014
171. Rosser EC, Blair PA, Mauri C. Cellular targets of regulatory B cell-mediated suppression. *Molecular Immunology* 2014;62(2):296-304. doi: 10.1016/j.molimm.2014.01.014

172. Berthelot JM, Jamin C, Amrouche K, et al. Regulatory B cells play a key role in immune system balance. *Joint Bone Spine* 2013;80(1):18-22. doi: 10.1016/j.jbspin.2012.04.010
173. Wang P, Wu P, Siegel MI, et al. Interleukin (IL)-10 inhibits nuclear factor kappa B (NF kappa B) activation in human monocytes. IL-10 and IL-4 suppress cytokine synthesis by different mechanisms. *Journal of Biological Chemistry* 1995;270(16):9558-63.
174. Li M, Flavell, RA. TGF-beta: a master of all T cell trades. *Cell* 2008;134(3):392-404.
175. Belkaid Y. Regulatory T cells and infection: a dangerous necessity. *Nature Reviews Immunology* 2007;7(11):875-88. doi: 10.1038/nri2189
176. Shouval DS, Ouahed J, Biswas A, et al. Interleukin 10 receptor signaling: master regulator of intestinal mucosal homeostasis in mice and humans. *Advances in Immunology* 2014;122:177-210. doi: 10.1016/B978-0-12-800267-4.00005-5
177. Verma R, Balakrishnan L, Sharma K, et al. A network map of Interleukin-10 signaling pathway. *Journal of Cell Communication and Signaling* 2016;10(1):61-7. doi: 10.1007/s12079-015-0302-x
178. Murray PJ. The primary mechanism of the IL-10-regulated antiinflammatory response is to selectively inhibit transcription. *Proceedings of the National Academy of Sciences of the United States of America* 2005;102(24):8686-91. doi: 10.1073/pnas.0500419102
179. Dhingra S, Sharma AK, Arora RC, et al. IL-10 attenuates TNF-alpha-induced NF kappaB pathway activation and cardiomyocyte apoptosis. *Cardiovascular Research* 2009;82(1):59-66. doi: 10.1093/cvr/cvp040
180. Thibodeau J, Bourgeois-Daigneault MC, Huppe G, et al. Interleukin-10-induced MARCH1 mediates intracellular sequestration of MHC class II in monocytes. *European Journal of Immunology* 2008;38(5):1225-30. doi: 10.1002/eji.200737902
181. Mittal SK, Roche PA. Suppression of antigen presentation by IL-10. *Current Opinion in Immunology* 2015;34:22-7. doi: 10.1016/j.coi.2014.12.009
182. Heine G, Drozdenko G, Grun JR, et al. Autocrine IL-10 promotes human B-cell differentiation into IgM- or IgG-secreting plasmablasts. *European Journal of Immunology* 2014;44(6):1615-21. doi: 10.1002/eji.201343822
183. Lundgren A, Stromberg E, Sjoling A, et al. Mucosal FOXP3-expressing CD4+ CD25high regulatory T cells in *Helicobacter pylori*-infected patients. *Infection and immunity* 2005;73(1):523-31. doi: 10.1128/IAI.73.1.523-531.2005
184. Enarsson K, Lundgren A, Kindlund B, et al. Function and recruitment of mucosal regulatory T cells in human chronic *Helicobacter pylori* infection and gastric adenocarcinoma. *Clinical Immunology* 2006;121(3):358-68. doi: 10.1016/j.clim.2006.07.002
185. Kandulski A, Malfertheiner P, Wex T. Role of regulatory T-cells in *H. pylori*-induced gastritis and gastric cancer. *Anticancer Research* 2010;30(4):1093-103.
186. Kandulski A, Wex T, Kuester D, et al. Naturally occurring regulatory T cells (CD4+, CD25high, FOXP3+) in the antrum and cardia are associated with higher *H. pylori* colonization and increased gene expression of TGF-beta1. *Helicobacter* 2008;13(4):295-303. doi: 10.1111/j.1523-5378.2008.00612.x

187. Iwaya Y, Kobayashi M, Momose M, et al. High levels of FOXP3(+) regulatory T cells in gastric MALT lymphoma predict responsiveness to *Helicobacter pylori* eradication. *Helicobacter* 2013;18(5):356-62. doi: 10.1111/hel.12051
188. Hussain K, Letley DP, Greenaway AB, et al. *Helicobacter pylori*-Mediated Protection from Allergy Is Associated with IL-10-Secreting Peripheral Blood Regulatory T Cells. *Front Immunol* 2016;7:71. doi: 10.3389/fimmu.2016.00071
189. Greenaway AB. *Helicobacter pylori* mediated immune regulation [PhD]. University of Nottingham, 2014.
190. Serrano C, Wright SW, Bimczok D, et al. Downregulated Th17 responses are associated with reduced gastritis in *Helicobacter pylori*-infected children. *Mucosal Immunology* 2013;6(5):950-59. doi: 10.1038/mi.2012.133
191. Kao JY, Zhang M, Miller MJ, et al. *Helicobacter pylori* immune escape is mediated by dendritic cell-induced Treg skewing and Th17 suppression in mice. *Gastroenterology* 2010;138(3):1046-54. doi: 10.1053/j.gastro.2009.11.043
192. Oertli M, Noben M, Engler DB, et al. *Helicobacter pylori* gamma-glutamyl transpeptidase and vacuolating cytotoxin promote gastric persistence and immune tolerance. *Proceedings of the National Academy of Sciences of the United States of America* 2013;110(8):3047-52. doi: 10.1073/pnas.1211248110
193. Wang WW, Yuan XL, Chen H, et al. CD19+CD24hiCD38hiBregs involved in downregulate helper T cells and upregulate regulatory T cells in gastric cancer. *Oncotarget* 2015;6(32):33486-99. doi: 10.18632/oncotarget.5588
194. Arnold IC, Lee JY, Amieva MR, et al. Tolerance rather than immunity protects from *Helicobacter pylori*-induced gastric preneoplasia. *Gastroenterology* 2011;140(1):199-209. doi: 10.1053/j.gastro.2010.06.047
195. NICE. Dyspepsia and gastro-oesophageal reflux disease: Investigation and management of dyspepsia, symptoms suggestive of gastro-oesophageal reflux disease, or both. In: Excellence NIfHaC, ed., 2014:1.4 Interventions for uninvestigated dyspepsia.
196. Walduck A, Andersen LP, Raghavan S. Inflammation, Immunity, and Vaccines for *Helicobacter pylori* Infection. *Helicobacter* 2015;20 Suppl 1:17-25. doi: 10.1111/hel.12252
197. Bogstedt AK, Nava S, Wadstrom T, et al. *Helicobacter pylori* infections in IgA deficiency: lack of role for the secretory immune system. *Clinical & Experimental Immunology* 1996;105(2):202-4.
198. Wotherspoon AC, Ortiz-Hidalgo C, Falzon MR, et al. *Helicobacter pylori*-associated gastritis and primary B-cell gastric lymphoma. *Lancet* 1991;338(8776):1175-6.
199. Stolte M, Bayerdorffer E, Morgner A, et al. *Helicobacter* and gastric MALT lymphoma. *Gut* 2002;50 Suppl 3:III19-24.
200. Gastric MALT lymphoma. In: Association L, ed., 2014.
201. Scott DW, Gascoyne RD. The tumour microenvironment in B cell lymphomas. *Nature Reviews Cancer* 2014;14(8):517-34. doi: 10.1038/nrc3774
202. Zucca E, Roggero E, Maggi-Solca N, et al. Prevalence of *Helicobacter pylori* and hepatitis C virus infections among non-Hodgkin's lymphoma patients in Southern Switzerland. *Haematologica* 2000;85(2):147-53.

203. D'Elios MM, Amedei A, Manghetti M, et al. Impaired T-cell regulation of B-cell growth in *Helicobacter pylori*--related gastric low-grade MALT lymphoma. *Gastroenterology* 1999;117(5):1105-12.
204. Zeng M, Mao XH, Li JX, et al. Efficacy, safety, and immunogenicity of an oral recombinant *Helicobacter pylori* vaccine in children in China: a randomised, double-blind, placebo-controlled, phase 3 trial. *Lancet* 2015;386(10002):1457-64. doi: 10.1016/S0140-6736(15)60310-5
205. Sutton P. At last, vaccine-induced protection against *Helicobacter pylori*. *Lancet* 2015 doi: 10.1016/S0140-6736(15)60579-7
206. Katz SI, Parker D, Turk JL. B-cell suppression of delayed hypersensitivity reactions. *Nature* 1974;251(5475):550-1.
207. Wolf SD, Dittel BN, Hardardottir F, et al. Experimental autoimmune encephalomyelitis induction in genetically B cell-deficient mice. *Journal of Experimental Medicine* 1996;184(6):2271-8.
208. Mizoguchi A, Mizoguchi E, Takedatsu H, et al. Chronic intestinal inflammatory condition generates IL-10-producing regulatory B cell subset characterized by CD1d upregulation. *Immunity* 2002;16(2):219-30.
209. Mizoguchi E, Mizoguchi A, Preffer FI, et al. Regulatory role of mature B cells in a murine model of inflammatory bowel disease. *International Immunology* 2000;12(5):597-605.
210. Tedder TF. B10 cells: a functionally defined regulatory B cell subset. *Journal of Immunology* 2015;194(4):1395-401. doi: 10.4049/jimmunol.1401329
211. Rosser EC, Mauri C. Regulatory B Cells: Origin, Phenotype, and Function. *Immunity* 2015;42(4):607-12. doi: 10.1016/j.immuni.2015.04.005
212. Rosser EC, Oleinika K, Tonon S, et al. Regulatory B cells are induced by gut microbiota-driven interleukin-1beta and interleukin-6 production. *Nature Medicine* 2014;20(11):1334-9. doi: 10.1038/nm.3680
213. Wang RX, Yu CR, Dambuza IM, et al. Interleukin-35 induces regulatory B cells that suppress autoimmune disease. *Nature Medicine* 2014;20(6):633-41. doi: 10.1038/nm.3554
214. Li X, Mai J, Virtue A, et al. IL-35 is a novel responsive anti-inflammatory cytokine--a new system of categorizing anti-inflammatory cytokines. *PLoS One* 2012;7(3):e33628. doi: 10.1371/journal.pone.0033628
215. Shen P, Roch T, Lampropoulou V, et al. IL-35-producing B cells are critical regulators of immunity during autoimmune and infectious diseases. *Nature* 2014;507(7492):366-70. doi: 10.1038/nature12979
216. Mauri C, Nistala K. Interleukin-35 takes the 'B' line. *Nature Medicine* 2014;20(6):580-1. doi: 10.1038/nm.3594
217. Yoshizaki A, Miyagaki T, DiLillo DJ, et al. Regulatory B cells control T-cell autoimmunity through IL-21-dependent cognate interactions. *Nature* 2012;491(7423):264-8. doi: 10.1038/nature11501
218. Yanaba K, Bouaziz JD, Haas KM, et al. A regulatory B cell subset with a unique CD1dhiCD5+ phenotype controls T cell-dependent inflammatory responses. *Immunity* 2008;28(5):639-50. doi: 10.1016/j.immuni.2008.03.017
219. Mauri C, Bosma A. Immune regulatory function of B cells. *Annual Review of Immunology* 2012;30:221-41. doi: 10.1146/annurev-immunol-020711-074934

220. Yanaba K, Bouaziz JD, Matsushita T, et al. The development and function of regulatory B cells expressing IL-10 (B10 cells) requires antigen receptor diversity and TLR signals. *Journal of Immunology* 2009;182(12):7459-72. doi: 10.4049/jimmunol.0900270
221. Matsushita T, Horikawa M, Iwata Y, et al. Regulatory B cells (B10 cells) and regulatory T cells have independent roles in controlling experimental autoimmune encephalomyelitis initiation and late-phase immunopathogenesis. *Journal of Immunology* 2010;185(4):2240-52. doi: 10.4049/jimmunol.1001307
222. Carter NA, Vasconcellos R, Rosser EC, et al. Mice lacking endogenous IL-10-producing regulatory B cells develop exacerbated disease and present with an increased frequency of Th1/Th17 but a decrease in regulatory T cells. *Journal of Immunology* 2011;186(10):5569-79. doi: 10.4049/jimmunol.1100284
223. Blair PA, Norena LY, Flores-Borja F, et al. CD19(+)CD24(hi)CD38(hi) B cells exhibit regulatory capacity in healthy individuals but are functionally impaired in systemic Lupus Erythematosus patients. *Immunity* 2010;32(1):129-40. doi: 10.1016/j.immuni.2009.11.009
224. Flores-Borja F, Bosma A, Ng D, et al. CD19+CD24hiCD38hi B cells maintain regulatory T cells while limiting TH1 and TH17 differentiation. *Science Translational Medicine* 2013;5(173):173ra23. doi: 10.1126/scitranslmed.3005407
225. Li G, Wulan H, Song Z, et al. Regulatory B Cell Function Is Suppressed by Smoking and Obesity in *H. pylori*-Infected Subjects and Is Correlated with Elevated Risk of Gastric Cancer. *PLoS One* 2015;10(7):e0134591. doi: 10.1371/journal.pone.0134591
226. Jamin C, Morva A, Lemoine S, et al. Regulatory B lymphocytes in humans: a potential role in autoimmunity. *Arthritis & Rheumatology* 2008;58(7):1900-6. doi: 10.1002/art.23487
227. Xiao S, Brooks CR, Sobel RA, et al. Tim-1 is essential for induction and maintenance of IL-10 in regulatory B cells and their regulation of tissue inflammation. *Journal of Immunology* 2015;194(4):1602-8. doi: 10.4049/jimmunol.1402632
228. Bosma A, Abdel-Gadir A, Isenberg DA, et al. Lipid-antigen presentation by CD1d(+) B cells is essential for the maintenance of invariant natural killer T cells. *Immunity* 2012;36(3):477-90. doi: 10.1016/j.immuni.2012.02.008
229. Gary-Gouy H, Harriague J, Bismuth G, et al. Human CD5 promotes B-cell survival through stimulation of autocrine IL-10 production. *Blood* 2002;100(13):4537-43. doi: 10.1182/blood-2002-05-1525
230. Diamant E, Melamed D. Class switch recombination in B lymphopoiesis: a potential pathway for B cell autoimmunity. *Autoimmunity Reviews* 2004;3(6):464-9. doi: 10.1016/j.autrev.2004.03.008
231. Kehry MR, Yamashita LC. Low-affinity IgE receptor (CD23) function on mouse B cells: role in IgE-dependent antigen focusing. *Proceedings of the National Academy of Sciences of the United States of America* 1989;86(19):7556-60.
232. Fang X, Zheng P, Tang J, et al. CD24: from A to Z. *Cellular & Molecular Immunology* 2010;7(2):100-3. doi: 10.1038/cmi.2009.119

233. Boyman O, Sprent J. The role of interleukin-2 during homeostasis and activation of the immune system. *Nature Reviews Immunology* 2012;12(3):180-90. doi: 10.1038/nri3156
234. Graham VA, Marzo AL, Tough DF. A role for CD44 in T cell development and function during direct competition between CD44+ and CD44- cells. *European Journal of Immunology* 2007;37(4):925-34. doi: 10.1002/eji.200635882
235. van de Veen W, Stanic B, Yaman G, et al. IgG4 production is confined to human IL-10-producing regulatory B cells that suppress antigen-specific immune responses. *Journal of Allergy and Clinical Immunology* 2013;131(4):1204-12. doi: 10.1016/j.jaci.2013.01.014
236. Garraud O, Borhis G, Badr G, et al. Revisiting the B-cell compartment in mouse and humans: more than one B-cell subset exists in the marginal zone and beyond. *BMC Immunology* 2012;13:63. doi: 10.1186/1471-2172-13-63
237. Cherukuri A, Cheng PC, Pierce SK. The role of the CD19/CD21 complex in B cell processing and presentation of complement-tagged antigens. *Journal of Immunology* 2001;167(1):163-72.
238. Borst J, Hendriks J, Xiao Y. CD27 and CD70 in T cell and B cell activation. *Current Opinion in Immunology* 2005;17(3):275-81. doi: 10.1016/j.coi.2005.04.004
239. Cobaleda C, Schebesta A, Delogu A, et al. Pax5: the guardian of B cell identity and function. *Nature Immunology* 2007;8(5):463-70. doi: 10.1038/ni1454
240. Matsumoto M, Fujii Y, Baba A, et al. The calcium sensors STIM1 and STIM2 control B cell regulatory function through interleukin-10 production. *Immunity* 2011;34(5):703-14. doi: 10.1016/j.immuni.2011.03.016
241. Carter NA, Rosser EC, Mauri C. Interleukin-10 produced by B cells is crucial for the suppression of Th17/Th1 responses, induction of T regulatory type 1 cells and reduction of collagen-induced arthritis. *Arthritis research & therapy* 2012;14(1):R32. doi: 10.1186/ar3736
242. Kalampokis I, Yoshizaki A, Tedder TF. IL-10-producing regulatory B cells (B10 cells) in autoimmune disease. *Arthritis research & therapy* 2013;15 Suppl 1:S1. doi: 10.1186/ar3907
243. Wei L, Wang J, Liu Y. Prior to Foxp3(+) regulatory T-cell induction, interleukin-10-producing B cells expand after *Helicobacter pylori* infection. *Pathogens and Disease* 2014;72(1):45-54. doi: 10.1111/2049-632X.12182
244. Nouel A, Pochard P, Simon Q, et al. B-Cells induce regulatory T cells through TGF-beta/IDO production in A CTLA-4 dependent manner. *Journal of Autoimmunity* 2015;59:53-60. doi: 10.1016/j.jaut.2015.02.004
245. Pennati A, Ng S, Wu Y, et al. Regulatory B Cells Induce Formation of IL-10-Expressing T Cells in Mice with Autoimmune Neuroinflammation. *Journal of Neuroscience* 2016;36(50):12598-610. doi: 10.1523/JNEUROSCI.1994-16.2016
246. Matsumoto M, Baba A, Yokota T, et al. Interleukin-10-producing plasmablasts exert regulatory function in autoimmune inflammation. *Immunity* 2014;41(6):1040-51. doi: 10.1016/j.immuni.2014.10.016
247. Shen P, Roch T, Lampropoulou V, et al. IL-35-producing B cells are critical regulators of immunity during autoimmune and infectious diseases. *Nature* 2014;507(7492):366-70. doi: 10.1038/nature12979

248. Maseda D, Smith SH, DiLillo DJ, et al. Regulatory B10 cells differentiate into antibody-secreting cells after transient IL-10 production in vivo. *Journal of Immunology* 2012;188(3):1036-48. doi: 10.4049/jimmunol.1102500
249. Qian L, Bian GR, Zhou Y, et al. Clinical significance of regulatory B cells in the peripheral blood of patients with oesophageal cancer. *Central-European Journal of Immunology* 2015;40(2):263-5. doi: 10.5114/ceji.2015.52840
250. Barsotti NS, Almeida RR, Costa PR, et al. IL-10-Producing Regulatory B Cells Are Decreased in Patients with Common Variable Immunodeficiency. *PLoS One* 2016;11(3):e0151761. doi: 10.1371/journal.pone.0151761
251. Li J, Shen C, Liu Y, et al. Impaired Function of CD5+CD19+CD1dhi B10 Cells on IgE Secretion in an Atopic Dermatitis-Like Mouse Model. *PLoS One* 2015;10(8):e0132173. doi: 10.1371/journal.pone.0132173
252. Yokoyama T, Yoshizaki A, Simon KL, et al. Age-Dependent Defects of Regulatory B Cells in Wiskott-Aldrich Syndrome Gene Knockout Mice. *PLoS One* 2015;10(10):e0139729. doi: 10.1371/journal.pone.0139729
253. Cuss AK, Avery DT, Cannons JL, et al. Expansion of functionally immature transitional B cells is associated with human-immunodeficient states characterized by impaired humoral immunity. *Journal of Immunology* 2006;176(3):1506-16.
254. Wei L, Wang J, Liu Y. Prior to Foxp3(+) regulatory T-cell induction, interleukin-10-producing B cells expand after *Helicobacter pylori* infection. *Pathog Dis* 2014;72(1):45-54. doi: 10.1111/2049-632X.12182
255. Liu H, Ruskon-Fourmestraux A, Lavergne-Slove A, et al. Resistance of t(11;18) positive gastric mucosa-associated lymphoid tissue lymphoma to *Helicobacter pylori* eradication therapy. *Lancet* 2001;357(9249):39-40. doi: 10.1016/S0140-6736(00)03571-6
256. Wong BC, Lam SK, Wong WM, et al. *Helicobacter pylori* eradication to prevent gastric cancer in a high-risk region of China: a randomized controlled trial. *Journal of the American Medical Association* 2004;291(2):187-94. doi: 10.1001/jama.291.2.187
257. Ricci V, Giannouli M, Romano M, et al. *Helicobacter pylori* gamma-glutamyl transpeptidase and its pathogenic role. *World Journal of Gastroenterology* 2014;20(3):630-8. doi: 10.3748/wjg.v20.i3.630
258. Vieira PL, Christensen JR, Minaee S, et al. IL-10-secreting regulatory T cells do not express Foxp3 but have comparable regulatory function to naturally occurring CD4+CD25+ regulatory T cells. *Journal of Immunology* 2004;172(10):5986-93.
259. Yap TW, Gan HM, Lee YP, et al. *Helicobacter pylori* Eradication Causes Perturbation of the Human Gut Microbiome in Young Adults. *PLoS One* 2016;11(3):e0151893. doi: 10.1371/journal.pone.0151893
260. Fessler J, Ficjan A, Duftner C, et al. The impact of aging on regulatory T-cells. *Frontiers in Immunology* 2013;4:231. doi: 10.3389/fimmu.2013.00231
261. Argent RH, Hale JL, El-Omar EM, et al. Differences in *Helicobacter pylori* CagA tyrosine phosphorylation motif patterns between western and East Asian strains, and influences on interleukin-8 secretion. *Journal of Medical Microbiology* 2008;57(Pt 9):1062-7. doi: 10.1099/jmm.0.2008/001818-0

262. Huang JQ, Hunt RH. Treatment after failure: the problem of "non-responders". *Gut* 1999;45 Suppl 1:I40-4.
263. Malfertheiner P, Megraud F, O'Morain C, et al. Current concepts in the management of *Helicobacter pylori* infection: the Maastricht III Consensus Report. *Gut* 2007;56(6):772-81. doi: 10.1136/gut.2006.101634
264. Fuhrman CA, Yeh WI, Seay HR, et al. Divergent Phenotypes of Human Regulatory T Cells Expressing the Receptors TIGIT and CD226. *Journal of Immunology* 2015;195(1):145-55. doi: 10.4049/jimmunol.1402381
265. Azuma T. *Helicobacter pylori* CagA protein variation associated with gastric cancer in Asia. *Journal of Gastroenterology* 2004;39(2):97-103. doi: 10.1007/s00535-003-1279-4
266. Graham DY, Opekun AR, Osato MS, et al. Challenge model for *Helicobacter pylori* infection in human volunteers. *Gut* 2004;53(9):1235-43. doi: 10.1136/gut.2003.037499
267. Aebischer T, Bumann D, Epple HJ, et al. Correlation of T cell response and bacterial clearance in human volunteers challenged with *Helicobacter pylori* revealed by randomised controlled vaccination with Ty21a-based Salmonella vaccines. *Gut* 2008;57(8):1065-72. doi: 10.1136/gut.2007.145839
268. Fulurija A, Lundin, S., Ee, H., Kumarasinghe M.P., Marshall, B.J. Unravelling the Immune Response to *Helicobacter pylori*: Results from a Human Challenge Study. *Gastroenterology* 2017;152(5):Supplement 1, S667–S68.
269. Chen Y, Blaser MJ. Inverse associations of *Helicobacter pylori* with asthma and allergy. *Archives of internal medicine* 2007;167(8):821-7. doi: 10.1001/archinte.167.8.821
270. Scaletsky IC, Aranda KR, Garcia GT, et al. Application of real-time PCR stool assay for *Helicobacter pylori* detection and clarithromycin susceptibility testing in Brazilian children. *Helicobacter* 2011;16(4):311-5. doi: 10.1111/j.1523-5378.2011.00845.x
271. Parmar S, Shpall EJ. Treg adoptive therapy: is more better? *Blood* 2016;127(8):962-3. doi: 10.1182/blood-2015-12-682492
272. Heimesaat MM, Fischer A, Plickert R, et al. *Helicobacter pylori* induced gastric immunopathology is associated with distinct microbiota changes in the large intestines of long-term infected Mongolian gerbils. *PLoS One* 2014;9(6):e100362. doi: 10.1371/journal.pone.0100362
273. Chatila T, Silverman L, Miller R, et al. Mechanisms of T cell activation by the calcium ionophore ionomycin. *Journal of Immunology* 1989;143(4):1283-9.
274. Pelchen-Matthews A, Parsons IJ, Marsh M. Phorbol ester-induced downregulation of CD4 is a multistep process involving dissociation from p56lck, increased association with clathrin-coated pits, and altered endosomal sorting. *Journal of Experimental Medicine* 1993;178(4):1209-22.
275. Cook K. The regulatory T-cell response to *Helicobacter pylori* infection. University of Nottingham, 2014.
276. Laboratory TJ. Mouse strain datasheet - 000664 2016 [Available from: https://www.jax.org/strain/000664.
277. Sheh A, Lee CW, Masumura K, et al. Mutagenic potency of *Helicobacter pylori* in the gastric mucosa of mice is determined by sex and duration of infection.

*Proceedings of the National Academy of Sciences of the United States of America* 2010;107(34):15217-22. doi: 10.1073/pnas.1009017107
278. Vandamme TF. Use of rodents as models of human diseases. *Journal of Pharmacy & Bioallied Sciences* 2014;6(1):2-9.
279. Buer J, Balling R. Mice, microbes and models of infection. *Nature Reviews Genetics* 2003;4(3):195-205. doi: 10.1038/nrg1019
280. Peek RM. *Helicobacter pylori* infection and disease: from humans to animal models. *Disease Models & Mechanisms* 2008;1(1):50-5. doi: 10.1242/dmm.000364
281. Ruiz VE, Sachdev M, Zhang S, et al. Isolating, immunophenotyping and ex vivo stimulation of CD4+ and CD8+ gastric lymphocytes during murine *Helicobacter pylori* infection. *Journal of Immunological Methods* 2012;384(1-2):157-63. doi: 10.1016/j.jim.2012.07.002
282. Zavros Y, Van Antwerp M, Merchant JL. Use of flow cytometry to quantify mouse gastric epithelial cell populations. *Digestive diseases and sciences* 2000;45(6):1192-9.
283. Cesta MF. Normal structure, function, and histology of the spleen. *Toxicologic Pathology* 2006;34(5):455-65. doi: 10.1080/01926230600867743
284. Iwata Y, Matsushita T, Horikawa M, et al. Characterization of a rare IL-10-competent B-cell subset in humans that parallels mouse regulatory B10 cells. *Blood* 2011;117(2):530-41. doi: 10.1182/blood-2010-07-294249
285. Aebischer T, Fischer A, Walduck A, et al. Vaccination prevents *Helicobacter pylori*-induced alterations of the gastric flora in mice. *FEMS Immunology and Medical Microbiology* 2006;46(2):221-9. doi: 10.1111/j.1574-695X.2005.00024.x
286. Thompson LJ, Danon SJ, Wilson JE, et al. Chronic *Helicobacter pylori* infection with Sydney strain 1 and a newly identified mouse-adapted strain (Sydney strain 2000) in C57BL/6 and BALB/c mice. *Infection and immunity* 2004;72(8):4668-79. doi: 10.1128/IAI.72.8.4668-4679.2004
287. Barrozo RM, Cooke CL, Hansen LM, et al. Functional plasticity in the type IV secretion system of *Helicobacter pylori*. *PLoS Pathogens* 2013;9(2):e1003189. doi: 10.1371/journal.ppat.1003189
288. Sheu BS, Yang HB, Wu JJ, et al. Development of *Helicobacter pylori* infection model in BALB/c mice with domestic *cagA*-positive and -negative strains in Taiwan. *Digestive diseases and sciences* 1999;44(5):868-75.
289. Mestas J, Hughes CC. Of mice and not men: differences between mouse and human immunology. *Journal of Immunology* 2004;172(5):2731-8.
290. Gordon CJ, Grafton G, Wood PM, et al. Modelling the human immune response: can mice be trusted? Commentary. *Current Opinion in Pharmacology* 2001;1(4):431-5.
291. Perfetto SP, Chattopadhyay PK, Roederer M. Seventeen-colour flow cytometry: unravelling the immune system. *Nature Reviews Immunology* 2004;4(8):648-55. doi: 10.1038/nri1416
292. Hulspas R, O'Gorman MR, Wood BL, et al. Considerations for the control of background fluorescence in clinical flow cytometry. *Cytometry Part B: Clinical Cytometry* 2009;76(6):355-64. doi: 10.1002/cyto.b.20485

293. Rostaing L, Tkaczuk J, Durand M, et al. Kinetics of intracytoplasmic Th1 and Th2 cytokine production assessed by flow cytometry following in vitro activation of peripheral blood mononuclear cells. *Cytometry* 1999;35(4):318-28.
294. McLaughlin BE, Baumgarth N, Bigos M, et al. Nine-color flow cytometry for accurate measurement of T cell subsets and cytokine responses. Part I: Panel design by an empiric approach. *Cytometry A* 2008;73(5):400-10. doi: 10.1002/cyto.a.20555
295. van der Vlugt LEPM. Toll-like Receptor Ligation for the Induction of Regulatory B cells. In: Vitale GaM, F., ed. Regulatory B Cells. 1 ed. New York: Humana Press 2014:127-41.
296. El-Omar EM, Carrington M, Chow WH, et al. Interleukin-1 polymorphisms associated with increased risk of gastric cancer. *Nature* 2000;404(6776):398-402. doi: 10.1038/35006081
297. Kearley J, Silver JS, Sanden C, et al. Cigarette smoke silences innate lymphoid cell function and facilitates an exacerbated type I interleukin-33-dependent response to infection. *Immunity* 2015;42(3):566-79. doi: 10.1016/j.immuni.2015.02.011
298. Bergman H. The efficacy of IL-33 as a serum tumour marker and the immunomodulatory effects of smoking in the context of *Helicobacter pylori*-induced gastritis and disease [BMedSci]. University of Nottingham, 2016.
299. Herzenberg LA, Tung J, Moore WA, et al. Interpreting flow cytometry data: a guide for the perplexed. *Nature Immunology* 2006;7(7):681-5. doi: 10.1038/ni0706-681
300. Maecker HaT, J. Selecting reagents for multicolor flow cytometry. In: Biosciences BD, ed., 2012:1-7.
301. Miyagaki T, Fujimoto M, Sato S. Regulatory B cells in human inflammatory and autoimmune diseases: from mouse models to clinical research. *International Immunology* 2015 doi: 10.1093/intimm/dxv026
302. Guo Y, Chan KH, Lai WH, et al. Human mesenchymal stem cells upregulate CD1dCD5(+) regulatory B cells in experimental autoimmune encephalomyelitis. *Neuroimmunomodulation* 2013;20(5):294-303. doi: 10.1159/000351450
303. Ray A, Basu S, Gharaibeh RZ, et al. Gut Microbial Dysbiosis Due to *Helicobacter* Drives an Increase in Marginal Zone B Cells in the Absence of IL-10 Signaling in Macrophages. *Journal of Immunology* 2015;195(7):3071-85. doi: 10.4049/jimmunol.1500153
304. Mauri C, Blair PA. The incognito journey of a regulatory B cell. *Immunity* 2014;41(6):878-80. doi: 10.1016/j.immuni.2014.12.003
305. Sicinschi LA, Correa P, Bravo LE, et al. Non-invasive genotyping of *Helicobacter pylori cagA*, *vacA*, and *hopQ* from asymptomatic children. *Helicobacter* 2012;17(2):96-106. doi: 10.1111/j.1523-5378.2011.00919.x
306. Vecsei A, Innerhofer A, Binder C, et al. Stool polymerase chain reaction for *Helicobacter pylori* detection and clarithromycin susceptibility testing in children. *Clinical Gastroenterology and Hepatology* 2010;8(3):309-12. doi: 10.1016/j.cgh.2009.12.002

307. Windsor HM, Ho GY, Marshall BJ. Successful recovery of *H. pylori* from rapid urease tests (CLO tests). *American Journal of Gastroenterology* 1999;94(11):3181-3. doi: 10.1111/j.1572-0241.1999.01515.x
308. Tang JH, Liu NJ, Cheng HT, et al. Endoscopic diagnosis of *Helicobacter pylori* infection by rapid urease test in bleeding peptic ulcers: a prospective case-control study. *Journal of clinical gastroenterology* 2009;43(2):133-9.
309. Dattilo M, Figura N. *Helicobacter pylori* infection, chronic gastritis, and proton pump inhibitors. *Journal of clinical gastroenterology* 1998;27 Suppl 1:S163-9.
310. Vaira D, Holton J, Menegatti M, et al. Review article: invasive and non-invasive tests for *Helicobacter pylori* infection. *Alimentary Pharmacology & Therapeutics* 2000;14 Suppl 3:13-22.
311. Andersen LP, Wadstrom, T. . In: H. L. T. Mobley GLM, S. L. Hazell, ed. Basic Bacteriology and Culture. Washington, DC.: ASM Press 2001:27-38.
312. Leal YA, Cedillo-Rivera R, Simon JA, et al. Utility of stool sample-based tests for the diagnosis of *Helicobacter pylori* infection in children. *Journal of Pediatric Gastroenterology and Nutrition* 2011;52(6):718-28. doi: 10.1097/MPG.0b013e3182077d33
313. Marchildon PA, Sugiyama T, Fukuda Y, et al. Evaluation of the effects of strain-specific antigen variation on the accuracy of serologic diagnosis of *Helicobacter pylori* infection. *Journal of clinical microbiology* 2003;41(4):1480-5.
314. Leal YA, Flores LL, Garcia-Cortes LB, et al. Antibody-based detection tests for the diagnosis of *Helicobacter pylori* infection in children: a meta-analysis. *PLoS One* 2008;3(11):e3751. doi: 10.1371/journal.pone.0003751
315. Savarino V, Vigneri S, Celle G. The 13C urea breath test in the diagnosis of *Helicobacter pylori* infection. *Gut* 1999;45 Suppl 1:I18-22.
316. Gisbert JP, Pajares JM. Review article: 13C-urea breath test in the diagnosis of *Helicobacter pylori* infection -- a critical review. *Alimentary Pharmacology & Therapeutics* 2004;20(10):1001-17. doi: 10.1111/j.1365-2036.2004.02203.x
317. Korkmaz H, Kesli R, Karabagli P, et al. Comparison of the diagnostic accuracy of five different stool antigen tests for the diagnosis of *Helicobacter pylori* infection. *Helicobacter* 2013;18(5):384-91. doi: 10.1111/hel.12053
318. Vaira D, Vakil N, Menegatti M, et al. The stool antigen test for detection of *Helicobacter pylori* after eradication therapy. *Annals of internal medicine* 2002;136(4):280-7.
319. Megraud F. *H. pylori* antibiotic resistance: prevalence, importance, and advances in testing. *Gut* 2004;53(9):1374-84. doi: 10.1136/gut.2003.022111
320. Bereswill S, Krainick C, Stahler F, et al. Analysis of the *rdxA* gene in high-level metronidazole-resistant clinical isolates confirms a limited use of *rdxA* mutations as a marker for prediction of metronidazole resistance in *Helicobacter pylori*. *FEMS Immunology and Medical Microbiology* 2003;36(3):193-8.
321. Lottspeich C, Schwarzer A, Panthel K, et al. Evaluation of the novel *Helicobacter pylori* ClariRes real-time PCR assay for detection and clarithromycin susceptibility testing of *H. pylori* in stool specimens from symptomatic children. *Journal of clinical microbiology* 2007;45(6):1718-22. doi: 10.1128/JCM.00103-07

322. Beckman E, Saracino I, Fiorini G, et al. A Novel stool PCR Test for *Helicobacter pylori* may Predict Clarithromycin Resistance and Patient Eradication at a High Rate. *Journal of clinical microbiology* 2017 doi: 10.1128/JCM.00506-17
323. UniProtKB: UniProt Consortium; 2017 [Available from: http://www.uniprot.org/uniprot/.
324. Ching CK, Wong BC, Kwok E, et al. Prevalence of CagA-bearing *Helicobacter pylori* strains detected by the anti-CagA assay in patients with peptic ulcer disease and in controls. *American Journal of Gastroenterology* 1996;91(5):949-53.
325. Fusconi M, Vaira D, Menegatti M, et al. Anti-CagA reactivity in *Helicobacter pylori*-negative subjects: a comparison of three different methods. *Digestive diseases and sciences* 1999;44(8):1691-5.
326. Rahman SH, Azam MG, Rahman MA, et al. Non-invasive diagnosis of *H. pylori* infection: evaluation of serological tests with and without current infection marker CIM. *World Journal of Gastroenterology* 2008;14(8):1231-6.
327. Weiss J, Mecca J, da Silva E, et al. Comparison of PCR and other diagnostic techniques for detection of *Helicobacter pylori* infection in dyspeptic patients. *Journal of clinical microbiology* 1994;32(7):1663-8.
328. van Doorn LJ, Figueiredo C, Sanna R, et al. Distinct variants of *Helicobacter pylori cagA* are associated with *vacA* subtypes. *Journal of clinical microbiology* 1999;37(7):2306-11.
329. Yamaoka Y, Kodama T, Graham DY, et al. Comparison of four serological tests to determine the CagA or VacA status of *Helicobacter pylori* strains. *Journal of clinical microbiology* 1998;36(11):3433-4.
330. Schembri MA, Lin SK, Lambert JR. Comparison of commercial diagnostic tests for *Helicobacter pylori* antibodies. *Journal of clinical microbiology* 1993;31(10):2621-4.
331. Reynders MB, Miendje Deyi VY, Dahma H, et al. Performance of individual *Helicobacter pylori* antigens in the immunoblot-based detection of *H. pylori* infection. *FEMS Immunology and Medical Microbiology* 2012;64(3):352-63. doi: 10.1111/j.1574-695X.2011.00920.x
332. Lage AP, Godfroid E, Fauconnier A, et al. Diagnosis of *Helicobacter pylori* infection by PCR: comparison with other invasive techniques and detection of *cagA* gene in gastric biopsy specimens. *Journal of clinical microbiology* 1995;33(10):2752-6.
333. Clayton CL, Kleanthous H, Coates PJ, et al. Sensitive detection of *Helicobacter pylori* by using polymerase chain reaction. *Journal of clinical microbiology* 1992;30(1):192-200.
334. K. Robinson JCA. *Helicobacter pylori*. In: Pina M. Fratamico JLS, Kim A. Brogden, ed. Sequelae and Long-Term Consequences of Infectious Diseases. Washington (DC): ASM Press 2009.
335. Thomas JE, Gibson GR, Darboe MK, et al. Isolation of *Helicobacter pylori* from human faeces. *Lancet* 1992;340(8829):1194-5.
336. Stauffer SH, Birkenheuer AJ, Levy MG, et al. Evaluation of four DNA extraction methods for the detection of *Tritrichomonas foetus* in feline stool specimens by polymerase chain reaction. *Journal of Veterinary Diagnostic Investigation* 2008;20(5):639-41.

337. Monteiro L, Bonnemaison D, Vekris A, et al. Complex polysaccharides as PCR inhibitors in feces: *Helicobacter pylori* model. *Journal of clinical microbiology* 1997;35(4):995-8.
338. Monteiro L, Gras N, Vidal R, et al. Detection of *Helicobacter pylori* DNA in human feces by PCR: DNA stability and removal of inhibitors. *Journal of microbiological methods* 2001;45(2):89-94.
339. Moreira D. Efficient removal of PCR inhibitors using agarose-embedded DNA preparations. *Nucleic acids research* 1998;26(13):3309-10.
340. Sicinschi LA, Correa P, Bravo LE, et al. Detection and typing of *Helicobacter pylori cagA*/*vacA* genes by radioactive, one-step polymerase chain reaction in stool samples from children. *Journal of microbiological methods* 2003;52(2):197-207.
341. Schabereiter-Gurtner C, Hirschl AM, Dragosics B, et al. Novel real-time PCR assay for detection of *Helicobacter pylori* infection and simultaneous clarithromycin susceptibility testing of stool and biopsy specimens. *Journal of clinical microbiology* 2004;42(10):4512-8. doi: 10.1128/JCM.42.10.4512-4518.2004
342. Hirai I, Sasaki T, Kimoto A, et al. Assessment of East Asian-type *cagA*-positive *Helicobacter pylori* using stool specimens from asymptomatic healthy Japanese individuals. *Journal of Medical Microbiology* 2009;58(Pt 9):1149-53. doi: 10.1099/jmm.0.010934-0
343. Liang S, Redlinger T. A protocol for isolating putative *Helicobacter pylori* from fecal specimens and genotyping using *vacA* alleles. *Helicobacter* 2003;8(5):561-7.
344. Horemans T, Deschacht M, Clais S, et al. An alternative, sensitive method to detect *Helicobacter pylori* DNA in feces. *Helicobacter* 2011;16(2):113-8. doi: 10.1111/j.1523-5378.2011.00819.x
345. Puz S, Innerhofer A, Ramharter M, et al. A novel noninvasive genotyping method of *Helicobacter pylori* using stool specimens. *Gastroenterology* 2008;135(5):1543-51. doi: 10.1053/j.gastro.2008.08.006
346. Kabir S. Detection of *Helicobacter pylori* DNA in feces and saliva by polymerase chain reaction: a review. *Helicobacter* 2004;9(2):115-23. doi: 10.1111/j.1083-4389.2004.00207.x
347. Mishra S, Singh V, Rao GR, et al. Prevalence of *Helicobacter pylori* in asymptomatic subjects--a nested PCR based study. *Infection, Genetics and Evolution* 2008;8(6):815-9. doi: 10.1016/j.meegid.2008.08.001
348. Rimbara E, Sasatsu M, Graham DY. PCR detection of *Helicobacter pylori* in clinical samples. *Methods in molecular biology* 2013;943:279-87. doi: 10.1007/978-1-60327-353-4_19
349. Goncalves MH, Silva CI, Braga-Neto MB, et al. *Helicobacter pylori* virulence genes detected by string PCR in children from an urban community in northeastern Brazil. *Journal of clinical microbiology* 2013;51(3):988-9. doi: 10.1128/JCM.02583-12
350. Narayanan GL. Determinants of vacuolating cytotoxin production in the gastric pathogen *Helicobacter pylori*. [PhD]. University of Nottingham, 2005.
351. Patel S. Determinants of *Helicobacter pylori* density in the human stomach and implications in disease [PhD]. University of Nottingham, 2011.

352. Iyengar V, Albaugh GP, Lohani A, et al. Human stools as a source of viable colonic epithelial cells. *Federation of American Societies for Experimental Biology* 1991;5(13):2856-9.
353. Barber RD, Harmer DW, Coleman RA, et al. *GAPDH* as a housekeeping gene: analysis of *GAPDH mRNA* expression in a panel of 72 human tissues. *Physiological genomics* 2005;21(3):389-95. doi: 10.1152/physiolgenomics.00025.2005
354. White AK, VanInsberghe M, Petriv OI, et al. High-throughput microfluidic single-cell RT-qPCR. *Proceedings of the National Academy of Sciences of the United States of America* 2011;108(34):13999-4004. doi: 10.1073/pnas.1019446108
355. Aktepe OC, Ciftci IH, Safak B, et al. Five methods for detection of *Helicobacter pylori* in the Turkish population. *World Journal of Gastroenterology* 2011;17(47):5172-6. doi: 10.3748/wjg.v17.i47.5172
356. Gorzelak MA, Gill SK, Tasnim N, et al. Methods for Improving Human Gut Microbiome Data by Reducing Variability through Sample Processing and Storage of Stool. *PLoS One* 2015;10(8):e0134802. doi: 10.1371/journal.pone.0134802
357. Sen N, Yilmaz O, Simsek I, et al. Detection of *Helicobacter pylori* DNA by a simple stool PCR method in adult dyspeptic patients. *Helicobacter* 2005;10(4):353-9. doi: 10.1111/j.1523-5378.2005.00326.x
358. Falsafi T, Favaedi R, Mahjoub F, et al. Application of stool-PCR test for diagnosis of *Helicobacter pylori* infection in children. *World Journal of Gastroenterology* 2009;15(4):484-8.
359. Zwet AAV. Use of PCR with Feces for Detection of *Helicobacter pylori* infections in patients. *Journal of clinical microbiology* 1994;32:1346-48.
360. Flores R, Shi J, Gail MH, et al. Association of fecal microbial diversity and taxonomy with selected enzymatic functions. *PLoS One* 2012;7(6):e39745. doi: 10.1371/journal.pone.0039745
361. Talarico S, Safaeian M, Gonzalez P, et al. Quantitative Detection and Genotyping of *Helicobacter pylori* from Stool using Droplet Digital PCR Reveals Variation in Bacterial Loads that Correlates with *cagA* Virulence Gene Carriage. *Helicobacter* 2015 doi: 10.1111/hel.12289
362. Enders G. Gut (Darm Mitt Charme). London, U.K.: Scribe 2015.
363. Timothy L. Cover MJB. Purification and Characterization of the Vacuolating Toxin from *Helicobacter pylori*. *Journal of Biological Chemistry* 1991;267(15):10570-75.
364. Jimenez FA. Studies on the microdiversity, localisation and serological typing of *Helicobacter pylori* vacuolating cytotoxin [PhD]. University of Nottingham, 2005.
365. Sarvaria A, Basar R, Mehta RS, et al. IL-10+ regulatory B cells are enriched in cord blood and may protect against cGVHD after cord blood transplantation. *Blood* 2016;128(10):1346-61. doi: 10.1182/blood-2016-01-695122
366. Klausner RD, Donaldson JG, Lippincott-Schwartz J. Brefeldin A: insights into the control of membrane traffic and organelle structure. *Journal of Cell Biology* 1992;116(5):1071-80.
367. Macian F. NFAT proteins: key regulators of T-cell development and function. *Nature Reviews Immunology* 2005;5(6):472-84. doi: 10.1038/nri1632

368. Peek RM, Jr., Fiske C, Wilson KT. Role of innate immunity in *Helicobacter pylori*-induced gastric malignancy. *Physiological Reviews* 2010;90(3):831-58. doi: 10.1152/physrev.00039.2009
369. WHO. Global priority list of antibiotic-resistant bacteria to guide research, discovery, and development of new antibiotics: WHO, 2017.
370. Spigaglia P. Recent advances in the understanding of antibiotic resistance in *Clostridium difficile* infection. *Therapeutic Advances in Infectious Disease* 2016;3(1):23-42. doi: 10.1177/2049936115622891
371. Bolan GA, Sparling PF, Wasserheit JN. The emerging threat of untreatable gonococcal infection. *New England Journal of Medicine* 2012;366(6):485-7. doi: 10.1056/NEJMp1112456
372. Allen VG, Mitterni L, Seah C, et al. *Neisseria gonorrhoeae* treatment failure and susceptibility to cefixime in Toronto, Canada. *Journal of the American Medical Association* 2013;309(2):163-70. doi: 10.1001/jama.2012.176575
373. Limbago BM, Kallen AJ, Zhu W, et al. Report of the 13th vancomycin-resistant *Staphylococcus aureus* isolate from the United States. *Journal of clinical microbiology* 2014;52(3):998-1002. doi: 10.1128/JCM.02187-13
374. Gould SJ. The evolution of life on the earth. *Scientific American* 1994;271(4):84-91.

## Appendix

A – Information given to patients participating in the Treg eradication study

Participant Information Sheet
(Final version 2.0: 30th June 2014)

Title of Study: **Study to Investigate Regulatory T lymphocyte Response to *Helicobacter pylori* Treatment**

Name of Researcher(s): Professor JC Atherton, Dr Jonathan White

We would like to invite you to take part in our research study. Before you decide we would like you to understand why the research is being done and what it would involve if you took part. One of our team will go through the information sheet with you and answer any questions you have. Talk to others about the study if you wish. Ask us if there is anything that is not clear.

**What is the purpose of the study?**

*Helicobacter pylori* (*H. pylori*) is a bacteria that lives in the stomach of approximately half of the world's population. It lives there for life, unless treatment is used to get rid of these bacteria. For the majority of people this bacterium does not cause any problems but in a few it could lead to ulceration in the stomach or first part of the small bowel (duodenum). In some cases it may be a risk factor for cancer of the stomach in a similar (but less strong) way that smoking may be a risk factor for lung cancer. Some individuals are more prone to developing complications associated with these bacteria than others because of two reasons:

1) Certain types of *H. pylori* cause more disease than others.
2) The ability of a person's body to fight the infection – also known as their immune response differs between individuals.

Professor Atherton's team are investigating the immune response to *H. pylori*. Regulatory T lymphocytes (Treg) are special immune cells stimulated by *H. pylori* that are vital for controlling the immune system and preventing localised irritation caused by *H. pylori*. However, we think that in some people, by giving medications to get rid of *H. pylori* we are actually lowering the number of these protective cells too. This might explain why in recent years when *H. pylori* has become less common and certain immune related conditions have become more common. We do not know what actually happens to your immune cells that suppress inflammation after *H. pylori* treatment and that is why we are doing the research.

We are collecting your information and blood samples so we can measure your body's immune response to *H. pylori* treatment. We would like to collect this

information to investigate how eradication treatment influences the immune response.

Previous research in this area has also looked at the effect of *H. pylori* on conditions such as asthma. Evidence shows that *H. pylori* may play a role in childhood when the immune system is developing. We want to follow up anyone who is currently or has previously been an asthma sufferer with extra lung function tests, even though is it very unlikely to have an effect on your symptoms.

This study will also form part of Dr Jonathan White's higher degree (PhD) which will be supervised by Professor Atherton.

**Why have I been invited?**

Patients attending the Nottingham University Hospital's outpatient department will be invited to take part in the study. You are being invited to take part because you have tested positive for *H. pylori*. We need approximately 50 people to take part to help us gather this information and would like to include people previously treated for *H. pylori* where treatment has not been successful as well as people that have not yet been treated.

**Do I have to take part?**

Taking part in this research is entirely voluntary. If you do decide to take part, you will be given this information sheet to keep and will be asked to sign a consent form to show that you have agreed to take part. If you decide to take part, you are still free to withdraw at any time without giving a reason.

**What will happen to me if I take part?**

If you are interested please attend your appointment as normal. During your appointment you will be approached by a member of Professor Atherton's team. They will discuss the study and answer any questions you may have. If you are willing, we will ask you to sign a consent form.

We plan to measure your body's Treg immune response by a simple blood test before and after you are given antibiotics to eradicate the bacteria. You will attend our Biomedical Research Unit at Queens Medical Centre either 5 or 7 occasions over the two year study period. Up to 50mls (approximately 1/5 of a cup) of blood will be taken at each visit, and if applicable (i.e. if you currently or have previously suffered from asthma we will do simple spirometry tests and ask you to complete an Asthma Quality of Life Questionnaire. If you are found to carry *H. pylori* you will be enrolled to Group 1 and will receive eradication treatment.

**Group 1 (untreated):**

After eradication treatment, a Urea Breath Test will be performed as part of normal clinical practice to ensure the antibiotics have worked. The Urea Breath test usually takes about 30 minutes, you will be asked to blow into a bag. Afterwards you drink orange juice containing 13C urea then blow into the bag again. The test does not involve any radiation and is completely safe. In some patients, eradication treatment for *H. pylori* may fail for unknown reasons. If it does not work, we will move these patients to Group 2. *However, you will not have any different tests to Group 1. We will just analyse your results in a different way. You will also receive further treatment as per normal clinical practice.

**Group 2 (treatment failed):**

Patients previously treated for *H. pylori* and treatment has failed will be allocated to this group; along with those who received treatment in group 1 which failed.

***** *Please note that groups 1 and 2 will receive exactly the same tests.*

Each group will have up to 50mls of blood taken at the first visit and at 2, 6, 12 and 24 months after eradication treatment. Before each blood test, you will have a repeat breath test to check that you still do not carry the bug.

If at your first visit your medical history identifies you as a current or previous asthmatic, we will perform spirometry, peak flows and an asthma quality of life questionnaire in addition to your blood tests at first visit, 12 and 24 months. Spirometry is a special test to measure breathing and is a useful way to monitor asthma. You will be required to blow as hard as you can into the mouth piece of the spirometer. This test may take between 10 and 30 minutes. Peak flow measurements are simple ways of measuring breathing that many of you may already do at home and will involve you blowing into a small handheld device, which normally takes 1 minute.

The estimated amount of time required at each visit to include blood tests, urea breath tests and spirometry is less than one and a half hours.

This study will end after two years and your participation will be complete. Hopefully, we will have found some exciting new answers in this field of research that will make a real difference!

**Expenses and payment**

Participants will not be paid to participate in the study; however, prescription costs and travel expenses will be reimbursed for participants' visits; participants will receive an inconvenience allowance of £50 to cover these costs; paid in two £25 instalments at the beginning of their participation in the trial and on them completing the trial.

**What are the possible disadvantages and risks of taking part?**

The only additional tests to what you would have undergone in normal clinical practice will be blood tests and if applicable spirometry, peak flow and asthma quality of life questionnaires.

We do not expect any change in your breathing symptoms during the time period of the study, but if there is some unexpected deterioration we will inform your responsible physician who will manage you further.

Blood testing may result in localised discomfort and/or slight bruising

**What are the possible benefits of taking part?**

We cannot promise the study will help you but the information we get from this study may help us to better understand *H. pylori* infection and come up with new novel ways to test and treat this infection. It also helps us to gather information that may influence future management of people with common disorders that may be influenced by these bacteria.

**What if there is a problem?**

If you have a concern about any aspect of this study, you should ask to speak to the researchers who will do their best to answer your questions. The researchers contact details are given at the end of this information sheet. If you remain unhappy and wish to complain formally, the National Health Service complaints procedure or NHS Patient Advice & Liaison Service (PALS) office is available to you and can be contacted on Free phone: 0800 183 0204 or [local contact details].

**Will my taking part in the study be kept confidential?**

We are bound by ethical and legal regulations to ensure any information related to you is kept safe. All information which is collected about you during the course of the research will be kept **strictly confidential**, stored in a secure and locked office, and on a password protected database. Any information about you which leaves the hospital will have your name and address removed and a unique code will be used so that you cannot be recognised from it.

If you join the study, some parts of your medical records and the data collected for the study will be looked at by authorised persons from the University of Nottingham who are organising the research. They may also be looked at by authorised people to check that the study is being carried out correctly. All will have a duty of confidentiality to you as a research participant and we will do our best to meet this duty.

Your personal data (address, telephone number) will be kept for 12 months after the end of the study so that we are able to contact you about the findings of the study.

All other data (research data) will be kept securely for 7 years. After this time your data will be disposed of securely. During this time, all precautions will be taken by all those involved to maintain your confidentiality, only members of the research team will have access to your personal data.

**What will happen if I don't want to carry on with the study?**

Your participation is voluntary and you are free to withdraw at any time, without giving any reason, and without your legal rights being affected. If you withdraw then the information collected so far cannot be erased and this information may still be used in the project analysis.

**Involvement of the General Practitioner/Family doctor (GP)**

With your consent, we will inform your General Practitioner of your participation in this study.

**What will happen to any samples I give?**

A variety of methods will be used to analyse the samples you provide us. In essence, we will be studying your body's immune response to *H. pylori* and how this changes after treatment. We will be concentrating specially on the immune cells which suppress inflammation in the body. These are called regulatory T cells.
After the study has ended, all remaining samples will be destroyed.

**Will any genetic tests be done?**

No genetic testing will be done.

**What will happen to the results of the research study?**

The results of this study are likely to be published in a scientific journal and presented at professional meetings. All participants' information will be anonymous. The results may also be written up as educational material by one of Professor Atherton's team.

**Who is organising and funding the research?**

This study is sponsored by The University of Nottingham.
The NIHR Nottingham Digestive Diseases Biomedical research unit at Nottingham University Hospitals is organising the research, working closely in partnership with The University of Nottingham.

**Who has reviewed the study?**

All research in the NHS is looked at by independent group of people, called a Research Ethics Committee, to protect your interests. This study has been reviewed and given favourable opinion by the Nottingham 1 Research Ethics Committee.

**CONSENT FORM**

**(Final version 1.0: 6th November 2012)**

Title of Study: **Study to Investigate Regulatory T lymphocyte Response to *Helicobacter pylori* Treatment**

**REC ref:** ***(to be added after approval given)***

**Name of Researcher**:

**Name of Participant:** **Please initial box**

I confirm that I have read and understood the information sheet version number ……dated..... for the above study and have had the opportunity to ask questions. ☐

I understand that my participation is voluntary and that I am free to withdraw at any time, without giving any reason, and without my medical care or legal rights being affected. I understand that should I withdraw, then the information collected so far cannot be erased and so may still be used in the project analysis. ☐

I understand that relevant sections of my medical notes and data collected in the study may be looked at by authorised individuals from the University of Nottingham, the research group and regulatory authorities where it is relevant to my taking part in this study. I give permission for these individuals to have access to these records and to collect, store, analyse and publish information obtained from my participation in this study. I understand that my personal details will be kept confidential. ☐

I understand and agree that a blood sample of up to 50mls will be taken on each visit and stored for analysis during this current study. ☐

I agree to having peak flow measurements, spirometry and completing an Asthma Quality of Life Questionnaire (if applicable). ☐

I agree to my GP being informed of my participation in this study. ☐

I agree to take part in this study. ☐

| _____ | _____ | _____ |
|---|---|---|
| Name of Participant | Date | Signature |
| _____ | _____ | _____ |
| Name of Person taking consent | Date | Signature |

3 copies: 1 for participant, 1 for the project notes and 1 for the medical notes

# Patient Information Sheet

## Influence of host and bacterial factors on the outcome of *Helicobacter pylori* infection – gastric tissue biopsy, blood and stool sample collection

You are due to have an endoscopy examination of your oesophagus (food-pipe), stomach, and duodenum (upper bowel). During this procedure we often routinely take small biopsy specimens (tiny snips of your bowel lining) to help in your diagnosis and treatment (for clinical use). As a leading UK Medical Research Centre, patients are often asked if they would like to help with research studies. You are invited to contribute extra biopsy specimens and a blood sample to be used for research. You will also be asked to provide a stool sample at this visit – details of this are below, you can still take part in this study without having to provide a stool sample.

Please take the time to read the following information carefully - this explains things in detail. If you have any questions or require further information after reading this information sheet there are contact details at the end of the sheet.

### *What is the purpose of the study?*

*Helicobacter pylori* (*Hp*) are bacteria that live in the stomach of about a third of people in the UK. In most people *Hp* infection does not cause problems, however in a small proportion the infection causes stomach or duodenal ulcers or stomach cancer. Professor Atherton's research group is studying factors which may explain why the infection leads to disease in some people but not others. These include:

i) Factors related to the person infected (host) e.g. how their immune system responds to the *Hp* infection
ii) Bacterial factors – some *Hp* strains cause more disease than others. Professor Atherton's group is studying factors that make these strains cause more disease.

The results from these will aid defining which Hp individuals develop disease and help develop simple non-invasive tests that may influence future practice.

### *Why have I been chosen?*

All patients scheduled to have an endoscopy examination of their oesophagus (food pipe),stomach and duodenum (upper bowel) are being invited to take part whether or not they have the infection, as we need infected people and uninfected people for comparison.

### *Do I have to take part?*

Taking part is entirely voluntary and if you decide not to take part it will not affect the standard of care you receive. If you decide to take part you are still free to withdraw at any time without giving a reason.

### *What will happen if I take part?*

If you are interested in participating in the study then please attend your endoscopy appointment as normal. During your visit you may be approached about the study by the doctor or a member of the research team. They will discuss the study with you and give you an opportunity to ask any questions. If you are happy to proceed you will be asked to sign a form to consent to extra biopsy samples being taken for

research. Please remember, you are under no obligation to take part. No more, than 8 research biopsy samples would be taken, and this will add about 2 minutes to the procedure. You will also be asked to contribute a blood sample of up to 50ml (this is the equivalent of about 3 and a half tablespoons).

Where possible we would also like you to give a stool sample at this visit, we appreciate that this may not be possible and if not arrangements can be made for you to provide a sample up to a week after your endoscopy visit – we can provide you with a sample container and gloves and ask that you to bring it into reception. *(*Please note: It is still possible to take part in the study without providing a stool sample).*

That will be the end of your participation in this study.

It may be useful for the study team to look at your medical notes before your hospital visit to see if you are suitable for the study. If would like to give permission for Prof Atherton or a member of his research team to do this then please complete the attached permission form and return it in the freepost envelope provided.

***What is a biopsy sample?***

Biopsy samples are fragments of the lining of the stomach or bowel that are about 1-3mm in diameter. They are taken by forceps that are passed down the endoscope and used to snip a small piece of lining. Passing the forceps takes about 10 seconds and snipping the lining about 1 second. It is painless and you will not be aware of the process. More details can be found in the endoscopy information leaflet.

***What are the possible disadvantages and risks of taking part?***

Taking biopsy samples is very safe. A small amount of bleeding occurs but this stops very quickly. In theory, significant bleeding or perforation of the bowel can occur but experience shows that this does not happen except in certain well recognised conditions of risk. In these specific cases we do not take biopsy samples. Taking a blood sample may cause mild discomfort and may leave a small bruise.

***What are the possible benefits of taking part?***

There are no benefits to you, but the information we get might improve our understanding of gastrointestinal disease, its causes and how to prevent or treat it.

***Will my taking part in the study be kept confidential?***

Yes. All the information about your participation in the study will be kept confidential. Your medical notes may be inspected by the study team to check if you are suitable for the study and to help analyse the results but your clinical details and results will be stored anonymously.

***What will happen if I don't want to carry on with the study?***

If you withdraw from the study, we will destroy all your remaining samples.

***What if there is a problem?***

If you have a concern or complaint about the study, this can be discussed with a research team member. If the problem persists, this can be brought to the attention of Professor Atherton. If you remain unhappy and wish to make a formal complaint the National Health Service complaints procedure will be available to you.

***What will happen to any samples I give?***

Your samples will be used for research into understanding why some people infected with *Hp* develop disease whilst the majority do not. With your permission we would also like to store any remaining samples for use in future related research into *Helicobacter pylori* infection. We would also like to ask your permission for some of your biopsy samples to be sent to other laboratories, some of which may be outside The European Union (EU) for analysis. This is to enable special research tests using equipment that we do not have available here. All your samples will have your details removed before they are sent so you will not be able to be identified from them.

***What will happen to the results of this research?***

We anticipate that the results from this study will be published in a scientific journal and will be presented at scientific meetings. All patient information will be kept anonymous and you will not be identified in any publication or presentation.

***Who is organising payment for the research?***

The University of Nottingham is organising the study which is funded by Professor Atherton's departmental funds. All research in the NHS is looked at by an independent group of people called a Research Ethics Committee to protect your safety, rights, wellbeing and dignity. This study has been reviewed and given favourable opinion by Nottingham Research Ethics Committee 2.

D – Consent form given to patients donating to the Nottingham Collection

**CONSENT FORM**

**Study Title: Influence of host and bacterial factors on the outcome of *Helicobacter pylori* infection – gastric tissue biopsy, blood and stool sample collection**

Name of Chief Investigator: Prof John Atherton

**Please initial box**

| | | |
|---|---|---|
| 1. | I confirm that I have read and understand the information sheet dated 18 December 2012 (version 2.1) for the above study. I have had the opportunity to consider the information, ask questions and have had these answered satisfactorily. | ☐ |
| 2. | I understand that my participation is voluntary and that I am free to withdraw at any time without giving any reason, without my medical care or legal rights being affected. | ☐ |
| 3. | I understand that relevant sections of my medical notes and data collected during the study may be looked at by responsible individuals from the University of Nottingham, the Research Group, from regulatory authorities or from the NHS Trust, where it is relevant to my taking part in this research. I give permission for these individuals to have access to my records. I understand that my personal details will not be recorded. | ☐ |
| 4. | a. I understand and agree that up to 8 additional biopsies will be taken and stored for analysis during this current study.<br><br>b. I agree that my biopsy samples may be sent to other researchers in outside laboratories (some of which may be outside the EU) for analysis. I understand that the samples will have any details that could identify me removed before sending. *(Optional)* | ☐<br><br>☐ |
| 5. | I understand and agree that a blood sample of up to 50mls will be taken and stored for analysis during this current study. | ☐ |
| 6. | OPTIONAL:<br>I understand and agree to provide a stool sample. The stool sample will be stored for analysis during this current study. | ☐ |
| 7. | I agree that if any samples are left over, at the end of this study, they can be stored and used for possible *Helicobacter pylori*-related future research. | ☐ |
| 8. | I agree to take part in the above study. | ☐ |

_____ _____ _____

Name of Patient Date Signature

| _____ | _____ | _____ |
| --- | --- | --- |
| Name of Person taking consent | Date | Signature |

1 copy for the patient, 1 copy to be place in the medical notes and 1 copy for the study file.

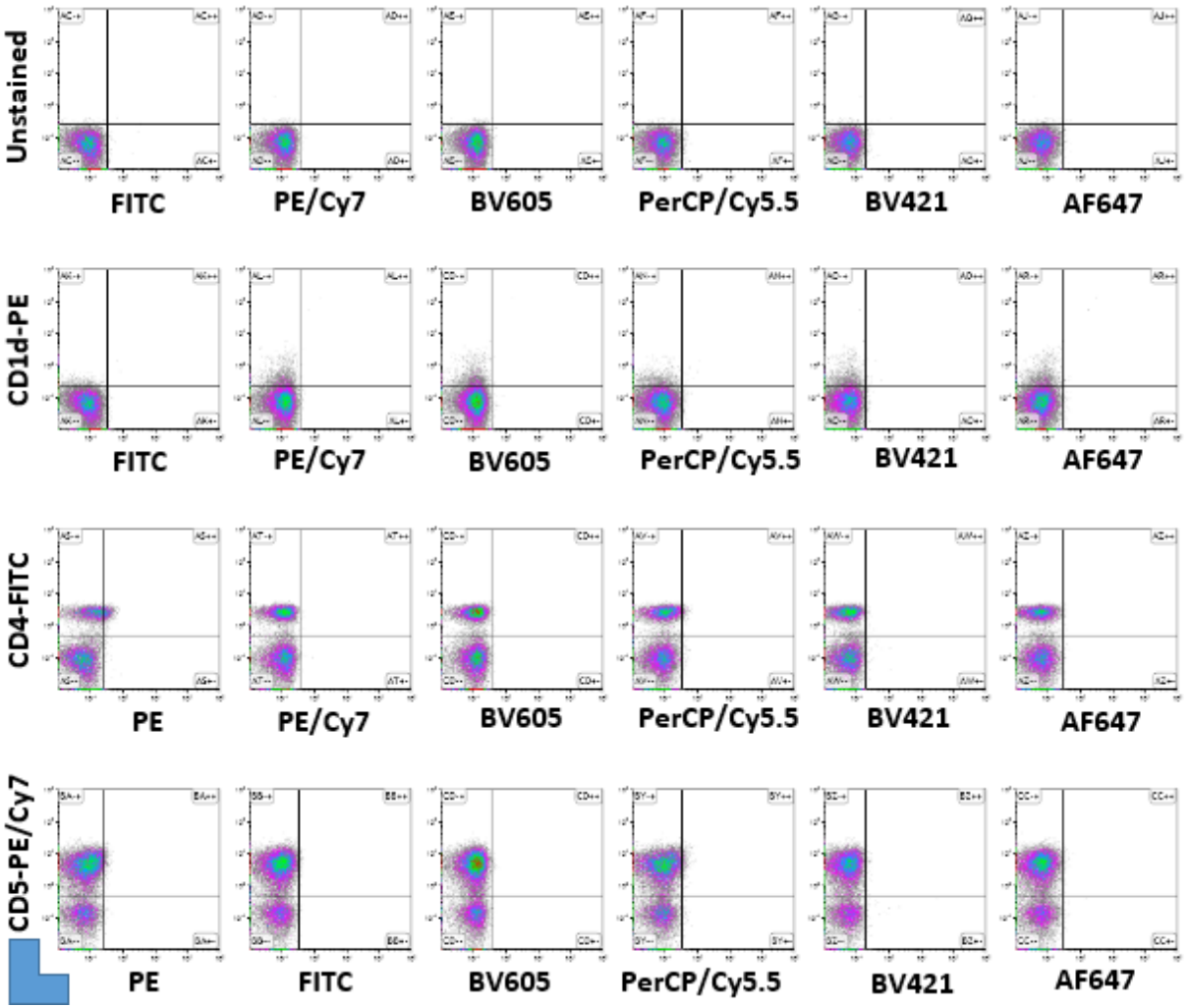
E – Clinical history of volunteers and patients who consented to participate in Breg/Treg study

| Patient | Sex | Age | *H. pylori* status | Ethnicity | Smoking status | Relevant clinical history | Indication for endoscopy | Endoscopy findings |
|---|---|---|---|---|---|---|---|---|
| Volunteer | - | - | Negative | - | Non-S | - | - | - |
| Volunteer | F | 26 | Negative | Caucasian | Non-S | - | - | - |
| Volunteer | M | 29 | Negative | Black | Non-S | - | - | - |
| P #880 | M | 69 | Negative | Caucasian | - | Serology negative | Dyspepsia | - |
| P #881 | F | 59 | Positive | Asian | Non-S | | IDA | Gastric atrophy |
| P #882 | M | 71 | Negative | - | Non-S | - | Reflux | - |
| P #883 | M | 80 | Negative | Caucasian | Non-S | - | IDA | - |
| P #887 | M | 49 | Negative | - | - | Serology negative | IDA | - |
| P #888 | F | 56 | Eradicated | - | Non-S | *H. pylori* eradication x2 2015 | Previous CLO/UBT+ | - |
| P #889 | M | 56 | Negative | Caucasian | Non-S | - | Dyspepsia | - |
| P #890 | M | 18 | Negative | Black | Non-S | - | - | - |
| P #891 | M | 32 | Positive | Black | S | *H. pylori* eradication 2014, *H. pylori* serology positive | - | - |
| P #892 | F | 71 | Eradicated | - | Non-S | *H. pylori* eradication 2015 | - | - |
| P #893 | F | 67 | Negative | - | Ex-S | - | IDA | - |
| P #895 | M | 47 | Positive | Asian | - | Serology negative | Dysphagia | - |
| P #896 | F | 34 | Positive | - | - | - | - | - |
| P #897 | M | 86 | Negative | - | Non-S | - | IDA | - |

| Patient | Sex | Age | *H. pylori* status | Ethnicity | Smoking status | Relevant clinical history | Indication for endoscopy | Endoscopy findings |
|---|---|---|---|---|---|---|---|---|
| P #898 | M | 65 | Positive | - | Non-S | - | Dyspepsia | Peptic ulcer |
| P #899 | M | 40 | Negative | Caucasian | Non-S | T2 Diabetes | Dyspepsia | - |
| P #902 | M | 61 | Negative | - | Non-S | - | Dyspepsia and gastric reflux | Moderate gastritis |
| P #904 | M | 52 | Negative | - | S | *H. pylori* eradication | Dyspepsia | - |
| P #905 | M | 72 | Negative | - | Non-S | - | IDA | - |
| P #906 | F | 38 | Positive | - | Non-S | *H. pylori* eradication | *H. pylori* culture | - |
| P #907 | F | 55 | Negative | - | Ex-S | *H. pylori* eradication UBT inconclusive Peptic ulcer x 2 | - | Peptic ulcer x 2 |
| P #908 | M | 79 | Negative | - | Non-S | Serology negative | IDA | Gastritis |
| P #910 | M | 38 | Positive | - | Non-S | - | - | - |
| Volunteer | M | 26 | Negative | Caucasian | Ex-S | - | - | - |
| T041M2V4 | M | 59 | Positive | Caucasian | Non-S | *H. pylori* eradication | Dyspepsia | Hiatus hernia |
| T048M2V4 | F | 65 | Positive | Caucasian | Non-S | *H. pylori* eradication | *H. pylori* culture | Peptic ulcer |
| T026M12 | M | 64 | Eradicated | Caucasian | Non-S | - | Abnormal CT scan | - |
| T029M12 | M | 53 | Eradicated | Asian | S | - | IDA | - |
| T014M24 | M | 60 | Eradicated | Caucasian | S | | Peptic ulcer pain | Peptic ulcer |
| T018M24 | F | 55 | Eradicated | Caucasian | Ex-S | - | Dyspepsia | - |
| T035M12 | M | 55 | Eradicated | Caucasian | Non-S | | Gastric reflux | Peptic ulcer |
| T036M12 | M | 70 | Eradicated | Caucasian | Non-S | - | Weight loss | Peptic ulcer |
| T037M12 | F | 59 | Eradicated | Caucasian | Non-S | - | Weight loss | Peptic ulcer |

| Patient | Sex | Age | *H. pylori* status | Ethnicity | Smoking status | Relevant clinical history | Indication for endoscopy | Endoscopy findings |
|---|---|---|---|---|---|---|---|---|
| T020M24 | M | 56 | Eradicated | Caucasian | Ex-S | - | Gastric reflux | Hiatus hernia |
| T038M12 | F | 69 | Eradicated | Caucasian | Non-S | - | IDA | Hiatus hernia |
| T040M12 | M | 67 | Eradicated | Caucasian | S | - | Gastric reflux | Hiatus hernia |
| T019M24 | M | 58 | Eradicated | Caucasian | Non-S | - | Dyspepsia | Hiatus hernia |
| T046M12 | F | 65 | Eradicated | Caucasian | Non-S | - | Dyspepsia | Normal |
| T021M24 | M | 51 | Eradicated | Caucasian | Non-S | - | IDA | Inflammation |
| T044M12 | M | 65 | Eradicated | Caucasian | S | - | Nausea/ Vomiting | Normal |
| T049M6 | F | 67 | Eradicated | Caucasian | S | - | Gastric reflux | Normal |

F – Representative single stain control plot diagrams in Breg/Treg study



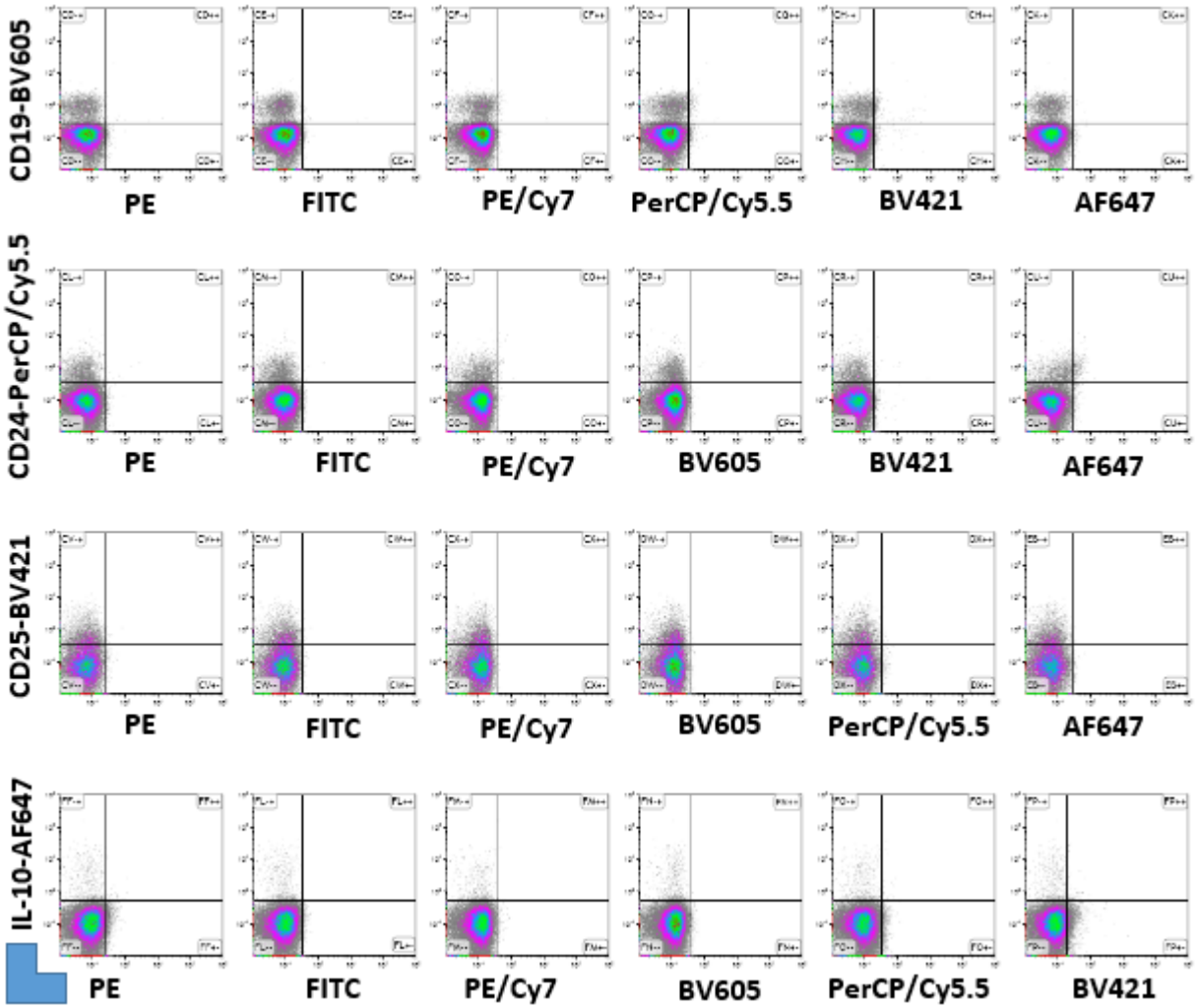
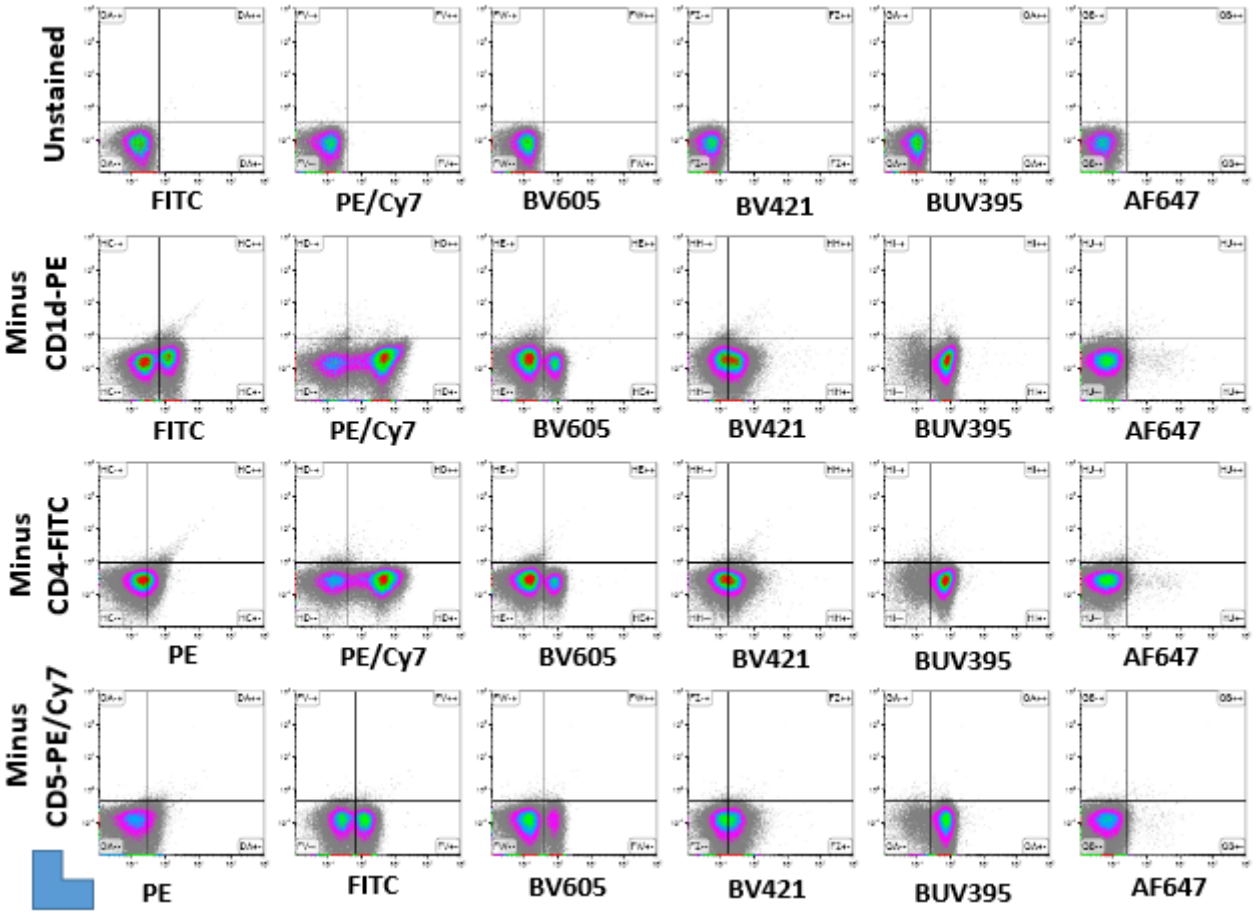

CD19-BV605
PE
FITC
PE/Cy7
PerCP/Cy5.5
BV421
AF647
CD24-PerCP/Cy5.5
PE
FITC
PE/Cy7
BV605
BV421
AF647
CD25-BV421
PE
FITC
PE/Cy7
BV605
PerCP/Cy5.5
AF647
IL-10-AF647
PE
FITC
PE/Cy7
BV605
PerCP/Cy5.5
BV421

**Figure F:** (Overleaf) Representative flow cytometry plots of human PBMCs stained with individual mouse and rat fluorochrome-conjugated antibodies, and assessed for the intensity of fluorescence and its detection in other channels. (Top to bottom) Unstained cells, anti-CD1d-PE, anti-CD4-FITC, anti-CD5-PE/Cy7, anti-CD19-BV605, anti-CD24-PerCP/Cy5.5, anti-CD25-BV421, and anti-IL-10-AF647.

G – Representative FMO experiment plot diagrams in Breg/Treg study



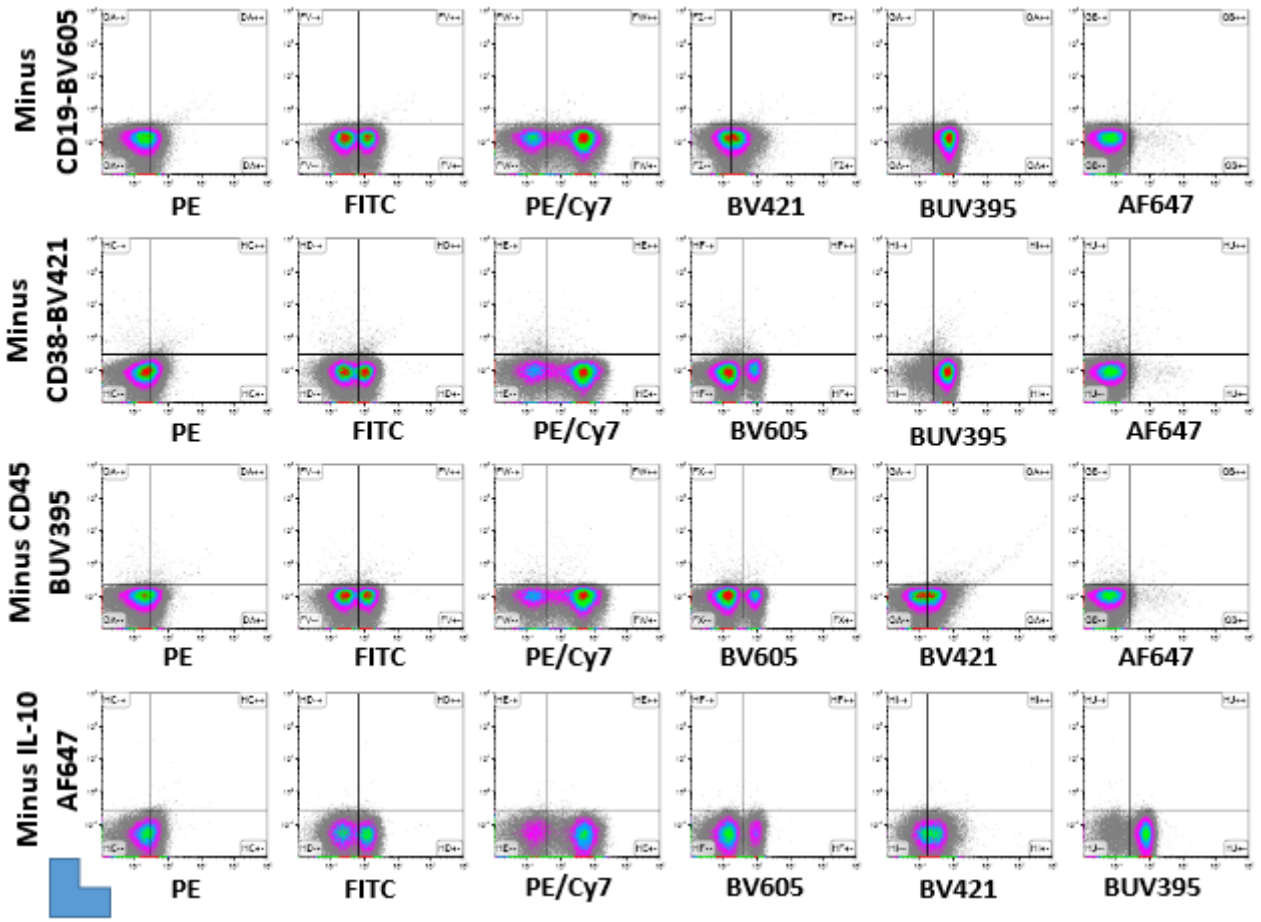
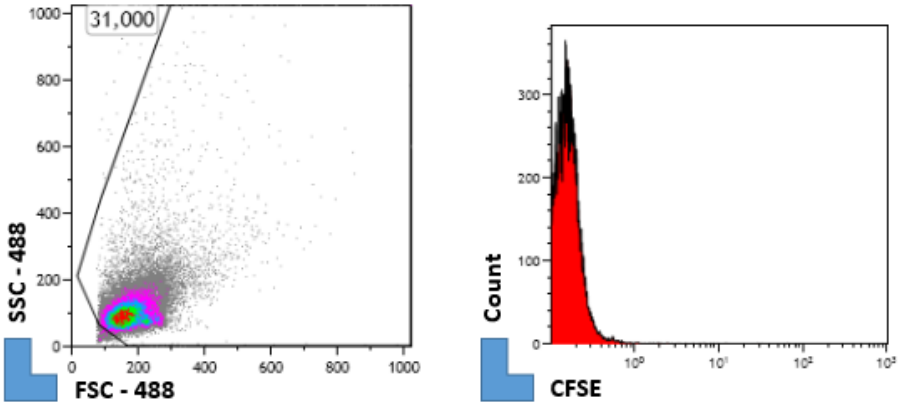

Minus CD19-BV605
PE
FITC
PE/Cy7
BV421
BUV395
AF647
Minus CD38-BV421
PE
FITC
PE/Cy7
BV605
BUV395
AF647
Minus CD45 BUV395
PE
FITC
PE/Cy7
BV605
BV421
AF647
Minus IL-10 AF647
PE
FITC
PE/Cy7
BV605
BV421
BUV395

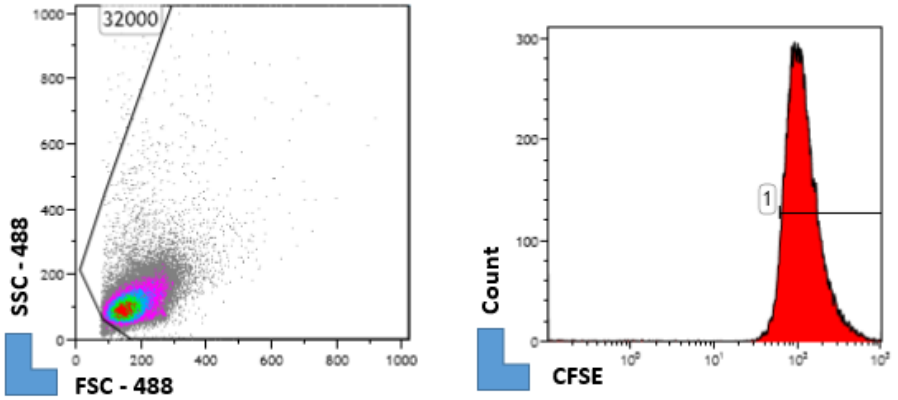
**Figure G:** (Overleaf) Representative flow cytometry plots of human PBMCs that were stained with a polychromatic panel of fluorochrome-conjugated antibodies to conduct an FMO analysis. This was to assess the level of background fluorescence between the different channels, and each tube were labelled with all antibodies minus one. (Top to bottom) Unstained control, all fluorochrome-conjugated antibodies minus anti-CD1d-PE, minus anti-CD4-FITC, minus anti-CD5-PE/Cy7, minus anti-CD19-BV605, minus anti-CD38-BV421, minus anti-CD45-BUV395, and minus anti-IL-10-AF647.

## H – Gating strategy for Tresps in suppression assay

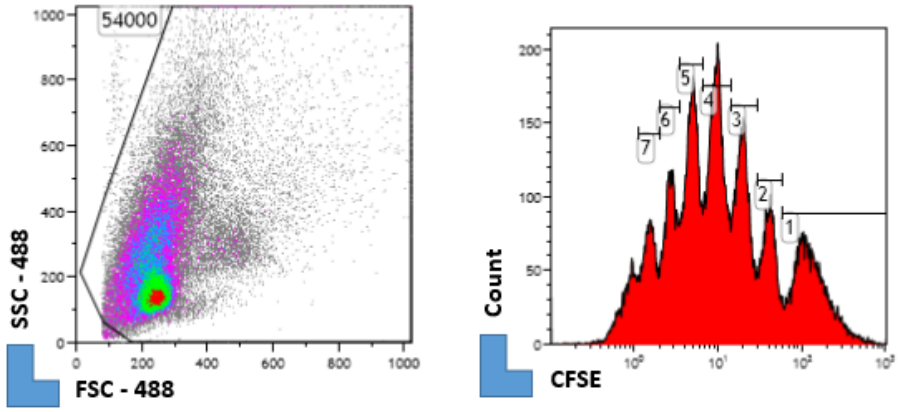
**A** Unlabelled CD4⁺CD25⁻ Tresp cells only



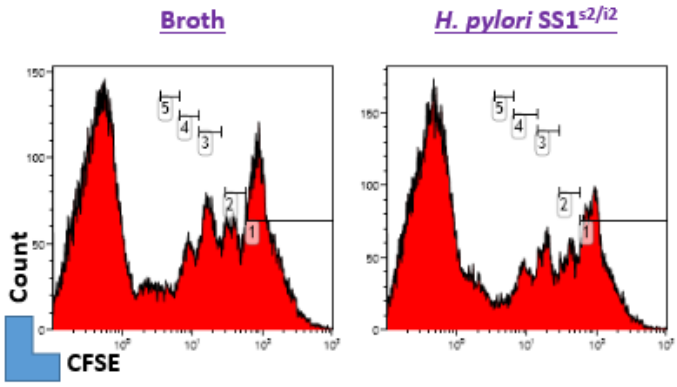

**B** Labelled CD4⁺CD25⁻ Tresp cells only



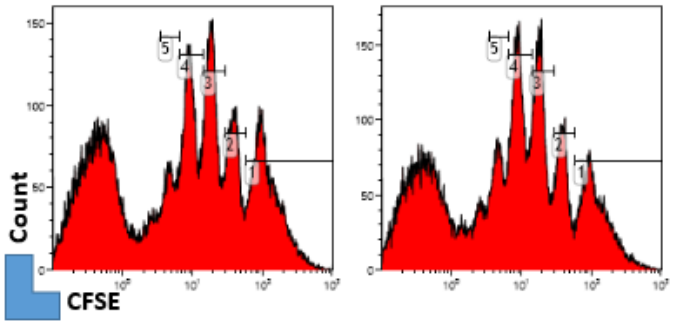

**C** Labelled CD4⁺CD25⁻ cells with CD3/CD28 beads



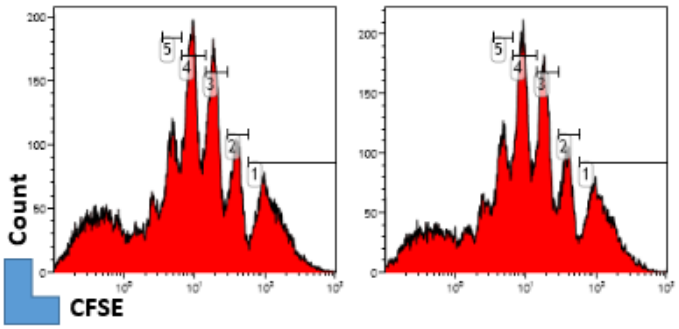
**D** 1:1 Treg:Tresp ratio




**E** 1:2 Treg:Tresp ratio




**F** 1:4 Treg:Tresp ratio




**G** 1:8 Treg:Tresp ratio

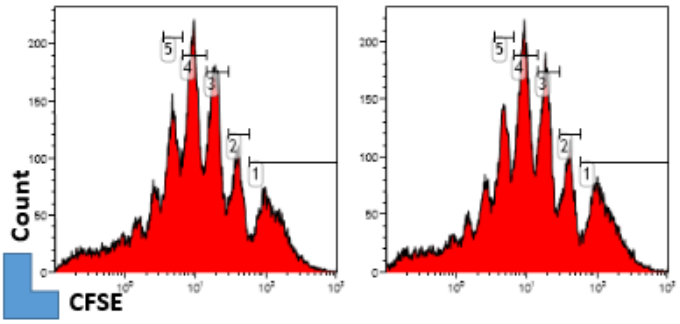


**Figure H:** (Overleaf) Representative flow cytometry plots and gating strategy used to identify the capacity of splenic $CD4^+CD25^+$ Tregs to suppress the proliferation of $CD4^+CD25^-$ Tresp cells in mice. Female C57BL/6 mice were orally dosed with Brucella broth (Broth), or infected with *H. pylori* SS1 wild-type strain ($SS1^{s2/i2}$) for 9 weeks. (A) Unlabelled Tresp cells only. (B) Labelled Tresp cells only. (C) Labelled Tresp cells with CD3/CD28 stimulation beads. (D-G) The proportion of CFSE-labelled Tresp proliferation in *H. pylori*-infected ($SS1^{s2/i2}$) and uninfected mice in different Treg:Tresp ratios, based on the peak gating strategy identified in (C).

I – Clinical history of patients who consented to participate in the Stool study

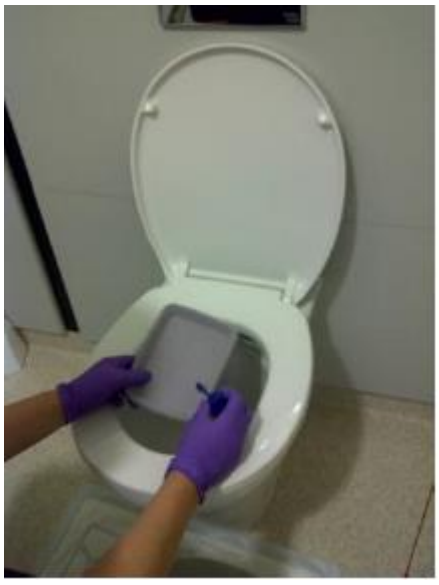
| Patient no. | Sex | Age | Symptoms and previous *H. pylori* testing | Previous *H. pylori* treatment | Endoscopy findings |
|---|---|---|---|---|---|
| 755 | F | 51 | Vomiting<br>Weight loss | No | Healed peptic ulcer |
| 764 | F | 49 | Dyspepsia | - | - |
| 775 | M | 53 | Reflux, Heartburn | Yes | Peptic ulcer |
| 779 | M | 36 | *H. pylori* C+S testing | Yes x 3 | Duodenal ulcer |
| 784 | M | 35 | *H. pylori* C+S testing | Yes x 4 | Peptic ulcer |
| 803 | F | 46 | *H. pylori* C+S testing<br>Persistent vomiting | - | Healed peptic ulcer |
| 810 | F | 42 | *H. pylori* C+S testing<br>Previous gastric ulcer | - | - |
| 812 | M | 77 | Dyspepsia<br>*H. pylori* C+S testing | Yes | - |
| 813 | M | 46 | *H. pylori* C+S testing | - | - |
| 849 | F | 75 | Reflux<br>Heartburn | - | - |
| 850 | M | 49 | *H. pylori* C+S testing | Yes x 2 | - |
| 856 | M | 63 | Dyspepsia | - | Peptic ulcer |
| 857 | F | 77 | Dyspepsia | - | - |
| 858 | M | 59 | Dyspepsia | Yes | - |
| 861 | F | 68 | Dyspepsia | - | - |
| 862 | F | 75 | Dyspepsia | - | - |

J – Information given to patients participating in the Stool study

**Stool Collection advice**

- Collect samples on a Monday, Tuesday or Wednesday.
- Place Gel pack in freezer overnight (ready to use the next day).
- The morning you collect the sample the Gel pack can be taken out of the freezer and will help keep stool sample cool.
- Put on plastic gloves.
- Place or hold the cardboard tray to collect the stool as passed.
- Remove the screw cap and spatula from the stool container and collect a cherry-sized piece of stool on the scoop (See Figure 1).
- Replace screw cap and close the container.
- Place the container in the double sample cool gel pack container provided.
- This will keep your samples cool when it is in the post.
- Dispose of gloves and cardboard in a plastic bag to be placed in any normal dustbin.
- Flush any leftover stool down the toilet.

**Figure 1.**





- Place the sample and the frozen gel pack in the postage pack provided and post.

**Thank you for your participation**

K – Comparing the response of lymphocytes to different stimulants

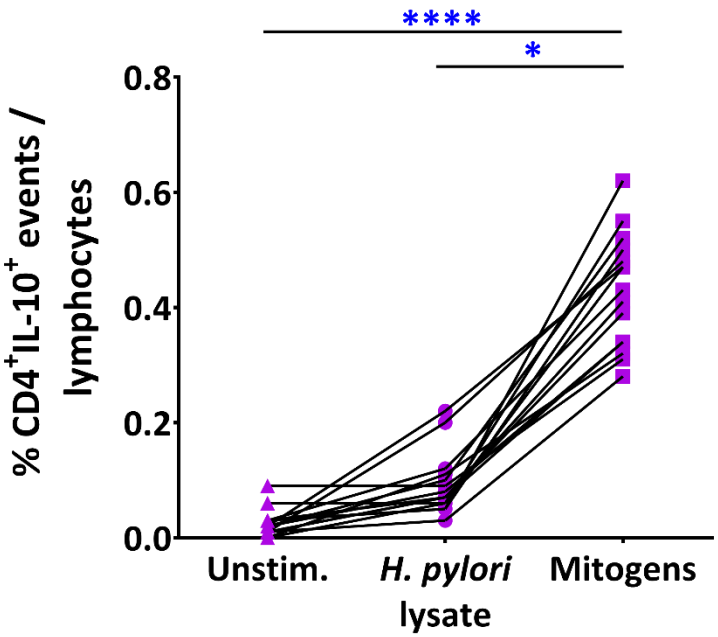



**Figure K**: Comparison of $CD4^+IL\text{-}10^+$ lymphocyte frequencies following *in vitro* stimulation of human PBMCs with *H. pylori* lysate antigen or mitogens. Cells were stimulated with *H. pylori* lysate for 16 hours, or with PMA, ionomycin and LPS for 6 hours (Mitogens), or left unstimulated (Unstim.) before being stained with different mouse and rat fluorochrome-conjugated antibodies and quantified on MoFlo Astrios or FC 500 (Beckman Coulter). Statistical analysis between all three paired groups was carried out using a 1-way ANOVA Friedman test with a post-hoc Dunn's test. The asterisks indicate the level of statistical significance, where * represents $p \leq 0.05$, and **** represents $p \leq 0.0001$.

## Quotation

*This is truly the Age of Bacteria*

*- as it was in the beginning,*

*is now*

*and ever shall be.*

- Stephen Jay Gould[374]